frontiers | Research Topics

The UN international day of families: Neurodegeneration as a result of genetic inheritance

Edited by
Prabhjyot Saini, Durga Attili, Stelios Ravanidis,
Iliyana Hristova Pacheva and Lucio Tremolizzo

Published in
Frontiers in Aging Neuroscience

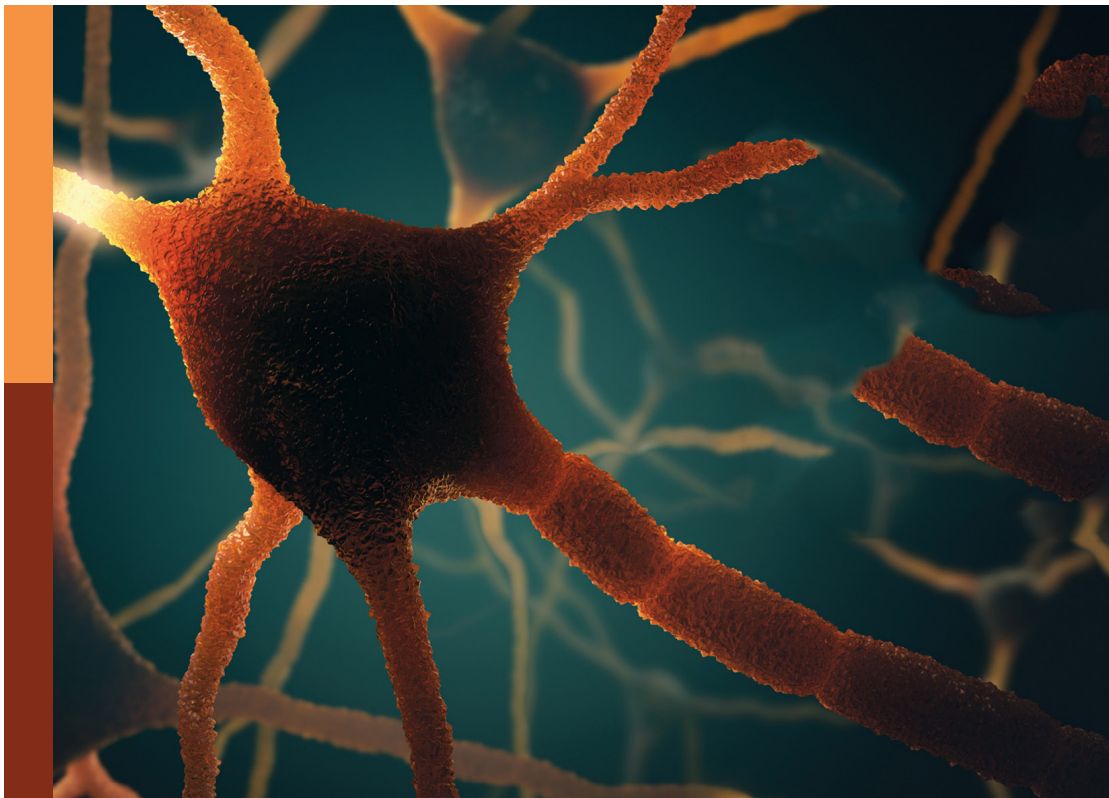

ISSN 1664-8714
ISBN 978-2-8325-3753-4
DOI 10.3389/978-2-8325-3753-4

About Frontiers

Frontiers is more than just an open access publisher of scholarly articles: it is a pioneering approach to the world of academia, radically improving the way scholarly research is managed. The grand vision of Frontiers is a world where all people have an equal opportunity to seek, share and generate knowledge. Frontiers provides immediate and permanent online open access to all its publications, but this alone is not enough to realize our grand goals.

Frontiers journal series

The Frontiers journal series is a multi-tier and interdisciplinary set of open-access, online journals, promising a paradigm shift from the current review, selection and dissemination processes in academic publishing. All Frontiers journals are driven by researchers for researchers; therefore, they constitute a service to the scholarly community. At the same time, the *Frontiers journal series* operates on a revolutionary invention, the tiered publishing system, initially addressing specific communities of scholars, and gradually climbing up to broader public understanding, thus serving the interests of the lay society, too.

Dedication to quality

Each Frontiers article is a landmark of the highest quality, thanks to genuinely collaborative interactions between authors and review editors, who include some of the world's best academicians. Research must be certified by peers before entering a stream of knowledge that may eventually reach the public - and shape society; therefore, Frontiers only applies the most rigorous and unbiased reviews. Frontiers revolutionizes research publishing by freely delivering the most outstanding research, evaluated with no bias from both the academic and social point of view. By applying the most advanced information technologies, Frontiers is catapulting scholarly publishing into a new generation.

What are Frontiers Research Topics?

Frontiers Research Topics are very popular trademarks of the *Frontiers journals series*: they are collections of at least ten articles, all centered on a particular subject. With their unique mix of varied contributions from Original Research to Review Articles, Frontiers Research Topics unify the most influential researchers, the latest key findings and historical advances in a hot research area.

Find out more on how to host your own Frontiers Research Topic or contribute to one as an author by contacting the Frontiers editorial office: frontiersin.org/about/contact

The UN international day of families: Neurodegeneration as a result of genetic inheritance

Topic editors

Prabhjyot Saini — Emory University, United States
Durga Attili — University of Michigan, United States
Stelios Ravanidis — ECONCARE Health Research and Consulting, Greece
Iliyana Hristova Pacheva — Plovdiv Medical University, Bulgaria
Lucio Tremolizzo — University of Milano-Bicocca, Italy

Citation

Saini, P., Attili, D., Ravanidis, S., Pacheva, I. H., Tremolizzo, L., eds. (2023). *The UN international day of families: Neurodegeneration as a result of genetic inheritance*. Lausanne: Frontiers Media SA. doi: 10.3389/978-2-8325-3753-4

Table of contents

frontiers | Frontiers in Aging Neuroscience

TYPE Editorial
PUBLISHED 06 October 2023
DOI 10.3389/fnagi.2023.1291613

OPEN ACCESS

EDITED AND REVIEWED BY
Kristy A. Nielson,
Marquette University, United States

*CORRESPONDENCE
Stylianos Ravanidis
✉ stelrav@hotmail.com

RECEIVED 09 September 2023
ACCEPTED 18 September 2023
PUBLISHED 06 October 2023

CITATION
Pacheva IH, Attili D and Ravanidis S (2023) Editorial: The UN international day of families: neurodegeneration as a result of genetic inheritance. *Front. Aging Neurosci.* 15:1291613. doi: 10.3389/fnagi.2023.1291613

Editorial: The UN international day of families: neurodegeneration as a result of genetic inheritance

Iliyana Hristova Pacheva[1], Durga Attili[2] and Stylianos Ravanidis[3]*

[1]Department of Pediatrics and Medical Genetics, Plovdiv Medical University, Plovdiv, Bulgaria, [2]Department of Pathology, University of Michigan Medical School, Ann Arbor, MI, United States, [3]ECONCARE LP, Athens, Greece

KEYWORDS

neurodegeneration, neurodegenerative diseases, genetic inheritance, Alzheimer's disease, Parkinson's disease, dementia, single nucleotide (nt) polymorphism (SNP), ischemic stroke

Editorial on the Research Topic
The UN international day of families: neurodegeneration as a result of genetic inheritance

Neurodegenerative diseases (NDs) represent a group of heterogeneous conditions affecting the motor and cognitive functions of patients. Alzheimer's (AD) and Parkinson's disease (PD) for example may be categorized as distinct NDs, however common overlapping traits occur, such as neuronal loss and accumulation of aggregated or misfolded proteins (Ruffini et al., 2020). Moreover, common malfunctions in cellular homeostasis processes take place resulting in impaired protein dynamics (Jellinger, 2010). Therefore, identifying and delineating the contribution of genetic inheritance in the malfunction of these processes could improve the prognosis and the therapeutic management of these patients. In this Research Topic we aimed to collect articles that discuss new research findings over the genetic inheritance in NDs.

Gao et al. explored the importance of presenilin-1 (PSEN1) in the regulation of amyloid β-protein 1-42 (Aβ42) accumulation related to familial AD. The authors examined the efficacy of angiotensin-converting enzyme (ACE), responsible for the conversion of neurotoxic Aβ42 to neuroprotective Aβ40, using experimental models containing wild-type (WT) and *PSEN1*-deficient fibroblasts. Altered glycosylation was observed in ACE purified from *PSEN1*-deficient fibroblasts while the Aβ42-to-Aβ40 conversion rate was reduced compared to WT counterparts. The reduced conversion ability of ACE was further found to be age-dependent, since adult brains demonstrated lower conversion capability. These results highlight the crucial contribution of PSEN1 in keeping low the levels of neurotoxic Aβ42 rendering it as an important target for AD therapeutic strategies.

One of the greatest genetic factors for AD and related dementias (ADRDs) is the $APOE^{\varepsilon 4}$allele (Zhao et al., 2020). Foley et al., aimed to delineate its contribution employing a new set of humanized *APOE* mouse models. The authors aimed to point out the unique effects of the heterozygote phenotype ($APOE^{\varepsilon 3/\varepsilon 4}$) in the pathogenetic mechanisms observed in ADRDs. Differential contributions of the two main genotypes ($APOE^{\varepsilon 3/\varepsilon 4}$ and $APOE^{\varepsilon 4/\varepsilon 4}$) on cortical gene expression were observed. These results highlight the importance of the *APOEε4* allele dosage-specific effects in the selection of the optimal therapy for clinical routine in patients suffering from AD-related dementia.

The phospholipid-transporting ATP binding cassette subfamily A member 7 (ABCA7) gene has been shown to have strong associations with AD (Stepler et al., 2022). In a case control study conducted by Wang L. et al. the association of a set of single nucleotide polymorphisms (SNPs) with AD was explored particularly for patients from southern China. The study detected 21 selected SNPs using molecular techniques. The ABCA7 rs3764650 SNP was positively correlated with AD morbidity. However, another ABCA7 SNP, rs4147929, was related to higher AD risk. These results suggest the involvement of *ABCA7* SNPs in AD and highlight the requirement for studies with larger patient cohorts.

Bartoletti-Stella et al. aimed to further identify pathogenic variants in genes as predictive risk factors for early-onset AD (EOAD). Using Next-Generation Sequencing (NGS) the authors assessed a panel of causal and risk factor genes for AD and dementia in Italian patients. Almost 11% of patients carried pathogenic or likely pathogenic variants in *PSEN1, PSEN2,* and *APP* while almost 8% of patients were homozygous for the ε4 *APOE* allele. Additionally, a significant fraction of patients carried only a variant in genes associated with other NDs. Therefore, genetic screening in EOAD patients could assist in their prognosis unraveling the pathogenic mechanisms that take place in AD and other forms of dementia.

In a last study for AD and related diseases, Liu et al. re-analyzed clinical data from literature from familial AD patients aiming to identify correlations between likely pathogenic amyloid precursor protein (APP) mutations, a major pathogenic gene for AD (Hinz and Geschwind, 2017), and phenotypical traits. Common clinical features such as amnesia, impairment in cognitive function and behavioral and psychological disorders were consistent with typical AD. The authors further reported different clinical manifestations depending on whether patients carried *APP* or *PSEN1/PSEN2* mutations thus potentially contributing to earlier clinical prognosis.

Loss-of-function mutations in *RAB39B* gene, a GTPase involved in intracellular vesicle trafficking (Cheng et al., 2002), are associated with early-onset Parkinson's disease (EOPD). Characteristic features of PD pathology, such as substantial loss of dopaminergic neurons in the substantia nigra and widespread Lewy body pathology were associated with Rab39b knockdown (Wilson et al., 2014). Wang Z. et al. aimed to further elucidate the role of RAB39B in PD pathogenesis. A typical PD model was induced by 1-methyl-4-phenyl-1,2,3,6-tetrahydropyridine (MPTP) to Rab39b knock-out (KO) mice**.** Both WT and Rab39b KO mice showed the same impairment in their motor activity and the same loss of dopaminergic neurons suggesting that RAB39B deficiency has no additive contribution to PD-like pathogenesis.

Aquaporin-4 (AQP4) plays a central role in the glymphatic system facilitating macromolecules draining to the interstitial fluid contributing to waste clearance in the brain (Mestre et al., 2018). Among the waste removed by AQP4, α-synuclein and Aβ are included, thus linking its function with PD (Zou et al., 2019) and AD (Iliff et al., 2012) pathologies. Fang et al. studied the association of AQP4 SNPs with motor and cognitive function in PD patients as well as the levels of neurotoxic species in the CSF. The AQP4 rs162009 SNP was associated with slower dementia conversion and better cognitive functions, lower Aβ deposition in different brain regions, while higher CSF levels of Aβ42 were observed in the subgroup of patients with REM sleep behavior disorder (RBD). The latter supports the notion that PD patients with sleep disorders demonstrate concomitant disruption of the glymphatic system (Bohnen and Hu, 2019). These results render the rs162009 SNP as an effective genetic prognostic marker for cognitive decline in PD patients potentially due to a malfunction in brain waste clearance system facilitated by sleep disruptions.

Rossi et al. aimed to identify the associated genetic variants of the semantic and right temporal variants of frontotemporal dementia (svFTD and rtvFTD). Twelve pathogenic or likely pathogenic variants were found in almost 40% of patients. These mutations were localized in genes implicated in processes such as autophagy. More importantly, these mutations may overlap with other neurodegenerative conditions such as AD and amyotrophic lateral sclerosis (ALS) indicating common pathogenetic mechanisms.

Thrombospondin-1 (THBS1) plasma levels have been shown to be elevated in ischemic stroke (IS) patients (Gao et al., 2015). Chen et al. evaluated the association of *THBS1* SNPs and the mRNA expression of THBS1 with the risk as well as the long-term outcome of IS. The authors reported no significant contribution of genotype and haplotype frequencies of rs2236741 and rs3743125. Risk of IS incidence or long-term death was not associated with any of the THBS1 variants. No further association was reported for *THBS1* mRNA expression levels as well, questioning the importance of THBS-1 in IS outcomes.

We believe that the present Research Topic articles highlights the important contribution of genetic inheritance in the pathogenetic malfunctions observed in NDs providing novel insights that need further research.

Author contributions

IHP: Writing—review and editing. DA: Writing—review and editing. SR: Writing—original draft, Writing-review and editing.

Acknowledgments

The authors would like to thank the rest of the Research Topic Dr. Lucio Tremolizzo and Dr. Prabhjyot Saini for their assistance in the organization of this effort.

Conflict of interest

SR is employed by ECONCARE LP, Athens, Greece.

The remaining authors declare that the research was conducted in the absence of any commercial or financial relationships that could be construed as a potential conflict of interest.

Publisher's note

the editors and the reviewers. Any product that may be evaluated in this article, or claim that may be made by its manufacturer, is not guaranteed or endorsed by the publisher.

References

Bohnen, N. I., and Hu, M. T. M. (2019). Sleep disturbance as potential risk and progression factor for Parkinson's Disease. *J. Parkinsons. Dis.* 9, 603–614. doi: 10.3233/JPD-191627

Cheng, H., Ma, Y., Ni, X., Jiang, M., Guo, L., Ying, K., et al. (2002). Isolation and characterization of a human novel RAB (RAB39B) gene. *Cytogenet. Genome Res.* 97, 72–75. doi: 10.1159/000064047

Gao, J. B., Tang, W. D., Wang, H. X., and Xu, Y. (2015). Predictive value of thrombospondin-1 for outcomes in patients with acute ischemic stroke. *Clin. Chim. Acta* 450, 176–180. doi: 10.1016/j.cca.2015.08.014

Hinz, F. I., and Geschwind, D. H. (2017). Molecular genetics of neurodegenerative dementias. *Cold Spring Harb. Perspect Biol.* 9, a023705. doi: 10.1101/cshperspect.a023705

Iliff, J. J., Wang, M., Liao, Y., Plogg, B. A., Peng, W., Gundersen, G. A., et al. (2012). A paravascular pathway facilitates CSF flow through the brain parenchyma and the clearance of interstitial solutes, including amyloid β. *Sci. Transl. Med.* 4, 111. doi: 10.1126/scitranslmed.3003748

Jellinger, K. A. (2010). Basic mechanisms of neurodegeneration: a critical update. *J. Cell Mol. Med.* 14, 457–487. doi: 10.1111/j.1582-4934.2010.01010.x

Mestre, H., Hablitz, L. M., Xavier, A. L., Feng, W., Zou, W., Pu, T., et al. (2018). Aquaporin-4-dependent glymphatic solute transport in the rodent brain. *Elife* 7, e40070. doi: 10.7554/eLife.40070.022

Ruffini, N., Klingenberg, S., Schweiger, S., and Gerber, S. (2020). Common factors in neurodegeneration: a meta-study revealing shared patterns on a multi-omics scale. *Cells* 9, 2642. doi: 10.3390/cells9122642

Stepler, K. E., Gillyard, T. R., Reed, C. B., Avery, T. M., Davis, J. S., Robinson, R. A. S., et al. (2022). ABCA7, a genetic risk factor associated with Alzheimer's disease risk in African Americans. *J. Alzheimers Dis.* 86, 5–19. doi: 10.3233/JAD-215306

Wilson, G. R., Sim, J. C. H., McLean, C., Giannandrea, M., Galea, C. A., Riseley, J. R., et al. (2014). Mutations in RAB39B cause X-linked intellectual disability and early-onset Parkinson disease with α-synuclein pathology. *Am. J. Hum. Genet.* 95, 729–735. doi: 10.1016/j.ajhg.2014.10.015

Zhao, N., Ren, Y., Yamazaki, Y., Qiao, W., Li, F., Felton, L. M., et al. (2020). Alzheimer's risk factors age, APOE genotype, and sex drive distinct molecular pathways. *Neuron* 106, 727–742. doi: 10.1016/j.neuron.2020.02.034

Zou, W., Pu, T., Feng, W., Lu, M., Zheng, Y., Du, R., et al. (2019). Blocking meningeal lymphatic drainage aggravates Parkinson's disease-like pathology in mice overexpressing mutated α-synuclein. *Transl. Neurodegener.* 8, 7. doi: 10.1186/s40035-019-0147-y

frontiers in Aging Neuroscience

ORIGINAL RESEARCH
published: 09 March 2022
doi: 10.3389/fnagi.2021.740491

Aquaporin-4 Polymorphisms Are Associated With Cognitive Performance in Parkinson's Disease

Yi Fang[1†], Shaobing Dai[2†], Chongyao Jin[1], Xiaoli Si[1], Luyan Gu[1], Zhe Song[1], Ting Gao[1], Ying Chen[1], Yaping Yan[1], Xinzhen Yin[1], Jiali Pu[1] and Baorong Zhang[1]**

[1]*Department of Neurology, Second Affiliated Hospital, School of Medicine, Zhejiang University, Hangzhou, China,*
[2]*Department of Anesthesiology, Women's Hospital, School of Medicine, Zhejiang University, Hangzhou, China*

Objective: Aquaporin-4 (AQP4) facilitates a sleep-enhanced interstitial brain waste clearance system. This study was conducted to determine the clinical implication of *AQP4* polymorphisms in Parkinson's disease (PD).

Methods: Three-hundred and eighty-two patients with PD and 180 healthy controls with a mean follow-up time of 66.1 months from the Parkinson's Progression Marker Initiative study were analyzed. We examined whether *AQP4* SNPs were associated with an altered rate of motor or cognitive decline using linear mixed model and Cox regression. We then investigated whether *AQP4* SNPs were associated with Aβ burden as measured by ^{18}F Florbetapir standard uptake values. Furthermore, we examined if *AQP4* SNPs moderated the association between REM sleep behavior disorder (RBD) and CSF biomarkers.

Results: In patients with PD, *AQP4* rs162009 (AA/AG vs. GG) was associated with slower dementia conversion, better performance in letter-number sequencing and symbol digit modalities, lower Aβ deposition in the putamen, anterior cingulum, and frontotemporal areas. In the subgroup of high RBD screening questionnaire score, rs162009 AA/AG had a higher CSF Aβ42 level. rs162009 AA/AG also had better performance in semantic fluency in healthy controls. Besides, rs68006382 (GG/GA vs. AA) was associated with faster progression to mild cognitive impairment, worse performance in letter-number sequencing, semantic fluency, and symbol digit modalities in patients with PD.

Interpretation: Genetic variations of *AQP4* and subsequent alterations of glymphatic efficacy might contribute to an altered rate of cognitive decline in PD. *AQP4* rs162009 is likely a novel genetic prognostic marker of glymphatic function and cognitive decline in PD.

Keywords: Parkinson's disease, cognitive dysfunction, aquaporin-4, amyloid plaque, REM sleep behavior disorder

OPEN ACCESS

Edited by:
Dennis Qing Wang, Southern Medical University, China

Reviewed by:
Julien Rossignol, Central Michigan University, United States
Sharad Purohit, Augusta University, United States
Rongfang Que, Southern Medical University, China

****Correspondence:***
Baorong Zhang
brzhang@zju.edu.cn
Jiali Pu
jialipu@zju.edu.cn

[†]These authors have contributed equally to this work and share first authorship

Specialty section:
This article was submitted to Parkinson's disease and aging-related movement disorders, a section of the journal Frontiers in Aging Neuroscience

Received: *13 July 2021*
Accepted: *04 October 2021*
Published: *09 March 2022*

Citation:
Fang Y, Dai S, Jin C, Si X, Gu L, Song Z, Gao T, Chen Y, Yan Y, Yin X, Pu J and Zhang B (2022) Aquaporin-4 Polymorphisms Are Associated With Cognitive Performance in Parkinson's Disease. Front. Aging Neurosci. 13:740491. doi: 10.3389/fnagi.2021.740491

INTRODUCTION

Aquaporin-4 (AQP4) is a water channel that lies at the astrocytic endfeet around perivascular space in the brain (Nagelhus and Ottersen, 2013). AQP4 plays a central role in the glymphatic system, which facilitates exchange between cerebrospinal fluid (CSF) and interstitial fluid, and drains macromolecules from the brain to the periphery (Mestre et al., 2018). Strikingly, the AQP4-facilitated glymphatic system clears interstitial brain waste,

including amyloid β (Aβ; Iliff et al., 2012), tau (Harrison et al., 2020), and α-synuclein (Zou et al., 2019) according to animal studies. The association between AQP4 and interstitial waste clearance was further validated by a postmortem study of aging human brains, which revealed a link between reduced perivascular localization of AQP4 and Aβ deposition (Zeppenfeld et al., 2017). In addition, Single Nucleotide Polymorphisms (SNPs) of the *AQP4* gene were associated with brain Aβ uptake on PET and the rate of cognitive decline in the spectrum of Alzheimer's disease (AD; Burfeind et al., 2017; Chandra et al., 2020).

Parkinson's disease (PD) is pathologically characterized by intraneuronal α-synuclein accumulation (Jakes et al., 1994), although extracellular α-synuclein is present and might contribute to the seeding of the disease (Lee et al., 2014). In addition, AD pathologies, including extracellular amyloid and tau aggregates, are also found in PD (Robinson et al., 2018). Amyloid deposition as measured by PET was positive in 34% of patients with PD dementia and 5% of patients with PD-mild cognitive impairment (MCI; Petrou et al., 2015). Furthermore, even subthreshold amyloid might contribute to cognitive decline in PD. In patients with PD, lower baseline CSF Aβ42 is associated with a faster rate of cognitive decline (Compta et al., 2013; Alves et al., 2014; Bäckström et al., 2015), worse performance in executive function (Compta et al., 2009; Stav et al., 2015), and delayed memory recall (Hall et al., 2015). Therefore, it is likely that clearing efficacy of synuclein and AD co-pathology are associated with an altered rate of motor or cognitive progression in PD.

Glymphatic fluid transport is known to be sleep-enhanced (Xie et al., 2013) and regulated by circadian rhythms (Hablitz et al., 2020). Disrupted sleep is a potential mechanism accounting for glymphatic dysfunction in PD. REM sleep behavior disorder (RBD) is one of the most characteristic sleep disorders in PD (Xie et al., 2019). Concomitant RBD in patients with PD is associated with faster motor progression, and worse cognitive function (Pagano et al., 2018; Zhang et al., 2020). These patients exhibit elevated synuclein deposition across the brain according to a postmortem study (Postuma et al., 2015). Interestingly, they are also inclined to have lower CSF Aβ42 and higher total tau/Aβ42 levels (Pagano et al., 2018). The elevated synuclein and amyloid burden are potentially attributable to the reduced efficacy of the AQP4-facilitated glymphatic system as a result of sleep disturbance (Bohnen and Hu, 2019).

In this study, using longitudinal data from the Parkinson's Progression Marker Initiative (PPMI), we tested the hypothesis that *AQP4* SNPs were associated with altered CSF or PET biomarker values and rate of motor or cognitive decline in PD. We also studied if *AQP4* SNPs modulate the association between RBD and CSF biomarkers.

MATERIALS AND METHODS

Study Participants

Major inclusion criteria for the PD cohort in the PPMI were as follows: (1) drug naïve; (2) diagnosed with PD within the past 2 years; (3) Hoehn and Yahr stage 1 or 2 at baseline; (4) age 30 years or older; and (5) striatal dopaminergic dysfunction on SPECT.

TABLE 1 | Demographic information and clinical characteristics of patients and healthy controls.

	Patients	Healthy controls
Age, y	61.83 ± 9.50	61.42 ± 10.63
Sex, male, n (%)	252 (66.0%)	117 (65.0%)
Years of education	15.56 ± 2.93	16.18 ± 2.91
*APOE*ε4 carriage	0.28 ± 0.50	0.28 ± 0.51
Baseline MDS-UPDRS I	5.43 ± 4.14	2.84 ± 2.80
Baseline MDS-UPDRS II	5.99 ± 4.24	0.40 ± 0.95
Baseline MDS-UPDRS III	20.96 ± 8.92	1.71 ± 2.16
Baseline MoCA	27.24 ± 0.11	28.23 ± 1.11
Baseline BJLOT	12.14 ± 2.92	12.50 ± 2.75
Baseline HVLT-total recall	45.84 ± 10.61	49.72 ± 9.78
Baseline LNS	11.59 ± 2.63	11.78 ± 2.76
Baseline SFT-T score	51.19 ± 9.86	52.71 ± 10.27
Baseline SDMT-T score	45.00 ± 9.07	50.68 ± 10.10
Baseline ESS	5.80 ± 3.47	5.63 ± 3.36
Baseline RBDSQ	4.53 ± 2.87	2.78 ± 2.29

MDS-UPDRS, Movement Disorder Society-sponsored revision of the Unified Parkinson's Disease Rating Scale; MoCA, Montreal Cognitive Assessment; BJLOT, Benton Judgment of line orientation test; HVLT, Hopkins verbal learning test; LNS, Letter-number sequencing; SFT, Semantic fluency test; SDMT, Symbol digit modalities; ESS, Epworth Sleepiness scale; RBDSQ, REM sleep behavior disorder screening questionnaire.

To exclude the potential confounding effect of race and ethnicity, non-Hispanic Caucasian patients and healthy controls (HC) were included in our analysis. Causes of exclusion include: (1) no CSF biomarker study result; and (2) no whole-genome sequencing data. Overall, 382 patients and 180 HCs were included, their demographic information and clinical characteristics are presented in **Table 1**.

Standard Protocol Approvals, Registrations, and Patient Consents

The study was approved by the institutional review board at each PPMI site. All patients signed an informed consent form before their participation in the PPMI study.

Clinical Assessment

Cognitive function was evaluated on a yearly basis. Cognitive tests included the Montreal Cognitive Assessment for global cognition, the Hopkins Verbal Learning Test (HVLT) for memory, the Benton Judgment of Line Orientation Test (BJLOT) for visuospatial perception, the Semantic Fluency Test (SFT) for executive function, the Letter-Number Sequencing (LNS) and the Symbol Digit Modality Test (SDMT) for working memory and attention-processing speed. Cognitive categorization of normal, MCI, and dementia was performed by investigators at each site in accordance with MDS criteria (Emre et al., 2007; Litvan et al., 2012).

Motor symptoms were evaluated at baseline, 3, 6, 9, 12, 18, 24, 30, 36, 42, 48, 54, 60, 72, 84, 96, and 108 months. We analyzed Hoehn and Yahr stage that was rated during the off condition (levodopa/dopaminergic agonist withheld for at least 6 h prior to the visit).

RBD was evaluated with an RBD screening questionnaire (RBDSQ). The optimal cutoff value for probable RBD in PD is 6 (Stiasny-Kolster et al., 2007; Nomura et al., 2011). RBD

symptoms are time-varying. To study if *AQP4* modulates the association between RBD and CSF biomarker, we stratified patients into subgroups by their averaged RBDSQ score in the first 3 years, as CSF samples were collected from baseline to the 3rd year. Overall, there are four expected visits for RBDSQ evaluation during this time frame (baseline, 1st, 2nd, and 3rd-year). Patients who were absent for two or more of these scheduled visits were excluded due to insufficient available data to characterize RBD symptoms within this time frame ($N = 40$). Then we stratified patients into a high RBDSQ group if averaged 3-year RBDSQ lies in the top one-third (RBDSQ ≥ 5.5, $N = 117$), and a low RBDSQ group if averaged 3-year RBDSQ lies in the least one-third (RBDSQ ≤ 3, $N = 113$).

Genotyping and SNP Pruning

Whole-genome sequencing data were downloaded from the PPMI database. SNP pruning was undertaken using PLINK (Purcell et al., 2007). Genetic variants of *AQP4* underwent quality control procedures. Specifically, SNPs that were not in Hardy-Weinberg equilibrium ($p < 0.05$), had a minor allele frequency of <5% were removed. Linkage disequilibrium-based SNP pruning was performed to reduce statistical redundancy and maintain coverage of the *AQP4* gene. SNP pruning parameters were as follows: window size 10, increment 5, and variance inflation factor 2. Two SNP pairs left after pruning were in high linkage disequilibrium (rs1058427 and rs12968026: $r^2 = 0.96$; rs335930 and rs455671: $r^2 = 0.86$). Therefore, rs12968026 and rs455671 were removed from further statistical analysis, leaving 11 SNPs. The information of these SNPs was displayed in **Table 2**, **Figure 1**, and **Supplementary Figure 1**.

A dominant model was used for all *AQP4* SNPs.

Aβ Retention by PET

Overall, 36 patients who met the inclusion criteria of the current study underwent a Florbetaben (FBB) PET imaging for *in vivo* imaging of Aβ plaques. We analyzed standard uptake values (SUVs) downloaded from the PPMI dataset. SUV ratios (SUVRs) were calculated using the cerebellar cortex as reference.

Measurement of CSF Biomarkers

CSF was collected at baseline, 6, 12, 24, and 36 months. Levels of CSF Aβ42, total tau (*t*-tau), and phosphorylated tau (*p*-tau) at threonine 181 position were measured using Elecsys electrochemiluminescence immunoassays on the cobas e 601 analysis platform. CSF α-synuclein concentrations were analyzed using commercially available enzyme-linked immunosorbent assay kits. These values were downloaded from the PPMI database.

Statistical Analysis

Clinical and biomarker data were downloaded from the PPMI database in December 2020. Statistical analysis was performed using SPSS (IBM Corp, Armonk NY, USA). Graphs were plotted using GraphPad (San Diego, CA, USA).

For longitudinal cognitive test score analysis, mixed models with random slope and intercept and unstructured covariance were used. Fixed effects include age at baseline, sex, baseline MoCA score, years of education, Apolipoprotein-E (*APOE*) ε4 carriage, and *AQP4* SNP of interest. The *AQP4* SNP by time interaction effect was also included as a fixed effect in separate models. Time was treated as a continuous variable. The patient number was listed as a random effect.

Cox proportional hazards regressions were performed to study if *AQP4* polymorphisms were associated with the rate of motor and cognitive deterioration. We defined events separately as: (1) progression to MCI for the first time; (2) progression to dementia for the first time; and (3) progression of Hoehn and Yahr stage for the first time. Age, sex, *APOE* ε4 carriage, years of education, and baseline MoCA score were covaried for conversion to MCI or dementia. Age, sex, baseline MDS-UPDRS-III, and levodopa equivalent dose were covaried for motor progression. Kaplan-Meier curves were plotted, and log-rank test results were presented.

APOE ε4 (Mata et al., 2014), glucocerebrosidase (*GBA*) variants (Alcalay et al., 2012), and Catechol-O-methyltransferase (*COMT*) $Val^{158}Met$ (rs4680; Egan et al., 2001; Williams-Gray et al., 2009) are previously established genetic markers of cognition in PD. *COMT* rs4680 data was extracted from whole-genome sequencing data. *GBA* variant summary from across different sequencing platforms was directly downloaded. Their distribution on *AQP4* SNPs was tested using the Chi-Square test.

The association between *AQP4* SNPs and SUVRs was examined using linear regression. Covariates included age, sex, *APOE* ε4 carriage, and disease duration at the time of PET scan.

CSF biomarkers (α-synuclein, Aβ, *t*-tau, *p*-tau) did not follow a normal distribution and were, therefore, log10 transformed in the statistical analysis. To determine whether CSF biomarkers differed with respect to *AQP4* polymorphisms across time, linear mixed models with random intercept were used. Fixed effects included age at baseline, sex, time, and *AQP4* SNP of interest. For CSF Aβ42, *APOE* ε4 carriage was also covaried. To determine whether *AQP4* SNPs moderate the association between RBD and CSF biomarkers, the RBDSQ subgroup by *AQP4* SNP interaction effect was tested.

To correct for multiple comparisons, the Benjamini-Hochberg procedure with a false discovery rate at 0.10 was used given the exploratory nature of this study. $p < 0.05$ was used as the threshold for statistical significance.

RESULT

AQP4 SNPs and Conversion to MCI and Dementia

We did not observe a significant association between *AQP4* SNPs and motor progression as reflected by MDS-UPDRS-III score increment in mixed model and Hoehn and Yahr stage progression in Cox regression.

However, after adjusting for age, sex, *APOE* ε4 carriage, and baseline MoCA score, minor allele carrier status of rs68006382 was associated with accelerated conversion to MCI (HR = 1.973, 95% CI = 1.246–3.123, $p = 0.004$; **Figure 2A**), but not dementia (HR = 1.512, 95% CI = 0.753–3.034, $p = 0.245$). In addition, minor allele carrier status of rs162009 was associated with slower conversion to MCI (HR = 0.646, 95%

TABLE 2 | *AQP4* SNPs being investigated in the current study.

	Annotation	Position (GRCh38)	Minor allele frequency	Previously reported associations
rs7240333 C/T	3'-UTR	18:26852848	0.098	
rs1058427 G/T	3'-UTR	18:26855131	0.115	Risk of cerebral edema (Appelboom et al., 2015)
rs3763043 C/T	3'-UTR	18:26855854	0.318	Risk of intracerebral hemorrhage (Dardiotis et al., 2019) and schizophrenia (Wu et al., 2020)
rs68006382 A/G	intron	18:26856555	0.205	
rs335930 A/C	intron	18:26856961	0.228	
rs71353405 C/T	intron	18:26857429	0.061	
rs74163677 G/A	intron	18:26861697	0.055	
rs162009 G/A	M23 promoter	18:26864250	0.344	
rs3763040 G/A	M23 promoter	18:26864410	0.192	Rate of cognitive decline in AD (Burfeind et al., 2017)
rs4800773 G/A	M23 promoter	18:26865017	0.356	
rs3875089 T/C	M23 promoter	18:26865469	0.149	Rate of cognitive decline in AD (Burfeind et al., 2017)

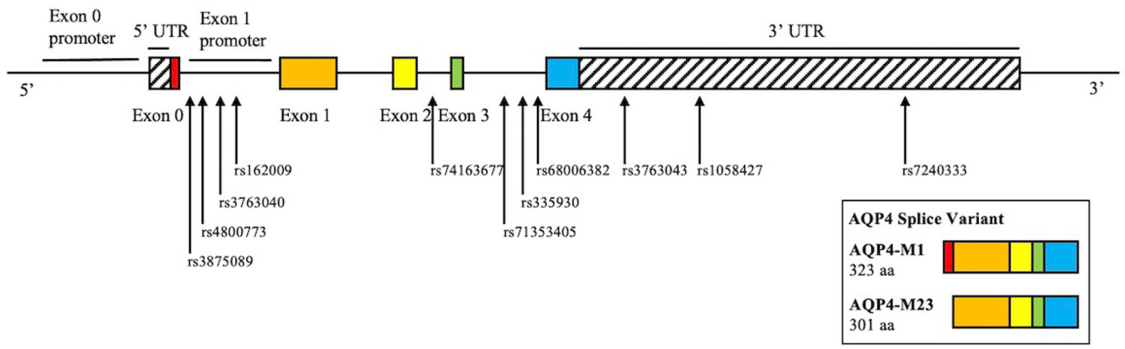

FIGURE 1 | Schematic illustration of the investigated SNPs in the *AQP4* gene. There are two isoforms of AQP4, M1, and M23. M1 consists of exon 0–4, M23 consists of exon 1–4. rs162009 locates in between exon 0 and 1, which presumably acts as the promoter of the M23 isoform.

CI = 0.409–1.019, p = 0.060), and dementia (HR = 0.473, 95% CI = 0.234–0.956, p = 0.037), although these effects were marginal (**Figures 3A,B**).

AQP4 SNPs and Performance in Cognitive Subdomains

The association between *AQP4* SNPs and cognitive subdomains is presented in **Table 3**.

Briefly, minor allele carrier status of rs68006382 was associated with worse performance in executive function, working memory, and attention (SFT: p = 0.001; LNS: p = 0.003; SDMT: p = 0.002; **Figures 2B–D**).

Minor allele carrier status of rs162009, on the other hand, was protective, with better performance in working memory and attention (LNS: p = 0.009; SDMT: p = 0.006; **Figures 3C,D**).

In addition, minor allele carrier status of rs3763043 and rs3763040 were associated with worse executive function (SFT: p = 0.003) and better visuospatial function (BJLOT: p = 0.007), respectively. Minor allele carrier of rs7240333 was associated with better memory (HVLT: p = 0.047), which was not significant after correction for multiple comparisons.

There was no significant SNP by time interaction effect in any of the tests. Notably, there was no significant main effect of time in HVLT (p = 0.457), LNS (p = 0.068), and SFT (p = 0.518), indicating the absence of decreasing scores in these subdomains over time. This was likely attributable to the high education level in the PPMI cohort, which amounts to an average of 15.56 years of education. Patients with a higher level of education are likely to have higher cognitive reserve and therefore slower cognitive decline in PD (Meng and D'Arcy, 2012; Hindle et al., 2014).

Association Between *AQP4* and *APOE* ε4, *COMT* Val^{158}Met, *GBA* Variants

Chi-Square test indicated that the distribution of *COMT* variants on rs3763043 minor allele carriers and non-carriers was statistically different (p = 0.027), indicating a potential confounding effect of *COMT* variants on the observed association between rs3763043 and SFT. The distribution of *APOE* ε4, *COMT* Val^{158}Met, *GBA* variants on other *AQP* SNPs minor allele carrier vs. non-carrier was not significant (**Supplementary Table 1**).

AQP4 SNPs and ^{18}F Florbetapir SUVR

Of the 36 patients who underwent ^{18}F Florbetapir imaging, six (16.7%) were amyloid positive, if a cut-off of 1.43 for composite SUVR was used (Bullich et al., 2017; Fiorenzato et al., 2018). The average disease duration at the time of PET imaging was 4.73 ± 1.71 years. There was no statistically significant association between SNPs and composite SUVRs, although rs162009 was marginally associated lower composite SUVRs (β = −0.076, SE = 0.044, p = 0.094).

Given the observed association between minor allele carriers of rs162009 and more preserved cognitive performance,

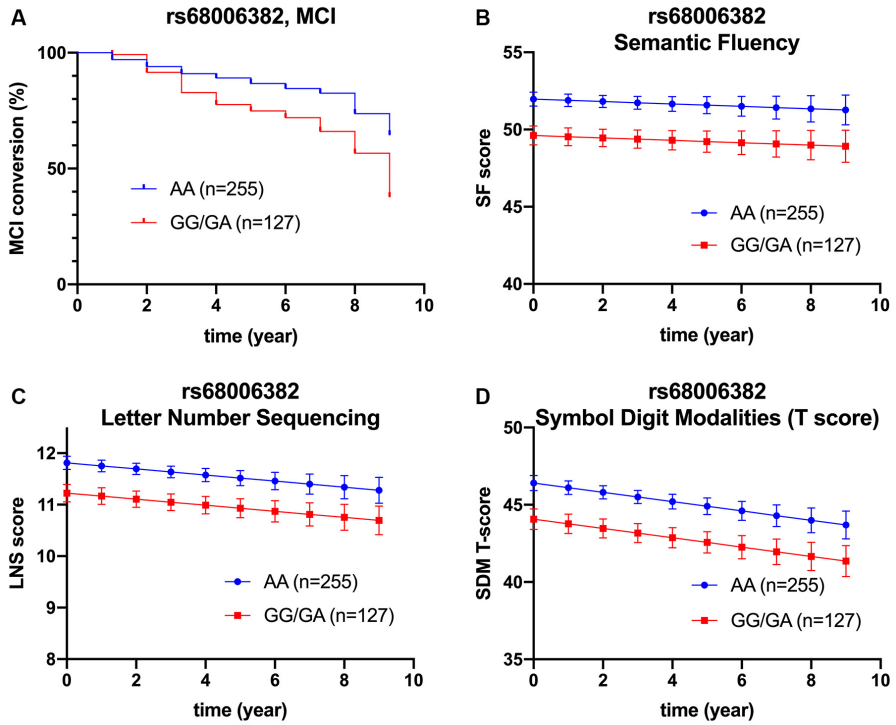

FIGURE 2 | Association between rs68006382 and cognition. rs68006382 (GG/GA vs. AA) had faster conversion to MCI (HR = 1.973, 95% CI = 1.246–3.123, p = 0.004) **(A)**. rs68006382 GG/GA genotype also had worse performance in semantic fluency test (β = −2.357, SE = 0.691, p = 0.001) **(B)**, letter-number sequencing (β = −0.587, SE = 0.193, p = 0.003) **(C)**, and symbol digit modalities test (β = −2.339, SE = 0.193, p = 0.002) **(D)**. Covariates for cox regression and linear mixed model included age, sex, *APOE* ε4 carriage, years of education, and baseline MoCA score. Lines in Panels **(B–D)** represent the estimated marginal mean from the mixed model. MCI, mild cognitive impairment.

we explored its association with SUVRs in cortical and subcortical regions of interest (**Table 4**). There were decreased SUVRs in putamen (p = 0.012) and anterior cingulum (p = 0.048) even with a limited sample size (n = 36; **Figure 3E**). In addition, minor allele carriers of rs162009 were marginally associated with lower amyloid burden in the temporal (p = 0.070) and frontal (p = 0.072) cortex.

The Interaction Between *AQP4* SNPs, Sleep Disturbance, and CSF Biomarkers

There was no significant association between *AQP4* SNPs and CSF biomarkers in the whole cohort. Then we examined the association between RBD and CSF biomarkers. Our analysis concords with a previous study that RBD is associated with lower CSF Aβ42 using the same PPMI database (Pagano et al., 2018). There was no such association between RBD and α-synuclein or tau. Given the proposed role of *AQP4* in solute drainage during sleep, we examined if *AQP4* SNPs modulate this association. After controlling for *APOE* ε4 carriage, age, sex and time, minor allele of rs162009 was associated with higher CSF Aβ42 level in the high RBDSQ subgroup (β = 0.081, SE = 0.033, p = 0.017), but not in the low RBDSQ subgroup (subgroup by SNP interaction effect: β = −0.056, SE = 0.023, p = 0.014; **Figure 3F**).

AQP4 SNPs and Cognitive Performance in Healthy Controls

The association between *AQP4* SNP and cognitive scales was demonstrated in **Table 5**. Notably, minor allele carrier status of rs162009 was associated with higher semantic fluency test performance (β = 2.209, SE = 0.913, p = 0.016), validating the association between rs162009 and cognitive performance observed in patients with PD.

In addition, multiple *AQP4* SNPs (rs3763043, rs68006382, and rs74163677) were associated with HVLT performance. However, these associations were likely attributable to the fact that AQP4 plays a role in synaptic plasticity and therefore learning and memory (Hubbard et al., 2018; Woo et al., 2018).

During follow-up, 6/180 (3.33%) and 1/180 (0.56%) HCs developed MCI and dementia, respectively. Therefore, we did not perform Cox regressions in HCs.

Besides, there was no significant distribution difference of *AQP4* SNPs in PD and HCs.

DISCUSSION

Given the previously established association between *AQP4* and cognitive performance in the spectrum of AD, we explored this association in a cohort of patients with PD. We found that

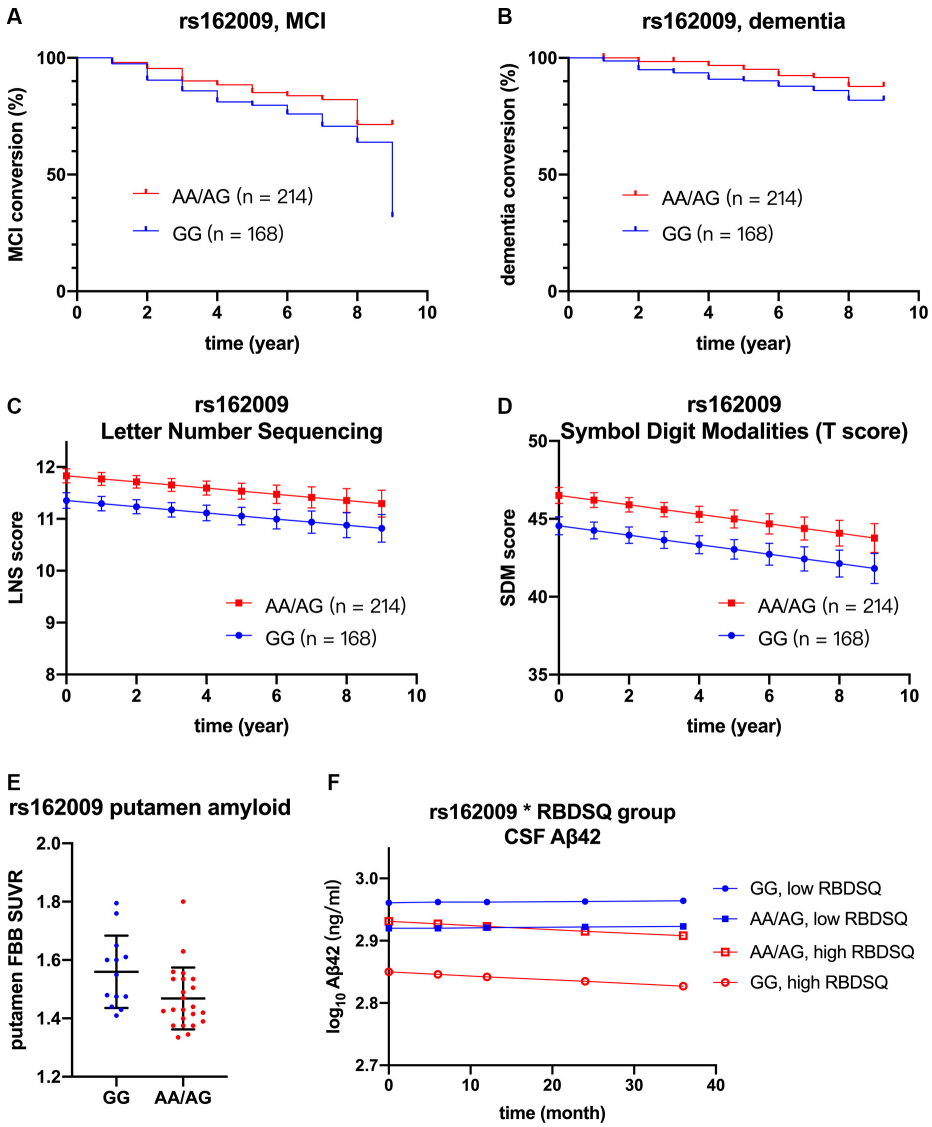

FIGURE 3 | Association between rs162009, cognition, and biomarkers. rs162009 (AA/AG vs. GG) had slower conversion to MCI (HR = 0.646, 95% CI = 0.409–1.019, $p = 0.060$) **(A)** and dementia (HR = 0.473, 95% CI = 0.234–0.957, $p = 0.037$) **(B)**, better performance in letter-number sequencing (β = 0.477, SE = 0.183, $p = 0.009$) **(C)**, and symbol digit modalities test (β = 2.401, SE = 1.953, $p = 0.006$) **(D)**. rs162009 AA/AG genotype also had lower putamen FBB SUVRs (β = −0.105, SE = 0.039, $p = 0.012$) **(E)**. In the subgroup of patients with high RBDSQ score (averaged score during the first 3 year ≥ 5.5, $N = 117$), patients with rs162009 AA/AG genotype had higher CSF Aβ42 levels (β = 0.081, SE = 0.033, $p = 0.017$), indicating its protective effect on Aβ deposition **(F)**. Covariates for cox regression and linear mixed model included age, sex, *APOE* ε4 carriage, years of education, and baseline MoCA score. Lines in Panels **(C,D,F)** represent the estimated marginal mean from the mixed model. FBB, ^{18}F Florbetaben; MCI, mild cognitive impairment; RBDSQ, Rapid Eye Movement Sleep Behavior Disorder Screening Questionnaire; SUVRs, standard uptake value ratios.

rs162009 was associated with slower dementia conversion, better performance in LNS and SDMT, and lower amyloid burden in the putamen and anterior cingulum. This variant was also associated with higher CSF Aβ in the subgroup with a high RBDSQ score. Besides, rs68006382 was associated with faster MCI conversion and worse performance in LNS, SFT, and SDMT.

The implication of rs162009 AA/AG genotype was more compelling as this variant was associated with both better cognitive performance and lower amyloid deposition in multiple regions. In addition, its protective effect on cognition was also seen in HCs. One of the potential mechanisms to back up these clinical findings is that rs162009 likely increases the transcription of AQP4-M23 isoform and improves the glymphatic fluid circulation. There are two AQP4 splice variants, the M1 and M23. The M1 variant tends to be evenly distributed across the astrocytic membrane, while the M23 variant primarily locates at the astrocytic endfeet (Smith et al., 2014). rs162009 locates between exon 0 and exon 1 of the *AQP4* gene (**Figure 1**), and putatively acts

TABLE 3 | *AQP4* SNPs and cognition in patients with PD.

	Hazard ratio (95% CI)		Cognitive subdomains (β estimate)				
	MCI	Dementia	BJLOT	HVLT	LNS	SF	SDMT
rs7240333	0.677 (0.355, 1.293)	0.556 (0.194, 1.595)	0.213	1.626	0.308	0.171	0.367
rs1058427	0.668 (0.347, 1.285)	0.564 (0.195, 1.637)	0.038	0.035	0.280	0.457	0.950
rs3763043	1.435 (0.899, 2.292)	1.295 (0.643, 2.606)	−0.089	−0.161	−0.068	**−1.931**[a]	−0.981
rs68006382	**1.973 (1.246, 3.123)**	1.512 (0.753, 3.034)	−0.229	−1.162	**−0.587**[a]	**−2.357**[a]	**−2.339**[a]
rs335930	0.932 (0.584, 1.485)	0.748 (0.366, 1.530)	−0.178	−0.017	−0.009	−0.387	0.235
rs71353405	0.971 (0.417, 2.258)	0.737 (0.174, 3.120)	−0.063	−1.085	0.150	0.499	−0.243
rs74163677	0.737 (0.365, 1.489)	0.529 (0.160, 1.750)	0.056	0.154	−0.126	−0.964	−0.600
rs162009	0.646 (0.409, 1.019)	**0.473 (0.234, 0.957)**	−0.129	0.583	**0.477**[a]	1.108	**1.953**[a]
rs3763040	0.784 (0.481, 1.277)	0.735 (0.348, 1.553)	**0.465**[a]	1.146	0.333	0.768	0.950
rs4800773	0.896 (0.560, 1.431)	1.034 (0.506, 2.112)	0.141	0.183	0.276	−0.388	−0.486
rs3875089	0.858 (0.490, 1.503)	1.001 (0.440, 2.279)	−0.026	−0.366	0.061	−0.537	0.049

[a]*Significant after correction of multiple comparisons. Covariates include age, sex, APOE ε4 carriage, years of education, and baseline MoCA score. BJLOT, Benton Judgment of line orientation test; HVLT, Hopkins verbal learning test (total recall); LNS, Letter-number sequencing; SFT, Semantic fluency test; SDMT, Symbol digit modalities test. Bold values are statistically significant.*

TABLE 4 | Association between rs162009 and ^{18}F Florbetapir SUVRs.

Regions of interest	β	SE	*p*	Adjusted r^2
putamen	−0.105	0.039	**0.012**	0.159
Anterior cingulum	−0.122	0.059	**0.048**	0.066
orbitofrontal	−0.084	0.042	0.056	0.077
Mesial temporal cortex	−0.065	0.034	0.068	0.046
Lateral temporal cortex	−0.067	0.036	0.070	0.082
Temporal cortex	−0.066	0.035	0.070	0.069
Frontal cortex	−0.084	0.045	0.072	0.102
Parietal cortex	−0.081	0.048	0.102	0.095
Rectus	−0.084	0.050	0.104	0.046
Occipital cortex	−0.062	0.041	0.139	0.018
Posterior cingulum	−0.078	0.066	0.245	−0.002
Thalamus	−0.040	0.052	0.449	−0.037
Caudate	−0.038	0.055	0.494	0.021
Pons	0.023	0.071	0.746	−0.132

FBB, ^{18}F Florbetaben; SUVRs, standard uptake value ratios. Bold values are statistically significant.

as a promoter for the AQP4-M23 splice variant, which potentially facilitates the the glymphatic fluid circulation (Iliff et al., 2012). However, this was primarily speculative, more mechanistic study is needed to explore the physiological effect of *AQP4* SNPs.

The current findings add weight to previous observations that even subthreshold amyloid contributes to cognitive decline in non-demented PD. Interestingly, we observed a link between rs162009 and decreased putamen amyloid deposition. Increased striatal amyloid deposition was a prominent feature in PD-dementia autopsy (Kalaitzakis et al., 2008; Hepp et al., 2016). PD patients with combined amyloid pathology in cortex and striatum were associated with worse cognition than those with cortical amyloid pathology alone (Shah et al., 2016). In line with AD, it has been proposed that amyloid deposits in the neocortex first and striatum later (Shah et al., 2016). Therefore, the association between rs162009 and putamen SUVR might correspond to the slowed dementia conversion. The lower amyloid burden in the anterior cingulum (Petersen and Posner, 2012) and frontotemporal area (Randolph et al., 1993; Forn et al., 2009) in rs162009 minor allele carriers might correspond to better attention and working memory performance in these patients. However, AQP4 might modulate cognition in PD through other mechanisms such as synaptic plasticity (Hubbard et al., 2018; Woo et al., 2018), and neuroimmunological regulation (Ikeshima-Kataoka, 2016; Tamtaji et al., 2019).

The association between rs162009 and CSF Aβ42 in the subgroup of high RBDSQ score provides a novel insight into

TABLE 5 | *AQP4* SNPs and cognition in healthy controls.

	BJLOT		HVLT		LNS		SF		SDMT	
	β	*p*	β	*p*	β	*p*	β	*p*	β	*p*
rs7240333	0.063	0.819	−0.451	0.676	−0.464	0.091	0.502	0.636	−0.961	0.379
rs1058427	0.046	0.872	−1.781	0.108	0.235	0.406	0.810	0.458	0.317	0.778
rs3763043	0.217	0.380	2.000	**0.038**	−0.025	0.921	−0.006	0.995	−0.135	0.891
rs68006382	0.150	0.543	2.954	**0.002**[a]	0.305	0.216	−0.119	0.900	−0.247	0.801
rs335930	0.178	0.473	−0.519	0.593	−0.093	0.708	0.903	0.345	−0.380	0.701
rs71353405	−0.278	0.441	−0.118	0.933	−0.320	0.377	0.578	0.678	1.231	0.391
rs74163677	0.702	0.122	−4.060	**0.022**	−0.510	0.262	−2.640	0.130	0.737	0.683
rs162009	0.241	0.315	0.087	0.926	0.162	0.499	2.209	**0.016**	0.895	0.348
rs3763040	−0.022	0.929	−0.847	0.379	−0.280	0.255	−0.269	0.777	−1.977	**0.042**
rs4800773	−0.003	0.991	−1.654	0.091	0.000	0.999	0.329	0.733	−1.382	0.164
rs3875089	0.152	0.556	−1.246	0.216	0.126	0.624	1.138	0.251	1.017	0.320

[a]*Significant after correction of multiple comparisons. BJLOT, Benton Judgment of line orientation test; HVLT, Hopkins verbal learning test (total recall); LNS, Letter-number sequencing; SFT, Semantic fluency test; SDMT, Symbol digit modalities test. Bold values are statistically significant.*

the interaction between RBD and AQP4-facilitated glymphatic clearance. Although glymphatic efficacy peaks during slow-wave sleep (Hablitz et al., 2019), changes in the EEG signature of non-REM sleep have been observed in patients with RBD (Sunwoo et al., 2020). Therefore, it is reasonable to assume that RBD reduces glymphatic capacity. In patients with high RBDSQ scores, disrupted sleep architecture likely reduced the clearing capacity of the glymphatic system, which is attributable to the *AQP4* polymorphisms. The absence of significant association in the low RBDSQ subgroup likely reflected a situation where the glymphatic capacity exceeds the clearing need due to intact sleep. This finding provides indirect evidence that amyloid deposition as a result of disrupted glymphatic clearance might contribute to cognitive decline in RBD. This finding also highlights the prospects of targeting amyloid with immunotherapy in a subgroup of patients with PD (for instance, RBD and non-carriers of rs162009 minor allele).

We did not observe a significant association between *AQP4* and motor progression or CSF α-synuclein. This was likely because α-synuclein was primarily intracellular, the need for interstitial clearance might be low when compared with extracellular Aβ. Although significant α-synuclein aggregation was reported in *Aqp4* knockout mice (Xue et al., 2019), single nucleotide polymorphisms in humans likely exert a much smaller effect than genetic knockout.

The major limitations of the current study are as follows: (1) Significant associations observed in the current study are likely to be false positive. More work in other cohorts is needed to verify the effect of *AQP4* SNPs on PD. (2) We observed a marginally significant effect of rs162009 on FBB SUVRs in a limited number of patients (n = 36). Future studies to validate the finding by expanding the patient sample size would be necessary. Besides, such a small number of patients who underwent FBB-PET would limit the statistical power to detect *AQP4* variants that are potentially associated with FBB SUV, especially for those SNPs that have low minor allele frequency. (3) Caution must be taken when interpreting the interaction effect between rs162009 and RBDSQ subgroup. It is also likely that abnormal neuronal activation as a result of sleep disturbance causes elevated production and release of Aβ (Ovsepian and O'Leary, 2016; Lucey, 2020). As Aβ measured by CSF or PET represents the balance of production and clearance, future studies to measure glymphatic activity *in vivo* would be necessary. (4) Measuring RBD symptoms with RBDSQ is prone to subjectivity (Halsband et al., 2018). More studies are warranted to validate and explore the effect of various types of sleep disturbance with objective sleep assessment equipment such as polysomnography and actigraphy.

CONCLUSIONS

Genetic variations of *AQP4* likely alter the glymphatic clearance of Aβ in the brain and subsequently the rate of cognitive decline in PD. *AQP4* rs162009 is likely a novel prognostic marker of cognitive decline in PD. Our findings also provide indirect evidence that in PD, AQP4-facilitated clearance of interstitial amyloid might be disrupted in patients with probable REM sleep behavior disorder.

DATA AVAILABILITY STATEMENT

Publicly available datasets were analyzed in this study. This data can be found here: https://www.ppmi-info.org/access-data-specimens/download-data.

ETHICS STATEMENT

Ethical approval was not provided for this study on human participants because this study obtained and analyzed data from the PPMI dataset. Ethical approval was obtained at each individual PPMI participating site. The patients/participants provided their written informed consent to participate in the PPMI study.

AUTHOR CONTRIBUTIONS

YF, JP, and BZ contributed to the conception and design of the study. YF, SD, and CJ performed the statistical analysis. YF and SD wrote the first draft of the manuscript. All authors contributed to the article and approved the submitted version.

FUNDING

This work was supported by the National Natural Science Foundation of China's Major Regional International Cooperation Project (No. 81520108010), the National Natural Science Foundation of China (No. 81771216), the Key Research and Development Program of Zhejiang Province (No. 2020C03020), and the Natural Science Foundation of Zhejiang Province (No. LY18H090003).

ACKNOWLEDGMENTS

For up-to-date information on Parkinson's Progression Markers Initiative visit www.ppmi-info.org. PPMI—a public-private partnership—is funded by the Michael J. Fox Foundation for Parkinson's Research funding partners Abbvie, Allergan, Amathus therapeutics, Avid Radiopharmaceuticals, Biogen, BioLegend, Bristol-Myers Squibb, Celgene, Denali, GE Healthcare, Genentech, GlaxoSmithKline, Handl Therapeutics, Insitro, Janssen Neuroscience, Lilly, Lundbeck, Merck, Meso Scale Discovery, Pfizer, Piramal, Prevail, Roche, Sanofi Genzyme, Servier, Takeda, Teva, UCB, Verily, Voyager Therapeutics, and Golub Capital. The full list of funding partners is found at www.ppmi-info.org/about-ppmi/who-we-are/study-sponsors.

SUPPLEMENTARY MATERIALS

The Supplementary Material for this article can be found online at: https://www.frontiersin.org/articles/10.3389/fnagi.2021.740491/full#supplementary-material.

REFERENCES

Alcalay, R. N., Caccappolo, E., Mejia-Santana, H., Tang, M.-X., Rosado, L., Orbe Reilly, M., et al. (2012). Cognitive performance of GBA mutation carriers with early-onset PD. *Neurology* 78, 1434–1440. doi: 10.1212/WNL.0b013e318253d54b

Alves, G., Lange, J., Blennow, K., Zetterberg, H., Andreasson, U., Forland, M. G., et al. (2014). CSF $A\beta_{42}$ predicts early-onset dementia in Parkinson disease. *Neurology* 82, 1784–1790. doi: 10.1212/WNL.0000000000000425

Appelboom, G., Bruce, S., Duren, A., Piazza, M., Monahan, A., Christophe, B., et al. (2015). Aquaporin-4 gene variant independently associated with oedema after intracerebral haemorrhage. *Neurol. Res.* 37, 657–661. doi: 10.1179/1743132815Y.0000000047

Bäckström, D. C., Eriksson Domellöf, M., Linder, J., Olsson, B., Öhrfelt, A., Trupp, M., et al. (2015). Cerebrospinal fluid patterns and the risk of future dementia in early, incident Parkinson disease. *JAMA Neurol.* 72, 1175–1182. doi: 10.1001/jamaneurol.2015.1449

Bohnen, N. I., and Hu, M. T. M. (2019). Sleep disturbance as potential risk and progression factor for Parkinson's disease. *J. Parkinsons Dis.* 9, 603–614. doi: 10.3233/JPD-191627

Bullich, S., Seibyl, J., Catafau, A. M., Jovalekic, A., Koglin, N., Barthel, H., et al. (2017). Optimized classification of 18F-Florbetaben PET scans as positive and negative using an SUVR quantitative approach and comparison to visual assessment. *Neuroimage Clin.* 15, 325–332. doi: 10.1016/j.nicl.2017.04.025

Burfeind, K. G., Murchison, C. F., Westaway, S. K., Simon, M. J., Erten-Lyons, D., Kaye, J. A., et al. (2017). The effects of noncoding aquaporin-4 single-nucleotide polymorphisms on cognition and functional progression of Alzheimer's disease. *Alzheimers Dement. (NY)* 3, 348–359. doi: 10.1016/j.trci.2017.05.001

Chandra, A., Farrell, C., Wilson, H., Dervenoulas, G., De Natale, E. R., and Politis, M. (2020). Aquaporin-4 polymorphisms predict amyloid burden and clinical outcome in the Alzheimer's disease spectrum. *Neurobiol. Aging* 97, 1–9. doi: 10.1016/j.neurobiolaging.2020.06.007

Compta, Y., Martí, M. J., Ibarretxe-Bilbao, N., Junqué, C., Valldeoriola, F., Muñoz, E., et al. (2009). Cerebrospinal tau, phospho-tau and beta-amyloid and neuropsychological functions in Parkinson's disease: CSF and neuropsychological markers in PD. *Mov. Disord.* 24, 2203–2210. doi: 10.1002/mds.22594

Compta, Y., Pereira, J. B., Ríos, J., Ibarretxe-Bilbao, N., Junqué, C., Bargalló, N., et al. (2013). Combined dementia-risk biomarkers in Parkinson's disease: a prospective longitudinal study. *Parkinsonism Relat. Disord.* 19, 717–724. doi: 10.1016/j.parkreldis.2013.03.009

Dardiotis, E., Siokas, V., Marogianni, C., Aloizou, A.-M., Sokratous, M., Paterakis, K., et al. (2019). AQP4 tag SNPs in patients with intracerebral hemorrhage in greek and polish population. *Neurosci. Lett.* 696, 156–161. doi: 10.1016/j.neulet.2018.12.025

Egan, M. F., Goldberg, T. E., Kolachana, B. S., Callicott, J. H., Mazzanti, C. M., Straub, R. E., et al. (2001). Effect of COMT Val108/158 Met genotype on frontal lobe function and risk for schizophrenia. *Proc. Natl. Acad. Sci. U S A* 98, 6917–6922. doi: 10.1073/pnas.111134598

Emre, M., Aarsland, D., Brown, R., Burn, D. J., Duyckaerts, C., Mizuno, Y., et al. (2007). Clinical diagnostic criteria for dementia associated with Parkinson's disease. *Mov. Disord.* 22, 1689–1707. doi: 10.1002/mds.21507

Fiorenzato, E., Biundo, R., Cecchin, D., Frigo, A. C., Kim, J., Weis, L., et al. (2018). Brain amyloid contribution to cognitive dysfunction in early-stage Parkinson's disease: the PPMI dataset. *J. Alzheimers Dis.* 66, 229–237. doi: 10.3233/JAD-180390

Forn, C., Belloch, V., Bustamante, J. C., Garbin, G., Parcet-Ibars, M. à., Sanjuan, A., et al. (2009). A symbol digit modalities test version suitable for functional MRI studies. *Neurosci. Lett.* 456, 11–14. doi: 10.1016/j.neulet.2009.03.081

Hablitz, L. M., Plá, V., Giannetto, M., Vinitsky, H. S., Stæger, F. F., Metcalfe, T., et al. (2020). Circadian control of brain glymphatic and lymphatic fluid flow. *Nat. Commun.* 11:4411. doi: 10.1038/s41467-020-18115-2

Hablitz, L. M., Vinitsky, H. S., Sun, Q., Stæger, F. F., Sigurdsson, B., Mortensen, K. N., et al. (2019). Increased glymphatic influx is correlated with high EEG delta power and low heart rate in mice under anesthesia. *Sci. Adv.* 5:eaav5447. doi: 10.1126/sciadv.aav5447

Hall, S., Surova, Y., Öhrfelt, A., Zetterberg, H., Lindqvist, D., and Hansson, O. (2015). CSF biomarkers and clinical progression of Parkinson disease. *Neurology* 84, 57–63. doi: 10.1212/WNL.0000000000001098

Halsband, C., Zapf, A., Sixel-Döring, F., Trenkwalder, C., and Mollenhauer, B. (2018). The REM sleep behavior disorder screening questionnaire is not valid in *de novo* Parkinson's disease. *Mov. Disord. Clin. Pract.* 5, 171–176. doi: 10.1002/mdc3.12591

Harrison, I. F., Ismail, O., Machhada, A., Colgan, N., Ohene, Y., Nahavandi, P., et al. (2020). Impaired glymphatic function and clearance of tau in an Alzheimer's disease model. *Brain* 143, 2576–2593. doi: 10.1093/brain/awaa179

Hepp, D. H., Vergoossen, D. L. E., Huisman, E., Lemstra, A. W., Bank, N. B., Berendse, H. W., et al. (2016). Distribution and load of amyloid-β pathology in Parkinson disease and dementia with lewy bodies. *J. Neuropathol. Exp. Neurol.* 75, 936–945. doi: 10.1093/jnen/nlw070

Hindle, J. V., Martyr, A., and Clare, L. (2014). Cognitive reserve in Parkinson's disease: a systematic review and meta-analysis. *Parkinsonism Relat. Disord.* 20, 1–7. doi: 10.1016/j.parkreldis.2013.08.010

Hubbard, J. A., Szu, J. I., and Binder, D. K. (2018). The role of aquaporin-4 in synaptic plasticity, memory and disease. *Brain Res. Bull.* 136, 118–129. doi: 10.1016/j.brainresbull.2017.02.011

Ikeshima-Kataoka, H. (2016). Neuroimmunological implications of AQP4 in astrocytes. *Int. J. Mol. Sci.* 17:1306. doi: 10.3390/ijms17081306

Iliff, J. J., Wang, M., Liao, Y., Plogg, B. A., Peng, W., Gundersen, G. A., et al. (2012). A paravascular pathway facilitates CSF flow through the brain parenchyma and the clearance of interstitial solutes, including amyloid. *Sci. Transl. Med.* 4:147ra111. doi: 10.1126/scitranslmed.3003748

Jakes, R., Spillantini, M. G., and Goedert, M. (1994). Identification of two distinct synucleins from human brain. *FEBS Lett.* 345, 27–32. doi: 10.1016/0014-5793(94)00395-5

Kalaitzakis, M. E., Graeber, M. B., Gentleman, S. M., and Pearce, R. K. B. (2008). Striatal β-amyloid deposition in Parkinson disease with dementia. *J. Neuropathol. Exp. Neurol.* 67, 155–161. doi: 10.1097/NEN.0b013e31816362aa

Lee, H.-J., Bae, E.-J., and Lee, S.-J. (2014). Extracellular α-synuclein—a novel and crucial factor in Lewy body diseases. *Nat. Rev. Neurol.* 10, 92–98. doi: 10.1038/nrneurol.2013.275

Litvan, I., Goldman, J. G., Tröster, A. I., Schmand, B. A., Weintraub, D., Petersen, R. C., et al. (2012). Diagnostic criteria for mild cognitive impairment in Parkinson's disease: movement disorder society task force guidelines: PD-MCI diagnostic criteria. *Mov. Disord.* 27, 349–356. doi: 10.1002/mds.24893

Lucey, B. P. (2020). It's complicated: the relationship between sleep and Alzheimer's disease in humans. *Neurobiol. Dis.* 144:105031. doi: 10.1016/j.nbd.2020.105031

Mata, I. F., Leverenz, J. B., Weintraub, D., Trojanowski, J. Q., Hurtig, H. I., Van Deerlin, V. M., et al. (2014). APOE, MAPT and SNCA genes and cognitive performance in Parkinson disease. *JAMA Neurol.* 71:1405. doi: 10.1001/jamaneurol.2014.1455

Meng, X., and D'Arcy, C. (2012). Education and dementia in the context of the cognitive reserve hypothesis: a systematic review with meta-analyses and qualitative analyses. *PLoS One* 7:e38268. doi: 10.1371/journal.pone.0038268

Mestre, H., Hablitz, L. M., Xavier, A. L., Feng, W., Zou, W., Pu, T., et al. (2018). Aquaporin-4-dependent glymphatic solute transport in the rodent brain. *eLife* 7:e40070. doi: 10.7554/eLife.40070

Nagelhus, E. A., and Ottersen, O. P. (2013). Physiological roles of aquaporin-4 in brain. *Physiol. Rev.* 93, 1543–1562. doi: 10.1152/physrev.00011.2013

Nomura, T., Inoue, Y., Kagimura, T., Uemura, Y., and Nakashima, K. (2011). Utility of the REM sleep behavior disorder screening questionnaire (RBDSQ) in Parkinson's disease patients. *Sleep Med.* 12, 711–713. doi: 10.1016/j.sleep.2011.01.015

Ovsepian, S. V., and O'Leary, V. B. (2016). Neuronal activity and amyloid plaque pathology: an update. *J. Alzheimers Dis.* 49, 13–19. doi: 10.3233/JAD-150544

Pagano, G., De Micco, R., Yousaf, T., Wilson, H., Chandra, A., and Politis, M. (2018). REM behavior disorder predicts motor progression and cognitive decline in Parkinson disease. *Neurology* 91, e894–e905. doi: 10.1212/WNL.0000000000006134

Petersen, S. E., and Posner, M. I. (2012). The attention system of the human brain: 20 years after. *Annu. Rev. Neurosci.* 35, 73–89. doi: 10.1146/annurev-neuro-062111-150525

Petrou, M., Dwamena, B. A., Foerster, B. R., MacEachern, M. P., Bohnen, N. I., Müller, M. L., et al. (2015). Amyloid deposition in Parkinson's disease and cognitive impairment: a systematic review: systematic review: amyloid in Parkinsonian dementia. *Mov. Disord.* 30, 928–935. doi: 10.1002/mds.26191

Postuma, R. B., Gagnon, J.-F., Bertrand, J.-A., Génier Marchand, D., and Montplaisir, J. Y. (2015). Parkinson risk in idiopathic REM sleep behavior disorder. *Neurology* 84, 1104–1113. doi: 10.1212/WNL.0000000000001364

Purcell, S., Neale, B., Todd-Brown, K., Thomas, L., Ferreira, M. A. R., Bender, D., et al. (2007). PLINK: a tool set for whole-genome association and population-based linkage analyses. *Am. J. Hum. Genet.* 81, 559–575. doi: 10.1086/519795

Randolph, C., Braun, A. R., Goldberg, T. E., and Chase, T. N. (1993). Semantic fluency in Alzheimer's, Parkinson's and Huntington's disease: dissociation of storage and retrieval failures. *Neuropsychology* 7, 82–88. doi: 10.1037/0894-4105.7.1.82

Robinson, J. L., Lee, E. B., Xie, S. X., Rennert, L., Suh, E., Bredenberg, C., et al. (2018). Neurodegenerative disease concomitant proteinopathies are prevalent, age-related and APOE4-associated. *Brain* 141, 2181–2193. doi: 10.1093/brain/awy146

Shah, N., Frey, K. A., Müller, L. T. M., Petrou, M., Kotagal, V., Koeppe, R. A., et al. (2016). Striatal and cortical β-amyloidopathy and cognition in Parkinson's disease: striatal β-amyloid and cognition in PD. *Mov. Disord.* 31, 111–117. doi: 10.1002/mds.26369

Smith, A. J., Jin, B.-J., Ratelade, J., and Verkman, A. S. (2014). Aggregation state determines the localization and function of M1- and M23-aquaporin-4 in astrocytes. *J. Cell Biol.* 204, 559–573. doi: 10.1083/jcb.201308118

Stav, A. L., Aarsland, D., Johansen, K. K., Hessen, E., Auning, E., and Fladby, T. (2015). Amyloid-β and α-synuclein cerebrospinal fluid biomarkers and cognition in early Parkinson's disease. *Parkinsonism Relat. Disord.* 21, 758–764. doi: 10.1016/j.parkreldis.2015.04.027

Stiasny-Kolster, K., Mayer, G., Schäfer, S., Möller, J. C., Heinzel-Gutenbrunner, M., and Oertel, W. H. (2007). The REM sleep behavior disorder screening questionnaire—A new diagnostic instrument. *Mov. Disord.* 22, 2386–2393. doi: 10.1002/mds.21740

Sunwoo, J.-S., Cha, K. S., Byun, J.-I., Jun, J.-S., Kim, T.-J., Shin, J.-W., et al. (2020). Nonrapid eye movement sleep electroencephalographic oscillations in idiopathic rapid eye movement sleep behavior disorder: a study of sleep spindles and slow oscillations. *Sleep* 44:zsaa160. doi: 10.1093/sleep/zsaa160

Tamtaji, O. R., Behnam, M., Pourattar, M. A., Jafarpour, H., and Asemi, Z. (2019). Aquaporin 4: a key player in Parkinson's disease. *J. Cell. Physiol.* 234, 21471–21478. doi: 10.1002/jcp.28871

Williams-Gray, C. H., Evans, J. R., Goris, A., Foltynie, T., Ban, M., Robbins, T. W., et al. (2009). The distinct cognitive syndromes of Parkinson's disease: 5 year follow-up of the CamPaIGN cohort. *Brain* 132, 2958–2969. doi: 10.1093/brain/awp245

Woo, J., Kim, J. E., Im, J. J., Lee, J., Jeong, H. S., Park, S., et al. (2018). Astrocytic water channel aquaporin-4 modulates brain plasticity in both mice and humans: a potential gliogenetic mechanism underlying language-associated learning. *Mol. Psychiatry* 23, 1021–1030. doi: 10.1038/mp.2017.113

Wu, Y.-F., Sytwu, H.-K., and Lung, F.-W. (2020). Polymorphisms in the human aquaporin 4 gene are associated with schizophrenia in the southern chinese han population: a case-control study. *Front. Psychiatry* 11:596. doi: 10.3389/fpsyt.2020.00596

Xie, F., Gao, X., Yang, W., Chang, Z., Yang, X., Wei, X., et al. (2019). Advances in the research of risk factors and prodromal biomarkers of Parkinson's disease. *ACS Chem. Neurosci.* 10, 973–990. doi: 10.1021/acschemneuro.8b00520

Xie, L., Kang, H., Xu, Q., Chen, M. J., Liao, Y., Thiyagarajan, M., et al. (2013). Sleep drives metabolite clearance from the adult brain. *Science* 342, 373–377. doi: 10.1126/science.1241224

Xue, X., Zhang, W., Zhu, J., Chen, X., Zhou, S., Xu, Z., et al. (2019). Aquaporin-4 deficiency reduces TGF-β1 in mouse midbrains and exacerbates pathology in experimental Parkinson's disease. *J. Cell. Mol. Med.* 23, 2568–2582. doi: 10.1111/jcmm.14147

Zeppenfeld, D. M., Simon, M., Haswell, J. D., D'Abreo, D., Murchison, C., Quinn, J. F., et al. (2017). Association of perivascular localization of aquaporin-4 with cognition and Alzheimer disease in aging brains. *JAMA Neurol.* 74, 91–99. doi: 10.1001/jamaneurol.2016.4370

Zhang, F., Niu, L., Liu, X., Liu, Y., Li, S., Yu, H., et al. (2020). Rapid eye movement sleep behavior disorder and neurodegenerative diseases: an update. *Aging Dis.* 11, 315–326. doi: 10.14336/AD.2019.0324

Zou, W., Pu, T., Feng, W., Lu, M., Zheng, Y., Du, R., et al. (2019). Blocking meningeal lymphatic drainage aggravates Parkinson's disease-like pathology in mice overexpressing mutated α-synuclein. *Transl. Neurodegener.* 8:7. doi: 10.1186/s40035-019-0147-y

Conflict of Interest: The authors declare that the research was conducted in the absence of any commercial or financial relationships that could be construed as a potential conflict of interest.

Publisher's Note: All claims expressed in this article are solely those of the authors and do not necessarily represent those of their affiliated organizations, or those of the publisher, the editors and the reviewers. Any product that may be evaluated in this article, or claim that may be made by its manufacturer, is not guaranteed or endorsed by the publisher.

frontiers in Aging Neuroscience

ORIGINAL RESEARCH
published: 16 March 2022
doi: 10.3389/fnagi.2022.838436

The *APOE*$^{\varepsilon 3/\varepsilon 4}$ Genotype Drives Distinct Gene Signatures in the Cortex of Young Mice

*Kate E. Foley[1,2], Amanda A. Hewes[1,3], Dylan T. Garceau[1], Kevin P. Kotredes[1], Gregory W. Carter[1,2,4], Michael Sasner[1] and Gareth R. Howell[1,2,4]**

[1] The Jackson Laboratory, Bar Harbor, ME, United States, [2] School of Graduate Biomedical Sciences, Tufts University School of Medicine, Boston, MA, United States, [3] Department of Psychology, University of Maine, Orono, ME, United States, [4] Graduate School of Biomedical Sciences and Engineering, University of Maine, Orono, ME, United States

OPEN ACCESS

Edited by:
Poornima Venkat, Henry Ford Health System, United States

Reviewed by:
Berislav Zlokovic, University of Southern California, United States
Xu Cui, Henry Ford Hospital, United States
Amy R. Nelson, University of South Alabama, United States

***Correspondence:**
Gareth R. Howell
Gareth.Howell@jax.org

Specialty section:
This article was submitted to Alzheimer's Disease and Related Dementias, a section of the journal Frontiers in Aging Neuroscience

Received: *17 December 2021*
Accepted: *14 February 2022*
Published: *16 March 2022*

Citation:
Foley KE, Hewes AA, Garceau DT, Kotredes KP, Carter GW, Sasner M and Howell GR (2022) The APOE$^{\varepsilon 3/\varepsilon 4}$ *Genotype Drives Distinct Gene Signatures in the Cortex of Young Mice. Front. Aging Neurosci. 14:838436. doi: 10.3389/fnagi.2022.838436*

Introduction: Restrictions on existing *APOE* mouse models have impacted research toward understanding the strongest genetic risk factor contributing to Alzheimer's disease (AD) and dementia, *APOE*$^{\varepsilon 4}$, by hindering observation of a key, common genotype in humans – *APOE*$^{\varepsilon 3/\varepsilon 4}$. Human studies are typically underpowered to address *APOE*$^{\varepsilon 4}$ allele risk as the *APOE*$^{\varepsilon 4/\varepsilon 4}$ genotype is rare, which leaves human and mouse research unsupported to evaluate the *APOE*$^{\varepsilon 3/\varepsilon 4}$ genotype on molecular and pathological risk for AD and dementia.

Methods: As a part of MODEL-AD, we created and validated new versions of humanized *APOE*$^{\varepsilon 3/\varepsilon 3}$ and *APOE*$^{\varepsilon 4/\varepsilon 4}$ mouse strains that, due to unrestricted breeding, allow for the evaluation of the *APOE*$^{\varepsilon 3/\varepsilon 4}$ genotype. As biometric measures are often translatable between mouse and human, we profiled circulating lipid concentrations. We also performed transcriptional profiling of the cerebral cortex at 2 and 4 months (mos), comparing *APOE*$^{\varepsilon 3/\varepsilon 4}$ and *APOE*$^{\varepsilon 4/\varepsilon 4}$ to the reference *APOE*$^{\varepsilon 3/\varepsilon 3}$ using linear modeling and WGCNA. Further, *APOE* mice were exercised and compared to litter-matched sedentary controls, to evaluate the interaction between *APOE*$^{\varepsilon 4}$ and exercise at a young age.

Results: Expression of human APOE isoforms were confirmed in *APOE*$^{\varepsilon 3/\varepsilon 3}$, *APOE*$^{\varepsilon 3/\varepsilon 4}$ and *APOE*$^{\varepsilon 4/\varepsilon 4}$ mouse brains. At two mos, cholesterol composition was influenced by sex, but not *APOE* genotype. Results show that the *APOE*$^{\varepsilon 3/\varepsilon 4}$ and *APOE*$^{\varepsilon 4/\varepsilon 4}$ genotype exert differential effects on cortical gene expression. *APOE*$^{\varepsilon 3/\varepsilon 4}$ uniquely impacts 'hormone regulation' and 'insulin signaling,' terms absent in *APOE*$^{\varepsilon 4/\varepsilon 4}$ data. At four mos, cholesterol and triglyceride levels were affected by sex and activity, with only triglyceride levels influenced by *APOE* genotype. Linear modeling revealed *APOE*$^{\varepsilon 3/\varepsilon 4}$, but not *APOE*$^{\varepsilon 4/\varepsilon 4}$, affected 'extracellular matrix' and 'blood coagulation' related terms. We confirmed these results using WGCNA, indicating robust, yet subtle, transcriptional patterns. While there was little evidence of *APOE* genotype by exercise interaction on the cortical transcriptome at this young age, running was predicted to

affect myelination and gliogenesis, independent of *APOE* genotype with few *APOE* genotype-specific affects identified.

Discussion: *APOE*$^{\varepsilon 4}$ allele dosage-specific effects were observed in circulating lipid levels and cortical transcriptional profiles. Future studies are needed to establish how these data may contribute to therapeutic development in *APOE*$^{\varepsilon 3/\varepsilon 4}$ and *APOE*$^{\varepsilon 4/\varepsilon 4}$ dementia patients.

Keywords: APOE4 and APOE3, APOE4 and AD risk, transcriptome (RNA-seq), exercise, Alzheimer's disease, dementia - Alzheimer's disease, dementia, cerebral cortex

INTRODUCTION

The ε*4* allele of apolipoprotein E (*APOE*), *APOE*$^{\varepsilon 4}$, has been identified as one of the greatest genetic risk factors for Alzheimer's disease (AD) and related dementias (ADRDs) (Rohn, 2014; Halliday et al., 2016; Riedel et al., 2016; Koizumi et al., 2018; Zhao et al., 2020). The ε*3* and ε*2* alleles of *APOE* confer neutral and protective risk, respectively. In late-onset AD (LOAD), allele frequencies vary between cases and controls, with *APOE*$^{\varepsilon 2}$, *APOE*$^{\varepsilon 3}$, and *APOE*$^{\varepsilon 4}$ present at a rate of 8%, 78%, and 14%, respectively, in unaffected subjects, and 4%, 59% and 37%, respectively, in affected subjects (Farrer et al., 1997). The frequency of LOAD increases from 20% in a non-carrier of *APOE*$^{\varepsilon 4}$, to 47% when carrying one copy, and up to 91% when carrying two copies (Bell et al., 2012). In VaD, *APOE*$^{\varepsilon 4}$ predisposes individuals for increased risk of cerebrovascular disease and ischemic stroke, potentially up to 30% (Belloy et al., 2019). With *APOE*$^{\varepsilon 4}$ being less frequent than *APOE*$^{\varepsilon 3}$, the more common risk genotype in at risk populations is *APOE*$^{\varepsilon 3/\varepsilon 4}$, with 41.1% of LOAD cases possessing the *APOE*$^{\varepsilon 3/\varepsilon 4}$ genotype compared to 14.8% with *APOE*$^{\varepsilon 4/\varepsilon 4}$ (Farrer et al., 1997).

Genetic variation between mouse strain *Apoe* has been proposed to modify phenotypes relevant to human aging and dementia (Neuner et al., 2019). However, mouse strains do not carry equivalent *Apoe* alleles to those observed in humans. Therefore, humanized *APOE* mice have contributed greatly to what we currently understand about the myriad of APOE mechanisms that may contribute risk for dementia. *APOE*$^{\varepsilon 4}$ is predicted to increase risk for multiple dementias through either gain of toxic function or loss of function which is context dependent (Belloy et al., 2019). Additionally, it is well understood that there are at least two major compartments by which APOE functions –peripherally (i.e., blood) and centrally (i.e., brain) (Chan et al., 1989; Hauser et al., 2011; Chernick et al., 2019). Peripheral APOE (also referred to as circulating APOE), produced primarily by liver hepatocytes, remains in the blood and circulatory system, and is thought to not cross the blood brain barrier (Liu et al., 2012). A primary role of circulating APOE is in lipid and cholesterol homeostasis with APOE functioning as a lipid trafficking protein. The lipid binding region and receptor binding region differ in affinity to its respective receptors between *APOE*$^{\varepsilon 2}$, *APOE*$^{\varepsilon 3}$, and *APOE*$^{\varepsilon 4}$. Cerebral APOE is produced mainly by astrocytes, however during stress can be upregulated and produced by microglia and possibly neurons (Chan et al., 1989; Hauser et al., 2011; Chernick et al., 2019). Studies have utilized humanized *APOE* mouse models crossed with amyloid and tau mouse models to show that, in addition to lipid trafficking, APOE functions in a variety of AD-relevant processes including amyloid clearance and tau-mediated neurodegeneration (Sullivan et al., 1997; Knouff et al., 1999; Huang et al., 2017; Liu et al., 2017; Shi et al., 2017; Huynh et al., 2019). However, these studies assessed homozygous *APOE*$^{\varepsilon 3/\varepsilon 3}$ and *APOE*$^{\varepsilon 4/\varepsilon 4}$, but not the heterozygous *APOE*$^{\varepsilon 3/\varepsilon 4}$ genotype.

Human and murine studies have parsed out important mechanisms by which the *APOE*$^{\varepsilon 4}$ allele differs in comparison to the *APOE*$^{\varepsilon 3}$ allele to increase detrimental brain pathology leading to AD and other dementias. However, little is known about the mechanisms by which *APOE*$^{\varepsilon 3}$ and *APOE*$^{\varepsilon 4}$ may interact in those with the *APOE*$^{\varepsilon 3/\varepsilon 4}$ genotype to affect risk for dementia. This lack of knowledge has been in part due to legal restrictions on the breeding of *APOE*$^{\varepsilon 4/\varepsilon 4}$ to *APOE*$^{\varepsilon 3/\varepsilon 3}$ mice to create *APOE*$^{\varepsilon 3/\varepsilon 4}$ mice. This limitation has also meant that experiments comparing *APOE*$^{\varepsilon 3/\varepsilon 3}$ to *APOE*$^{\varepsilon 4/\varepsilon 4}$ were often not performed in litter-matched mice. It has been shown that the APOE$^{\varepsilon 4}$ isoform is degraded at a higher rate by astrocytes compared to the APOE$^{\varepsilon 3}$ isoform (Ramaswamy et al., 2005; Riedel et al., 2016). Others have shown differential bioenergetics in male *APOE*$^{\varepsilon 3/\varepsilon 4}$ mice compared to male *APOE*$^{\varepsilon 3/\varepsilon 3}$ mice (Area-Gomez et al., 2020). Nonetheless, much is still to be learned about the global consequences of the *APOE*$^{\varepsilon 3/\varepsilon 4}$ genotype. It is conceivable there may be compensatory, dominant, or *APOE*$^{\varepsilon 4}$ dose-dependent effects on molecular changes predisposing risk for ADRDs.

To improve translatability of *APOE* mouse models to enable new discoveries for human biology, here we describe the creation of a new set of humanized *APOE* mouse models, using a similar design to models commonly used (Sullivan et al., 1997; Knouff et al., 1999). There are no breeding or distribution restrictions on these new humanized *APOE* models. Further, we used our new humanized *APOE* mouse models to test our hypothesis that *APOE*$^{\varepsilon 3/\varepsilon 4}$ mice show characteristics that may modify risk for dementias that are distinct from *APOE*$^{\varepsilon 4/\varepsilon 4}$ mice. First, we assessed male and female *APOE* mice, examining the effects of sex and *APOE*$^{\varepsilon 4}$ at 2 months (2 mos) of age. We next evaluated a cohort at 4 months (4 mos) which also including a running cohort to evaluate the potential interactions between *APOE*$^{\varepsilon 4}$

Abbreviations: LOAD, late onset Alzheimer's disease; VaD, vascular dementia; HDR, homology directed recombination; VLDL, very low density lipoprotein; LDL, low density lipoprotein; HDL, high density lipoprotein; NEFA, non-esterified fatty acids; WGCNA, weighted gene co-expression network analysis; GO, gene ontology.

and exercise. Lipid profiling was performed on plasma samples while RNA-seq was performed on the cerebral cortex. Linear modeling, a mathematical approach widely used for analyzing transcriptomic data in both humans and mice, was used identify the contribution of main and interacting factors (genotype, sex, activity) on the cortical transcriptome (Wang and Brinton, 2016; Belloy et al., 2019; Williams et al., 2020). Results revealed significant differences between the *APOE* genotypes in both the periphery and the cortex supporting our hypothesis that the $APOE^{\varepsilon 3/\varepsilon 4}$ genotype exerts unique effects compared to the $APOE^{\varepsilon 4/\varepsilon 4}$ genotype.

MATERIALS AND METHODS

Mouse Husbandry

All experiments involving mice were conducted with approval and accordance described in the Guide for the Care and Use of Laboratory Animals of the National Institutes of Health. All experiments were approved by the Animal Care and Use Committee at The Jackson Laboratory. Mice were kept in a 12/12-h light/dark cycle and fed *ad libitum* 6% kcal fat standard mouse chow.

Creation of Humanized Apolipoprotein E Mouse Strains

Humanized *APOE* mice were created in collaboration with the Genetic Engineering Technologies core at The Jackson Laboratory. The mouse *Apoe* gene is located on chromosome 7 at 19,696,109–19,699,166. An $APOE^{\varepsilon 4}$ gene-targeting construct was made that included 4980 bp of mouse sequence, which defined the mouse 5' homology arm including exon 1 of mouse *Apoe*, 4292 bp of human $APOE^{\varepsilon 4}$ sequence including human protein coding exons 2–4 of the human gene as well as an additional 1.5 kb of flanking human sequence after the 3′UTR to include any potential regulatory sequences. Exon 4 contained sequence that encoded the $APOE^{\varepsilon 4}$ isoform (nucleotide sequence for arginine at R130 and R176). The predicted protein sequence in our humanized $APOE^{\varepsilon 4}$ mouse model is 317 amino acids and includes the18 amino acid signal peptide at the N-terminus. As in all *APOE* isoforms, the 18 amino acid leader sequence is cleaved resulting in the mature 299 amino acid protein, with the amino acids that define $APOE^{\varepsilon 4}$ located at positions 112 and 158 (Mahley and Rall, 2000; Rohn and Moore, 2017). A Frt-neo-Frt (FNF) selection cassette was inserted after the human sequence followed by a Nde1 restriction site (for ease of Southern screening). The FNF cassette was followed by 5166 bp of mouse sequence, the 3' homology arm. The resulting 14,438 bp synthesized construct was cloned into pBlight vector using recombineering techniques, producing a construct called mApoE_hAPOE4_PGKneo_mAPOE for gene targeting in embryonic stem cells. The $APOE^{\varepsilon 4}$ gene-targeting construct was introduced into cultured embryonic stem (ES) cells of a C57BL/6J (B6) mouse strain by electroporation. Homologous recombination produced loci that retained all normal mouse regulatory sequences (plus non-coding exon one) together with the human $APOE^{\varepsilon 4}$ protein-encoding exons 2–4 (**Figure 1A**). Transfected ES cells were screened by Southern blot to ensure correct targeting. Three clones were identified that were correctly targeted. ES cells containing the correctly targeted locus were introduced into albino B6 embryos, and the resultant chimeric mice were bred with B6 mice. Offspring carrying the modified locus in the germline were interbred to generate the homozygous genetically modified genome. All F1 matings produced normal litter sizes with a Mendelian distribution of the locus. Heterozygous animals were crossed to FLP recombinase expression mice (JAX Stock No. 005703) to remove the FRT site flanked PGK-neo cassette. Mice that no longer contained the FRT flanked PGK-neo cassette were then backcrossed to B6 at least once to remove the FLP recombinase transgene. SNP analysis was performed to validate the B6 background. Offspring that were negative for the FLP recombinase transgene were then interbred and maintained as $APOE^{\varepsilon 4/\varepsilon 4}$ homozygous mice (JAX Stock No. 000664).

The $APOE^{\varepsilon 3}$ model was generated using CRISPR/Cas9-mediated gene targeting in $APOE^{\varepsilon 4}$ zygotes (**Figure 1A**). An $APOE^{\varepsilon 4}$ specific sgRNA (GCGGACATGGAGGACGTGCG CGG; PAM site is underlined) was used to target the human knock-in allele just downstream of the valine codon that defines the $APOE^{\varepsilon 4}$ allele, and a 129 nt single stranded oligonucleotide (GAGACGCGGGCACGGCTGTCCAAGGAGCTGCAGGCGG CGCAGGCCCGGCTGGGCGCGGACATGGAGGACGTc**T**GC GGCCGCCTGGTGCAGTACCGCGGCGAGGTGCAGGCCA TGCTCGGCCA) including the CGC->**T**GC substitution (bold) to change arginine to cysteine and silent mutation GTG-GTC (underlined) to prevent re-cutting. Putative founders were bred to B6 mice for at least four generations and then interbred to be maintained as $APOE^{\varepsilon 3/\varepsilon 3}$ homozygous mice (JAX Stock No. 029018).

To create experimental cohorts, $APOE^{\varepsilon 3/\varepsilon 3}$ mice were crossed to $APOE^{\varepsilon 4/\varepsilon 4}$ mice to generate $APOE^{\varepsilon 3/\varepsilon 4}$ mice, which were then intercrossed to give cohorts of litter-matched mice of all required genotypes ($APOE^{\varepsilon 3/\varepsilon 3}$, $APOE^{\varepsilon 3/\varepsilon 4}$, and $APOE^{\varepsilon 4/\varepsilon 4}$). Three separate cohorts of mice were used in this study. The first was aged to 2 mos for strain validation including western blotting. The second was aged to 2 mos for peripheral and cortical assessments. The third was aged to 1 mo, when half were provided a running wheel, and subsequently assessed at 4 mos along with sedentary controls.

Genotyping of Apolipoprotein E Mice

Genotyping to differentiate between $APOE^{\varepsilon 3}$ and $APOE^{\varepsilon 4}$ alleles for our experimental cohorts was performed *via* ear punch at 1 mo of age. A gel-based PCR assay was used to determine insertion of the humanized construct (**Figure 1B**). Primers included a common forward spanning over intron 1 and exon 2 (AATTTTTCCCTCCGCAGACT), a wild type (WT) mouse reverse in intron 2 (ACAGCTGCTCAGGGCTATTG), and a humanized reverse (AGGAGGTTGAGGTGAGGATG). A band for WT (wild type – mouse control, no humanized insertion) shows at 244 bp, while the humanized insertion results in a 148 bp band. To differentiate between the $APOE^{\varepsilon 3}$ and $APOE^{\varepsilon 4}$ alleles,

Sanger sequencing was used to identify CT for $APOE^{\varepsilon 3}$, and GC for $APOE^{\varepsilon 4}$, and a double peak signifying the presence of both $APOE^{\varepsilon 3}$ and $APOE^{\varepsilon 4}$ (GT) (**Figure 1C**).

Validation of Apolipoprotein E Expression by Western Blotting

Snap-frozen hemispheres were homogenized by hard tissue homogenizer (USA Scientific, Ocala, FL, United States) and lysed in 700 mL RIPA buffer (R0278, Sigma, St. Louis, MO, United States) supplemented with 100× protease and phosphatase inhibitor reagents (1861281, Thermo Fisher Scientific, Waltham, MA, United States). Lysates were incubated for 1 h at 4°C before pelleting insoluble proteins by spinning at 4°C, 11,000 × *g* for 15 min. Protein concentration was determined by Bradford protein assay (Biorad, Hercules, CA, United States), according to manufacturer's instructions. Samples were mixed with 10× Laemlli buffer (42556.01, Amsbio, Cambridge, MA, United States), boiled for 10 min, and run on 12% SDS PAGE gels (456-1044, BioRad) with colorimetric ladder (RPN800E, GE, Boston, MA, United States). Gels were transferred to PVDF membranes for immunoblotting and imaging using an iBlot2 dry blotting system (Thermo Fisher). Membranes were blocked in 5% non-fat dry milk in 1XPBS + 0.1% Tween20 for 1 h prior to incubating with primary antibodies diluted in 5% non-fat dry milk in 1XPBS + 0.1% Tween20 for 1 h at room temperature. Membranes were washed in 1XPBS + 0.1% Tween20 before incubating with secondary antibodies diluted in 5% non-fat dry milk in 1XPBS + 0.1% Tween20. HRP-conjugated secondary antibodies targeting primary antibody host IgG were incubated at 1 h at room temperature. Membranes were washed in 1XPBS + 0.1% Tween20 before digital imaging with SuperSignal West Pico PLUS chemiluminescent substrate (34579, Thermo Fisher). Antibodies used include: Pan human APOE (AB947, Millipore, Burlington, MA, United States); Mouse Apoe (NB100-240, Novus Biologicals, Centennial, CO, United States); human $APOE^{\varepsilon 4}$ (NBP1-49529, Novus Biologicals); Actin (ab179467, Abcam, Cambridge, United Kingdom).

For $APOE^{\varepsilon 4}$ quantification, western blots were run as stated above with modifications. Protein extraction was performed on snap frozen cerebral cortex tissue in 700–1000 mL RIPA buffer supplemented with cOmplete Mini Protease Inhibitor Cocktail (Millipore Sigma, 11836153001), 100 uM PMSF, and 100 μM Na3V4O. Protein was quantified by Bradford Protein Assay as stated above. Samples were mixed with 2× Laemmli buffer and RIPA buffer to dilute all proteins to 100 μg/μl/sample. Samples were heated for 5 min at 95°C, and run on 4–20% gradient gels (BioRad, 4561096) with Full Range Rainbow Recombinant Protein Molecular Marker ladder (RPN800E). Gels were transferred to nitrocellulose membranes (Thermo Fisher, IB301001) using the iBlot system (Thermo Fisher) for immunoblotting. Membranes were blocked in 5% non-fat dry milk in 1XPBS + 0.1% Tween20 for 1 h. Primary antibodies were diluted in 5% non-fat dry milk in 1XPBS + 0.1% Tween20 and incubated overnight at 4°C moving. Membranes were washed in 5% non-fat dry milk in 1XPBS + 0.1%Tween20 and then incubated. Secondary antibodies were also diluted in 5% non-fat dry milk in 1XPBS + 0.1% Tween20 for 2 h at room temperature. Membranes were washed again in 5% non-fat dry milk in 1XPBS + 0.1%Tween20 and exposed to Amersham ECL Western Blotting Detection Reagent (RPN2109, Cytiva, Marlborough, MA, United States) just prior to digital imaging on the Azure Biosystems c600 (Azure Biosystems, Dublin, CA, United States). Actin and $APOE^{\varepsilon 4}$ were quantified in ImageJ (FIJI).

Exercise by Voluntary Running

At first, mice were group housed (two or three per pen) and were provided access to low profile saucer wheels (Innovive Inc.) 24 h a day from 1 mo to 4 mos. Sedentary mice were not provided access to running wheels. At 4 mos, just prior to harvest, mice were separated and individually housed with a trackable low-profile running wheel (Med Associates Inc.) or no wheel access. Rotations per minute during lights out (12 h, 6:00 pm – 6:00 am) were quantified. This time period was used as it is when mice are naturally awake and active. Running wheel rotations were measured in 1-min bins to allow for distance traveled (sum of rotations) calculated per mouse each night. Average rotations were calculated per mouse. Average speed while active was calculated by isolating the minute intervals where activity was measured (>0) and averaging the number of rotations for the minutes active. Percent of time at each speed was calculated by totaling the number of minute bins that mice ran between 0, 1–30 rotations, 31–70 rotations, 71–100 rotations, and 100+ rotations and dividing by the total amount of minutes tracked. Any nights that had fewer than 700 min tracked were excluded from analysis.

Harvesting, Tissue Preparation and Blood Lipid Profiling Assessment

All mice were euthanized by intraperitoneal injection of a lethal dose of Ketamine (100 mg/ml)/Xylazine (20 mg/ml) and blood was collected in K2 EDTA (1.0 mg) microtainer tubes (BD, Franklin Lakes, NJ, United States) through approved cardiac puncture protocols. Mice were perfused intracardially with 1XPBS. Brains were carefully dissected then hemisected sagittally, and the cortex (Ctx) was then carefully isolated and snap frozen in solid CO_2 for RNA-sequencing and cholesterol profiling. Blood was kept at room temperature for at least 30 min to prevent clotting, and then centrifuged at 21°C for 10 min at 5000 rpm. Plasma was carefully collected. Plasma and brain lipid concentrations were characterized on the Beckman Coulter AU680 chemistry analyzer.

RNA Extraction, Library Construction, RNA Sequencing, and RNA Sequencing Quality Control

RNA sequencing (RNA-seq) was performed by The Jackson Laboratory Genome Technologies Core. RNA extraction involved homogenization with TRIzol (Invitrogen, Waltham, MA, United States) as previously described (Soto et al., 2015). RNA was isolated and purified using the QIAGEN miRNeasy mini extraction kit (Qiagen, Hilden, Germany) in accordance with manufacturer's instructions. RNA quality was measured *via*

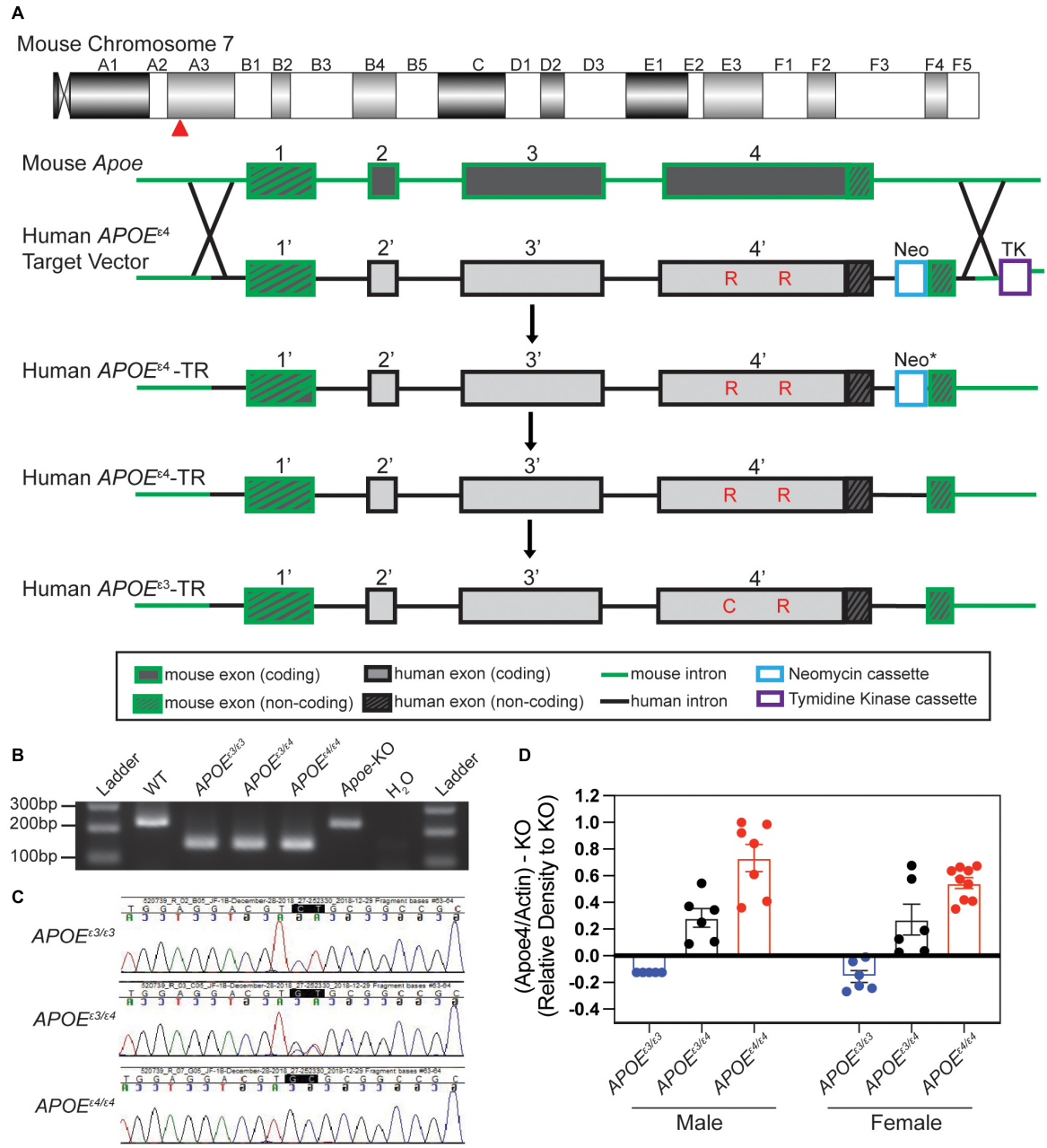

FIGURE 1 | Creation and validation of *APOE* allelic series. **(A)** Schematic of human *APOE* allele insertion at the mouse *Apoe* locus on chromosome 7. Exon 1 remained unchanged (mouse) and exons 2–4 were replaced with human *APOE*$^{\varepsilon 4}$ sequence through homology directed repair (HDR). The neomycin cassette was removed (* indicated by asterisk) through Flp-Frt breeding (Flp-Frt sites not shown). The *APOE*$^{\varepsilon 3}$ SNP was changed through CRISPR mediated endonuclease activity. Critical amino acids differing between *APOE*$^{\varepsilon 4}$ and *APOE*$^{\varepsilon 3}$ noted in red. **(B)** PCR based assay to identify humanized *APOE* insertions at exon 2 vs. WT mouse *Apoe* (no insertion) at exon 2. **(C)** Sanger sequencing to distinguish *APOE*$^{\varepsilon 3}$ and/or *APOE*$^{\varepsilon 4}$ alleles. **(D)** Western blotting revealed significant differences in APOE$^{\varepsilon 4}$ levels between genotypes.

the Bioanalyzer 2100 (Agilent, Santa Clara, CA, United States) and poly(A) RNA-seq sequencing libraries were compiled by TruSeq RNA Sample preparation kit v2 (Illumina, San Diego, CA, United States). Quantification was performed using qPCR (Kapa Biosystems). RNA-seq was performed on the HiSeq 4000 platform (Illumina) for 2 × 100 bp reads for a total of 45 million reads according to the manufacturer's instructions. Quality control for each sample was completed using NGSQCToolkit v2.3 which removed adaptors and trimmed low quality bases (Phred < 30) (Patel and Jain, 2012). To quantify gene expression of the trimmed reads, we used RSEM v1.2.12 which uses Bowtie2 v2.2.0 for alignment of these reads (Langmead et al., 2009). We

used a custom mouse genome including mm-10 based upon the B6 reference genome, with the addition of the human *APOE* gene for continuity.

Linear Modeling and Functional Enrichment

Genes were filtered by (1) removing all genes that did not vary in expression (gene count change across all samples was 0) and (2) removing all genes that did not have at least five reads in 50% of the samples. Remaining genes were normalized using DEseq2 (Love et al., 2014). Variance stabilizing transformation (vst) was then performed. Principal component analysis (PCA) identified three outliers from the 2 mo dataset, and five outliers from the 4 mo dataset which were excluded from further analysis. *APOE* genotype will be referred to as 'genotype.' A linear model was used on the normalized counts to identify genes significantly fit by the predictors of our model: sex, genotype, and sex-genotype in the 2 mo dataset, and sex, genotype, activity, and genotype-activity in the 4 mo dataset. Reference data in the model were 'female $APOE^{\varepsilon 3/\varepsilon 3}$' for 2 mo and 'female sedentary $APOE^{\varepsilon 3/\varepsilon 3}$, for 4 mo data. The linear model was performed on 18,402 genes for 2 mos and on 18,987 genes for 4 mos. Nominal significant genes were identified per predictor term (sex, genotype, etc.) based upon $Pr(>|t|< 0.05)$. Functional enrichment for each linear model predictor term was performed using the clusterProfiler package with $p < 0.10$ to determine significant GO terms (Yu et al., 2012). Bonferroni Hochberg (BH) conditions were chosen for pAdjustMethod. Background lists consisted of all genes prior to significant geneset filtering.

Comparison of $APOE^{\varepsilon 3/3}$ and $APOE^{\varepsilon 4/4}$ Samples to Zhao et al.

Previously published cortical transcriptional data was accessed through the AD Knowledge Portal. Gene expression from Zhao et al. (2020) utilized conditional quantile normalization (CQN)-normalized log2RPKM values. Samples from 3 mo mice were filtered for, and then used for PCA clustering. To match previous publications, no scaling or centering was used in this PCA. Linear modeling was run on 19,120 genes across 32 samples with factors for sex, genotype, and sex-genotype. Significant genes were identified per predictor term (sex, genotype, etc.) based upon $Pr(> | t| < 0.05)$. Functional enrichment for each linear model predictor term was performed using the clusterProfiler package with $p < 0.05$ to determine significant GO terms (Yu et al., 2012).

Cell Type Specific Enrichment

Publicly available cell type gene expression was downloaded from the brainrna-seq.org dataset generated by the Barres laboratory (Zhang et al., 2014, 2016). Significant genes from linear model results from 2- and 4- mo data were cross referenced to this dataset. Some genes in our datasets were not found in the brainRNA-seq dataset and were excluded. Number of genes per cell type was expressed as a percentage of a specific cell type divided by all genes that were able to be cross referenced for the linear model predictor terms.

Weighted Gene Co-expression Network Analysis

Weighted gene co-expression network analysis required the WGCNA package by Horvath and Langfelder (Langfelder and Horvath, 2008, 2012). Normalized and variance transformed data (vst) without outliers was used to build weight gene co-expression networks. First, all samples passed the function goodSamplesGenes to check for incomplete sample data. Samples were clustered to identify outliers using hierarchical clustering; two samples were excluded from further analysis. Next, the soft-thresholding power (b) was chosen by calculating scale-free topology through the relationship between power and scale independence which resulted in a softPower of 5. Then 18 modules were clustered based upon minModuleSize = 30, and a mergeCutHeight = 0.4. These values were chosen based off previous studies with similar methods to achieve non-redundant smaller modules (Zhao et al., 2020). Module eigengenes for each module were identified and the correlation to sex, genotype, and activity was computed. The p values were then corrected for multiple testing both within and across terms by calculating false discovery rates. Genes in each module were annotated by using the AnnotationDbi package (Hervé Pagès et al., 2020). Module membership (module eigengene correlated with gene expression) was regressed against gene significance (the correlation between the linear model predictor term and each individual gene) to identify highly correlated modules (Pearson correlation). Genes in a module were processed through clusterProfiler to identify functional enrichment.

Neuronal Counts

To quantify neuronal cell number, 4 mo female sedentary mice were evaluated as previous studies would suggest they would be the most susceptible to neuronal loss. Two of each genotype (six samples total) were stained in replicates of three (three brain slices) and then evaluated for NEUN+ DAPI+ cells in the cortex above the CA1 in the hippocampus. Brains were cryosectioned at 20 mm onto slides. Sections were blocked for 1 h in 2%PBT + 10% Normal Goat Serum. Primary antibody NEUN (abcam, ab104225) was diluted in 2% PBT + 10% Normal Goat Serum and kept at 4°C overnight. Slides were washed 3 × 10 min in 2% PBT. Secondary antibody (goat anti rabbit 488) was diluted in 2%PBT and kept for 3 h at room temperature. A representative cortical section was imaged on a Leica SP8 confocal microscope at 1 um step size for 20 um. Images were quantified identically with the spots feature through IMARIS software for NEUN+ and DAPI+ cells.

Statistical Analysis

Statistical analysis for 2 mo biometric data including cholesterol composition, triglyceride, unfasted glucose, and non-esterified fatty acids (NEFA) were calculated by two-way ANOVA (interactions tested: sex-genotype, main effects: sex, genotype), and a *post hoc* Tukey test in GraphPad Prism v7.0a. Outliers were identified by ROUT (Q = 1.0%) using GraphPad Prism v7.0a. Statistical analysis for 4 mo biometric data was performed by three-way ANOVA (interactions tested: sex-genotype-activity,

genotype-activity, sex-activity, sex-genotype, main effects tested: sex, activity, genotype) followed by a TukeyHSD *post hoc* test in R v1.2.1335. Terms were considered significant if $p < 0.05$. *Post hoc* tests were used to determine differences between genotypes per sex, significant effects between genotypes and sexes were not reported (i.e., female-sed-$APOE^{\varepsilon 3/\varepsilon 4}$ to male-sed-$APOE^{\varepsilon 3/\varepsilon 3}$). All weight and biometric data included groups of 5–16 mice per sex/genotype/activity. Transcriptional profiling was performed on groups of six mice per sex/genotype/activity. Details of statistical analyses of linear modeling, functional enrichment, and WGCNA data are provided above.

RESULTS

Creation of Humanized $APOE^{\varepsilon 3/\varepsilon 3}$, $APOE^{\varepsilon 3/\varepsilon 4}$, and $APOE^{\varepsilon 4/\varepsilon 4}$ Mice

Humanized $APOE^{\varepsilon 3/\varepsilon 3}$ and $APOE^{\varepsilon 4/\varepsilon 4}$ mice were created on C57BL/6J (B6) mouse strain using a similar design to that described previously (**Supplementary Figure 1A**, see the section "Materials and Methods") (Sullivan et al., 1997; Knouff et al., 1999). Briefly, exons two through four of the mouse *Apoe* gene were replaced by sequence encoding the equivalent region in human the $APOE^{\varepsilon 4}$ gene through homologous directed repair (HDR) (**Figure 1A** and **Supplementary Figures 1B,C**). The $APOE^{\varepsilon 3}$ allele was produced by CRISPR-Cas9 of $APOE^{\varepsilon 4/\varepsilon 4}$ mice (**Figures 1B,C**). A PCR-based assay combined with Sanger sequencing was used to confirm humanized *APOE* alleles (**Figures 1B,C**). Protein was confirmed by western blotting with human APOE protein present in all humanized APOE mice. $APOE^{\varepsilon 4}$ protein only detectable in $APOE^{\varepsilon 3/\varepsilon 4}$ and $APOE^{\varepsilon 4/\varepsilon 4}$ mice in a relative abundance of 0.38 and 0.49, respectively (**Figure 1D** and **Supplementary Figures 2**,**3**).

To evaluate whether $APOE^{\varepsilon 4}$ dosage affected body weight and circulating lipids, two translatable biometric measurements, litter-matched male and female $APOE^{\varepsilon 3/\varepsilon 3}$, $APOE^{\varepsilon 3/\varepsilon 4}$ and $APOE^{\varepsilon 4/\varepsilon 4}$ mice were assayed at 2 mos. As expected, body weight was significantly different between sexes, with males weighing more than females. However, body weight was not affected by *APOE* genotype (**Figure 2A**). Total cholesterol, HDL, and unfasted glucose levels in plasma showed a significant main effect of sex, with males showing higher concentrations than females (**Figures 2B,D,F**). There was a significant interaction between sex and *APOE* genotype for LDL with the sexes showing differing trends in $APOE^{\varepsilon 3/\varepsilon 4}$ mice (**Figure 2C**). Plasma triglyceride levels, and brain total cholesterol, HDL, and LDL concentrations did not show an effect of sex or *APOE* genotype (**Figure 2E** and **Supplementary Figure 4**).

Cortical Transcriptional Profiling Reveals Unique Effects of $APOE^{\varepsilon 3/\varepsilon 4}$ Genotype at 2 Months

We hypothesized that compared to $APOE^{\varepsilon 4/\varepsilon 4}$, the $APOE^{\varepsilon 3/\varepsilon 4}$ genotype may differentially modulate cerebral processes. To assess this, RNA-seq was performed on cortical tissue collected from litter-matched male and female mice at 2 mos. Principal component analysis (PCA) showed clear separation between the sexes. There was no separation based on *APOE* genotype (**Figures 3A,B**) which agreed with previous studies (Zhao et al., 2020). Using $APOE^{\varepsilon 3/\varepsilon 3}$ as the 'control' genotype, linear modeling identified genes that varied as a function of sex, *APOE* genotype, and the interaction between sex and *APOE* genotype (**Figure 3C**, see the section "Materials and Methods"). Only 127 genes were in common between the 487 $APOE^{\varepsilon 3/\varepsilon 4}$ and the 518 $APOE^{\varepsilon 4/\varepsilon 4}$ genes (**Figure 3D**). GO terms enriched for the 360 unique $APOE^{\varepsilon 3/\varepsilon 4}$ genes included 'regulation of hormone levels,' 'regulation of hormone secretion,' and 'insulin secretion' (**Figure 3E** and **Supplementary Figure 7**). Hormone signaling, particularly in the glucose/insulin pathway, is disrupted in $APOE^{\varepsilon 4}$ individuals and can increase the severity of dementia (Peila et al., 2002; Irie et al., 2008). No GO terms were enriched for either the 127 intersection genes or the 391 genes unique to $APOE^{\varepsilon 4/\varepsilon 4}$, suggesting multiple unrelated processes may be more subtly affected. Interestingly, $APOE^{\varepsilon 4/\varepsilon 4}$ unique genes included angiogenesis-related *Acvrl1*, *Ang*, *Eng*, *Vegfc,* and cell adhesion-related *Fermt3*, *Itga2b*, *Itga5*. *Ang* can function by endothelial nuclear translocation to stimulate endothelial angiogenesis, while *Vegfc* is involved in vascular permeability (Moroianu and Riordan, 1994; Gao and Xu, 2008; Tammela et al., 2008; Miyake et al., 2015; Nagai and Minami, 2015; Apte et al., 2019). Both *Itga2b* and *Itga5* are receptors for fibrinogen and fibronectin, involved in the blood clotting cascade, while *Fermt3* is involved in leukocyte adhesion to endothelial cells (Varner et al., 1995; Oksala et al., 2015; Botero et al., 2020). RNA *in situ* hybridization (Allen Brain Atlas) and single cell sequencing of vascular-related cells confirm both *Acvrl1* (activin A receptor like Type 1) and *Eng* (endoglin) are expressed by vascular cells, including endothelial cells (**Supplementary Figures 5**, **6**; Lein et al., 2007; Vanlandewijck et al., 2018).

Cell type analysis revealed that while the $APOE^{\varepsilon 3/\varepsilon 4}$ unique genes are expressed in multiple cell types, the majority of these genes are expressed by endothelial cells and astrocytes. In contrast, the majority of $APOE^{\varepsilon 4/\varepsilon 4}$ unique genes are expressed by neurons (**Figure 3F**). This further supports subtle but unique effects of *APOE* genotype to the cerebral cortex at a young age that may predispose for AD and dementia later in life.

Sex and Physical Activity, but Not Apolipoprotein E Genotype Influence Peripheral Cholesterol Composition at 4 Months

Physical activity, especially running, has been widely considered a prevention, reducing risk for age-dependent cognitive decline and dementia. However, exercise may not prevent dementia in all individuals. We hypothesized that this may be due in part to genetics. To begin to test this we determined whether the effects of exercise are influenced by *APOE* genotype in young mice. Litter-matched male and female $APOE^{\varepsilon 3/\varepsilon 3}$, $APOE^{\varepsilon 3/\varepsilon 4}$ and $APOE^{\varepsilon 4/\varepsilon 4}$ mice were given access to a voluntary running wheel for 12 weeks from 1 mo to 4 mos (**Figure 4A**, see the section "Materials and Methods"). There was expected variation between mice for amount of

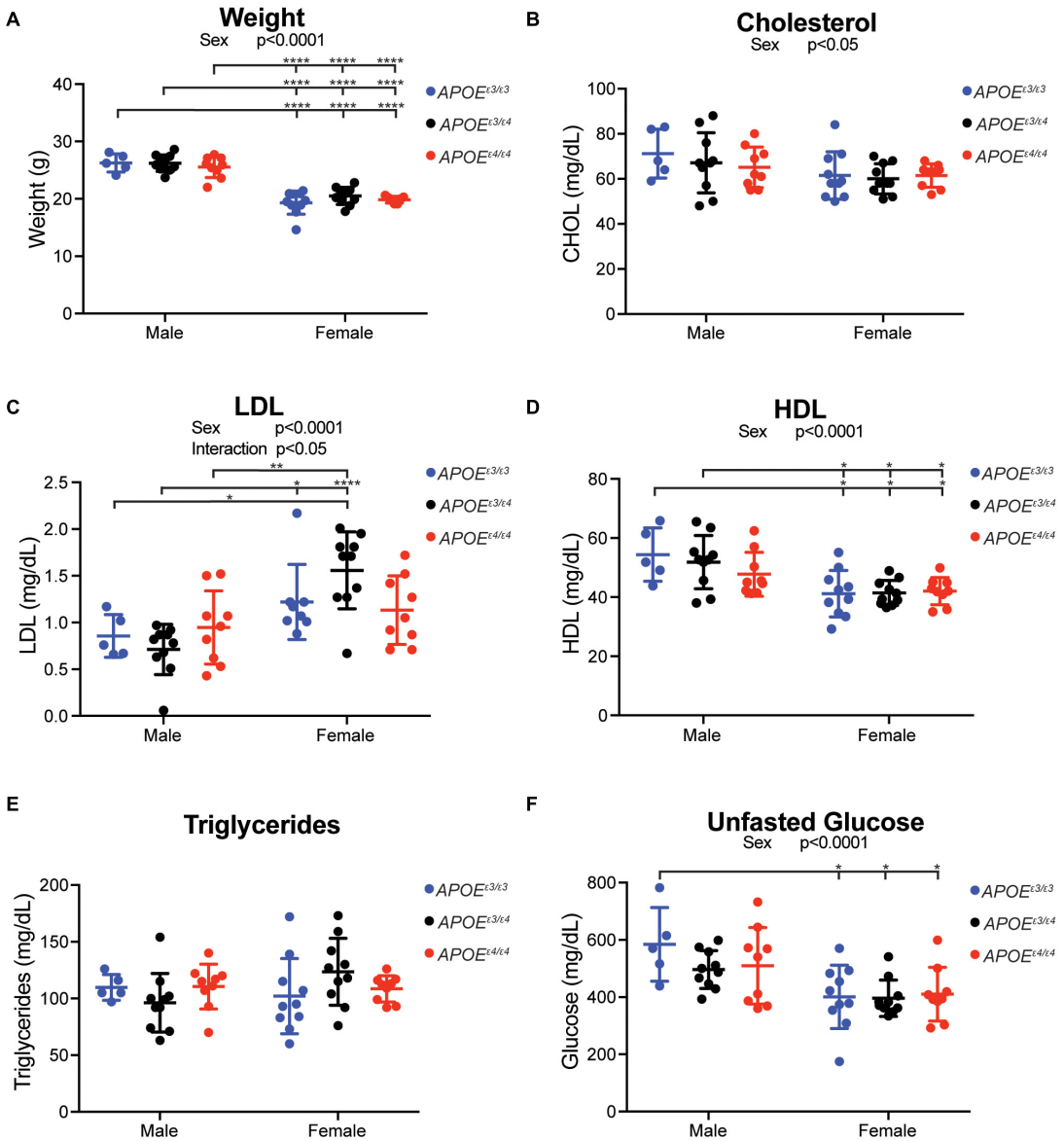

FIGURE 2 | Plasma cholesterol composition affected by sex, but not *APOE* genotype, at 2 months. **(A)** Weight (grams, g) at harvest in both male and female *APOE* mice showed expected significant sex differences across all genotypes. **(B)** Total plasma cholesterol concentration revealed a significant effect of sex. **(C)** Low density lipoprotein (LDL) concentration showed a significant interactive effect between *APOE* genotype and sex, as well as a main effect of sex. **(D)** High density lipoprotein concentration (HDL) showed a significant effect of sex. **(E)** Triglyceride concentration showed no effect by *APOE* genotype or sex. **(F)** Unfasted glucose showed a significant sex effect. Significant ANOVA results are stated under the title of the graph, significant Tukey *post hoc* results are shown on graph between significant groups. All significance data can be found in **Supplementary Table 1**.

time spent running and there were no differences in average rotations or running speed between *APOE* genotypes for both sexes, indicating activity may be compared across genotypes as it is not a confound (**Supplementary Figures 8A–F**). As has been shown before, female mice tended to run farther than male mice (Foley et al., 2019). As expected, there was a significant difference in weight between sexes at 4 mos, but there were no differences between the *APOE* genotypes or running and sedentary groups for either sex (**Figures 4B–D**).

Apolipoprotein E genotype did not significantly influence total cholesterol, LDL or HDL which agrees with previous findings in other *APOE* mouse models (Knouff et al., 1999; Mann et al., 2004). There was also no effect of *APOE* genotype on unfasted glucose, or NEFA concentrations in the plasma (**Figures 4E–G,I,J**). However, there was an effect of sex for total cholesterol, LDL, HDL and unfasted glucose levels, with males having higher total cholesterol, HDL, and unfasted glucose and lower LDL than females (**Figures 4E–G,I**). There was also an interaction between sex and activity for total cholesterol and HDL, suggesting

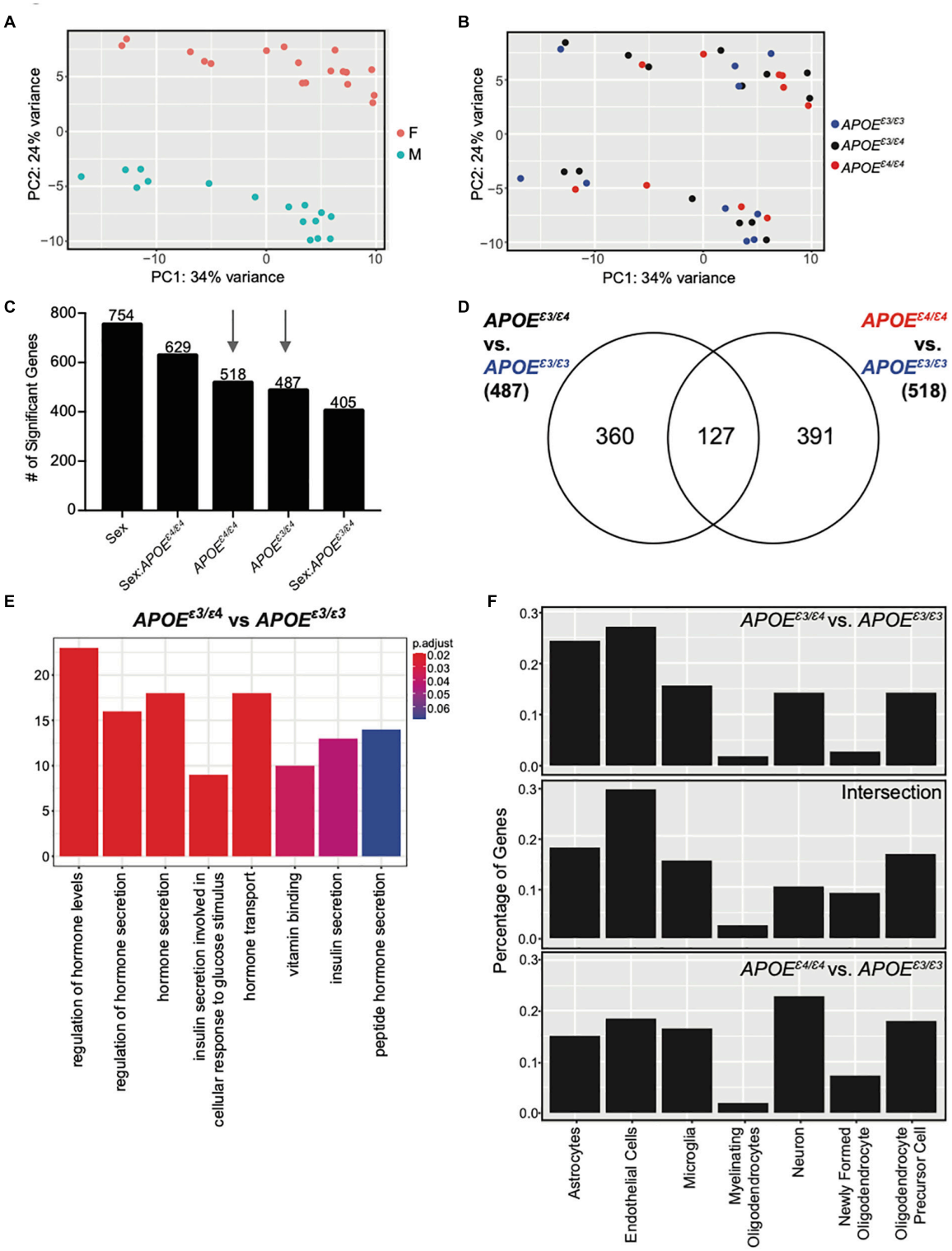

FIGURE 3 | Cortical transcriptome analysis revealed unique functional enrichment for the *APOE*$^{\varepsilon 3/\varepsilon 4}$ genotype at 2 months. **(A)** PCA showed distinct clusters of male and female samples. **(B)** PCA showed samples do not cluster by *APOE* genotype at two mos. **(C)** Number of significant genes for each linear model predictor term ($p < 0.05$). **(D)** Number of significant genes unique to 2-month *APOE*$^{\varepsilon 4/\varepsilon 4}$ and *APOE*$^{\varepsilon 4/\varepsilon 4}$ when compared to *APOE*$^{\varepsilon 3/\varepsilon 3}$, as well as the number of significant genes intersecting both lists. **(E)** Functional enrichment of the 360 significant genes ($p < 0.10$) unique to *APOE*$^{\varepsilon 3/\varepsilon 4}$ compared to *APOE*$^{\varepsilon 3/\varepsilon 3}$. **(F)** Percentage of genes expressed by cell type according to the BrainRNAseq dataset.

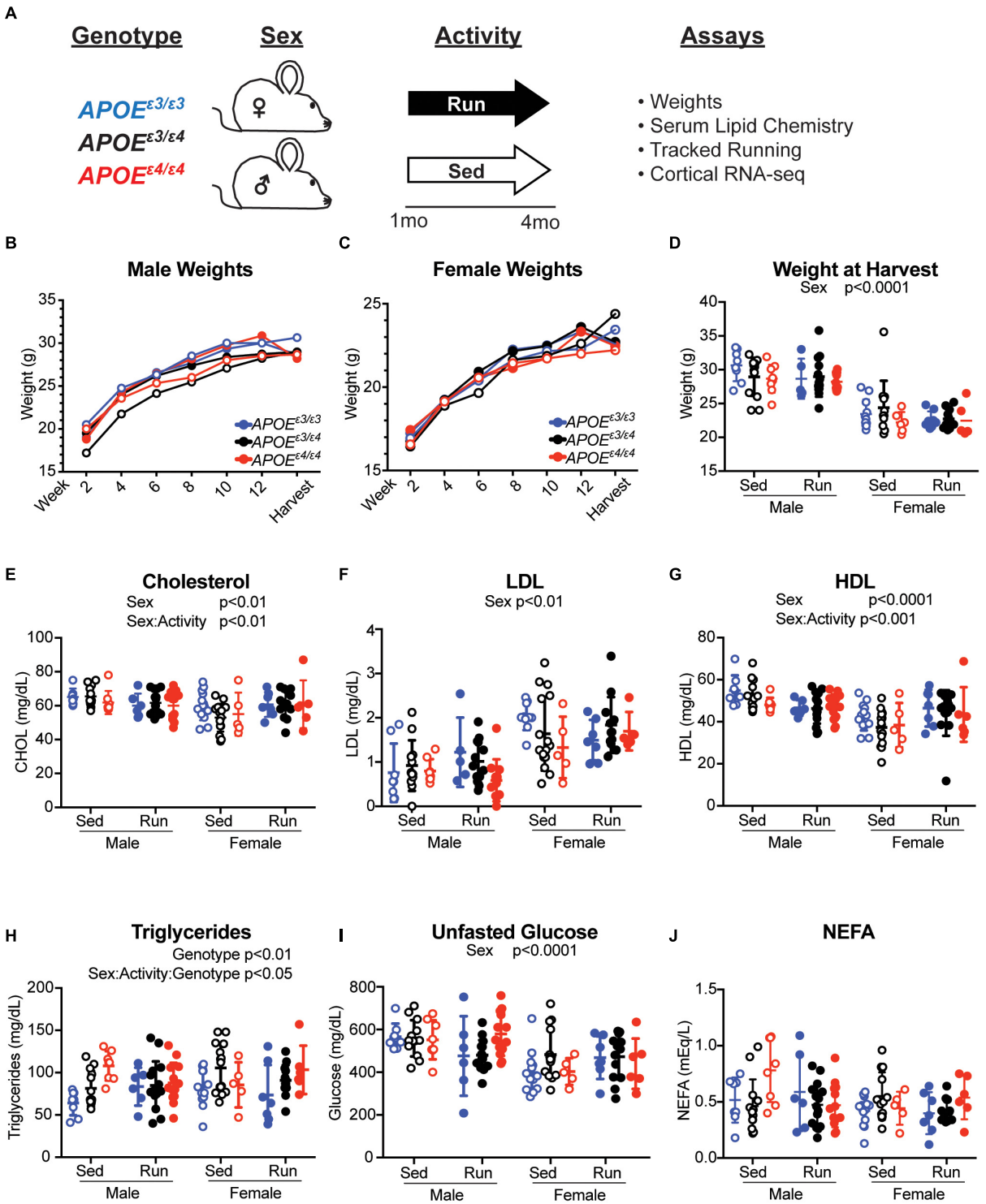

FIGURE 4 | *APOE* genotype did not affect weight or cholesterol composition at 4 months. **(A)** Schematic of experiment and timeline. **(B,C)** Weights of male **(B)** and female **(C)** mice over the course of the running experiment. **(D)** Weight at harvest of both male and female mice across *APOE* genotypes showed a significant effect of sex. **(E)** Plasma total cholesterol concentrations revealed a main effect of sex and an interactive effect between sex and activity. **(F)** LDL concentration revealed a significant effect of sex. **(G)** HDL concentration revealed a significant effect of sex and interactive effect between sex and activity. **(H)** Triglyceride concentrations revealed a significant effect of *APOE* genotype and an interactive effect between sex, activity and *APOE* genotype. **(I)** Unfasted glucose concentrations revealed an effect of sex. **(J)** Non-esterified fatty acid (NEFA) concentrations revealed no significant effects. Significant ANOVA results are stated under the title of the graph, significant Tukey *post hoc* results can be found in **Supplementary Table 2**.

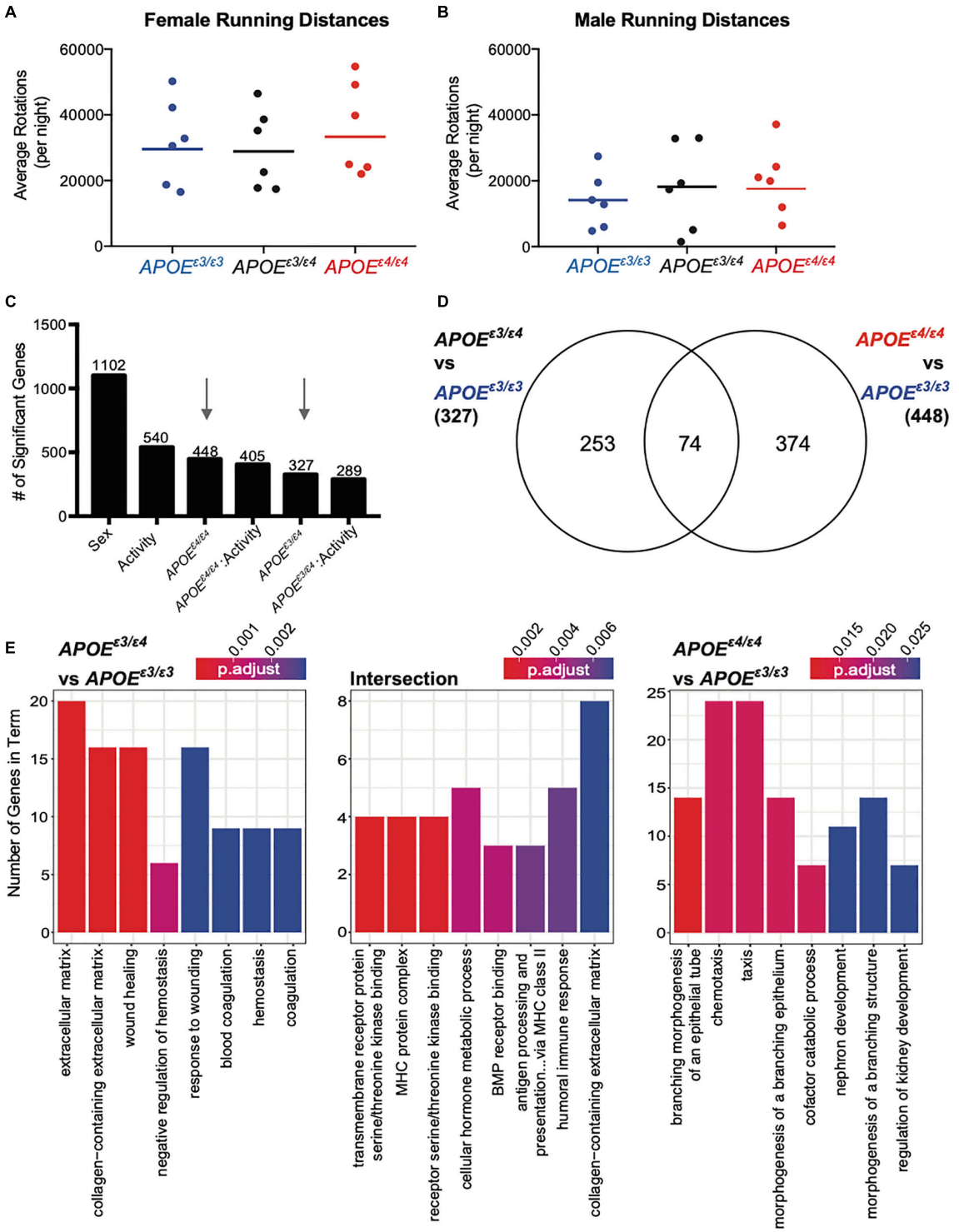

FIGURE 5 | Significant genes unique for *APOE*$^{\varepsilon 3/\varepsilon 4}$ genotype showed functional enrichment for 'extracellular matrix' and 'response to wounding' at 4 months. **(A,B)** Average number of rotations per night during the dark cycle for female **(A)** and males **(B)** across all *APOE* genotypes for the six mice per group that were selected for RNA-seq. Mean is representative of all mice, including those that were not sequenced (see also **Supplementary Figure 8**). **(C)** Number of significant genes per each linear model predictor term. Red arrows highlight *APOE*$^{\varepsilon 4/\varepsilon 4}$ and *APOE*$^{\varepsilon 3/\varepsilon 4}$ terms used in panel **(D)**. **(D)** Number of significant genes unique to *APOE*$^{\varepsilon 3/\varepsilon 4}$ when compared to *APOE*$^{\varepsilon 3/\varepsilon 3}$, and *APOE*$^{\varepsilon 4/\varepsilon 4}$ compared to *APOE*$^{\varepsilon 3/\varepsilon 3}$, as well as the number of significant genes intersecting both groups. **(E)** Functional enrichment of the 253 genes unique to *APOE*$^{\varepsilon 3/\varepsilon 4}$ compared to *APOE*$^{\varepsilon 3/\varepsilon 3}$ (left), 374 genes unique to *APOE*$^{\varepsilon 4/\varepsilon 4}$ compared to *APOE*$^{\varepsilon 3/\varepsilon 3}$ (right) and 74 intersection genes between the two groups (middle) ($p < 0.05$).

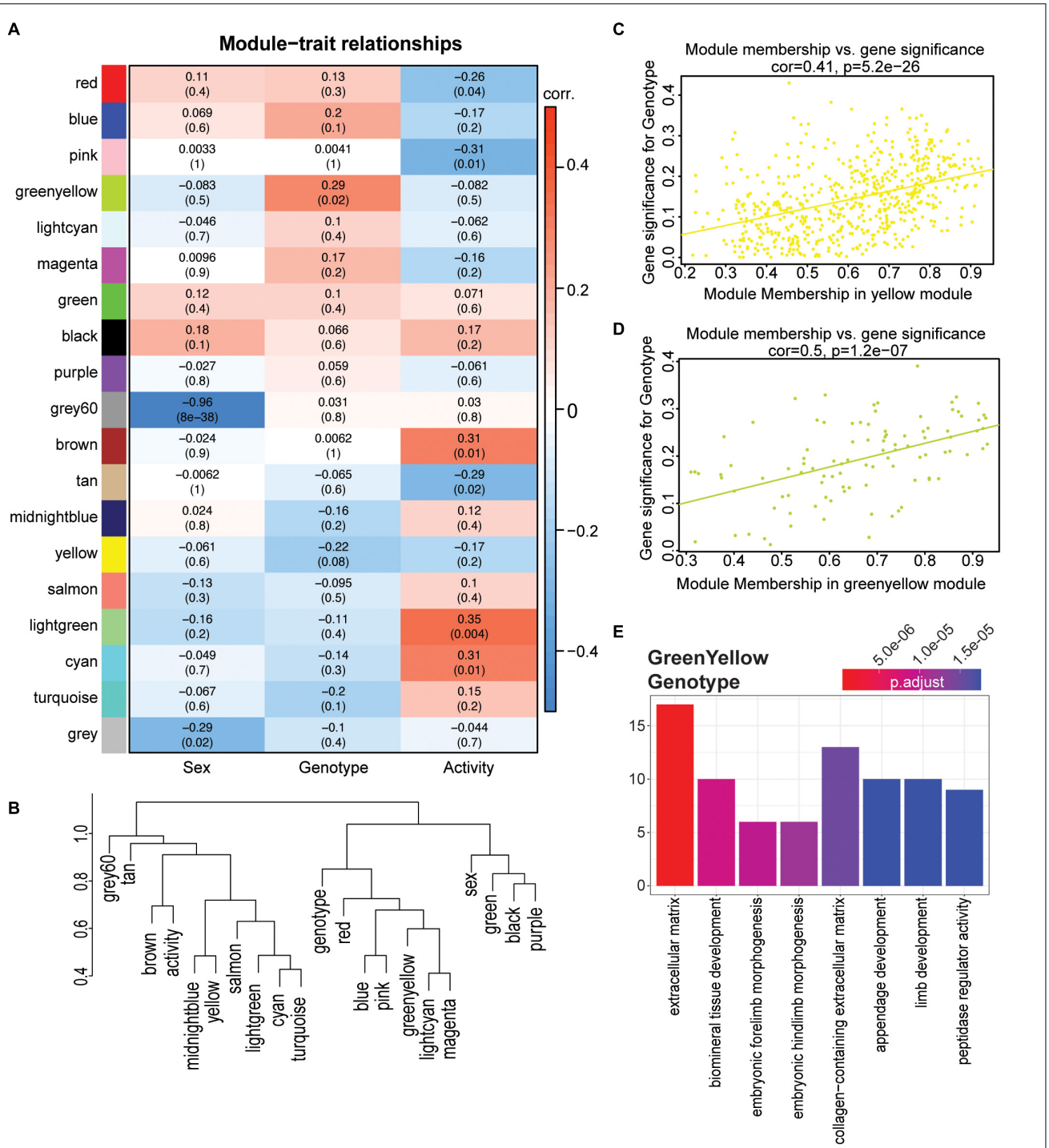

FIGURE 6 | WGCNA confirmed functional enrichment of GO terms relating to extracellular matrix and morphogenesis is affected by *APOE* genotype. **(A)** Heatmap of module correlation and FDR values for sex, *APOE* genotype, and activity ($p < 0.10$). **(B)** Eigengene dendrogram of each module and sex, *APOE* genotype and activity. *Y* axis is a measure of dissimilarity. **(C,D)** Gene significance regressed against module membership to show correlation and significance for the yellow **(C)** and greenyellow **(D)** modules for *APOE* genotype. **(E)** Functional enrichment of the genes in the greenyellow module which is significant for *APOE* genotype ($p < 0.05$).

the effect of activity on plasma cholesterol may be sex-specific at a young age (**Figures 4E,G** and **Supplementary Table 2**). There was a significant sex-activity-genotype interaction on triglyceride concentration (**Figure 4H**). Across total cholesterol and HDL concentration, there was an interesting sex-activity interaction, with activity appearing to have differential effects

per sex. In total cholesterol and HDL there was an overall decrease in lipid concentration with running in males, however in females, there was an overall increase in these lipids. These results suggest that activity may have different effects on circulating lipid concentrations due to sex-based differences. Together, the effects of exercise on cholesterol composition were subtle and not influenced by *APOE* genotype, whereas triglyceride concentrations were influenced by sex, activity, and *APOE* genotype.

Unique $APOE^{\varepsilon 3/\varepsilon 4}$ Genes Enrich for Extracellular Matrix (ECM)- and Coagulation-Related Terms

To determine whether the effects of $APOE^{\varepsilon 4}$ on the brain are modified by running in an *APOE* genotype-specific manner, cortical transcriptional profiling and linear modeling were performed (see the section "Materials and Methods"). Genes significantly associated with sex, $APOE^{\varepsilon 3/\varepsilon 4}$, $APOE^{\varepsilon 4/\varepsilon 4}$, activity and the interactions were identified (**Figures 5A–C** and **Supplementary Figures 8C,D**; Foley et al., 2019). The largest number of genes were significant for sex which enriched for 'response to interferon beta,' 'response to virus,' and 'innate immune response,' including known AD and dementia risk genes *Clu,* and *Plgc2*, suggesting a difference in immune function between the sexes (**Supplementary Figure 10**). There was no enrichment for the 540 genes significant for activity, suggesting multiple processes affected. Of the 540 genes, *Cx3cr1* and Csf1r were significant and have been previously implicated in maintaining microglia homeostasis, suggesting microglia response may be affected by activity across *APOE* genotypes (Keren-Shaul et al., 2017).

Of the 327 genes significant for $APOE^{\varepsilon 3/\varepsilon 4}$ and the 448 genes significant for $APOE^{\varepsilon 4/\varepsilon 4}$ only 74 intersected (22% from $APOE^{\varepsilon 3/\varepsilon 4}$ genes, 17% from $APOE^{\varepsilon 4/\varepsilon 4}$ genes) (**Figure 5D**) which was similar to our findings at 2 mos. Of the 253 genes unique for $APOE^{\varepsilon 3/\varepsilon 4}$ 63 genes were downregulated (negative β value) and 190 were upregulated (β value). The 253 $APOE^{\varepsilon 3/\varepsilon 4}$ unique genes enriched for GO terms such as 'extracellular matrix,' 'collagen-containing extracellular matrix,' and 'wound healing' (**Figure 5E** and **Supplementary Figure 12A**). The 374 $APOE^{\varepsilon 4/\varepsilon 4}$ unique genes enriched for 'branching morphogenesis of an epithelial tube,' 'chemeotaxis' and 'taxis,' including genes such as *Gli3*, *Cx3cr1*, and *Ccr1* (**Figure 5C** and **Supplementary Figure 11A**). Of the 374 genes there were 183 downregulated and 191 genes upregulated, indicated by a negative and a positive β-value, respectively. The 74 intersecting genes enriched for 'MHC protein complex' and 'BMP receptor binding' including genes associated with these GO terms included *Bmp5*, *Bmp6*, and *Spp1* (**Supplementary Figure 11B**). BMP (bone morphogenetic protein) signaling has been previously implicated in vascular development and more importantly, abnormal BMP protein expression can lead to vascular dysfunction, suggesting another pathway by which the $APOE^{\varepsilon 4}$ allele influences AD and dementia pathologies (Garcia de Vinuesa et al., 2016). Of these 74 intersecting genes, 19 genes were downregulated and 55 genes upregulated, although the degree of regulation (β value) was different.

While many cell types can contribute to the extracellular matrix (ECM)- and coagulation-related pathways, endothelial cells contributed to 33% of the unique genes that were in the $APOE^{\varepsilon 3/\varepsilon 4}$ dataset (**Supplementary Figure 12B**). The cell types enriched for intersection genes included both oligodendrocyte precursor cells, as well as microglia (**Supplementary Figure 12B**). No specific cell types appeared to be responsible for $APOE^{\varepsilon 4/\varepsilon 4}$ unique genes. While there is no single cell type contributing to the $APOE^{\varepsilon 4/\varepsilon 4}$-dependent transcriptional differences, endothelial cells may be critical drivers of transcriptional differences in $APOE^{\varepsilon 3/\varepsilon 4}$ mice (**Supplementary Figure 12B**). Interestingly, our data for $APOE^{\varepsilon 4/\varepsilon 4}$-specific changes only minimally overlapped with previous studies (**Supplementary Figure 13**), differences likely due to dissimilarities in study design and environment (Zhao et al., 2020). The $APOE^{\varepsilon 3/\varepsilon 4}$ genotype was not studied previously (Zhao et al., 2020).

In examining genes unique to $APOE^{\varepsilon 3/\varepsilon 4}$ genotype and expressed by endothelial cells we observed several annexin genes. Both *Anxa1* and *Anxa2* contributed to the enrichment terms 'extracellular matrix,' 'response to wound healing,' and 'coagulation.' *Anxa2* has direct effects on the plasminogen/fibrin clotting response (**Supplementary Figure 12C**; Ling et al., 2004). While we expected a linear increase in gene expression with increasing $APOE^{\varepsilon 4}$ gene dose, for endothelial-expressed *Anxa1*, *Anxa2*, and *Anxa3*, there was a significant increase in the $APOE^{\varepsilon 3/\varepsilon 4}$ genotype when compared to $APOE^{\varepsilon 3/\varepsilon 3}$, but not a significant increase in the $APOE^{\varepsilon 4/\varepsilon 4}$ genotype when compared to $APOE^{\varepsilon 3/\varepsilon 3}$. This pattern suggests that expression of some genes was differentially affected by the combination of the $APOE^{\varepsilon 3}$ and $APOE^{\varepsilon 4}$ allele.

To determine whether exercise effects the cortex in an *APOE* genotype-specific manner, we compared the genes for activity-$APOE^{\varepsilon 3/\varepsilon 4}$ with activity-$APOE^{\varepsilon 4/\varepsilon 4}$. Only 17% of activity-$APOE^{\varepsilon 3/\varepsilon 4}$, and 12% of activity-$APOE^{\varepsilon 4/\varepsilon 4}$ genes overlapped (**Supplementary Figure 14A**). Three intersection genes enriched for 'anoikis' (consisting of *Src*, *Tfdp1* and *Bmf*), suggesting a common cell death response between genotypes in response to activity (**Supplementary Figures 14B,C**). Together, these data show that exercise and *APOE* genotype do not appear to overtly interact on a transcriptional level in 4 mo mice.

Weighted Gene Co-expression Network Analysis Confirms Apolipoprotein E Genotype-Specific Effects but Shows No Genotype by Activity-Specific Effects

While linear modeling indicated subtle changes at the gene level, to ensure these changes were robust we employed a second approach, weighted gene co-expression network analysis (WGCNA) on the same 4 mo dataset. We used WGCNA to create modules of groups of genes across the entire dataset, thus reducing complexity of the large number of input genes to produce biologically relevant modules. This method differs from linear modeling by grouping genes into modules, including genes that may not be significant on the gene level, but still contribute

to the coordination of a significant biological process. Nineteen modules were identified, and two modules were significantly correlated with sex (grey60, gray), two modules significantly correlated for genotype (yellow and greenyellow), and six modules significantly correlated for activity (cyan, lightgreen, tan, brown, pink, and red) (**Figure 6A**, see the section "Materials and Methods"). No modules were significant across multiple terms. Module eigengenes were calculated and dissimilarity plotted to visualize the relationship between modules and terms (**Figure 6B**). Both the yellow and greenyellow modules were significantly correlated to *APOE* genotype (**Figures 6C,D**). The yellow module showed no enrichment, however the genes in the greenyellow module enriched for 'extracellular matrix,' 'embryonic morphogenesis,' and 'collagen-containing extracellular matrix' and showed distinct differences between $APOE^{\varepsilon 3/\varepsilon 3}$ and both $APOE^{\varepsilon 3/\varepsilon 4}$ and $APOE^{\varepsilon 4/\varepsilon 4}$ (**Figure 6C** and **Supplementary Figure 14D**). Confirming our previous findings, these data suggest that *APOE* genotype affects the extracellular matrix, collagen, and morphogenesis (**Figure 4**).

The cyan and tan modules were significantly correlated for activity, and cyan enriched for 'ensheathment of neurons,' 'myelination,' and 'gliogenesis,' while the tan module enriched for 'skeletal muscle cell differentiation,' and 'skeletal muscle organ development' (**Supplementary Figures 15A–D**). However, no modules were significant for both *APOE* genotype and activity. These data support our previous findings by linear modeling that suggest the effects of exercise on cortical gene expression are not significantly impacted by *APOE* genotype, at least at this young age.

DISCUSSION

In this study, we demonstrated the importance of including the $APOE^{\varepsilon 3/\varepsilon 4}$ genotype to study the biology of APOE. $APOE^{\varepsilon 3/\varepsilon 4}$ is more common than $APOE^{\varepsilon 4/\varepsilon 4}$ across Caucasian, African America, Hispanic, and Japanese populations, which means there is a stark disconnect between genotypes evaluated in current mouse models to those present in human studies (Farrer et al., 1997). In human studies, the rarity of $APOE^{\varepsilon 4/\varepsilon 4}$ individuals results in a clustering of both $APOE^{\varepsilon 3/\varepsilon 4}$ and $APOE^{\varepsilon 4/\varepsilon 4}$ (often referred to as '$APOE^{\varepsilon 4}$+' or '$APOE^{\varepsilon 4}$ carriers'). These studies have been instrumental in understanding the effect of $APOE^{\varepsilon 4}$ on cognitive health trajectories in humans, finding key biomarkers (e.g., soluble PDGFRβ) that are $APOE^{\varepsilon 4}$+ carrier specific, however the next step requires determining whether this is relevant for $APOE^{\varepsilon 3/\varepsilon 4}$ and $APOE^{\varepsilon 4/\varepsilon 4}$ similarly (Montagne et al., 2020). While informational, these strategies obfuscate differences between the two risk genotypes with the $APOE^{\varepsilon 3/\varepsilon 4}$ effect likely dominating the findings. In contrast, the vast majority of mouse studies performed to date primarily contrast the $APOE^{\varepsilon 4/\varepsilon 4}$ genotype with the $APOE^{\varepsilon 3/\varepsilon 3}$ genotype. Our transcriptome profiling approach predicts the $APOE^{\varepsilon 3/\varepsilon 4}$ genotype exerts unique effects on the cortex, therefore supporting more studies in mouse models to understand mechanisms by which the $APOE^{\varepsilon 3/\varepsilon 4}$ genotype increases risk for ADRDs. Our new humanized *APOE* mouse models and data help to facilitate these mechanistic studies.

Our results indicate that *APOE* genotype did not affect total cholesterol, HDL, or LDL levels in the blood at 2 and 4 mos. These data confirm reports using other humanized *APOE* models, where no *APOE* genotype differences were observed in plasma total cholesterol, HDL, or triglyceride in female mice between 2 and 5 mos (Knouff et al., 1999; Mann et al., 2004). It is of note that there are well-established differences in cholesterol composition between humans and mice due, at least in part, to a lack of cholesterol ester transfer protein (CETP) in mice which aids in the transfer of cholesterol esters depending on triglyceride concentration status (Davidson, 2010). This inability to properly transfer cholesteryl esters and triglycerides results in higher HDL and lower LDL levels in mice (Mabuchi et al., 2014). Cholesterol composition in heterozygous *APOE* genotypes throughout aging are still necessary, as this is when *APOE* genotype differences are reported to become more prominent.

Human studies have reported differences in triglycerides due to *APOE* genotype, with an increase in circulating triglyceride levels for each copy of $APOE^{\varepsilon 4}$. In our study, there was no *APOE* genotype effect on triglyceride levels at 2 mos, but differences were observed at 4 mos (Huang, 2010; Belloy et al., 2019). Data from other humanized *APOE* mice agreed with our 2 mo findings showing no significant difference in triglyceride concentrations between $APOE^{\varepsilon 3/\varepsilon 3}$ and $APOE^{\varepsilon 4/\varepsilon 4}$ mice (Knouff et al., 1999; Mann et al., 2004). While these findings indicate that *APOE* genotype does not affect lipid homeostasis at an early age, genotype-specific differences may come apparent at older ages – studies that are ongoing.

The $APOE^{\varepsilon 3/\varepsilon 4}$ genotype uniquely affected the cortical transcriptome at 2 and 4 mos (using $APOE^{\varepsilon 3/\varepsilon 3}$ as reference in our linear model). At 2 mos, genes unique for $APOE^{\varepsilon 3/\varepsilon 4}$ enriched for 'regulation of hormone levels' and 'insulin secretion.' At 4 mos, genes unique for $APOE^{\varepsilon 3/\varepsilon 4}$ enriched for 'extracellular matrix,' 'collagen-containing extracellular matrix,' and 'blood coagulation,' suggesting that the cerebrovasculature may be compromised. Our cell type analysis showed a greater contribution by endothelial cells in $APOE^{\varepsilon 3/\varepsilon 4}$ for these cerebrovascular terms, however this data is not inclusive of all cells in the cerebrovasculature, such as pericytes which have been shown to be impacted by *APOE* genotype (Montagne et al., 2020). Overall, these data supported our hypothesis that the $APOE^{\varepsilon 3/\varepsilon 4}$ risk genotype confers unique effects compared to $APOE^{\varepsilon 4/\varepsilon 4}$ and signify the need to better understand the effect of heterozygous *APOE* genotypes and how these differences may play a role in risk for dementia. Linear modeling is commonly used to identify significant changes to biological systems, and this is the case for the genotype differences identified in this study.

A previous study using other humanized *APOE* mice sought to examine early transcriptome and proteome changes in the $APOE^{\varepsilon 4/\varepsilon 4}$, $APOE^{\varepsilon 3/\varepsilon 3}$ and $APOE^{\varepsilon 2/\varepsilon 2}$ mouse cortex (Zhao et al., 2020). Analysis of their data with our linear modeling approach identified differences in the number of significant genes found between the two studies. We predict these differences are more likely due to study design, mouse cohort generation, mouse husbandry, environment, tissue harvesting,

and sequencing platform rather than inherent differences between the humanized *APOE* models. However, future studies are necessary to compare the available humanized *APOE* models under the same conditions.

$APOE^{\varepsilon 4}$ carrier females are at a greater risk dementia than their male counterparts. Postmenopausal females account for over 60% of AD cases (Riedel et al., 2016; Mosconi et al., 2018). In women, one $APOE^{\varepsilon 4}$ allele causes an increase in dementia risk equivalent to two $APOE^{\varepsilon 4/\varepsilon 4}$ alleles in men (Riedel et al., 2016). Our study supports that sex-specific $APOE^{\varepsilon 4}$ effects begin early in adolescence/adulthood and would be predicted to exacerbate dementia pathophysiology later in life. When examining the effect of sex by genotype interactions for $APOE^{\varepsilon 4}$ status at 2 mos and then 4 mos, there were more genes significant for sex-$APOE^{\varepsilon 4/\varepsilon 4}$, than sex-$APOE^{\varepsilon 3/\varepsilon 4}$. These data indicate that *APOE* genotype interacts with sex-specific characteristics even at younger ages (as early as adolescence) to differentially predispose females and males to dementia later in life.

The molecular effects of exercise in the context *APOE* genotype are not known. With previous studies suggesting that up to a third of LOAD cases may be prevented by physical activity, it is of the utmost importance to understand the interactions between genetic risk and exercise (Norton et al., 2014). To elucidate the effects of exercise on dementia related pathology, most exercise-based murine studies utilized amyloidogenic models relevant to AD or middle cerebral artery occlusion models of VaD (Yuede et al., 2009; Otsuka et al., 2016; Choi et al., 2018; Khodadadi et al., 2018; Rezaei et al., 2018; Zhang et al., 2018). The few studies that have determined whether exercise is beneficial in the context of *APOE* utilized mostly *APOE* knockout mice (Nichol et al., 2009; Soto et al., 2015; Di Cataldo et al., 2016; Jakic et al., 2019; Zheng and Cai, 2019; Chaudhari et al., 2020). Our experimental design suggests exercise affects young mice in subtle ways that are not greatly impacted by *APOE* genotype, however aging studies may reveal greater *APOE* and exercise interactions. Linear modeling identified genes relevant to ECM health, the blood clotting cascade, development, and microglia homeostasis, all processes that play a role in modulating risk for ADRDs. Separately, WGCNA identified a module that correlated with activity which contained genes that enriched for myelination and gliogenesis (**Supplementary Figure 15C**). Previous studies have shown that voluntary exercise impacts myelination by increasing the proliferation oligodendrocyte precursor cells and mature oligodendrocytes in the motor cortex (Zheng et al., 2019).

Surprisingly, in our study, there were no significant functional enrichment terms for the genes unique to activity-$APOE^{\varepsilon 3/\varepsilon 4}$ and activity-$APOE^{\varepsilon 4/\varepsilon 4}$. It will be important to understand whether longer term exercise paradigms are impacted by *APOE* genotype. $APOE^{\varepsilon 4}$ exhibits harmful effects on the brain, predisposing for AD and cognitive decline. In general, few studies have determined whether long-term exercise is beneficial in the context of *APOE* risk genotypes. Exercise may mitigate or exacerbate $APOE^{\varepsilon 4}$-dependent risk depending on the specific biological process considered.

CONCLUSION

These novel *APOE* models increase the ability to elucidate the mechanisms by which heterozygous *APOE* genotypes increase risk for AD and dementia. Our study predicts important unique effects of the $APOE^{\varepsilon 3/\varepsilon 4}$ genotype on AD-relevant phenotypes including biometrics and cortical gene expression. These differences need to be better understood to properly determine whether the mechanisms increasing risk for diseases such as AD and related dementias in those carrying one *APOE* $^{\varepsilon 4}$ allele are different from those carrying two, particularly as differential *APOE* genotype effects may be exacerbated at older ages. This work supports that research and therapies need to account for the impact of *APOE* $^{\varepsilon 4}$ allele dosage on ADRD risk and pathology.

DATA AVAILABILITY STATEMENT

The data presented in the study are publicly available via www.synapse.org, Synapse ID:syn26561824.

ETHICS STATEMENT

The animal study was reviewed and approved by Animal Care and Use Committee at The Jackson Laboratory.

AUTHOR CONTRIBUTIONS

MS, GC, and GH designed *APOE* mouse models. KF and GH conceived and designed this project and wrote and prepared this manuscript. AH, DG, KK, and KF validated the *APOE* mouse models. KF performed mouse experiments, data collection, and bioinformatic analysis. KF, GC, and GH consulted for statistical approach and analysis. All authors read and approved the final manuscript.

FUNDING

This work was supported by T32HD007065 to KF. Also, the authors are especially grateful to Tucker Taft and his wife Phyllis R. Yale, and the estate of Bennett Bradford and his daughter, Deborah Landry. Their generous and thoughtful support of Alzheimer's research at The Jackson Laboratory supported this study. These funding sources supported study design, data collection and interpretation, and writing of the manuscript. This study is part of the Model Organism Development and Evaluation for Late-onset Alzheimer's Disease (MODEL-AD) consortium funded by the National Institute on Aging. MODEL-AD comprises the Indiana University/The Jackson Laboratory MODEL-AD Center U54 AG054345 led by Bruce T. Lamb, GC, GH, and Paul R. Territo and the University of California, Irvine MODEL-AD Center U54 AG054349 led by Frank M. LaFerla and Andrea J. Tenner. This work was also supported by the

National Institutes of Health grant to The Jackson Laboratory Nathan Shock Center of Excellence in the Basic Biology of Aging (AG038070). The funding organizations played no role in the design and conduct of the study; in the management, analysis, and interpretation of the data; or in the preparation, review, or approval of the article.

ACKNOWLEDGMENTS

We gratefully acknowledge the contribution of Judy Morgan and Leslie Goodwin and the Genetic Engineering Technology Scientific service at The Jackson Laboratory for technical help in generating the mouse models in this publication. We wish to thank Todd Hoffert from Clinical Assessment Services for blood chemistry, Heidi Munger and the Genome Technologies group for RNA-sequencing, and Tim Stearns and Vivek Philip from Computational Sciences.

SUPPLEMENTARY MATERIAL

The Supplementary Material for this article can be found online at: https://www.frontiersin.org/articles/10.3389/fnagi.2022.838436/full#supplementary-material

REFERENCES

Apte, R. S., Chen, D. S., and Ferrara, N. (2019). VEGF in signaling and disease: beyond discovery and development. *Cell* 176, 1248–1264. doi: 10.1016/j.cell.2019.01.021

Area-Gomez, E., Larrea, D., Pera, M., Agrawal, R. R., Guilfoyle, D. N., Pirhaji, L., et al. (2020). APOE4 is associated with differential regional vulnerability to bioenergetic deficits in aged APOE mice. *Sci. Rep.* 10:4277. doi: 10.1038/s41598-020-61142-8

Bell, R. D., Winkler, E. A., Singh, I., Sagare, A. P., Deane, R., Wu, Z., et al. (2012). Apolipoprotein E controls cerebrovascular integrity *via* cyclophilin A. *Nature* 485, 512–516. doi: 10.1038/nature11087

Belloy, M. E., Napolioni, V., and Greicius, M. D. (2019). A quarter century of APOE and Alzheimer's disease: progress to date and the path forward. *Neuron* 101, 820–838. doi: 10.1016/j.neuron.2019.01.056

Botero, J. P., Lee, K., Branchford, B. R., Bray, P. F., Freson, K., Lambert, M. P., et al. (2020). Glanzmann thrombasthenia: genetic basis and clinical correlates. *Haematologica* 105, 888–894. doi: 10.3324/haematol.2018.214239

Chan, M. Y., Zhao, X. L., and Ogle, C. W. (1989). A comparative study on the hepatic toxicity and metabolism of *Crotalaria assamica* and *Eupatorium* species. *Am. J. Chin. Med.* 17, 165–170. doi: 10.1142/S0192415X89000255

Chaudhari, K., Wong, J. M., Vann, P. H., Como, T., O'Bryant, S. E., and Sumien, N. (2020). ApoE genotype-dependent response to antioxidant and exercise interventions on brain function. *Antioxidants* 9:553. doi: 10.3390/antiox9060553

Chernick, D., Ortiz-Valle, S., Jeong, A., Qu, W., and Li, L. (2019). Peripheral versus central nervous system APOE in Alzheimer's disease: Interplay across the blood-brain barrier. *Neurosci. Lett.* 708:134306. doi: 10.1016/j.neulet.2019.134306

Choi, S. H., Bylykbashi, E., Chatila, Z. K., Lee, S. W., Pulli, B., Clemenson, G. D., et al. (2018). Combined adult neurogenesis and BDNF mimic exercise effects on cognition in an Alzheimer's mouse model. *Science* 361:eaan8821. doi: 10.1126/science.aan8821

Davidson, M. H. (2010). Update on CETP inhibition. *J. Clin. Lipidol.* 4, 394–398. doi: 10.1016/j.jacl.2010.08.003

Di Cataldo, V., Geloen, A., Langlois, J. B., Chauveau, F., Theze, B., Hubert, V., et al. (2016). Exercise does not protect against peripheral and central effects of a high cholesterol diet given ad libitum in Old ApoE(-/-) Mice. *Front. Physiol.* 7:453. doi: 10.3389/fphys.2016.00453

Farrer, L. A., Cupples, L. A., Haines, J. L., Hyman, B., Kukull, W. A., Mayeux, R., et al. (1997). Effects of age, sex, and ethnicity on the association between apolipoprotein E genotype and Alzheimer disease. A meta-analysis. APOE and Alzheimer Disease Meta Analysis Consortium. *JAMA* 278, 1349–1356.

Foley, K. E., Yang, H. S., Graham, L. C., and Howell, G. R. (2019). Transcriptional profiling predicts running promotes cerebrovascular remodeling in young but not midlife mice. *BMC Genomics* 20:860. doi: 10.1186/s12864-019-6230-z

Gao, X., and Xu, Z. (2008). Mechanisms of action of angiogenin. *Acta Biochim. Biophys. Sin.* 40, 619–624. doi: 10.1111/j.1745-7270.2008.00442.x

Garcia de Vinuesa, A., Abdelilah-Seyfried, S., Knaus, P., Zwijsen, A., and Bailly, S. (2016). BMP signaling in vascular biology and dysfunction. *Cytokine Growth Factor Rev.* 27, 65–79. doi: 10.1016/j.cytogfr.2015.12.005

Halliday, M. R., Rege, S. V., Ma, Q., Zhao, Z., Miller, C. A., Winkler, E. A., et al. (2016). Accelerated pericyte degeneration and blood-brain barrier breakdown in apolipoprotein E4 carriers with Alzheimer's disease. *J. Cereb. Blood Flow Metab.* 36, 216–227. doi: 10.1038/jcbfm.2015.44

Hauser, P. S., Narayanaswami, V., and Ryan, R. O. (2011). Apolipoprotein E: from lipid transport to neurobiology. *Prog. Lipid Res.* 50, 62–74. doi: 10.1016/j.plipres.2010.09.001

Hervé Pagès, M. C., Falcon, S., and Li, N. (2020). *AnnotationDbi: Manipulation of SQLite-based annotations in Bioconductor. 1.56. 2.* Available online at: https://bioconductor.org/packages/AnnotationDbi

Huang, Y. (2010). Mechanisms linking apolipoprotein E isoforms with cardiovascular and neurological diseases. *Curr. Opin. Lipidol.* 21, 337–345. doi: 10.1097/MOL.0b013e32833af368

Huang, Y. A., Zhou, B., Wernig, M., and Sudhof, T. C. (2017). ApoE2, ApoE3, and ApoE4 Differentially Stimulate APP Transcription and Abeta Secretion. *Cell* 168, 427–441.e21. doi: 10.1016/j.cell.2016.12.044

Huynh, T. V., Wang, C., Tran, A. C., Tabor, G. T., Mahan, T. E., Francis, C. M., et al. (2019). Lack of hepatic apoE does not influence early Abeta deposition: observations from a new APOE knock-in model. *Mol. Neurodegener.* 14:37. doi: 10.1186/s13024-019-0337-1

Irie, F., Fitzpatrick, A. L., Lopez, O. L., Kuller, L. H., Peila, R., Newman, A. B., et al. (2008). Enhanced risk for Alzheimer disease in persons with type 2 diabetes and APOE epsilon4: the Cardiovascular Health Study Cognition Study. *Arch. Neurol.* 65, 89–93. doi: 10.1001/archneurol.2007.29

Jakic, B., Carlsson, M., Buszko, M., Cappellano, G., Ploner, C., Onestingel, E., et al. (2019). The Effects of Endurance Exercise and Diet on Atherosclerosis in Young and Aged ApoE-/- and Wild-Type Mice. *Gerontology* 65, 45–56. doi: 10.1159/000492571

Keren-Shaul, H., Spinrad, A., Weiner, A., Matcovitch-Natan, O., Dvir-Szternfeld, R., Ulland, T. K., et al. (2017). A unique microglia type associated with restricting development of alzheimer's disease. *Cell* 169, 1276–1290.e17. doi: 10.1016/j.cell.2017.05.018

Khodadadi, D., Gharakhanlou, R., Naghdi, N., Salimi, M., Azimi, M., Shahed, A., et al. (2018). Treadmill exercise ameliorates spatial learning and memory deficits through improving the clearance of peripheral and central amyloid-beta levels. *Neurochem. Res.* 43, 1561–1574. doi: 10.1007/s11064-018-2571-2

Knouff, C., Hinsdale, M. E., Mezdour, H., Altenburg, M. K., Watanabe, M., Quarfordt, S. H., et al. (1999). Apo E structure determines VLDL clearance and atherosclerosis risk in mice. *J. Clin. Invest.* 103, 1579–1586. doi: 10.1172/JCI6172

Koizumi, K., Hattori, Y., Ahn, S. J., Buendia, I., Ciacciarelli, A., Uekawa, K., et al. (2018). Apoepsilon4 disrupts neurovascular regulation and undermines white matter integrity and cognitive function. *Nat. Commun.* 9:3816. doi: 10.1038/s41467-018-06301-2

Langfelder, P., and Horvath, S. (2008). WGCNA: an R package for weighted correlation network analysis. *BMC Bioinformatics* 9:559. doi: 10.1186/1471-2105-9-559

Langfelder, P., and Horvath, S. (2012). Fast R functions for robust correlations and hierarchical clustering. *J. Stat. Softw.* 46:i11.

Langmead, B., Trapnell, C., Pop, M., and Salzberg, S. L. (2009). Ultrafast and memory-efficient alignment of short DNA sequences to the human genome. *Genome Biol.* 10:R25. doi: 10.1186/gb-2009-10-3-r25

Lein, E. S., Hawrylycz, M. J., Ao, N., Ayres, M., Bensinger, A., Bernard, A., et al. (2007). Genome-wide atlas of gene expression in the adult mouse brain. *Nature* 445, 168–176.

Ling, Q., Jacovina, A. T., Deora, A., Febbraio, M., Simantov, R., Silverstein, R. L., et al. (2004). Annexin II regulates fibrin homeostasis and neoangiogenesis *in vivo*. *J. Clin. Invest.* 113, 38–48. doi: 10.1172/JCI19684

Liu, C. C., Zhao, N., Fu, Y., Wang, N., Linares, C., Tsai, C. W., et al. (2017). ApoE4 Accelerates Early Seeding of Amyloid Pathology. *Neuron* 96, 1024–1032.e3. doi: 10.1016/j.neuron.2017.11.013

Liu, M., Kuhel, D. G., Shen, L., Hui, D. Y., and Woods, S. C. (2012). Apolipoprotein E does not cross the blood-cerebrospinal fluid barrier, as revealed by an improved technique for sampling CSF from mice. *Am. J. Physiol. Regul. Integr. Comp. Physiol.* 303, R903–R908. doi: 10.1152/ajpregu.00219.2012

Love, M. I., Huber, W., and Anders, S. (2014). Moderated estimation of fold change and dispersion for RNA-seq data with DESeq2. *Genome Biol.* 15:550. doi: 10.1186/s13059-014-0550-8

Mabuchi, H., Nohara, A., and Inazu, A. (2014). Cholesteryl ester transfer protein (CETP) deficiency and CETP inhibitors. *Mol. Cells* 37, 777–784. doi: 10.14348/molcells.2014.0265

Mahley, R. W., and Rall, S. C. Jr. (2000). Apolipoprotein E: far more than a lipid transport protein. *Annu. Rev. Genomics Hum. Genet.* 1, 507–537. doi: 10.1146/annurev.genom.1.1.507

Mann, K. M., Thorngate, F. E., Katoh-Fukui, Y., Hamanaka, H., Williams, D. L., Fujita, S., et al. (2004). Independent effects of APOE on cholesterol metabolism and brain Abeta levels in an Alzheimer disease mouse model. *Hum. Mol. Genet.* 13, 1959–1968. doi: 10.1093/hmg/ddh199

Miyake, M., Goodison, S., Lawton, A., Gomes-Giacoia, E., and Rosser, C. J. (2015). Angiogenin promotes tumoral growth and angiogenesis by regulating matrix metallopeptidase-2 expression *via* the ERK1/2 pathway. *Oncogene* 34, 890–901. doi: 10.1038/onc.2014.2

Montagne, A., Nation, D. A., Sagare, A. P., Barisano, G., Sweeney, M. D., Chakhoyan, A., et al. (2020). APOE4 leads to blood-brain barrier dysfunction predicting cognitive decline. *Nature* 581, 71–76. doi: 10.1038/s41586-020-2247-3

Moroianu, J., and Riordan, J. F. (1994). Nuclear translocation of angiogenin in proliferating endothelial cells is essential to its angiogenic activity. *Proc. Natl. Acad. Sci. U.S.A.* 91, 1677–1681. doi: 10.1073/pnas.91.5.1677

Mosconi, L., Rahman, A., Diaz, I., Wu, X., Scheyer, O., Hristov, H. W., et al. (2018). Increased Alzheimer's risk during the menopause transition: a 3-year longitudinal brain imaging study. *PLoS One* 13:e0207885. doi: 10.1371/journal.pone.0207885

Nagai, N., and Minami, T. (2015). Emerging Role of VEGFC in pathological angiogenesis. *EBioMedicine* 2, 1588–1589. doi: 10.1016/j.ebiom.2015.11.006

Neuner, S. M., Heuer, S. E., Huentelman, M. J., O'Connell, K. M. S., and Kaczorowski, C. C. (2019). Harnessing genetic complexity to enhance translatability of Alzheimer's disease mouse models: a path toward precision medicine. *Neuron* 101, 399–411.e5. doi: 10.1016/j.neuron.2018.11.040

Nichol, K., Deeny, S. P., Seif, J., Camaclang, K., and Cotman, C. W. (2009). Exercise improves cognition and hippocampal plasticity in APOE epsilon4 mice. *Alzheimers Dement.* 5, 287–294. doi: 10.1016/j.jalz.2009.02.006

Norton, S., Matthews, F. E., Barnes, D. E., Yaffe, K., and Brayne, C. (2014). Potential for primary prevention of Alzheimer's disease: an analysis of population-based data. *Lancet Neurol.* 13, 788–794. doi: 10.1016/S1474-4422(14)70136-X

Oksala, N., Parssinen, J., Seppala, I., Klopp, N., Illig, T., Laaksonen, R., et al. (2015). Kindlin 3 (FERMT3) is associated with unstable atherosclerotic plaques, anti-inflammatory type II macrophages and upregulation of beta-2 integrins in all major arterial beds. *Atherosclerosis* 242, 145–154. doi: 10.1016/j.atherosclerosis.2015.06.058

Otsuka, S., Sakakima, H., Sumizono, M., Takada, S., Terashi, T., and Yoshida, Y. (2016). The neuroprotective effects of preconditioning exercise on brain damage and neurotrophic factors after focal brain ischemia in rats. *Behav. Brain Res.* 303, 9–18. doi: 10.1016/j.bbr.2016.01.049

Patel, R. K., and Jain, M. (2012). NGS QC Toolkit: a toolkit for quality control of next generation sequencing data. *PLoS One* 7:e30619. doi: 10.1371/journal.pone.0030619

Peila, R., Rodriguez, B. L., Launer, L. J., and Honolulu-Asia Aging, S. (2002). Type 2 diabetes, APOE gene, and the risk for dementia and related pathologies: the Honolulu-Asia Aging Study. *Diabetes* 51, 1256–1262. doi: 10.2337/diabetes.51.4.1256

Ramaswamy, G., Xu, Q., Huang, Y., and Weisgraber, K. H. (2005). Effect of domain interaction on apolipoprotein E levels in mouse brain. *J. Neurosci.* 25, 10658–10663. doi: 10.1523/JNEUROSCI.1922-05.2005

Rezaei, R., Nasoohi, S., Haghparast, A., Khodagholi, F., Bigdeli, M. R., and Nourshahi, M. (2018). High intensity exercise preconditioning provides differential protection against brain injury following experimental stroke. *Life Sci.* 207, 30–35. doi: 10.1016/j.lfs.2018.03.007

Riedel, B. C., Thompson, P. M., and Brinton, R. D. (2016). Age, APOE and sex: triad of risk of Alzheimer's disease. *J. Steroid. Biochem. Mol. Biol.* 160, 134–147. doi: 10.1016/j.jsbmb.2016.03.012

Rohn, T. T. (2014). Is apolipoprotein E4 an important risk factor for vascular dementia? *Int. J. Clin. Exp. Pathol.* 7, 3504–3511.

Rohn, T. T., and Moore, Z. D. (2017). Nuclear Localization of Apolipoprotein E4: a new trick for an old protein. *Int. J. Neurol. Neurother.* 4:067. doi: 10.23937/2378-3001/1410067

Shi, Y., Yamada, K., Liddelow, S. A., Smith, S. T., Zhao, L., Luo, W., et al. (2017). ApoE4 markedly exacerbates tau-mediated neurodegeneration in a mouse model of tauopathy. *Nature* 549, 523–527. doi: 10.1038/nature24016

Soto, I., Graham, L. C., Richter, H. J., Simeone, S. N., Radell, J. E., Grabowska, W., et al. (2015). APOE stabilization by exercise prevents aging neurovascular dysfunction and complement induction. *PLoS Biol.* 13:e1002279. doi: 10.1371/journal.pbio.1002279

Sullivan, P. M., Mezdour, H., Aratani, Y., Knouff, C., Najib, J., Reddick, R. L., et al. (1997). Targeted replacement of the mouse apolipoprotein E gene with the common human APOE3 allele enhances diet-induced hypercholesterolemia and atherosclerosis. *J. Biol. Chem.* 272, 17972–17980. doi: 10.1074/jbc.272.29.17972

Tammela, T., Zarkada, G., Wallgard, E., Murtomaki, A., Suchting, S., Wirzenius, M., et al. (2008). Blocking VEGFR-3 suppresses angiogenic sprouting and vascular network formation. *Nature* 454, 656–660. doi: 10.1038/nature07083

Vanlandewijck, M., He, L., Mae, M. A., Andrae, J., Ando, K., Del Gaudio, F., et al. (2018). A molecular atlas of cell types and zonation in the brain vasculature. *Nature* 554, 475–480.

Varner, J. A., Brooks, P. C., and Cheresh, D. A. (1995). REVIEW: the integrin alpha V beta 3: angiogenesis and apoptosis. *Cell Adhes. Commun.* 3, 367–374. doi: 10.3109/15419069509081020

Wang, Y., and Brinton, R. D. (2016). Triad of risk for late onset Alzheimer's: mitochondrial haplotype, APOE genotype and chromosomal sex. *Front. Aging Neurosci.* 8:232. doi: 10.3389/fnagi.2016.00232

Williams, T., Borchelt, D. R., and Chakrabarty, P. (2020). Therapeutic approaches targeting Apolipoprotein E function in Alzheimer's disease. *Mol. Neurodegener.* 15:8. doi: 10.1186/s13024-020-0358-9

Yu, G., Wang, L. G., Han, Y., and He, Q. Y. (2012). clusterProfiler: an R package for comparing biological themes among gene clusters. *OMICS* 16, 284–287. doi: 10.1089/omi.2011.0118

Yuede, C. M., Zimmerman, S. D., Dong, H., Kling, M. J., Bero, A. W., Holtzman, D. M., et al. (2009). Effects of voluntary and forced exercise on plaque deposition, hippocampal volume, and behavior in the Tg2576 mouse model of Alzheimer's disease. *Neurobiol. Dis.* 35, 426–432. doi: 10.1016/j.nbd.2009.06.002

Zhang, J., Guo, Y., Wang, Y., Song, L., Zhang, R., and Du, Y. (2018). Long-term treadmill exercise attenuates Abeta burdens and astrocyte activation in APP/PS1 mouse model of Alzheimer's disease. *Neurosci. Lett.* 666, 70–77. doi: 10.1016/j.neulet.2017.12.025

Zhang, Y., Chen, K., Sloan, S. A., Bennett, M. L., Scholze, A. R., O'Keeffe, S., et al. (2014). An RNA-sequencing transcriptome and splicing database of glia, neurons, and vascular cells of the cerebral cortex. *J. Neurosci.* 34, 11929–11947.

Zhang, Y., Sloan, S. A., Clarke, L. E., Caneda, C., Plaza, C. A., Blumenthal, P. D., et al. (2016). Purification and Characterization of Progenitor and Mature Human Astrocytes Reveals Transcriptional and Functional Differences with Mouse. *Neuron* 89, 37–53. doi: 10.1016/j.neuron.2015.11.013

Zhao, N., Ren, Y., Yamazaki, Y., Qiao, W., Li, F., Felton, L. M., et al. (2020). Alzheimer's Risk Factors Age, APOE Genotype, and Sex Drive Distinct Molecular Pathways. *Neuron* 106, 727–742.e6.

Zheng, F., and Cai, Y. (2019). Concurrent exercise improves insulin resistance and nonalcoholic fatty liver disease by upregulating PPAR-gamma and genes involved in the beta-oxidation of fatty acids in ApoE-KO mice fed a high-fat diet. *Lipids Health Dis.* 18:6. doi: 10.1186/s12944-018-0933-z

Zheng, J., Sun, X., Ma, C., Li, B. M., and Luo, F. (2019). Voluntary wheel running promotes myelination in the motor cortex through Wnt signaling in mice. *Mol. Brain* 12:85. doi: 10.1186/s13041-019-0506-8

Conflict of Interest: The authors declare that the research was conducted in the absence of any commercial or financial relationships that could be construed as a potential conflict of interest.

frontiers | Frontiers in Aging Neuroscience

ORIGINAL RESEARCH
published: 25 May 2022
doi: 10.3389/fnagi.2022.819499

Analysis of Genetic Association Between *ABCA7* Polymorphism and Alzheimer's Disease Risk in the Southern Chinese Population

Lijun Wang[1], Yang Jiao[1], Aonan Zhao[1], Xiaomeng Xu[1], Guanyu Ye[1], Yichi Zhang[1], Ying Wang[1], Yulei Deng[1], Wei Xu[1] and Jun Liu[1,2]**

[1] Department of Neurology and Institute of Neurology, Ruijin Hospital, Shanghai Jiao Tong University School of Medicine, Shanghai, China, [2] CAS Center for Excellence in Brain Science and Intelligence Technology, Ruijin Hospital, Shanghai Jiao Tong University School of Medicine, Shanghai, China

OPEN ACCESS

Edited by:
Nilton Custodio, Peruvian Institute of Neurosciences (IPN), Peru

Reviewed by:
Mario Reynaldo Cornejo-Olivas, National Institute of Neurological Sciences, Peru
Claudio Villegas-Llerena, Universidad de San Martín de Porres, Peru

***Correspondence:**
Wei Xu
xw11246@rjh.com.cn
Jun Liu
jly0520@hotmail.com

Specialty section:
This article was submitted to Alzheimer's Disease and Related Dementias, a section of the journal Frontiers in Aging Neuroscience

Received: 21 November 2021
Accepted: 19 April 2022
Published: 25 May 2022

Citation:
Wang L, Jiao Y, Zhao A, Xu X, Ye G, Zhang Y, Wang Y, Deng Y, Xu W and Liu J (2022) Analysis of Genetic Association Between ABCA7 Polymorphism and Alzheimer's Disease Risk in the Southern Chinese Population. Front. Aging Neurosci. 14:819499. doi: 10.3389/fnagi.2022.819499

Objective: The study aimed to clarify the association of the 21 single nucleotide polymorphisms (SNPs) with Alzheimer's disease (AD) in the population of southern China.

Methods: A case-control study was conducted with a total sample size of 490 subjects (246 patients with AD and 244 age- and gender-matched healthy controls) enrolled in this study. Twenty-one selected SNPs were detected using SNaPshot assay and polymerase chain reaction (PCR) technique. Then, we assessed how these SNPs correlated with AD susceptibility.

Results: The results showed that rs3764650 of *ABCA7* was closely correlated with risen AD morbidity in the allele [P = 0.010, odds ratio (OR) = 1.43, 95% confidence interval (CI) 1.09–1.89], dominant (P = 0.004, OR = 1.71, 95% CI 1.19–2.46), and additive (P = 0.012, OR = 1.42, 95% CI 1.08–1.86) models. However, rs4147929 of *ABCA7* was related to higher AD risk in the allele (P = 0.006, OR = 1.45, 95% CI 1.11–1.89), dominant (P = 0.012, OR = 1.59, 95% CI 1.11–2.27), and additive (P = 0.010, OR = 1.40, 95% CI 1.08–1.81) models. In addition, the frequencies of the G-allele at rs3764650 (P = 0.030) and the A-allele at rs4147929 (P = 0.001) in AD were statistically higher in *APOE* ε4 carriers in comparison to non-carriers.

Conclusion: This study demonstrated that the G-allele at rs3764650 and the A-allele at rs4147929 appeared at higher risk for developing AD, particularly in *APOE* ε4 carriers. Moreover, it was observed that rs3764650 and rs4147929 of *ABCA7* were linked to AD. More in-depth research with a relatively large sample is needed to make the results more convincing.

Keywords: Alzheimer's disease, *ABCA7*, rs4147929, rs3764650, single nucleotide polymorphisms

INTRODUCTION

Alzheimer's disease (AD), an eye-catching neurodegenerative disorder in the elderly, has an increased burden dramatically on the global economic development and health care systems (Alzheimer's Association, 2021). It is characterized by progressive deterioration of cognitive function and function impairment resulting from extracellular deposition of β-amyloid (Aβ) plaques and neuronal accumulation of neurofibrillary tangles formed by hyperphosphorylated tau protein and brain atrophy (Blennow et al., 2006; De Strooper and Karran, 2016; DeTure and Dickson, 2019; Andrews et al., 2020). Genetic factors play a crucial role in the pathogenesis of AD (Jansen et al., 2019; Kunkle et al., 2019). The most strongly and consistently associated with AD risk gene is *apolipoprotein E* (*APOE*) (Liu et al., 2013; Yamazaki et al., 2019; Serrano-Pozo et al., 2021). Previous genome-wide association studies (GWASs) have found and defined up to 20 AD susceptibility loci, including *ABCA7*, *BIN1, CLU, CR1, PICALM*, *SORL1,* and so on (Harold et al., 2009; Lambert et al., 2009, 2013; Steinberg et al., 2015; Vardarajan et al., 2015; Giri et al., 2016; Kunkle et al., 2019). Recently, studies have reported that *GRN, TMEM106B, Complement C7, RBFOX1* genes are associated with AD in various cohorts (Viswanathan et al., 2009; Lee et al., 2011; Rutherford et al., 2012; Lu et al., 2014; Jun et al., 2016; Xu et al., 2017; Kunkle et al., 2019; Hu et al., 2021). In addition, hippocampal sclerosis of aging (HS-Aging) is a common, high morbidity brain disorder that occurs in the elderly with a clinical course similar to AD. *ABCC9* and *KCNMB2* have previously been shown to be associated with HS-Aging (Nelson et al., 2014; Nho and Saykin, 2016; Katsumata et al., 2017; Dugan et al., 2021). However, most of these studies were performed statistically limited in Caucasian populations, and the inheritance of AD in other populations is relatively limited. Repeating the GWAS results in different ethnic groups can help identify SNPs that are associated with AD (Chanock et al., 2007). However, the results in other populations of European descent were inconsistent with those in the southern Chinese population. Therefore, how these candidate loci and AD in the southern Chinese population are related was still not clear. Consequently, in the present study, 21 SNPs were selected from the above studies to investigate how genes affected the AD morbidity of the southern Chinese.

MATERIALS AND METHODS

Study Design and Participants

A sum of 246 patients with AD (137 females and 109 males, average age ± *SD*: 71.26 ± 8.46 years) were collected from September 2016 to September 2020 from the neurology outpatient clinic at Ruijin Hospital affiliated with Shanghai Jiao Tong University School of Medicine. Patients with AD dementia fulfilled the National Institute of Neurological and Communicative Disorders and Stroke–Alzheimer's Disease and Related Disorders Association (NINCDS-ADRDA) criteria for probable AD (Dubois et al., 2007). Global cognitive abilities were measured on a scale of 0 (severely impaired) to 30 points (no impaired) using the Mini-mental Status Evaluation (MMSE) test and at least one other cognitive deficit beyond memory impairment. All participants involved were assessed by more than two neurologists with profound experience and received a couple of standard tests, including but not limited to physical examinations, medical history, and neuropsychological and neuroimaging examinations. Conversely, participants recorded with other neurological disorders, which could cause dementia were excluded (McKhann et al., 2011; Janelidze et al., 2018). So, a final total of 244 healthy controls (HC) matched for age and gender (137 females and 107 males, average age ± *SD*: 71.10 ± 8.31) were voluntarily enrolled in Shanghai, China. Healthy subjects were strictly evaluated by doctors to confirm that they have no symptoms of cognitive decline and do not comply with the criteria for mild cognitive impairment (MCI) or AD dementia (McKhann et al., 2011; Jack et al., 2018). Demographic information of the participants was presented in **Table 1**. This research was authorized by the Committee on Medical Ethics of Ruijin Hospital affiliated with Shanghai Jiao Tong University School of Medicine. A signed informed consent by the Declaration of Helsinki was submitted by the participants.

DNA Extraction and Genotype Analysis

The genomic DNA was extracted from blood (2 ml) stored in an ethylene diamine tetraacetie acid (EDTA) anticoagulation tube using the phenol-chloroform-isopropyl alcohol method. Polymerase chain reaction (PCR) and extension primers scheme were achieved through Primer 5 software (PREMIER Biosoft International, Version 5.00). PCR materials were conducted by purification with phosphorylase (FastAP, Applied Biosystems) and exonuclease I (EXO I, Applied Biosystems). A consequent extension was applied by the ABI SNaPshot Multiplex Kit (Applied Biosystems). Extended products were purified with FastAP and loaded into ABI3730xl (Applied Biosystems). GeneMapper 4.0 (Applied Biosystems) was used to conduct data analysis. The SNaPshot technique (Applied Biosystems) was utilized for genotyping of SNPs. The following SNPs were tested: rs10792832, rs11136000, rs11218343, rs1990620, rs1990622, rs3173615, rs34860942, rs3764650, rs3792646, rs3818361, rs3851179, rs4147929, rs56081887, rs5848, rs6656401, rs6701713, rs6733839, rs704180, rs744373, rs9331888, and rs9637454. The SNPs rs429358 and rs7412 of the *APOE* gene were determined by Sanger sequencing. Details of primers were described in **Supplementary Table 1**.

Statistical Analysis

Statistical evaluations involved in the paper were conducted using SPSS software (two-sided significance level: P-value < 0.05) (version 26.0; IBM SPSS) or PLINK (Purcell et al., 2007) version 1.9.[1] The SNP with minor allele frequencies (MAF) < 0.01, call rate $< 95\%$, or not in Hardy-Weinberg equilibrium (HWE) were excluded. Differences in age, education level, and MMSE score between the two groups were examined for continuous variables using the Student's t-test or non-parametric Mann-Whitney U-test. Dichotomous variables (such as gender, genotype distribution, allele frequency, and HWE) evaluations

[1]http://pngu.mgh.harvard.edu/purcell/plink/

were conducted by the chi-square test. Then, logistic regression analysis adjusting for age and gender was used to figure out the odds ratio (OR) and 95% confidence intervals (CI) under varied genetic models (allele, dominant, recessive, and additive). It was defined that "A" means the major allele and "a" is the minor allele in the paper. We also defined dominant as 1 (aa + Aa) vs. 0 (AA), recessive as 1 (aa) vs. 0 (AA + Aa), and additive as 0 (AA) vs. 1 (Aa) vs. 2 (aa). Furthermore, the Bonferroni correction method was applied to perform multiple tests with aim to make the conclusion statistically convincing. G*Power software was used to evaluate all the SNPs' genetic power.

RESULTS

Demographic Characteristics of the Subjects

A total of 246 patients with AD and 244 age- and gender-matched healthy controls were enrolled. No statistically significant difference was found in age and gender between AD and the control group (all $P > 0.05$). In addition, patients with AD were less educated in comparison to the control group ($P < 0.001$), which matched well with the previous studies (Xu et al., 2016; Larsson et al., 2017). Patients with AD showed statistically significant lower MMSE scores compared with healthy controls ($P < 0.001$). Moreover, the patients with AD showed a much higher proportion of *APOE* ε4 allele carriers than the control subjects ($P < 0.001$). Detailed information about the participants was summarized in **Table 1**.

TABLE 1 | Demographic and clinical characteristics of subjects included in the study.

Characteristics	AD (*n* = 246)	CN (*n* = 244)	*P*-value
Age, years	71.26 ± 8.46	71.10 ± 8.31	0.835
Education, years	8.82 ± 4.53	10.90 ± 3.84	**<0.001**
MMSE	15.72 ± 6.28	28.81 ± 1.26	**<0.001**
Female, *n* (%)	137 (55.69)	137 (56.15)	0.919
APOE genotype, *n* (%)			
ε2/ε2	2 (0.81)	2 (0.82)	
ε2/ε3	20 (8.13)	28 (11.48)	
ε2/ε4	4 (1.63)	5 (2.05)	
ε3/ε3	98 (39.84)	160 (65.57)	
ε3/ε4	90 (36.59)	49 (20.08)	
ε4/ε4	32 (13.01)	0 (0)	
APOE ε4 carriers, *n* (%)	126 (51.22)	54 (22.13)	**<0.001**

AD, Alzheimer's Disease; APOE, Apolipoprotein E; MMSE, Mini Mental Status Evaluation. Demographic data were measured using non-parametric Mann-Whitney U-test for skewed distribution variable. For gender, genotype distribution and allele frequencies, values were expressed as number (%) using chi-square test. Bold values denote significant difference.

Association Analysis of Single Nucleotide Polymorphisms and Alzheimer's Disease in Various Genetic Models

The genotype distribution of all SNPs in AD and controls was consistent with HWE. The minimum allele and genotype frequencies for all related SNPs were shown in **Supplementary Table 2**. Significant statistical differences were noted in the allele frequencies of rs3764650 ($P = 0.010$) and rs4147929 ($P = 0.006$) between patients with AD and the healthy ones. Regarding SNP genotype frequencies, it was detected that at rs3764650, the genotypes TT and GT experienced a higher risk for AD than the genotype GG, while at rs4147929, the genotypes GG and AG experienced a higher risk of AD than the genotype AA. Also, statistically significant difference also existed between patients with AD and controls of genotype frequencies in rs3764650 ($P = 0.015$) and rs4147929 ($P = 0.030$). The higher *APOE* level enhanced the risk of developing AD as shown in **Table 1**. Hence, these data were stratified by *APOE* ε4 levels to determine whether they impacted the correlation between SNPs and AD susceptibility. Among *APOE* ε4 carriers, the allele and genotype frequencies of *ABCA7* rs3764650 were substantially different between AD and control cases [allele: $P = 0.030$, odds ratio (OR) = 1.80, 95% confidence interval (CI) 1.05–3.06, genotype: $P = 0.034$], and allele G was higher in the AD group than that in the control group (**Table 2A**). After adjusting for age and gender, the dominant and additive models of rs3764650 were nominally significantly related to AD (dominant model: $P = 0.016$, OR = 2.32, 95% CI 1.17–4.59; additive model: $P = 0.043$, OR = 1.77, 95% CI 1.02–3.08) (**Table 2A**). However, after the Bonferroni correction, these associations did not persist. Moreover, among *APOE* ε4 carriers, the allele and genotype frequencies of *ABCA7* rs4147929 showed the obvious difference between patients with AD and healthy controls (allele: $P = 0.001$, OR = 2.49, 95% CI 1.42–4.37, genotype: $P = 0.003$), with allele A higher in the case group than that in the control group (**Table 2B**). After adjusting for age and gender, the dominant and additive models of rs4147929 were related to AD (dominant model: $P = 0.002$, OR = 3.06, 95% CI 1.52–6.17; additive model: $P = 0.004$, OR = 2.33, 95% CI 1.31–4.13) (**Table 2B**). Bonferroni correction was needed to confirm the relationship. To further examine the *ABCA7* genetic association of AD, four genetic models including allele, dominant, recessive, and additive models were analyzed by logistic regression (**Table 3** and **Supplementary Table 3**). The results revealed that rs3764650 of *ABCA7* was correlated with the AD morbidity in the allele model ($P = 0.010$, OR = 1.43, 95% CI 1.09–1.89) without adjusting the age and gender, dominant ($P = 0.004$, OR = 1.71, 95% CI 1.19–2.46), and additive ($P = 0.012$, OR = 1.42, 95% CI 1.08–1.86) models after adjusting the age and gender. In addition, rs4147929 of *ABCA7* was correlated with the risk of developing AD in the allele ($P = 0.006$, OR = 1.45, 95% CI 1.11–1.89) without adjusting the age and gender, dominant ($P = 0.012$, OR = 1.59, 95% CI 1.11–2.27) and additive ($P = 0.010$, OR = 1.40, 95% CI 1.08–1.81) models after adjusting the age and gender. Again, the conclusion also needs to be confirmed by Bonferroni correction.

DISCUSSION

The interaction between rs3764650 and rs4147929 of *ABCA7* and the risk factors of AD in southern China was validated in the

TABLE 2A | Association of rs3764650 of *ABCA7* gene with AD risk stratified by *APOE* ε4 status.

rs3764650	MAF (AD/control)	Allele		Genotype	Dominant model (adjusted)		Recessive model (adjusted)		Additive model (adjusted)	
		P-value	OR (95% CI)	*P*-value	*P*-value	OR (95% CI)	*P*-value	OR (95% CI)	*P*-value	OR (95% CI)
Total	0.356/0.278	0.010	1.43 (1.09–1.89)	0.015	0.004	1.71 (1.19–2.46)	0.419	1.27 (0.71–2.26)	0.012	1.42 (1.08–1.86)
APOE ε4(+)	0.349/0.230	**0.030**	1.80 (1.05–3.06)	**0.034**	**0.016**	2.32 (1.17–4.59)	0.709	1.26 (0.38–4.13)	**0.043**	1.77 (1.02–3.08)
APOE ε4(-)	0.363/0.291	0.066	1.38 (0.98–1.96)	0.187	0.083	1.51 (0.95–2.42)	0.335	1.42 (0.70–2.87)	0.085	1.35 (0.96–1.89)

TABLE 2B | Association of rs4147929 of *ABCA7* gene with AD risk stratified by *APOE* ε4 status.

rs4147929	MAF (AD/control)	Allele		Genotype	Dominant model (adjusted)		Recessive model (adjusted)		Additive model (adjusted)	
		P-value	OR (95% CI)	*P*-value	*P*-value	OR (95% CI)	*P*-value	OR (95% CI)	*P*-value	OR (95% CI)
Total	0.382/0.299	0.006	1.45 (1.11–1.89)	0.030	0.012	1.59 (1.11–2.27)	0.101	1.54 (0.92–2.59)	0.010	1.40 (1.08–1.81)
APOE ε4(+)	0.369/0.190	**0.001**	2.49 (1.42–4.37)	**0.003**	**0.002**	3.06 (1.52–6.17)	0.200	2.32 (0.64–8.36)	**0.004**	2.33 (1.31–4.13)
APOE ε4(-)	0.396/0.327	0.083	1.35 (0.96–1.89)	0.236	0.290	1.29 (0.81–2.06)	0.119	1.64 (0.88–3.07)	0.129	1.28 (0.93–1.77)

AD, Alzheimer's Disease; Allele, minor allele; CI, confidence interval; MAF, minor allele frequency; OR, odds ratio. Dominant was defined as 1 (aa + Aa) vs. 0 (AA), recessive was defined as 1 (aa) vs. 0 (AA + Aa), and additive was defined as 0 (AA) vs. 1 (Aa) vs. 2 (aa). (A: major allele, a: minor allele). P allele and P genotype was examined using Chi-square test. P-value was adjusted for age and gender by logistic regression analysis. Bold values were indicated the significant results.

TABLE 3 | Association of SNPs of candidate genes and odds ratio to AD risk.

Gene	SNP	Minor allele	Allele model			Dominant model (Adjusted)			Recessive model (Adjusted)			Additive model (Adjusted)		
			P-value	OR	95% CI	*P*-value	OR	95% CI	*P*-value	OR	95% CI	*P*-value	OR	95% CI
ABCA7	rs3764650	**G**	**0.010**	1.43	1.09–1.89	**0.004**	1.71	1.19–2.46	0.419	1.27	0.71–2.26	**0.012**	1.42	1.08–1.86
ABCA7	rs4147929	**A**	**0.006**	1.45	1.11–1.89	**0.012**	1.59	1.11–2.27	0.101	1.54	0.92–2.59	**0.010**	1.40	1.08–1.81

AD, Alzheimer's Disease; CI, confidence interval; OR, odds ratio; SNP, single nucleotide polymorphism. P allele was examined using the Chi-square test. P-value was adjusted for age and gender with logistic regression. Bold indicates statistically significant values.

paper. Differences among *APOE* ε4 carriers were more dominant when allele and genotype distributions were stratified by *APOE* ε4 status. It was found that individuals with a heterozygote GT at rs3764650 had a higher susceptibility to AD, while individuals with heterozygote AG at rs4147929 suffered higher AD morbidity. But the relationship between the remaining SNPs and AD was not replicated in the southern Chinese group. Similarly, varied populations could suffer different AD risk genetic variants. Last but not least, the relatively limited sample compared to recent consortium-based GWAS may lead to the dismissal of replication.

A highly conserved protein, a part of the ABCB family of ATP-binding cassette (ABC) transporters, was encoded by the *ABCA7*, which was known as ATP-binding cassette subfamily A member 7 (Takahashi et al., 2005). The *ABCA7* also plays a role in the transportation of cholesterol across membranes (Le Guennec et al., 2016), particularly in the hippocampal CA1 neurons and microglia (Kim et al., 2005), suggesting a role in amyloid clearance and fibril formation (Chan et al., 2008; Aikawa et al., 2018). Recently, some studies investigated the interaction between *ABCA7* rs3764650 polymorphism and the morbidity of AD. However, the results were controversial (Hollingworth et al., 2011; Allen et al., 2012; Lambert et al., 2013; Reitz et al., 2013). Our study confirmed that *ABCA7* rs3764650 might be important genetic factor in the pathophysiology of AD. Furthermore, previous researchers found that the *ABCA7* rs4147929 might be a predisposing factor for late-onset AD (Hollingworth et al., 2011; Lambert et al., 2013; Talebi et al., 2020). In line with that, this study provides supportive evidence for the relationship between rs4147929 and AD. However, it should be noted that the conclusion needs further verification. Meanwhile, the shortcoming of our study is that there is no distinction between early-onset and late-onset AD, and further

subgroup research stratified by age of onset will be carried out in the future.

The research plays an important role in figuring out the basic genes of AD in the Asian population and offers useful findings that genetic risk factors varied in different populations. It should be noted that there are certain limitations in the study. Most importantly, the relatively small-sized sample due to its single-centered nature may affect the validity. A consequent meta-analysis of the Asian population with a bigger sample size should be conducted. Secondly, follow-up studies are required to evaluate more participants' loci for AD susceptibility. Simultaneously, the participants involved here should be followed regularly to find their cognitive variations and figure out the association between genetic polymorphisms and clinical performance. Last but not least, we will conduct a comprehensive neuropsychological battery to assess cognitive function in the future study.

CONCLUSION

In summary, this study suggested that the G-allele at rs3764650 and the A-allele at rs4147929 appeared at higher risk for developing AD in the southern Chinese population, particularly in *APOE* ε4 carriers. In addition, rs3764650 and rs4147929 of *ABCA7* were observed to be associated with AD. Further investigations on the role of the risk genes in the pathogenesis of AD are essential in the following research.

DATA AVAILABILITY STATEMENT

The original contributions presented in the study are included in the article/**Supplementary Material**, further inquiries can be directed to the corresponding author/s.

ETHICS STATEMENT

The studies involving human participants were reviewed and approved by this research was permitted by the Committee on Medical Ethics of Ruijin Hospital Affiliated to Shanghai Jiao Tong University School of Medicine. The patients/participants provided their written informed consent to participate in this study.

AUTHOR CONTRIBUTIONS

JL and WX conceived and designed the studies. LW analyzed the results and wrote the manuscript. LW, YJ, AZ, XX, GY, YZ, YW, and YD performed the research. All authors contributed to the article and approved the submitted version.

FUNDING

This work was supported by the National Natural Science Foundation of China (82071415 and 81873778).

ACKNOWLEDGMENTS

We thank all the patients and healthy controls who participated in this study.

SUPPLEMENTARY MATERIAL

The Supplementary Material for this article can be found online at: https://www.frontiersin.org/articles/10.3389/fnagi.2022.819499/full#supplementary-material

REFERENCES

Aikawa, T., Holm, M. L., and Kanekiyo, T. (2018). Abca7 and pathogenic pathways of alzheimer's disease. *Brain Sci.* 8:27.

Allen, M., Zou, F., Chai, H. S., Younkin, C. S., Crook, J., Pankratz, V. S., et al. (2012). Novel late-onset alzheimer disease loci variants associate with brain gene expression. *Neurology* 79, 221–228. doi: 10.1212/WNL.0b013e3182605801

Alzheimer's Association (2021). 2021 Alzheimer's disease facts and figures. *Alzheimers Dement.* 17, 327–406. doi: 10.1002/alz.12328

Andrews, S. J., Fulton-Howard, B., and Goate, A. (2020). Interpretation of risk loci from genome-wide association studies of alzheimer's disease. *Lancet Neurol.* 19, 326–335. doi: 10.1016/S1474-4422(19)30435-1

Blennow, K., de Leon, M. J., and Zetterberg, H. (2006). Alzheimer's disease. *Lancet* 368, 387–403.

Chan, S. L., Kim, W. S., Kwok, J. B., Hill, A. F., Cappai, R., Rye, K. A., et al. (2008). Atp-binding cassette transporter a7 regulates processing of amyloid precursor protein in vitro. *J. Neurochem.* 106, 793–804. doi: 10.1111/j.1471-4159.2008.05433.x

Chanock, S. J., Manolio, T., Boehnke, M., Boerwinkle, E., Hunter, D. J., Thomas, G., et al. (2007). Replicating genotype-phenotype associations. *Nature* 447, 655–660.

De Strooper, B., and Karran, E. (2016). The cellular phase of alzheimer's disease. *Cell* 164, 603–615.

DeTure, M. A., and Dickson, D. W. (2019). The neuropathological diagnosis of alzheimer's disease. *Mol. Neurodegener.* 14:32.

Dubois, B., Feldman, H. H., Jacova, C., DeKosky, S. T., Barberger-Gateau, P., Cummings, J., et al. (2007). Research criteria for the diagnosis of alzheimer's disease: revising the nincds–adrda criteria. *Lancet Neurol.* 6, 734–746. doi: 10.1016/S1474-4422(07)70178-3

Dugan, A. J., Nelson, P. T., Katsumata, Y., Shade, L. M. P., Boehme, K. L., Teylan, M. A., et al. (2021). Analysis of genes (tmem106b, grn, abcc9, kcnmb2, and apoe) implicated in risk for late-nc and hippocampal sclerosis provides pathogenetic insights: a retrospective genetic association study. *Acta Neuropathol. Commun.* 9:152. doi: 10.1186/s40478-021-01250-2

Giri, M., Zhang, M., and Lu, Y. (2016). Genes associated with alzheimer's disease: an overview and current status. *Clin. Interv. Aging* 11, 665–681. doi: 10.2147/CIA.S105769

Harold, D., Abraham, R., Hollingworth, P., Sims, R., Gerrish, A., Hamshere, M. L., et al. (2009). Genome-wide association study identifies variants at clu and picalm associated with alzheimer's disease. *Nat. Genet.* 41, 1088–1093. doi: 10.1038/ng.440

Hollingworth, P., Harold, D., Sims, R., Gerrish, A., Lambert, J. C., Carrasquillo, M. M., et al. (2011). Common variants at abca7, ms4a6a/ms4a4e, epha1, cd33 and cd2ap are associated with alzheimer's disease. *Nat. Genet.* 43, 429–435. doi: 10.1038/ng.803

Hu, Y., Sun, J. Y., Zhang, Y., Zhang, H., Gao, S., Wang, T., et al. (2021). Rs1990622 variant associates with alzheimer's disease and regulates tmem106b expression in human brain tissues. *BMC Med.* 19:11. doi: 10.1186/s12916-020-01883-5

Jack, C. R. Jr., Bennett, D. A., Blennow, K., Carrillo, M. C., Dunn, B., Haeberlein, S. B., et al. (2018). Nia-aa research framework: toward a biological definition of

alzheimer's disease. *Alzheimers Dement.* 14, 535–562. doi: 10.1016/j.jalz.2018.02.018

Janelidze, S., Mattsson, N., Stomrud, E., Lindberg, O., Palmqvist, S., Zetterberg, H., et al. (2018). Csf biomarkers of neuroinflammation and cerebrovascular dysfunction in early alzheimer disease. *Neurology.* 91, e867–e877. doi: 10.1212/WNL.0000000000006082

Jansen, I. E., Savage, J. E., Watanabe, K., Bryois, J., Williams, D. M., Steinberg, S., et al. (2019). Genome-wide meta-analysis identifies new loci and functional pathways influencing alzheimer's disease risk. *Nat. Genet.* 51, 404–413.

Jun, G., Ibrahim-Verbaas, C. A., Vronskaya, M., Lambert, J. C., Chung, J., Naj, A. C., et al. (2016). A novel alzheimer disease locus located near the gene encoding tau protein. *Mol. Psychiatry* 21, 108–117. doi: 10.1038/mp.2015.23

Katsumata, Y., Nelson, P. T., Ellingson, S. R., and Fardo, D. W. (2017). Gene-based association study of genes linked to hippocampal sclerosis of aging neuropathology: Grn, tmem106b, abcc9, and kcnmb2. *Neurobiol. Aging* 53, 193.e17-193.e25. doi: 10.1016/j.neurobiolaging.2017.01.003

Kim, W. S., Fitzgerald, M. L., Kang, K., Okuhira, K., Bell, S. A., Manning, J. J., et al. (2005). Abca7 null mice retain normal macrophage phosphatidylcholine and cholesterol efflux activity despite alterations in adipose mass and serum cholesterol levels. *J. Biol. Chem.* 280, 3989–3995. doi: 10.1074/jbc.M412602200

Kunkle, B. W., Grenier-Boley, B., Sims, R., Bis, J. C., Damotte, V., Naj, A. C., et al. (2019). Genetic meta-analysis of diagnosed alzheimer's disease identifies new risk loci and implicates abeta, tau, immunity and lipid processing. *Nat. Genet.* 51, 414–430.

Lambert, J. C., Heath, S., Even, G., Campion, D., Sleegers, K., Hiltunen, M., et al. (2009). Genome-wide association study identifies variants at clu and cr1 associated with alzheimer's disease. *Nat. Genet.* 41, 1094–1099. doi: 10.1038/ng.439

Lambert, J. C., Ibrahim-Verbaas, C. A., Harold, D., Naj, A. C., Sims, R., Bellenguez, C., et al. (2013). Meta-analysis of 74,046 individuals identifies 11 new susceptibility loci for alzheimer's disease. *Nat. Genet.* 45, 1452–1458. doi: 10.1038/ng.2802

Larsson, S. C., Traylor, M., Malik, R., Dichgans, M., Burgess, S., Markus, H. S., et al. (2017). Modifiable pathways in alzheimer's disease: mendelian randomisation analysis. *BMJ* 359:j5375. doi: 10.1136/bmj.j5375

Le Guennec, K., Nicolas, G., Quenez, O., Charbonnier, C., Wallon, D., Bellenguez, C., et al. (2016). ABCA7 rare variants and Alzheimer disease risk. *Neurology* 86, 2134–2137.

Lee, M. J., Chen, T. F., Cheng, T. W., and Chiu, M. J. (2011). Rs5848 variant of progranulin gene is a risk of alzheimer's disease in the taiwanese population. *Neurodegener. Dis.* 8, 216–220. doi: 10.1159/000322538

Liu, C. C., Liu, C. C., Kanekiyo, T., Xu, H., and Bu, G. (2013). Apolipoprotein e and alzheimer disease: risk, mechanisms and therapy. *Nat. Rev. Neurol.* 9, 106–118. doi: 10.1038/nrneurol.2012.263

Lu, R. C., Wang, H., Tan, M. S., Yu, J. T., and Tan, L. (2014). Tmem106b and apoe polymorphisms interact to confer risk for late-onset alzheimer's disease in han chinese. *J. Neural Transm.* 121, 283–287. doi: 10.1007/s00702-013-1106-x

McKhann, G. M., Knopman, D. S., Chertkow, H., Hyman, B. T., Jack, C. R. Jr., Kawas, C. H., et al. (2011). The diagnosis of dementia due to alzheimer's disease: recommendations from the national institute on aging-alzheimer's association workgroups on diagnostic guidelines for alzheimer's disease. *Alzheimers Dement.* 7, 263–269. doi: 10.1016/j.jalz.2011.03.005

Nelson, P. T., Estus, S., Abner, E. L., Parikh, I., Malik, M., Neltner, J. H., et al. (2014). Abcc9 gene polymorphism is associated with hippocampal sclerosis of aging pathology. *Acta Neuropathol.* 127, 825–843. doi: 10.1007/s00401-014-1282-2

Nho, K., and Saykin, A. J. (2016). Alzheimer's disease neuroimaging I, Nelson PT. Hippocampal sclerosis of aging, a common alzheimer's disease 'mimic': risk genotypes are associated with brain atrophy outside the temporal lobe. *J. Alzheimers Dis.* 52, 373–383. doi: 10.3233/JAD-160077

Purcell, S., Neale, B., Todd-Brown, K., Thomas, L., Ferreira, M. A., Bender, D., et al. (2007). Plink: a tool set for whole-genome association and population-based linkage analyses. *Am. J. Hum. Genet.* 81, 559–575. doi: 10.1086/519795

Reitz, C., Jun, G., Naj, A., Rajbhandary, R., Vardarajan, B. N., Wang, L. S., et al. (2013). Variants in the atp-binding cassette transporter (abca7), apolipoprotein e 4,and the risk of late-onset alzheimer disease in african americans. *JAMA* 309, 1483–1492. doi: 10.1001/jama.2013.2973

Rutherford, N. J., Carrasquillo, M. M., Li, M., Bisceglio, G., Menke, J., and Josephs, K. A. (2012). TMEM106B risk variant is implicated in the pathologic presentation of Alzheimer disease. *Neurology* 79, 717–718. doi: 10.1212/WNL.0b013e318264e3ac

Serrano-Pozo, A., Das, S., and Hyman, B. T. (2021). Apoe and alzheimer's disease: advances in genetics, pathophysiology, and therapeutic approaches. *Lancet Neurol.* 20, 68–80. doi: 10.1016/S1474-4422(20)30412-9

Steinberg, S., Stefansson, H., Jonsson, T., Johannsdottir, H., Ingason, A., Helgason, H., et al. (2015). Loss-of-function variants in abca7 confer risk of alzheimer's disease. *Nat. Genet.* 47, 445–447. doi: 10.1038/ng.3246

Takahashi, K., Kimura, Y., Nagata, K., Yamamoto, A., Matsuo, M., and Ueda, K. (2005). Abc proteins: key molecules for lipid homeostasis. *Med. Mol. Morphol.* 38, 2–12. doi: 10.1007/s00795-004-0278-8

Talebi, M., Delpak, A., Khalaj-Kondori, M., Sadigh-Eteghad, S., Talebi, M., Mehdizadeh, E., et al. (2020). Abca7 and epha1 genes polymorphisms in late-onset alzheimer's disease. *J. Mol. Neurosci.* 70, 167–173.

Vardarajan, B. N., Zhang, Y., Lee, J. H., Cheng, R., Bohm, C., Ghani, M., et al. (2015). Coding mutations insorl1and alzheimer disease. *Ann. Neurol.* 77, 215–227.

Viswanathan, J., Makinen, P., Helisalmi, S., Haapasalo, A., Soininen, H., and Hiltunen, M. (2009). An association study between granulin gene polymorphisms and alzheimer's disease in finnish population. *Am. J. Med. Genet. B Neuropsychiatr. Genet.* 150B, 747–750. doi: 10.1002/ajmg.b.30889

Xu, H. M., Tan, L., Wan, Y., Tan, M. S., Zhang, W., Zheng, Z. J., et al. (2017). Pgrn is associated with late-onset alzheimer's disease: a case-control replication study and meta-analysis. *Mol. Neurobiol.* 54, 1187–1195. doi: 10.1007/s12035-016-9698-4

Xu, W., Tan, L., Wang, H. F., Tan, M. S., Tan, L., Li, J. Q., et al. (2016). Education and risk of dementia: dose-response meta-analysis of prospective cohort studies. *Mol. Neurobiol.* 53, 3113–3123. doi: 10.1007/s12035-015-9211-5

Yamazaki, Y., Zhao, N., Caulfield, T. R., Liu, C. C., and Bu, G. (2019). Apolipoprotein e and alzheimer disease: pathobiology and targeting strategies. *Nat. Rev. Neurol.* 15, 501–518. doi: 10.1038/s41582-019-0228-7

Conflict of Interest: The authors declare that the research was conducted in the absence of any commercial or financial relationships that could be construed as a potential conflict of interest.

frontiers | Frontiers in Aging Neuroscience

TYPE Original Research
PUBLISHED 05 September 2022
DOI 10.3389/fnagi.2022.969817

OPEN ACCESS

EDITED BY
Robert Petersen,
Central Michigan University,
United States

REVIEWED BY
Valentina Bessi,
University of Florence, Italy
Valerio Napolioni,
University of Camerino, Italy
Anastasia Gurinovich,
Tufts Medical Center, United States

*CORRESPONDENCE
Sabina Capellari
sabina.capellari@unibo.it

†These authors have contributed equally to this work and share first authorship

SPECIALTY SECTION
This article was submitted to Alzheimer's Disease and Related Dementias, a section of the journal Frontiers in Aging Neuroscience

RECEIVED 15 June 2022
ACCEPTED 02 August 2022
PUBLISHED 05 September 2022

CITATION
Bartoletti-Stella A, Tarozzi M, Mengozzi G, Asirelli F, Brancaleoni L, Mometto N, Stanzani-Maserati M, Baiardi S, Linarello S, Spallazzi M, Pantieri R, Ferriani E, Caffarra P, Liguori R, Parchi P and Capellari S (2022) Dementia-related genetic variants in an Italian population of early-onset Alzheimer's disease. *Front. Aging Neurosci.* 14:969817. doi: 10.3389/fnagi.2022.969817

Dementia-related genetic variants in an Italian population of early-onset Alzheimer's disease

Anna Bartoletti-Stella[1†], Martina Tarozzi[1†], Giacomo Mengozzi[2], Francesca Asirelli[3], Laura Brancaleoni[2,4], Nicola Mometto[5], Michelangelo Stanzani-Maserati[2], Simone Baiardi[1,2], Simona Linarello[6], Marco Spallazzi[7], Roberta Pantieri[2], Elisa Ferriani[8], Paolo Caffarra[9], Rocco Liguori[2,10], Piero Parchi[2,10] and Sabina Capellari[2,10]*

[1]Department of Experimental Diagnostic and Specialty Medicine (DIMES), University of Bologna, Bologna, Italy, [2]IRCCS Istituto delle Scienze Neurologiche di Bologna, Bellaria Hospital, Bologna, Italy, [3]Department of Medical Science and Surgery (DIMEC), University of Bologna, Bologna, Italy, [4]Neurologia e Rete Stroke Metropolitana, Ospedale Maggiore, Bologna, Italy, [5]UOC Neurologia, Ospedale Guglielmo da Saliceto, Piacenza, Italy, [6]Programma Cure Intermedie - Azienda USL di Bologna, Bologna, Italy, [7]U.O. di Neurologia, Azienda Ospedaliero-Universitaria, Parma, Italy, [8]UOC Psicologia Clinica Ospedaliera, Ospedale Bellaria, Azienda USL di Bologna, Bologna, Italy, [9]Unità di Neuroscienze, Università di Parma, Parma, Italy, [10]Department of Biomedical and NeuroMotor Sciences (DIBINEM), University of Bologna, Bologna, Italy

Early-onset Alzheimer's disease (EOAD) is the most common form of early-onset dementia. Although three major genes have been identified as causative, the genetic contribution to the disease remains unsolved in many patients. Recent studies have identified pathogenic variants in genes representing a risk factor for developing Alzheimer's disease (AD) and in causative genes for other degenerative dementias as responsible for EOAD. To study them further, we investigated a panel of candidate genes in 102 Italian EOAD patients, 45.10% of whom had a positive family history and 21.74% with a strong family history of dementia. We found that 10.78% of patients carried pathogenic or likely pathogenic variants, including a novel variant, in *PSEN1*, *PSEN2*, or *APP*, and 7.84% showed homozygosity for the ε4 *APOE* allele. Additionally, 7.84% of patients had a moderate risk allele in *PSEN1*, *PSEN2*, or *TREM2* genes. Besides, we observed that 12.75% of our patients carried only a variant in genes associated with other neurodegenerative diseases. The combination of these variants contributes to explain 46% of cases with a definite familiarity and 32% of sporadic forms. Our results confirm the importance of extensive

genetic screening in EOAD for clinical purposes, to select patients for future treatments and to contribute to the definition of overlapping pathogenic mechanisms between AD and other forms of dementia.

KEYWORDS

Alzheimer's disease, early onset Alzheimer disease, next generation sequencing, genetic heterogeneity, mutation screening

Introduction

Alzheimer's disease (AD) is the most common form of dementia in the elderly and is associated with environmental and genetic components. Approximately 10% of patients with AD have an early onset disease (<65 years, EOAD) (Cacace et al., 2016) in which the heritability is between 92 and 100% (Wingo et al., 2012). Conversely, late onset AD (LOAD) is genetically more complex with heritability estimates of 58–70% (Gatz et al., 2006; Wingo et al., 2012). Still, the genetic factors identified account only for a portion of the genetic basis of the disease. To date, only about 33% of the genetic variance in sporadic AD is accounted for by common variants, and ultra-rare, rare and low-frequency variants that typically have a more harmful impact on protein function may be significant to the 'missing heritability' of AD (Khani et al., 2022). A proportion of 35–60% of EOAD patients have at least one affected first-degree relative (Campion et al., 1999; Brickell et al., 2006), while in 10–15%, the inheritance is autosomal dominant. Pathogenic variants in presenilin 1 (*PSEN1*), presenilin 2 (*PSEN2*) and amyloid precursor protein (*APP*) genes, the main autosomal dominant genetic causes, explain 5–10% of EOAD and about 50% of familial forms (Cacace et al., 2016). New data suggest that a mix of common and rare variants may cause unexplained cases that follow a non-Mendelian pattern of inheritance (Mrdjen et al., 2019). On the other hand, sporadic LOAD is considered a complex trait for which approximately 40 disease-associated genes/loci have been reported, exerting moderate to high pathogenic effects (Kunkle et al., 2019; Bellenguez et al., 2020), which have often been confirmed in EOAD (Cochran et al., 2019; Lacour et al., 2019). Among these, the ε4 allele of the apolipoprotein E (*APOE*) gene is not only a major genetic risk factor for LOAD, increasing the risk of disease by 3-fold in heterozygous and 15-fold in homozygous carriers (Genin et al., 2011), but also for EOAD. In these patients, the risk of disease increases more significantly than in LOADs in both ε4 homozygous and heterozygous carriers with a positive family history (Cochran et al., 2019). Furthermore, truncating and pathogenic variants in the ATP binding cassette subfamily A member 7 (*ABCA7*), Sortilin-related receptor 1, (*SORL1*), and Triggering receptor expressed on myeloid cells 2, (*TREM2*) genes were shown to act in a Mendelian mode in EOAD (Bellenguez et al., 2017). Additionally, a role in the disease was demonstrated for variants in genes involved in other types of neurodegenerative dementia (Cacace et al., 2016; Bartoletti-Stella et al., 2018, 2020; Sassi et al., 2018; Bonvicini et al., 2019; Giau et al., 2019; Wang et al., 2019; Park et al., 2020; Tarozzi et al., 2022), supporting the hypothesis of overlapping molecular mechanisms and a shared genetic basis. It is also likely that variants specific to individual populations, and thus difficult to detect with genome-wide ass1ociation study (GWAS) approaches unless the population is homogenous, may explain at least a portion of the missing heritability of EOAD. In addition, other inheritance patterns should be considered, e.g., autosomal recessive loci might cause EOAD (Moreno-Grau et al., 2021).

To investigate the role of rare variants in a well-characterized EOAD population of Italian origin, we analyzed 102 EOAD patients by a Next-Generation Sequencing (NGS) multigene panel covering causal and risk factor genes for AD and genes related to other forms of dementia.

Materials and methods

Participants

The EOAD consecutive unrelated patients referred to the Cognitive Disorders and Dementia Center of the UOC Clinica Neurologica, IRCCS Institute of Neurological Sciences of Bologna, from 2004 to 2019, either as outpatients, inpatients, or sent for genetic analysis, were recruited.

The AD was diagnosed according to the 2011 NIA-AA and International Working Group 2 criteria (McKhann et al., 2011; Dubois et al., 2014). All patients had evidence of AD pathophysiological process as defined by the presence of a characteristic AD CSF biomarker profile, calculated using in-house cutoff values [phosphorylated (p)-tau/Aβ42 ratio > 0.108 and total Aβ42/Aβ40 ratio < 0.68] as reported in Abu-Rumeileh et al. (2018). The strength of a patient's family history was quantified with the modified Goldman score (Goldman et al., 2005) as reported in Cochran et al. (2019). Briefly, S1 Score: at least three people in two generations affected by EOAD, with one being a first-degree relative of the other two; S1.5 is the same

as S1 but LOAD instead of EOAD; S2: at least three relatives with AD without complete autosomal dominant inheritance; S3: a single first- or second-degree family member affected with EOAD; S3.5 same as S3 but LOAD instead of EOAD. We considered patients with strong familiarity those with S1 and S1.5 scores, and with moderate family history if linked to S2, S3 or S3.5 scores.

Next generation sequencing

Genomic DNA from peripheral blood was isolated using the Maxwell 16 extractor (Promega, Madison, WI, United States) and quantified using the Quantus Fluorometer (Promega) with QuantiFluor double-stranded DNA system. Genetic screening was performed by Next Generation Sequencing (NGS) multigene panels, by using either one of the following panels: amplicon-based Illumina panel (Bartoletti-Stella et al., 2018) and probe-based Illumina panel (Truseq Neurodegeneration Illumina). Sequencing was performed on a MiSeq or NextSeq 500 sequencer using Illumina V2 reagent kit, with 2 × 150 bp paired end read cycles. Sequencing data were analyzed with an in-house bioinformatic pipeline: trimming and quality assessment of raw reads was performed with Trimmomatic (Bolger et al., 2014), mapping was performed with Burrows-Wheeler Aligner (Li and Durbin, 2009) using bwa-mem algorithm on the reference genome GRCh37/Hg19. Variant calling was performed with Strelka2 (Kim et al., 2018). Variant filtration and depth of coverage analysis were performed using Genome Analysis Toolkit (GATK) v4 (McKenna et al., 2010).

Variant classification

Variants annotation and selection were performed with BaseSpace Variant Interpreter (Illumina, CA, United States). Variants [single-nucleotide variants (SNV) and small indels] in the coding region or in the flanking 7 bp were filtered and selected with the following criteria: (i) sequence read depth at least 10× (ii) for heterozygous variants, an allelic balance value in the range of 0.30 and 0.70 (iii) Minor Allele Frequency (MAF) in the European population reported on the Genome Aggregation Database (GnomAD) (Karczewski et al., 2020) < 1%. Selected variants were classified according to the American College of Medical Genetics and Genomics guidance for the interpretation of sequence variants (Richards et al., 2015). Those reported in ClinVar (Landrum et al., 2018) or HGMD (Stenson et al., 2003) databases were classified accordingly as known disease-causing variants (Pathogenic) or variants of uncertain significance (VUS). To predict the pathogenicity of never reported variants, we performed several *in silico* analyses. The functional consequences of missense variants were predicted by four *in silico* models: Polyphen2 (Adzhubei et al., 2013), M-CAP (Jagadeesh et al., 2016), CADD v1.4 (Kircher et al., 2014), and MutationTaster (Schwarz et al., 2014), intronic splicing variants by: NetGene2 (Hebsgaard et al., 1996), MaxEntScan and Human Splicing Finder[1], while silent variants by MutationTaster (Schwarz et al., 2014), CADD (Kircher et al., 2014), and FATHMM XF[2]. Allele frequencies were compared with those reported in the Genome Aggregation Database (GnomAD v2.1.1). Variant calling files (VCF) related to the analyzed genomic regions were reported in the **Supplementary File**.

Copy number variation analysis in Alzheimer's disease causative genes

A preliminary *in silico* copy number variation analysis was performed on the sequencing data using the CNVkit (Talevich et al., 2016). Results for *APP*, *PSEN1*, and *PSEN2* genes were validated using a Multiplex Ligation-dependent Probe Amplification (MLPA) assay (MRC Holland). The results of the MLPA analysis were analyzed with Coffalyzer.net.

APOE genotyping

Genotyping of *APOE* was performed by restriction fragment length polymorphism according to Wenham et al. (1991).

Clinical classification of variants

According to Cochran et al. (2019), pathogenic and likely pathogenic variants were returned as "diagnostic." Variants classified in ClinVar or HGMD database as of uncertain significance (VUS) identified in AD-Causative genes or AD-risk factor genes (*TREM2*, *ABCA7*, and *SORL1*) were considered as risk factor alleles. We considered contributor of disease variants reported in ClinVar or HGMD as uncertain significance if found in fEOAD and if enriched in our AD cohort than GnomAD European non-finish population (v.2.1.1), assessed with Fisher's exact Test and Benjamini–Hochberg false discovery rate correction, p-value < 0.05.

Statistical analysis

Variant zygosity was extracted from the VCF files and allele frequencies of our dataset were compared with those reported in GnomAD. Statistical significance ($p < 0.05$) of variant allele

1 www.umd.be/HSF/

2 https://fathmm.biocompute.org.uk/fathmm-xf/

frequencies between our dataset and those reported in GnomAD for the European (non-Finnish) population was assessed with Fisher's exact Test and Benjamini–Hochberg false discovery rate correction. All tables report only adjusted *p*-values.

Results

Study population

The cohort included 102 patients diagnosed with EOAD; in one the diagnosis was neuropathologically confirmed (0.98%), in 72 was defined as "probable" (70.59%), and in 29 as "possible" (28.43%) with evidence of the AD pathophysiological process (McKhann et al., 2011). According to the International Working Group 2 criteria, a "typical" AD phenotype was found in 58 individuals (56.8%), the frontal variant in 15 (14.7%), the logopenic variant in 14 (13.7%), and the posterior variant in 15 (14.7%). The mean of age at onset (AAO) was 56.88 ± 5.84 years, while 10 patients presented the first symptoms before the age of 51. Forty-nine patients were male (48.04%), 46 showed a positive family history (45.10%), of whom 10 were classified as having a strong family history (21.74% of all family cases) (**Table 1**). Dimensionality reduction plots performed with Principal Component Analysis (PCA) and t-distributed stochastic neighbor embedding (t-SNE, Jaccard similarity used as metric, right panel) show an overall homogenous genetic background in our EOAD cohort, with no confounders caused by the geographical origin of the patients (**Supplementary Figure 1**).

TABLE 1 Clinical features of study population.

Patients/Clinical characteristics	*N* (102)	%
Gender		
Male	49	48.04
Female	53	51.96
Age at onset (y)		
Mean ± *SD*	56.88 ± 5.84	
Diagnosis[1]		
Possible	29	28.43
Probable	72	70.59
Certain	1	0.98
Family history		
fEOAD	46	45.10
Strong fh (GS 1 or 1,5)	10	21.74
Moderate fh (GS 2-3-3.5)	36	78.26
sEOAD	56	54.90

EOAD, early onset Alzheimer disease; fEOAD, familial EOAD; fh, positive family history, *N*, number; GS, Goldman score, standard deviation, sEOAD, sporadic EOAD, y, years.
[1]According to the International Working Group 2 criteria (Dubois et al., 2014).

Analysis of causative genes: *APP, PSEN1*, and *PSEN2*

We found 17 different rare variants (MAF < 0.01) in the AD causative genes *APP*, *PSEN1*, and *PSEN2* (**Table 2**). Nine (8.82%) patients carried a "diagnostic" variant; seven had a positive family history, although a strong familiarity was established only in two. All identified variants had been previously reported, with the only exception of p.Leu85Phe in the *PSEN1* gene (**Table 2**), which was not even present in the GnomAD. The carrier had a posterior variant of AD, with positive familial history. Two patients (AD#101 and AD#043) carried two variants, one in the *APP* and *PSEN1* genes, and the second in the *PSEN1* and *PSEN2* genes. No CNV were identified in AD-causative gene. Six rare variants were previously reported in the ClinVar or HGMD database as likely benign or of uncertain significance (*APP* p.Phe435=, *PSEN1* p.Arg35Gln, *PSEN2* p.Arg62His, p.Arg71Trp, p.Met174Val, p.Ser236=) (**Table 2**).

APOE genotype

Eight patients (7.84%), all negative for variants in AD causative genes, carried the *APOE* ε4/ε4 genotype (Cochran et al., 2019). Seven of them had a positive family history, while familiarity was strong in two. Thirty-two (31.37%) patients showed heterozygosity for the *APOE* ε4 allele: thirty carried the *APOE* ε3/ε4 and two the *APOE* ε2/ε4 genotype. The frequency of heterozygosity for the *APOE* ε4 allele was not increased in patients with a positive family history.

Variants in *TREM2* gene

Like *APOE* ε4, pathogenic variants in *TREM2* also increase a person's odds of developing late-onset AD from three- to 12-fold (Wolfe et al., 2019).

We identified five different variants in this gene, all singletons, in four patients (**Table 3**). One patient (AD#026) carried two variants. The variants discovered were not strictly deleterious: four were previously reported in the ClinVar database as benign, and one as VUS.

Variants in dementia-associated genes

Given the common mechanisms previously reported between AD and other neurodegenerative diseases (Bartoletti-Stella et al., 2018; Park et al., 2020), we also collected data on likely pathogenic rare variants in genes that play a role in other dementias.

After applying the filtering criteria, we identified 33 different rare variants in 12 genes (**Table 4**). Variants previously reported

10.3389/fnagi.2022.969817

TABLE 2 Rare variants in AD-causative genes identified in this study.

Gene	ID patient	FH score	Nucleotide change	Protein change	Pathogenicity ClinVar/HGMD	Clinical significance	Frequency GnomAD (EU)[1]	*P*-value[2]
APP	AD#089	3.5	c.1305C > T	p.Phe435=	Benign/NR	Benign	132/128888	0.23
	AD#101	3.5	c.2137G > A	p.Ala713Thr	Conflicting interpretations of pathogenicity: likely pathogenic (1); uncertain significance (2)/Alzheimer disease	Diagnostic	4/129100	0.01
	AD#010	3.5	c.2229C > T	p.Thr743=	NR/NR/prediction: likely benign[3]	Benign	NR	NA
PSEN1	AD#043	0	c.104G > A	p.Arg35Gln	Conflicting interpretation of pathogenicity uncertain significance (3); Benign (1); likely benign (1)/Alzheimer disease?	Risk factor	37/129122	0.08
	AD#102	3.5	c.253C > T	p.Leu85Phe	NR/NR/prediction: probable pathogenic	Diagnostic	NR	NA
	AD#055	1.5	c.275G > C	p.Cys92Ser	Pathogenic/Alzheimer disease	Diagnostic	NR	NA
	AD#001	3.5	c.497T > A	p.Leu166His	NR/Alzheimer disease, early-onset	Diagnostic	NR	NA
	AD#057	3.5	c.617G > C	p.Gly206Ala	Pathogenic/Alzheimer disease	Diagnostic	NR	NA
	AD#012	1	c.791C > T	p.Pro264Leu	Pathogenic/Alzheimer disease	Diagnostic	NR	NA
	AD#002	3.5	c.1172T > C	p.Val391Ala	NR/Alzheimer disease	Diagnostic	NR	NA
	AD#101	3.5	c.1315A > G	p.Ile439Val	NR/Alzheimer disease	Diagnostic	NR	NA
	AD#022	0	c.185G > A	p.Arg62His	Benign/Alzheimer disease?	Benign	300/128852	0.41
PSEN2	AD#097	0	c.211C > T	p.Arg71Trp	Benign/Alzheimer disease?	Risk factor	506/129030	0.51
	AD#098	0						
	AD#077	0						
	AD#035	3	c.520A > G	p.Met174Val	Benign/Alzheimer disease?	Contributor of disease	44/129182	<0.0001
	AD#091	3.5						
	AD#043	0	c.668G > C	p.Gly223Ala	NR/Alzheimer disease	Diagnostic	NR	NA
	AD#065	3.5	c.708T > C	p.Ser236=	Benign/NR	Likely benign	791/129088	0.4
	AD#053	0	c.1186C > T	p.Leu396Phe	NR/Alzheimer disease	Diagnostic	1/113608	0.01

AD, Alzheimer disease, FH, family history, NR, Not reported, NA, not applicable. [1]Population allele frequencies referred to the European (non-Finnish) population reported on GnomAD v2.1.1, expressed as Allele count (Alt/total). [2]*P*-value Fisher's exact test, BH correction. [3]Never reported variants in the *APP* gene not located in the exon 16 and 17 (Cacace et al., 2016) have been considered likely benign. Novel variants have been classified as "likely pathogenic" if at least three tools out of the four used showed potentially pathogenic effects (**Supplementary Table 2**).

TABLE 3 Rare variants in AD-risk gene *TREM2* identified in this study.

ID patient	FH score	Nucleotide change	Protein change	Pathogenicity ClinVar/HGMD	Clinical classification	Frequency GnomAD (EU)[1]	*P*-value[2]
AD#085	0	c.140G > A	p.Arg47His	Likely benign/Alzheimer disease, increased risk	Risk factor	315/127748	0.18
AD#026	3	c.287C > A	p.Thr96Lys	Benign/frontotemporal dementia, increased risk	Risk factor	130/129182	0.08
		c.632T > C	p.Leu211Pro	Benign/Alzheimer disease, increased risk	Risk factor	144/129164	0.11
AD#045	0	c.407G > A	p.Arg136Gln	Uncertain significance/Alzheimer disease?	Risk factor	17/128820	0.02
AD#089	3.5	c.668C > T	p.Thr223Ile	Benign/Alzheimer disease?	Risk factor	49/129176	0.05

AD, Alzheimer disease, FH, family history. [1]Population allele frequencies referred to the European (non-Finnish) population reported on GnomAD v2.1.1, expressed as Allele count (Alt/total). [2]*P*-value Fisher's exact test, BH correction.

TABLE 4 Rare variants in other dementia causative genes identified in this study.

Gene	ID patient	FH score	Nucleotide change	Protein change	Pathogenicity ClinVar/HGMD	Frequency GnomAD (EU)[1]	*P*-value[2]
CCNF	AD#020	0	c.353T > C	p.Val118Ala	NR/NR/prediction – Likely pathogenic	1/111550	0.02
	AD#079	1.5	c.656T > C	p.Leu219Pro	NR/NR/prediction – Likely pathogenic	5/111832	0.03
CHCHD10	AD#068	0	c.354C > A	p.Asp118Glu	Uncertain significance/NR	NR	NA
CSF1R	AD#081	0	c.1400C > T	p.Thr467Met	NR/NR/prediction – Likely benign	5/113734	0.03
	AD#057	3.5	c.1477A > G	p.Ser493Gly	NR/NR/prediction – Likely benign	NR	NA
	AD#044	0	c.2850C > A	p.His950Gln	NR/NR/prediction – Likely benign	2/113066	0.02
			c.2851C > A	p.Leu951Met	NR/NR/prediction – Likely benign	2/113102	0.02
DCTN1	AD#102	3.5	c.586A > G	p.Ile196Val	Conflicting interpretations of pathogenicity. Uncertain significance (2); Benign (6)/abnormal cellular organization.	649/105456	1
	AD#030	0	c.1361T > C	p.Val454Ala	NR/NR/prediction – Likely pathogenic	NR	NA
	AD#100	3	c.1480G > A	p.Ala494Thr	Uncertain significance/amyotrophic lateral sclerosis, phenotype modifiers?	4/128890	0.03
	AD#067	0	c.1555A > G	p.Lys519Glu	NR/NR prediction: Likely pathogenic	NR	NA
	AD#070	1	c.2278A > G	p.Met760Val	Conflicting interpretation of pathogenicity Uncertain significance (2) Benign (2) Likely benign (1)/NR	10/129140	0.03
	AD#078	0	c.2989C > T	p.Arg997Trp	Uncertain significance/amyotrophic lateral sclerosis.	1/113370	0.02
FIG4	AD#080	0	c.2200G > A	p.Glu734Lys	Uncertain significance/NR	15/113494	0.04
	AD#097	0	c.2467C > T	p.Gln823Ter*	Pathogenic/NR	7/129138	0.03
FUS	AD#039	0	c.430_447del	p.Gly144_Tyr149del	Conflicting interpretations of pathogenicity. Pathogenic (1); likely pathogenic (1); uncertain significance (1)/NR	10/113750	0.03
	AD#033	1.5	c.681_686del	p.Gly230_Gly231del	Conflicting interpretations of pathogenicity benign (1) uncertain significance (1)/NR	56/117710	
	AD#049	3.5					0.11
MAPT	AD#039	0	c.121G > A	p.Ala41Thr	Uncertain significance/Alzheimer disease?	6/128512	0.03
	AD#017	3.5	c.454G > A	p.Ala152Thr	Conflicting interpretation of pathogenicity uncertain significance (2) benign (1) likely benign (2)/neurodegeneration	297/129002	0.39
NOTCH3	AD#085	0	c.1505C > T	p.Ser502Phe	Uncertain significance/NR	9/75540	0.04
	AD#071	3	c.3315C > T	p.Gly1105=	NR/NR/prediction: likely benign	1/113330	0.02
	AD#099	0	c.3535A > G	p.Asn1179Asp	NR/NR/prediction: likely pathogenic	NR	NA
	AD#074	3.5	c.4461C > T	p.Gly1487=	NR/NR/prediction: likely benign	NR	NA
	AD#093	3.5	c.5816-6C > T		NR/NR prediction: likely benign	6/113474	0.03
OPTN	AD#010	3.5	c.448C > T	p.Leu150=	NR/NR prediction: likely benign	7/129170	0.03
	AD#091	3.5	c.941A > T	p.Gln314Leu	Conflicting interpretations of pathogenicity pathogenic (1) uncertain significance (1)/amyotrophic lateral sclerosis	38/129076	0.08
	AD#069	0	c.1401 + 4A > G		Uncertain significance/amyotrophic lateral sclerosis	17/129180	0.05
	AD#053	0	c.1643G > A	p.Arg548Gln	Uncertain significance/NR	9/129122	0.03
SQSTM1	AD#066	0	c.315C > T	p.Cys105=	NR/NR prediction: likely benign	NR	NA
	AD#092	3.5	c.960G > A	p.Gly320=	NR/NR prediction: likely benign	1/81718	0.02
	AD#032	3.5	c.1175C > T	p.Pro392Leu	Conflicting interpretations of pathogenicity pathogenic (4) likely pathogenic (1) uncertain significance (2) benign (1)/paget disease of bone	173/128718	0.27
TYROBP	AD#077	0	c.140T > C	p.Val47Ala	Uncertain significance – Alzheimer disease, early onset?	14/128556	0.04
UBQLN2	AD#095	0	c.1461C > A	p.Thr487=	Conflicting interpretations of pathogenicity uncertain significance (1); benign (5); likely benign (1)/NR	787/87391	1

Only variants not previously defined as benign/likely benign in ClinVar and MAF < 0.01 referred to the European (non-Finnish) population reported on GnomAD v2.1.1. were selected and reported. Prediction of variant pathogenicity were reported in the **Supplementary Tables 2–4**. AD, Alzheimer disease, FH, family history, NR. Not reported RE, reported. [1]Population allele frequencies referred to the European (non-Finnish) population reported on GnomAD v2.1.1. [2]*P*-value Fisher's exact test. *Variant homozygous.

as pathogenic or likely pathogenic were identified in patients with motor neuron disease (*FUS* p.Gly144_Tyr149del, *DCTN1* p.Arg997Trp, *OPTN* p. Gln314Leu and c.1401 + 4A > G, *SQSTM1* p.Pro392Leu) and amyotrophic lateral sclerosis (ALS)-Charcot-Marie-Tooth disease type 4 (*FIG4* p.Gln823Ter). Five previously unreported variants were classified as likely pathogenic (**Table 5**) by *in silico* prediction. These variants map to the *CCNF*, *DCTN1*, and *NOTCH3* genes, which are involved in the ALS/frontotemporal dementia (FTD) spectrum (**Supplementary Table 2**). In addition, *NOTCH3* variants have been previously associated with AD risk (Patel et al., 2019).

Among the VUS, two were identified in the *MAPT* gene. Although *MAPT* pathogenic variants are typically associated with FTD (Cruts et al., 2012), these variants have already been reported in patients with AD (Cochran et al., 2019). One of them (p.Ala152Thr) has been identified as a risk factor for several neurodegenerative diseases, including AD (Sydow et al., 2016). The other *MAPT* variant (p.Ala41Thr) occurred in a patient also carrying a pathogenic mutation in the *FUS* gene (AD#039).

Due to the heterogeneity of genetic factors contributing to neurodegeneration, pathogenic/likely pathogenic variants and VUS have been considered as weak allele risk factors (Dilliott et al., 2021). Carriers of these variants were equally distributed between the familial and sporadic groups (Fisher exact test p-value = 1).

Missing heritability: Role of rare variants in other Alzheimer's disease-risk factor genes

Rare pathogenic variants in AD causative genes, homozygosity for *APOE* ε4/ε4, risk factor alleles and likely pathogenic variants in genes related to other forms of neurodegenerative dementias explain 46% of familial and 32% of sporadic patients in our cohort (**Figure 1**). In recent years, more than 40 AD-associated genes/loci have been identified by GWAS, and subsequent sequencing projects have highlighted

TABLE 5 Rare variants in AD-risk genes *ABAC7* and *SORL1* identified in this study.

Gene	ID patient	FH score	Nucleotide change	Protein change	Pathogenicity reported in ClinVar/HGMD	Possible role in EOAD	Frequency GnomAD (EU)[1]	*P*-value[2]
ABCA7	AD#009	0	c.2126_2132del AGCAGGG	p.Glu709Al afsTer86	Conflicting interpretations of pathogenicity; risk factor Uncertain significance (1) likely benign (1)/NR	Reported AD risk (De Roeck et al., 2019) risk factor	250/104264	0.18
	AD#052	3.5	c.2476G > A	p.Gly826Arg	NR/NR Prediction: likely pathogenic	Risk factor	95/126126	0.08
	AD#088	0	c.2629G > A	p.Ala877Thr	NR/NR Prediction: likely benign	Likely benign	1014/127604	0.41
	AD#006	0	c.3412A > C	p.Ser1138Arg	NR/NR Prediction: likely pathogenic	Risk factor	1/76428	0.01
	AD#009	0	c.3472 + 5G > C		NR/NR Prediction: likely benign	Possibly affecting splicing (Le Guennec et al., 2016) – Risk factor	2/112726	0.01
	AD#083	0	c.4343G > A	p.Gly1448Asp	NR/NR Prediction: likely benign	Likely benign	72/127544	0.07
	AD#007	0	c.4795G > A	p.Val1599Met	Likely benign/autism?	Likely benign	554/129150	0.28
	AD#028	3.5	c.5570 + 5G > C		Uncertain significance/Alzheimer disease?	Reported AD risk (De Roeck et al., 2019) risk factor	432/114436	0.05
	AD#099	0						
SORL1	AD#094	3.5	c.133G > T	p.Asp45Tyr	NR/NR Prediction: likely pathogenic	Risk factor	4/39936	0.02
	AD#052	3.5	c.1805C > T	p.Ser602Leu	NR/Alzheimer disease?	Risk factor	NR	NA
	AD#096	0	c.3346A > G	p.Ile1116Val	Benign/Alzheimer disease, late-onset?	Likely benign	1065/129098	0.41
	AD#062	0	c.4077C > T	p.Cys1359=	Uncertain significance/NR	Risk factor	33/129196	0.03
	AD#097	0	c.5448T > C	p.Tyr1816=	Benign/NR	Likely benign	285/128866	0.18
	AD#088	0	c.6150A > G	p.Glu2050=	NR/NR Prediction: likely benign	Likely benign	1/113030	0.01

AD, Alzheimer disease, FH, family history, NA, not applicable, NR. Not reported. [1]Population allele frequencies referred to the European (non-Finnish) population reported on GnomAD v2.1.1, expressed as Allele count (Alt/total). [2]*P*-value Fisher's exact test, BH correction.

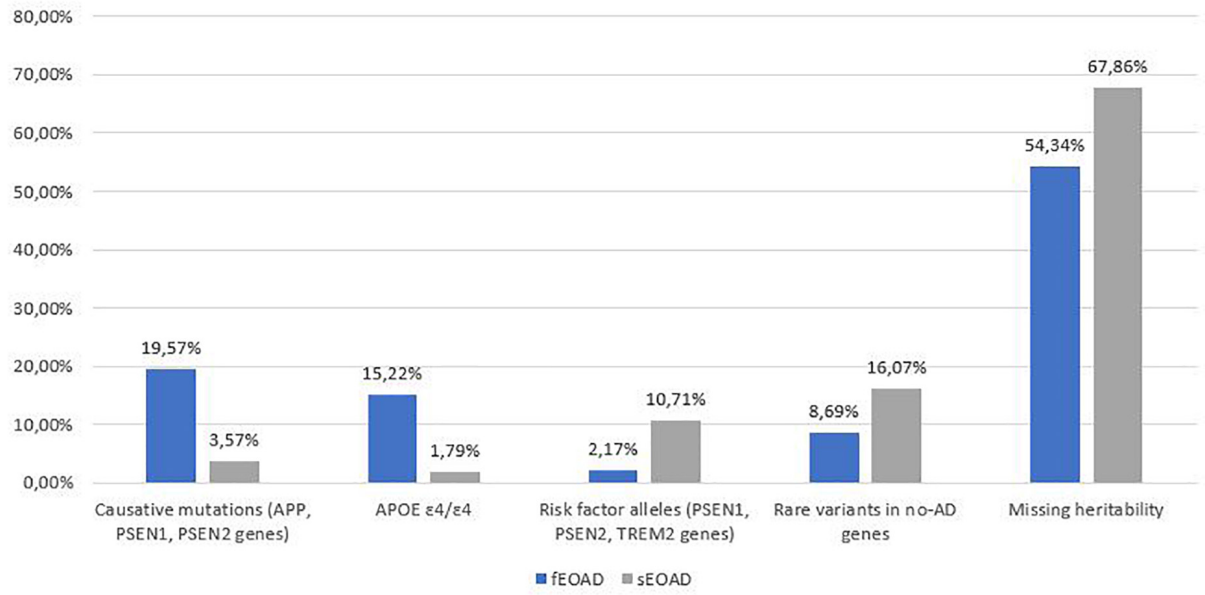

FIGURE 1
Summary of genetic variants identified in the 102 AD patients, divided into familial (fEOAD) and sporadic patients (sEOAD). Causative mutations included diagnostic and strong contributor alleles in *APP*, *PSEN1,* and *PSEN2* genes, moderate risk alleles included variant not strictly pathogenic in *APP*, *PSEN1*, *PSEN2,* and *TREM2* genes, rare variants in no-AD genes included pathogenic/likely pathogenic/VUS (uncertain significant variants or with major evidence of pathogenicity in ClinVar and/or HGMD) variants in genes causative for other type of dementia (**Supplementary Table 1**).

the role of rare variants in these genes in EOAD (Bellenguez et al., 2020; Wightman et al., 2021). In a pilot cohort of EOADs without causative variants (n = 30) we analyzed 34 genes (**Supplementary Table 1**), identified as susceptibility factors for AD, for the presence of rare and possibly pathogenic variants.

Most of the variants identified were in the *ABCA7* (n = 8; one in two patients) and *SORL1* (n = 6) genes (**Table 5**). Of these, two in the *ABCA7* gene were previously reported PTV (protein truncating variants) (**Table 5**). Among them, the c.2126_2132delAGCAGG p.Glu709AlafsTer86 variant was classified as a contributor to the disease (De Roeck et al., 2019). We also found three rare missense variants in the coding sequence of *SORL1*, one of which (p.Asp45Tyr) was classified as a likely pathogenic variant. Among the possibly pathogenic variants in *ABCA7* and *SORL1*, five had a positive association in our cohort compared to the frequency in the European population (**Table 5**). The remaining missense or silent variants were considered as rare benign variants (**Table 5** and **Supplementary Tables 2–4**).

Additionally, 26 rare variants of potential interest (**Table 6**) were identified in 17 of the 32 other AD susceptibility genes analyzed (**Supplementary Table 1**). All identified variants were singleton except for the *FERMT2* p.Thr513Met variant. Only three variants were reported in ClinVar or HGMD databases, all classified as VUS. Variants in the *BIN1* gene (p.Asn232Lys, and c.1462-3C > T) were linked to myopathy, while the variant in *PTK2B* was associated with Parkinson's disease. As for the remaining variants, eight were classified as likely pathogenic by *in silico* analyses (**Table 6** and **Supplementary Tables 2–4**).

In conclusion, 63% of the examined patients presented at least one likely pathogenic variant or a rare VUS in AD-susceptibility genes (**Tables 5**, **6**), suggesting that they might also confer risk for the development of EOAD. Familial and sporadic patients did not show a different distribution of these variants.

Discussion

Clarifying the genetic and molecular basis of EOAD and its clinical variability is crucial for improving diagnostic screening and developing more effective, and possibly preventive, disease modifying treatments.

Since a concern in genetic studies of AD patients is that at least some variants are private or specific to certain populations, we analyzed a well-characterized single-center cohort of 102 patients by a NGS panel including AD causative genes, risk factors and genes involved in other types of dementia.

We found a pathogenic mutation in one of the three AD-causing genes in 8.82% of patients, in agreement with the expected maximum of 11% reported in the literature (Mendez, 2019). These include a novel, likely pathogenic variant, *PSEN1* c.253C > T p.Leu85Phe. According to Guerreiro algorithm (Guerreiro et al., 2010), this variant can be defined as probably pathogenic: it maps to the first transmembrane domain, is

TABLE 6 Rare variants in GWAS genes identified in this study.

Gene	ID patient	FH score	Nucleotide change	Protein change	Pathogenicity ClinVar/HGMD	Frequency GnomAD (EU)[1]	*P*-value
ADAM10	AD#060	0	c.112A > G	p.Asn38Asp	NR/NR prediction: likely benign	NR	NA
	AD#065	3.5	c.556dupC	p.Gln186ProfsTer19	NR/NR prediction: likely pathogenic	NR	NA
BIN1	AD#095	0	c.696C > A	p.Asn232Lys	Uncertain significance (myopathy)/NR	98/129022	0.08
	AD#009	0	c.865G > A	p.Ala289Thr	NR/NR prediction: likely benign	3/94156	0.01
	AD#082	0	c.1462-3C > T		Uncertain significance (myopathy)/NR	16/128710	0.02
CLU	AD#096	0	c.509C > T	p.Thr170Met	NR/NR prediction: likely benign	2/113698	0.01
CR1	AD#062	0	c.4956G > A	p.Pro1652=	NR/NR prediction: likely benign	NR	NA
	AD#075	0	c.4356T > C	p.Cys1452=	NR/NR prediction: likely benign	1084/128002	0.50
ELAVL1	AD#010	3.5	c.765C > T	p.Ala255=	NR/NA prediction: likely benign	29/129192	0.04
EP300	AD#098	0	c.2194C > T	p.Pro732Ser	NR/NR prediction: likely pathogenic	NR	NA
EPHA1	AD#010	3.5	c.928A > G	p.Ile310Val	NR/NR prediction: likely benign	1/113284	0.01
FERMT2	AD#028	3.5	c.1077G > C	p.Gly359=	NR/NA prediction: likely benign	1083/127414	0.41
	AD#058	0	c.1538C > T	p.Thr513Met	NR/NA prediction: likely pathogenic	487/129124	0.05
	AD#060	0					
INPP5D	AD#090	0	c.470G > A	p.Arg157Gln	NR/NR prediction: likely pathogenic	300/127840	0.18
	AD#089	3.5	c.2085C > T	p.Pro695=	NR/NR prediction: likely benign	107/128314	0.08
MARK2	AD#090	0	c.1611C > T	p.Ser537=	NR/NA prediction: likely benign	5/108824	0.01
MARK4	AD#060	0	c.1553C > T	p.Pro518Leu	NR/NR prediction: likely benign	196/129058	0.14
PICALM	AD#014	0	c.1231G > C	p.Ala411Pro	NR/NR prediction: likely pathogenic	321/128802	0.18
PLCG2	AD#032	3.5	c.3379C > A	p.Pro1127Thr	NR/NR prediction: likely pathogenic	3/128682	0.01
	AD#083	0	c.408G > A	p.Ala136=	NR/NR prediction: likely benign	1/128708	0.01
PTK2B	AD#010	3.5	c.2591C > T	p.Ala864Val	NR/Parkinson disease?	275/129154	0.18
RIN3	AD#022	0	c.2377T > C	p.Tyr793His	NR/NA prediction: likely pathogenic	896/129136	0.40
TOMM40	AD#082	0	c.384C > G	p.Asn128Lys	NR/NR prediction: likely benign	4/113466	0.01
ZCWPW1	AD#052	3.5	c.1834C > T	p.Leu612=	NR/NR prediction: likely benign	1126/128540	0.41
	AD#097	0	c.314A > G	p.Glu105Gly	NR/NA prediction: likely pathogenic	623/128268	0.30
	AD#088	0	c.283-5T > G		NR/NR prediction: likely benign	1072/128080	0.41

Only variants not previously defined as benign/likely benign in ClinVar and MAF < 0.01 referred to the European (non-Finnish) population reported on GnomAD v2.1.1. were reported. Novel variants have been classified as "likely pathogenic" if at least three tools out of the four used showed potentially pathogenic effects (**Supplementary Table 2**). AD, Alzheimer disease, FH, family history; NR, not reported; NA, not applicable. [1]Population allele frequencies referred to the European (non-Finnish) population reported on GnomAD v2.1.1, expressed as Allele count (Alt/total).

defined as damaging by *in silico* tools (**Supplementary Table 2**), a causative mutation in the same codon (p.Leu85Pro) has been described in patients with EOAD (Ataka et al., 2004), and the residue is conserved in *PSEN2* (p.Leu91). *PSEN2* mutations are considered very rare but have the highest frequency in Spain and Italy (Cai et al., 2015). In agreement, we identified four possibly pathogenic missense variants in this gene, two possibly pathogenic missense variants, p.Gly223Ala and p.Leu396Phe, both in patients with no family history of AD, and two rare variants, p.Met174Val and p.Arg71Trp, which have a questionable classification. These variants were initially described as possibly pathogenic (Guerreiro et al., 2010) but subsequently found in healthy controls. Thus, they are currently classified as non-pathogenic (Alzforum Mutation database[3]). We demonstrated a positive association with the risk of developing EOAD for the *PSEN2* p.Met174Val variant, compared with the non-Finnish European allele frequency reported in GnomAD, having found it in two patients with EOAD and positive family history. This variants could be considered a contributing factor to the disease.

Given the previously reported common mechanisms between AD and other dementias (Bartoletti-Stella et al., 2018; Giau et al., 2019), we also collected data on likely pathogenic rare variants in genes implicated in other dementias. Of the 33 rare variants identified in 12 genes, 10 were pathogenic or likely pathogenic, nine VUS, equally distributed between the familial and sporadic EOAD (**Table 4**). Most of them were in genes causal for the ALS/FTD continuum. Thus, our study supports the view that AD and other neurodegenerative diseases might represent shades of the same disease spectrum, and that extended genetic testing of causative genes for other degenerative dementias should be offered to patients diagnosed with EOAD (Bartoletti-Stella et al., 2018 Giau et al., 2019). In agreement with this hypothesis, Spina et al., 2021, found at least one non-AD neuropathological diagnosis in 98% of patients with EOAD. Due to the heterogeneity of genetic factors contributing to neurodegeneration, and the equal distribution between sporadic and familial forms, we consider pathogenic/hypothetical pathogenic variants and variants with

3 https://www.alzforum.org/mutations

uncertain significance in these genes to be weak risk factors (Dilliott et al., 2021).

Concerning the main known risk factors for AD, homozygosity for *APOE* ε4 allele has previously been reported to be associated with a significantly increased risk of EOAD than of LOAD, regardless of family history (van Duijn et al., 1994; BLACKER et al., 1997; Cochran et al., 2019); in agreement, it reaches 7.84% in our dataset. This evidence confirms previous data suggesting that APOE may strongly influence AD risk at younger ages, but as age increases, the effect of *APOE* is reduced, and other risk variants start to play a more significant role in AD risk (Bellou et al., 2020). These include variants in *ABCA7*, *SORL1*, and *TREM2* gene. Regarding *TREM2*, a significant exome-wide association between the p.Arg47His variant and the risk of EOAD has been reported while rare *TREM2* variants have been associated with Aβ deposition, Aβ uptake by microglia, and increased tau in CSF (Gratuze et al., 2018). Together, these data suggest a connection with EOAD neuropathologic findings, and both the amyloid and tau hypotheses of AD (Ayodele et al., 2021). Furthermore, in patients with autosomal-dominant AD, CSF Aβ42 decline, cortical atrophy and cognitive impairment were lower in patients with high soluble receptor stub (Morenas-Rodríguez et al., 2022). In the *TREM2* coding region we found five rare VUS (one patient carried two variants), two of which (p.Arg136Gln, p.Thr223Ile) showed a higher allele frequency in EOAD than the European population reported on GnomAD (**Table 3**). The p.Arg136Gln variant causes the substitution of an arginine residue required for optimal binding of extracellular ligands, and other known missense variants were found in familial and early onset forms of the disease (Sirkis et al., 2016). In agreement with a previous study (Bellenguez et al., 2017), we considered these variants as risk factor/weak contributor to the disease.

Our results are therefore consistent with previous findings and strengthen the potential role of these rare variants as risk factors.

Recent meta-analyses and GWAS have shown a fivefold increased risk, similar to that of *APOE*-ε4 carriers, of developing EOAD with rare variants in *SORL1* (Ayodele et al., 2021) and a study that used the Exome Aggregation Consortium (ExAC; ExAC browser is not available anymore, and it is now part of the gnomAD) database established that pathogenic *SORL1* variants increase AD risk by 12-fold, as well as causing an earlier age of onset (58.6 ± 5.2 years) (Holstege et al., 2017). Moreover, protein-truncating variants in *SORL1* were observed exclusively in AD patients, and are highly penetrant, whereas two *SORL1* missense mutations (p.R1303C and p.G1732A) and a splice site variant (c.3050-2A > G) have been shown to segregate with disease in families affected by autosomal dominant AD (Holstege et al., 2017). Among the six rare variants in the *SORL1* gene identified in our cohort, p.Asp45Tyr and p.Ser402Leu were found in two familial patients. The variant p.Asp45Tyr was never previously reported and classified as possibly pathogenic.

In addition, we identified five unreported missense variants in *ABCA7*, (**Table 2**), a gene containing risk factors for developing both EOAD and LOAD due to its role in amyloid clearance and decreasing Aβ production through interference with APP processing (Satoh et al., 2015; De Roeck et al., 2017; Sleegers and Van Broeckhoven, 2019). In addition, *ABCA7* has been shown to provide a greater predisposition to develop AD than the APOE ε4 allele in African American adults. To date, four autosomal dominant AD families are known in which rare *ABCA7* PTC and missense variants segregated with the disease (Hoogmartens et al., 2021). Although our variants are missense, they may likely act as essential contributors to EOAD susceptibility, albeit with variable penetrance (Khani et al., 2022).

Lastly, in EOAD without causative mutations or *APOE* ε4/ε4, we analyzed 34 genes previously identified as susceptibility factors for AD. We found an average of 0.6 rare variants in each patient in 14 of them, also confirming in EOAD patients a high amount of risk factors.

Overall, the extended genetic analysis of a well-defined cohort of Italian EOAD patients showed that in cases without dominant pathogenic variants in *PSEN1*, *PSEN2* and *APP*, there is an enrichment for multiple pathogenic/likely pathogenic variants in genes associated with risk factors for AD, covering 38% of our cohort, supporting the extreme genetic heterogeneity of EOAD. Independently of family history, a high proportion of EOAD patients carried genetic risk factors, suggesting oligogenic determinism, particularly in individuals without familiarity. Therefore, our data also highlight the role of rare variants especially in sporadic EOAD, each exerting a moderate to high pathogenic effect and corroborate an extended analysis to identify variants implicated in the disease.

We also confirmed enrichment of *APOE* ε4/ε4 homozygosity and rare pathogenic/likely pathogenic variants in *SORL1*, *TREM2,* and *ABCA7* (Khani et al., 2022). Additionally, we found a substantial proportion of pathogenic variants in several autosomal dominant genes, causal in other dementias or previously identified as risk factors for AD, most often in patients with positive familiarity, providing evidence to the hypothesis that many different rare mutations usually detected only in a single family or in small populations could be causal in familial EOAD.

In summary, our study describes new pathogenic variants in AD linked genes, *PSEN1*, *ABCA7*, *SORL1,* and contributes to disentangle the broad genetic landscape of Italian EOAD. The results suggest that a systematic application of comprehensive genetic assessments could aid in the interpretation of early-onset dementia cases by providing a molecular basis to their phenotypic heterogeneity and potentially in enabling future personalized medicine approaches.

Data availability statement

The datasets presented in this study can be found in online repositories and the study is deposited in the European Nucleotide Archive (ENA, https://www.ebi.ac.uk/ena/) EMBLEBI repository, accession number PRJEB55143 (ERP140024).

Ethics statement

Ethical approval of the study was obtained by the ethical board Area Vasta Emilia Centro, (AVEC). The patients/participants provided their written informed consent to participate in this study.

Author contributions

AB-S and MT: manuscript drafting and revising, data collection, analysis, and interpretation of data. GM, FA, LB, NM, MS-M, SB, SL, MS, RP, EF, PC, RL, and PP: data collection and revision of the manuscript. SC: study concept and design, drafting and revising the manuscript, analysis and interpretation of data, and study supervision. All authors contributed to the article and approved the submitted version.

Funding

This work was funded by the Italian Ministry of Research RFO and by Fondazione del Monte.

Acknowledgments

The authors acknowledge the patients and their families; the Italian Ministry of Research RFO and Fondazione del Monte.

Conflict of interest

The authors declare that the research was conducted in the absence of any commercial or financial relationships that could be construed as a potential conflict of interest.

Publisher's note

All claims expressed in this article are solely those of the authors and do not necessarily represent those of their affiliated organizations, or those of the publisher, the editors and the reviewers. Any product that may be evaluated in this article, or claim that may be made by its manufacturer, is not guaranteed or endorsed by the publisher.

Supplementary material

The Supplementary Material for this article can be found online at: https://www.frontiersin.org/articles/10.3389/fnagi.2022.969817/full#supplementary-material

References

Abu-Rumeileh, S., Mometto, N., Bartoletti-Stella, A., Polischi, B., Oppi, F., Poda, R., et al. (2018). Cerebrospinal fluid biomarkers in patients with frontotemporal dementia spectrum: a single-center study. *J. Alzheimers Dis.* 66, 551–563. doi: 10.3233/JAD-180409

Adzhubei, I., Jordan, D. M., and Sunyaev, S. R. (2013). Predicting functional effect of human missense mutations using PolyPhen-2. *Curr. Protoc. Hum. Genet.* 7:20. doi: 10.1002/0471142905.hg0720s76

Ataka, S., Tomiyama, T., Takuma, H., Yamashita, T., Shimada, H., Tsutada, T., et al. (2004). A novel presenilin-1 mutation (Leu85Pro) in early-onset Alzheimer disease with spastic paraparesis. *Arch. Neurol.* 61, 1773–1776. doi: 10.1001/archneur.61.11.1773

Ayodele, T., Rogaeva, E., Kurup, J. T., Beecham, G., and Reitz, C. (2021). Early-onset Alzheimer's disease: what is missing in research? *Curr. Neurol. Neurosci. Rep.* 21:4. doi: 10.1007/s11910-020-01090-y

Bartoletti-Stella, A., Baiardi, S., Stanzani-Maserati, M., Piras, S., Caffarra, P., Raggi, A., et al. (2018). Identification of rare genetic variants in Italian patients with dementia by targeted gene sequencing. *Neurobiol. Aging* 66, 180.e23–180.e31. doi: 10.1016/j.neurobiolaging.2018.02.006

Bartoletti-Stella, A., De Pasqua, S., Baiardi, S., Bartolomei, I., Mengozzi, G., Orio, G., et al. (2020). Characterization of novel progranulin gene variants in Italian patients with neurodegenerative diseases. *Neurobiol. Aging* 97, .e7–.e145. doi: 10.1016/j.neurobiolaging.2020.05.004

Bellenguez, C., Charbonnier, C., Grenier-Boley, B., Quenez, O., Le Guennec, K., Nicolas, G., et al. (2017). Contribution to Alzheimer's disease risk of rare variants in TREM2, SORL1, and ABCA7 in 1779 cases and 1273 controls. *Neurobiol. Aging* 59, 220.e1–220.e9. doi: 10.1016/j.neurobiolaging.2017.07.001

Bellenguez, C., Grenier-Boley, B., and Lambert, J. C. (2020). Genetics of Alzheimer's disease: where we are, and where we are going. *Curr. Opin. Neurobiol.* 61, 40–48. doi: 10.1016/j.conb.2019.11.024

Bellou, E., Baker, E., Leonenko, G., Bracher-Smith, M., Daunt, P., Menzies, G., et al. (2020). Age-dependent effect of APOE and polygenic component on Alzheimer's disease. *Neurobiol. Aging* 93, 69–77. doi: 10.1016/j.neurobiolaging.2020.04.024

BLACKER, D., Haines, J. L., Rodes, L., Terwedow, H., Go, R. C., Harrell, L. E., et al. (1997). ApoE-4 and age at onset of Alzheimer's disease: The NIMH genetics initiative. *Neurology* 48, 139–147. doi: 10.1212/wnl.48.1.139

Bolger, A. M., Lohse, M., and Usadel, B. (2014). Trimmomatic: a flexible trimmer for Illumina sequence data. *Bioinformatics* 30, 2114–2120. doi: 10.1093/bioinformatics/btu170

Bonvicini, C., Scassellati, C., Benussi, L., Di Maria, E., Maj, C., Ciani, M., et al. (2019). Next generation sequencing analysis in early onset dementia patients. *J. Alzheimers Dis.* 67, 243–256. doi: 10.3233/JAD-180482

Brickell, K. L., Steinbart, E. J., Rumbaugh, M., Payami, H., Schellenberg, G. D., Van Deerlin, V., et al. (2006). Early-onset Alzheimer disease in families with

late-onset Alzheimer disease: a potential important subtype of familial Alzheimer disease. *Arch. Neurol.* 63, 1307–1311. doi: 10.1001/archneur.63.9.1307

Cacace, R., Sleegers, K., and Van Broeckhoven, C. (2016). Molecular genetics of early-onset Alzheimer's disease revisited. *Alzheimers Dement.* 12, 733–748. doi: 10.1016/j.jalz.2016.01.012

Cai, Y., An, S. S., and Kim, S. (2015). Mutations in presenilin 2 and its implications in Alzheimer's disease and other dementia-associated disorders. *Clin. Interv. Aging* 10, 1163–1172. doi: 10.2147/CIA.S85808

Campion, D., Dumanchin, C., Hannequin, D., Dubois, B., Belliard, S., Puel, M., et al. (1999). Early-onset autosomal dominant Alzheimer disease: prevalence, genetic heterogeneity, and mutation spectrum. *Am. J. Hum. Genet.* 65, 664–670. doi: 10.1086/302553

Cochran, J. N., McKinley, E. C., Cochran, M., Amaral, M. D., Moyers, B. A., Lasseigne, B. N., et al. (2019). Genome sequencing for early-onset or atypical dementia: high diagnostic yield and frequent observation of multiple contributory alleles. *Cold Spring Harb. Mol. Case Stud.* 5:a003491. doi: 10.1101/mcs.a003491

Cruts, M., Theuns, J., and Van Broeckhoven, C. (2012). Locus-specific mutation databases for neurodegenerative brain diseases. *Hum. Mutat.* 33, 1340–1344. doi: 10.1002/humu.22117

De Roeck, A., Van Broeckhoven, C., and Sleegers, K. (2019). The role of ABCA7 in Alzheimer's disease: Evidence from genomics, transcriptomics and methylomics. *Acta Neuropathol.* 138, 201–220. doi: 10.1007/s00401-019-01994-1

De Roeck, A., Van den Bossche, T., van der Zee, J., Verheijen, J., De Coster, W., Van Dongen, J., et al. (2017). Deleterious ABCA7 mutations and transcript rescue mechanisms in early onset Alzheimer's disease. *Acta Neuropathol.* 134, 475–487. doi: 10.1007/s00401-017-1714-x

Dilliott, A. A., Abdelhady, A., Sunderland, K. M., Farhan, S. M. K., Abrahao, A., Binns, M. A., et al. (2021). Contribution of rare variant associations to neurodegenerative disease presentation. *NPJ Genom. Med.* 6:80. doi: 10.1038/s41525-021-00243-3

Dubois, B., Feldman, H. H., Jacova, C., Hampel, H., Molinuevo, J. L., Blennow, K., et al. (2014). Advancing research diagnostic criteria for Alzheimer's disease: the IWG-2 criteria. *Lancet Neurol.* 13, 614–629. doi: 10.1016/S1474-4422(14)70090-0

Gatz, M., Reynolds, C. A., Fratiglioni, L., Johansson, B., Mortimer, J. A., Berg, S., et al. (2006). Role of genes and environments for explaining Alzheimer disease. *Arch. Gen. Psychiatry* 63, 168–174. doi: 10.1001/archpsyc.63.2.168

Genin, E., Hannequin, D., Wallon, D., Sleegers, K., Hiltunen, M., Combarros, O., et al. (2011). APOE and Alzheimer disease: a major gene with semi-dominant inheritance. *Mol. Psychiatry* 16:903. doi: 10.1038/mp.2011.52.-7

Giau, V. V., Bagyinszky, E., Yang, Y. S., Youn, Y. C., An, S. S. A., and Kim, S. Y. (2019). Genetic analyses of early-onset Alzheimer's disease using next generation sequencing. *Sci. Rep.* 9:8368.

Goldman, J. S., Farmer, J. M., Wood, E. M., Johnson, J. K., Boxer, A., Neuhaus, J., et al. (2005). Comparison of family histories in FTLD subtypes and related tauopathies. *Neurology* 65, 1817–1819. doi: 10.1212/01.wnl.0000187068.92184.63

Gratuze, M., Leyns, C. E. G., and Holtzman, D. M. (2018). New insights into the role of TREM2 in Alzheimer's disease. *Mol. Neurodegener.* 13:66. doi: 10.1186/s13024-018-0298-9

Guerreiro, R. J., Baquero, M., Blesa, R., Boada, M., Brás, J. M., Bullido, M. J., et al. (2010). Genetic screening of Alzheimer's disease genes in Iberian and African samples yields novel mutations in presenilins and APP. *Neurobiol. Aging.* 31, 725–731. doi: 10.1016/j.neurobiolaging.2008.06.012

Hebsgaard, S. M., Korning, P. G., Tolstrup, N., Engelbrecht, J., Rouzé, P., and Brunak, S. (1996). Splice site prediction in Arabidopsis thaliana pre-mRNA by combining local and global sequence information. *Nucleic Acids Res.* 24, 3439–3452. doi: 10.1093/nar/24.17.3439

Holstege, H., van der Lee, S. J., Hulsman, M., Wong, T. H., van Rooij, J. G., Weiss, M., et al. (2017). Characterization of pathogenic SORL1 genetic variants for association with Alzheimer's disease: a clinical interpretation strategy. *Eur. J. Hum. Genet.* 25, 973–981. doi: 10.1038/ejhg.2017.87

Hoogmartens, J., Cacace, R., and Van Broeckhoven, C. (2021). Insight into the genetic etiology of Alzheimer's disease: a comprehensive review of the role of rare variants. *Alzheimers Dement.* 13:e12155. doi: 10.1002/dad2.12155

Jagadeesh, K. A., Wenger, A. M., Berger, M. J., Guturu, H., Stenson, P. D., Cooper, D. N., et al. (2016). M-CAP eliminates a majority of variants of uncertain significance in clinical exomes at high sensitivity. *Nat. Genet.* 48, 1581–1586. doi: 10.1038/ng.3703

Karczewski, K. J., Francioli, L. C., Tiao, G., Cummings, B. B., Alföldi, J., Wang, Q., et al. (2020). The mutational constraint spectrum quantified from variation in 141,456 humans. *Nature* 581, 434–443. doi: 10.1038/s41586-020-2308-7

Khani, M., Gibbons, E., Bras, J., and Guerreiro, R. (2022). Challenge accepted: uncovering the role of rare genetic variants in Alzheimer's disease. *Mol. Neurodegener.* 17:3. doi: 10.1186/s13024-021-00505-9

Kim, S., Scheffler, K., Halpern, A. L., Bekritsky, M. A., Noh, E., Källberg, M., et al. (2018). Strelka2: fast and accurate calling of germline and somatic variants. *Nat. Methods* 15, 591–594. doi: 10.1038/s41592-018-0051-x

Kircher, M., Witten, D. M., Jain, P., O'Roak, B. J., Cooper, G. M., and Shendure, J. A. (2014). general framework for estimating the relative pathogenicity of human genetic variants. *Nat. Genet.* 46, 310–315. doi: 10.1038/ng.2892

Kunkle, B. W., Grenier-Boley, B., Sims, R., Bis, J. C., Damotte, V., Naj, A. C., et al. (2019). Genetic meta-analysis of diagnosed Alzheimer's disease identifies new risk loci and implicates Aβ, tau, immunity and lipid processing. *Nat. Genet.* 51, 414–430. doi: 10.1038/s41588-019-0358-2

Lacour, M., Quenez, O., Rovelet-Lecrux, A., Salomon, B., Rousseau, S., Richard, A. C., et al. (2019). Causative mutations and genetic risk factors in sporadic early onset Alzheimer's disease before 51 years. *J. Alzheimers Dis.* 71, 227–243. doi: 10.3233/JAD-190193

Landrum, M. J., Lee, J. M., Benson, M., Brown, G. R., Chao, C., Chitipiralla, S., et al. (2018). ClinVar: improving access to variant interpretations and supporting evidence. *Nucleic Acids Res.* 46, D1062–D1067. doi: 10.1093/nar/gkx1153

Le Guennec, K., Nicolas, G., Quenez, O., Charbonnier, C., Wallon, D., Bellenguez, C., et al. (2016). ABCA7 rare variants and Alzheimer disease risk. *Neurology* 86, 2134–2137. doi: 10.1212/WNL.0000000000002627

Li, H., and Durbin, R. (2009). Fast and accurate short read alignment with Burrows-Wheeler transform. *Bioinformatics* 25, 1754–1760. doi: 10.1093/bioinformatics/btp324

McKenna, A., Hanna, M., Banks, E., Sivachenko, A., Cibulskis, K., Kernytsky, A., et al. (2010). The genome analysis toolkit: a MapReduce framework for analyzing next-generation DNA sequencing data. *Genome Res.* 20, 1297–1303. doi: 10.1101/gr.107524.110

McKhann, G. M., Knopman, D. S., Chertkow, H., Hyman, B. T., Jack, C. R. Jr., Kawas, C. H., et al. (2011). The diagnosis of dementia due to Alzheimer's disease: Recommendations from the National Institute on Aging-Alzheimer's Association workgroups on diagnostic guidelines for Alzheimer's disease. *Alzheimers Dement.* 7, 263–269. doi: 10.1016/j.jalz.2011.03.005

Mendez, M. F. (2019). Early-onset alzheimer disease and its variants. *Continuum* 25, 34–51. doi: 10.1212/CON.0000000000000687

Morenas-Rodríguez, E., Li, Y., Nuscher, B., Franzmeier, N., Xiong, C., Suárez-Calvet, M., et al. (2022). Soluble TREM2 in CSF and its association with other biomarkers and cognition in autosomal-dominant Alzheimer's disease: a longitudinal observational study. *Lancet Neurol.* 21, 329–341. doi: 10.1016/S1474-4422(22)00027-8

Moreno-Grau, S., Fernández, M. V., de Rojas, I., Garcia-González, P., Hernández, I., Farias, F., et al. (2021). Long runs of homozygosity are associated with Alzheimer's disease. *Transl. Psychiatry* 11:142. doi: 10.1038/s41398-020-01145-1

Mrdjen, D., Fox, E. J., Bukhari, S. A., Montine, K. S., Bendall, S. C., and Montine, T. J. (2019). The basis of cellular and regional vulnerability in Alzheimer's disease. *Acta Neuropathol.* 138, 729–749. doi: 10.1007/s00401-019-02054-4

Park, J. E., Kim, H. J., Kim, Y. E., Jang, H., Cho, S. H., Kim, S. J., et al. (2020). Analysis of dementia-related gene variants in APOE ε4 noncarrying Korean patients with early-onset Alzheimer's disease. *Neurobiol. Aging* 85, 155.e5–155.e8. doi: 10.1016/j.neurobiolaging.2019.05.009

Patel, D., Mez, J., Vardarajan, B. N., Staley, L., Chung, J., Zhang, X., et al. (2019). Association of rare coding mutations with alzheimer disease and other dementias among adults of european ancestry. *JAMA Netw. Open* 2:e191350. doi: 10.1001/jamanetworkopen.2019.1350

Richards, S., Aziz, N., Bale, S., Bick, D., Das, S., Gastier-Foster, J., et al. (2015). Standards and guidelines for the interpretation of sequence variants: a joint consensus recommendation of the american college of medical genetics and genomics and the association for molecular pathology. *Genet. Med.* 17, 405–424. doi: 10.1038/gim.2015.30

Sassi, C., Nalls, M. A., Ridge, P. G., Gibbs, J. R., Lupton, M. K., Troakes, C., et al. (2018). Mendelian adult-onset leukodystrophy genes in Alzheimer's disease: Critical influence of CSF1R and NOTCH3. *Neurobiol. Aging* 66, 179.e17–179.e179. doi: 10.1016/j.neurobiolaging.2018.01.015

Satoh, K., Abe-Dohmae, S., Yokoyama, S., St George-Hyslop, P., and Fraser, P. E. (2015). ATP-binding cassette transporter A7 (ABCA7) loss of function alters Alzheimer amyloid processing. *J. Biol. Chem.* 290, 24152–24165. doi: 10.1074/jbc.M115.655076

Schwarz, J. M., Cooper, D. N., Schuelke, M., and Seelow, D. (2014). MutationTaster2: mutation prediction for the deep-sequencing age. *Nat. Methods* 11, 361–362. doi: 10.1038/nmeth.2890

Sirkis, D. W., Bonham, L. W., Aparicio, R. E., Geier, E. G., Ramos, E. M., Wang, Q., et al. (2016). Rare TREM2 variants associated with Alzheimer's disease display reduced cell surface expression. *Acta Neuropathol. Commun.* 4:98. doi: 10.1186/s40478-016-0367-7

Sleegers, K., and Van Broeckhoven, C. (2019). Novel Alzheimer's disease risk genes: exhaustive investigation is paramount. *Acta Neuropathol.* 138, 171–172. doi: 10.1007/s00401-019-02041-9

Spina, S., La Joie, R., Petersen, C., Nolan, A. L., Cuevas, D., Cosme, C., et al. (2021). Comorbid neuropathological diagnoses in early versus late-onset Alzheimer's disease. *Brain* 144, 2186–2198. doi: 10.1093/brain/awab099

Stenson, P. D., Ball, E. V., Mort, M., Phillips, A. D., Shiel, J. A., Thomas, N. S., et al. (2003). Human Gene Mutation Database (HGMD): 2003 update. *Hum. Mutat.* 21, 577–581. doi: 10.1002/humu.10212

Sydow, A., Hochgräfe, K., Könen, S., Cadinu, D., Matenia, D., Petrova, O., et al. (2016). Age-dependent neuroinflammation and cognitive decline in a novel Ala152Thr-Tau transgenic mouse model of PSP and AD. *Acta Neuropathol. Commun.* 4:17. doi: 10.1186/s40478-016-0281-z

Talevich, E., Shain, A. H., Botton, T., and Bastian, B. C. (2016). CNVkit: genome-wide copy number detection and visualization from targeted DNA sequencing. *PLoS Comput. Biol.* 12:e1004873. doi: 10.1371/journal.pcbi.1004873

Tarozzi, M., Bartoletti-Stella, A., Dall'Olio, D., Matteuzzi, T., Baiardi, S., Parchi, P., et al. (2022). Identification of recurrent genetic patterns from targeted sequencing panels with advanced data science: a case-study on sporadic and genetic neurodegenerative diseases. *BMC Med. Genomics* 15:26. doi: 10.1186/s12920-022-01173-4

van Duijn, C. M., de Knijff, P., Cruts, M., Wehnert, A., Havekes, L. M., Hofman, A., et al. (1994). Apolipoprotein E4 allele in a population-based study of early-onset Alzheimer's disease. *Nat. Genet.* 7, 74–78. doi: 10.1038/ng0594-74

Wang, G., Zhang, D. F., Jiang, H. Y., Fan, Y., Ma, L., Shen, Z., et al. (2019). Mutation and association analyses of dementia-causal genes in Han Chinese patients with early-onset and familial Alzheimer's disease. *J. Psychiatr. Res.* 113, 141–147. doi: 10.1016/j.jpsychires.2019.03.026

Wenham, P. R., Price, W. H., and Blandell, G. (1991). Apolipoprotein E genotyping by one-stage PCR. *Lancet* 337, 1158–1159. doi: 10.1016/0140-6736(91)92823-k

Wightman, D. P., Jansen, I. E., Savage, J. E., Shadrin, A. A., Bahrami, S., Holland, D., et al. (2021). A genome-wide association study with 1,126,563 individuals identifies new risk loci for Alzheimer's disease. *Nat. Genet.* 53, 1276–1282. doi: 10.1038/s41588-021-00921-z

Wingo, T. S., Lah, J. J., Levey, A. I., and Cutler, D. J. (2012). Autosomal recessive causes likely in early-onset Alzheimer disease. *Arch. Neurol.* 69, 59–64. doi: 10.1001/archneurol.2011.221

Wolfe, C. M., Fitz, N. F., Nam, K. N., Lefterov, I., and Koldamova, R. (2019). The role of apoe and trem2 in Alzheimer' s disease—current understanding and perspectives. *Int. J. Mol. Sci.* 20:81. doi: 10.3390/ijms20010081

frontiers | Frontiers in Aging Neuroscience

TYPE Original Research
PUBLISHED 23 September 2022
DOI 10.3389/fnagi.2022.1006473

OPEN ACCESS

EDITED BY
Xiao-Qiao Dong,
Hangzhou First People's Hospital, China

REVIEWED BY
Jiemiao Hu,
Ningbo Hangzhou Bay Hospital, China
Guo-Feng Yu,
The Quzhou Affiliated Hospital of Wenzhou Medical University, China

*CORRESPONDENCE
Chong Shen
sc@njmu.edu.cn

†These authors have contributed equally to this work and share first authorship

SPECIALTY SECTION
This article was submitted to Cellular and Molecular Mechanisms of Brain-aging, a section of the journal Frontiers in Aging Neuroscience

RECEIVED 29 July 2022
ACCEPTED 05 September 2022
PUBLISHED 23 September 2022

CITATION
Chen C, Chen X, Yang S, Li Q, Ren Z, Wang L, Jiang Y, Gu X, Liu F, Mu J, Liu L, Wang Y, Li J, Yu Y, Zhang J and Shen C (2022) Association of *THBS1* genetic variants and mRNA expression with the risks of ischemic stroke and long-term death after stroke. *Front. Aging Neurosci.* 14:1006473. doi: 10.3389/fnagi.2022.1006473

Association of *THBS1* genetic variants and mRNA expression with the risks of ischemic stroke and long-term death after stroke

Changying Chen[1†], Xuemei Chen[2†], Siyuan Yang[3], Qingqing Li[3], Zhanyun Ren[4], Lu Wang[5], Yuzhang Jiang[6], Xincheng Gu[1], Fangyuan Liu[1], Jialing Mu[1], Lihua Liu[5], Yi Wang[5], Junrong Li[2], Yanhua Yu[2], Jun Zhang[7] and Chong Shen[1*]

[1]Department of Epidemiology, School of Public Health, Nanjing Medical University, Nanjing, China, [2]Department of Neurology, The Affiliated Jiangning Hospital of Nanjing Medical University, Nanjing, China, [3]Department of Neurology, The Affiliated Hospital of Xuzhou Medical University, Xuzhou, China, [4]Department of Neurology, The Affiliated Yixing Hospital of Jiangsu University, Yixing, China, [5]Department of Neurology, Jurong Hospital Affiliated to Jiangsu University, Jurong People's Hospital, Jurong, China, [6]Department of Medical Laboratory, Huai'an First People's Hospital, The Affiliated Huai'an No.1 People's Hospital of Nanjing Medical University, Huai'an, China, [7]Suzhou Center for Disease Control and Prevention, Suzhou, China

Background: Thrombospondin-1 (THBS1) derived from platelets and acted as a critical mediator of hemostasis promoting platelet activation in thrombus formation. The biological connection of genetic variants and mRNA expression of *THBS1* with ischemic stroke (IS) warrants further validation with population-based evidence.

Objective: To evaluate the association of single nucleotide polymorphisms (SNPs) and mRNA expression of *THBS1* with the risks of IS and long-term death after stroke.

Methods: A case-control study consisted of 4,584 IS patients recruited from five hospitals in Jiangsu, China, and 4,663 age-gender-matched controls free of IS. A cohort study enrolled 4,098 participants free of stroke and lasted from 2009 to 2022. Early collected 3158 IS patients aged between 35 and 80 years were followed up an average of 5.86-year to follow up their long-term death outcomes. Two tagSNPs of the *THBS1* gene, rs2236471 and rs3743125, were genotyped in all subjects and *THBS1* mRNA expression of peripheral leukocyte was measured using RT-qPCR in 314 IS cases and 314 controls.

Results: There is no significant difference in genotype and haplotype frequencies of rs2236741 and rs3743125 between IS cases and controls (all $P > 0.05$). Furthermore, the cohort studies did not observe significant associations between *THBS1* variants and the risk of IS incidence or long-term death after IS (all $P > 0.05$). The *THBS1* mRNA expression level ($2^{-\Delta\Delta CT}$) in IS

cases was approximately equal to that in controls (1.01 vs. 0.99, $P = 0.833$). In addition, *THBS1* mRNA expression had no significant association with all-cause death, stroke death, and IS death of IS patients (all $P > 0.05$).

Conclusion: Therefore, our study suggested that there is no significant association of *THBS1* polymorphisms and mRNA expression level with the risk of IS and long-term death after IS.

KEYWORDS

thrombospondin-1, mRNA expression, ischemic stroke, case control study, cohort study

Introduction

Stroke affects 13.7 million people worldwide every year and it is the second leading cause of death, with 5.5 million people dying from it annually (Feigin et al., 2018). The main subtypes of stroke include ischemic stroke (IS) and hemorrhagic stroke (HS). IS, making up ∼71% of all strokes, was defined as infarction of the brain, spinal cord, or retina (Virani et al., 2021). As the 2020 report on cardiovascular health and diseases burden in China, the number of patients suffering from stroke in China was about 13 million at present and the deaths of stroke among Chinese residents accounted for 22.33% of the total deaths (Xiao et al., 2021). Thus, exploring the cause of stroke is important as it can guide therapeutic strategies for the prevention of stroke.

Previous studies presented that a history of hypertension or diabetes mellitus, high levels of blood pressure, smoking, high alcohol consumption were considered as the modifiable risk factors for IS (O'Donnell et al., 2010), while age, gender, and genetic factors are non-modifiable risk factors (Campbell et al., 2019). The estimated heritability of IS was about 37.9% when calculated by current genome-wide complex trait analysis (Bevan et al., 2012). Therefore, the missing heritability of IS and gene-environment interaction remain further exploration.

Thrombospondin-1 (THBS1) is a multifunctional glycoprotein released from platelets, macrophages, and adipocytes (Baenziger et al., 1972; Jaffe et al., 1985; Varma et al., 2008). Endogenous THBS1 is necessary for platelet aggregation and adhesion by overcoming the antithrombotic activity of physiologic nitric oxid (NO) (Isenberg et al., 2008). Besides, THBS1 is a critical mediator of hemostasis that promotes platelet activation by modulating inhibitory cyclic adenosine monophosphate (cAMP) signaling at sites of vascular injury (Aburima et al., 2021). Additionally, THBS1 participates in a wide range of physiological and pathological processes such as tissue remodeling, wound healing, angiogenesis, and inflammation (Sweetwyne and Murphy-Ullrich, 2012). THBS1 is also known to regulate the activation of transforming growth factor-β1 (*TGF-β1*) (Sweetwyne and Murphy-Ullrich, 2012), which makes a difference in restenosis after angioplasty, atherosclerosis, and angiogenesis (August and Suthanthiran, 2006). Above all functions may be involved in the pathophysiology of IS, with common sources of embolism being large artery atherosclerosis (Campbell et al., 2019).

Previous studies showed that genetic variants in the *THBS1* gene were associated with variation in pulmonary artery systolic pressure (Jacob et al., 2017), and chronic ocular surface inflammation after refractive surgery (Contreras-Ruiz et al., 2014). Besides, the coding polymorphism G1678A (rs2292305) was identified as a susceptible locus for cerebral thrombosis in a Chinese population (Liu et al., 2004) and the *THBS1* CT genotype was associated with a reduced risk of developing gastric cancer (Hong et al., 2015). Furthermore, the visceral *THBS1* mRNA expression was positively associated with abdominal obesity, hyperglycemia, and hypertension (Matsuo et al., 2015). Additionally, plasma THBS1 level elevated in patients with IS compared to the controls (Gao et al., 2015) as well as at 2h after tPA-treatment (Navarro-Sobrino et al., 2011). Thus, the serum THBS1 level was proposed to be an independent predictor of favorable outcome at baseline and after 6 months (Gao et al., 2015; Al Qawasmeh et al., 2020). Therefore, further population-based studies would be warranted to validate the association between *THBS1* and IS.

Therefore, this research aimed to investigate whether the genetic variants and mRNA expression of *THBS1* was associated with the susceptibility to developing IS and the long-term death after stroke by conducting the case-control and cohort studies in the Chinese population.

Materials and methods

Population in the case-control study

A total of 4,584 IS cases were recruited from five different hospitals in Jiangsu province, China, which included Jurong

People's Hospital, Nanjing Jiangning Hospital, Yixing People's Hospital, the Affiliated Hospital of Xuzhou Medical University, and Huai'an First People's Hospital from 2009 to 2021. Included patients were diagnosed according to the computed tomography (CT), magnetic resonance imaging (MRI), or angiography with symptoms lasting more than 24 h. Excluded patients were those who had non-atherosclerotic ischemic stroke, acute coronary syndrome, tumor, autoimmune disease, or severe kidney failure according to the patient's history of disease, admission diagnosis and discharge diagnosis. Besides, we use the TOAST (Trial of ORG 10172 in Acute Stroke Treatment) criteria to group the IS subjects. The TOAST classification denotes five subtypes of ischemic stroke: large-artery atherosclerosis (LAA), cardioembolism (CE), small-vessel occlusion (SVO), stroke of other determined etiology (SOE), and stroke of undetermined etiology (SUE). 4,663 controls free of stroke were randomly sampled from local communities and matched to the cases on age (±2 years) and gender. Subjects with acute coronary syndrome, tumor, autoimmune disease, and severe kidney failure were also excluded from the study. Additionally, we chose 314 pairs of IS cases and controls to detect *THBS1* mRNA expression from 2019 to 2021. IS cases had a definite TOAST type and qualified retention samples. The controls were selected from the cohorts in the same or adjacent areas of IS cases using age- and gender- matching method. For above 314 IS patients, we collected the National Institutes of Health Stroke Scale (NIHSS) score and modified Rankin scale (mRS) score of IS patients when discharge, and followed-up their NIHSS scores and mRS scores at 1, 3, and 6 months after discharge. Demographic and clinical characteristics of the study subjects in above two parts were listed in **Table 1**.

Population and outcome in the cohort study

This research incorporated two prospective cohort studies. The community-based cohort study was conducted from 2009 to 2022, which recruited 4128 participants from Guanlin Town and Xushe Town, Yixing city (Jiangsu, China). 4098 baseline subjects without stroke were followed up until May 25, 2022 for stroke onset. The detailed information about this cohort has been described previously (Dong et al., 2021).

The hospital-based cohort study enrolled 3158 IS patients aged between 35 and 80 years from Yixing People's Hospital and followed an average of 5.86-year to record their long-term death outcome based on the annual death data from Yixing Center for Disease Control and Prevention. The follow-up period ended on May 25, 2022. The four endpoints were all-cause death, stroke death, IS death, and HS death. Finally, we observed a total of 488 deaths, among which 245 died from stroke and over half of the stroke-induced deaths were attributed to IS (n = 161). Meanwhile, we collected outcome of the long-term death from local Centers for Disease Control and Prevention (CDC) to assessment the prognosis of IS patients comprehensively, including all-cause death, stroke death, and IS death. Followed up to May 13, 2022, we observed a total of 28 deaths. Of the 20 deaths from stroke, 13 deaths were attributed to IS.

Demographic and clinical characteristics of the study population in the two cohort studies were summarized in **Supplementary Table 2**.

The case-control and cohort studies were all approved by the Research Ethics Committee of Nanjing Medical University (#2018571) and all participants signed the informed consent voluntarily.

Questionnaire survey and physical examination

Demographic characteristics, smoking and drinking habits, diseases history, and medication history were collected by questionnaire survey. All investigators were trained and qualified uniformly. Subjects who have ever smoked one pack of cigarettes a day in the past were considered smokers. Drinker was defined as individuals drinking alcohol at least three times daily. Physical examination including systolic blood pressure (SBP, mmHg) and diastolic blood pressure (DBP, mmHg) were measured at least three times.

Hypertension was defined as a self-reported history of hypertension, or elevated levels of blood pressure (SBP $\geq$ 140 mmHg, DBP $\geq$ 90 mmHg), or taking antihypertensive drugs recently. Those with fasting blood glucose level (GLU) $\geq$ 7.0 mmol/L, or self-reported history of diabetes, or taking hypoglycemic drugs were considered as diabetes. Dyslipidemia was defined as abnormal changes in lipid levels [total cholesterol (TC) $\geq$ 6.2 mmol/L, triglyceride (TG) $\geq$ 2.3 mmol/L, low-density lipoprotein-cholesterol (LDL-C) $\geq$ 4.1 mmol/L, high-density lipoprotein-cholesterol (HDL-C) $<$ 1.04 mmol/L], or self-reported diagnosis of dyslipidemia, or currently taking lipid-lowering drugs.

Blood sample collection and biochemical index detection

Venous peripheral blood was collected from each subject after 8 h from the last meal into vacuum anticoagulation tubes with ethylene diamine tetraacetic acid dipotassium salt (EDTA-K2) and stored at −20°C. Leukocytes were obtained by gradient centrifugation from a subgroup of the study population. GLU was measured using the glucose oxidase method. TC was detected by the cholesterol oxidase-peroxidase method. TG was detected by the glycerophosphate oxidase-peroxidase method. HDL-C was detected by the catalase removal method and LDL-C was measured by sulfuric acid precipitation method.

TABLE 1 Demographic and clinical characteristics of the study population.

Characteristics	Group	Case-control study								Cohort study (n = 4098)
		Total population				Subgroups for mRNA comparison				
		Control (n = 4663)	IS (n = 4584)	Z/χ^2	P	Control (n = 314)	IS (n = 314)	Z/χ^2	P	
Age (year)		66 (60, 72)	66 (59, 72)	0.924	0.355[a]	66 (56, 73)	68 (57, 74)	1.386	0.166[a]	59 (52, 67)
Gender [n (%)]	Male	1941 (41.6)	2722 (59.4)	291.499	<0.001[b]	182 (58.0)	182 (58.0)	<0.001	1.000[b]	1663 (40.6)
	Female	2722 (58.4)	1862 (40.6)			132 (42.0)	132 (42.0)			2435 (59.4)
SBP (mmHg)		139 (127, 152)	150 (134, 161)	20.050	<0.001[a]	148 (133, 158)	154 (138, 168)	3.288	0.001[a]	134 (123, 141)
DBP (mmHg)		81 (74, 88)	87 (80, 95)	23.086	<0.001[a]	84 (76, 92)	85 (76, 95)	0.769	0.442[a]	82 (78, 89)
GLU (mmol/L)		5.45 (4.97, 5.97)	5.35 (4.56, 5.63)	16.924	<0.001[a]	5.86 (5.27, 6.76)	5.48 (4.88, 6.52)	3.875	<0.001[a]	5.28 (4.85, 5.80)
TC (mmol/L)		4.93 (4.32, 5.60)	4.52 (3.83, 5.28)	19.287	<0.001[a]	4.77 (4.21, 5.53)	4.45 (3.67, 5.15)	5.116	<0.001[a]	4.80 (4.22, 5.45)
TG (mmol/L)		1.36 (0.96, 1.96)	1.38 (0.98, 2.04)	1.822	0.068[a]	1.34 (0.92, 1.90)	1.28 (0.99, 1.88)	0.054	0.957[a]	1.32 (0.90, 2.00)
HDL-C (mmol/L)		1.32 (1.14, 1.54)	1.14 (0.97, 1.34)	28.142	<0.001[a]	1.31 (1.09, 1.56)	1.09 (0.93, 1.30)	8.119	<0.001[a]	1.33 (1.13, 1.55)
LDL-C (mmol/L)		2.71 (2.21, 3.21)	2.64 (2.09, 3.19)	3.724	<0.001[a]	2.73 (2.207, 3.24)	2.71 (2.03, 3.25)	0.702	0.483[a]	2.65 (2.20, 3.11)
Smoking [n (%)]	No	3725 (79.9)	3570 (77.9)	5.578	0.018[b]	232 (73.9)	266 (84.7)	11.214	0.001[b]	3103 (75.7)
	Yes	938 (20.1)	1014 (22.1)			82 (26.1)	48 (15.3)			995 (24.3)
Drinking [n (%)]	No	3748 (80.4)	3968 (86.6)	63.996	<0.001[b]	220 (70.1)	283 (90.1)	39.643	<0.001[b]	3215 (78.5)
	Yes	915 (19.6)	616 (13.4)			94 (29.9)	31 (9.9)			883 (21.5)
Hypertension [n (%)]	No	2327 (49.9)	734 (16.0)	1198.984	<0.001[b]	85 (27.1)	42 (13.4)	18.250	<0.001[b]	2110 (51.5)
	Yes	2336 (50.1)	3850 (84.0)			229 (72.9)	272 (86.6)			1988 (48.5)
Diabetes [n (%)]	No	4000 (85.8)	3327 (72.6)	244.928	<0.001[b]	236 (75.2)	208 (66.2)	6.027	0.014[b]	3634 (88.7)
	Yes	663 (14.2)	1257 (27.4)			78 (24.8)	106 (33.8)			464 (11.3)
Dyslipidemia [n (%)]	No	2891 (62.0)	2693 (58.7)	10.213	0.001[b]	152 (48.4)	241 (76.8)	53.862	<0.001[b]	1642 (40.1)
	Yes	1772 (38.0)	1891 (41.3)			162 (51.6)	73 (23.2)			2456 (59.9)

[a]Mann-Whitney U-test; [b]χ^2-test; IS, ischemic stroke; SBP, systolic blood pressure; DBP, diastolic blood pressure; GLU, glucose; TC, total cholesterol; TG, triglyceride; HDL-C, high-density lipoprotein-cholesterol; LDL-C, low-density lipoprotein-cholesterol.

10.3389/fnagi.2022.1006473

Single nucleotide polymorphism selection and genotyping

The *THBS1* gene (Gene ID: 7057, Locus NC_000015.10) locates on chromosome 15q14 and spans 18,388 bp, and consists of 22 exons. We searched the SNPs from the upstream 2 kb to the downstream 1 kb and selected tagging SNPs (tagSNPs) through the database of the Chinese Han population in Beijing (CHB) and China of the International Hap MAP Project. Three tagSNPs (tagSNPs rs2292305, etc. tagSNP rs2236741, and tagSNP rs2292304) would be available for candidate SNP selection. Included tagSNPs met the criteria of minor allele frequency (MAF) $\geq$ 0.05 and linkage disequilibrium (LD) $r^2 \geq 0.8$. A functional candidate strategy was also applied to select potential functional SNPs on the bioinformatics effect prediction website SNPinfo Web Server.[1] The SNP function prediction results of rs2292305 showed no informed predictive biological function, therefore, we selected the closely linked tagSNP rs3743125 ($r^2 = 0.932$) with a prior predictive biological function as the substitute. We did not include rs2292304 because its probes and primers were not designed successfully. Finally, two tagSNPs of *THBS1* gene, rs2236471 (C > T) and rs3743125 (G > A) were selected and genotyped in this study. Detailed biological information and function prediction were summarized in **Supplementary Table 1**.

DNA was extracted from the unfrozen venous peripheral blood using the protein precipitation method (Eaglink, EGEN2024, China) and then preserved at −20°C. Each DNA sample was quantified using the NanoDrop 2000 spectrophotometer (Thermo Fisher Scientific, Waltham, MA). The polymerase chain reaction (PCR) TaqMan MGB probe assay was performed to amplify the two SNPs in the GeneAmp® PCR system 9700 thermal cycle (Applied Biosystems, Foster City, CA). The results were post-read on the 7900HT real-time PCR system (Applied Biosystems, Foster City, CA) with the Sequence Detection System (SDS) 2.4 software. The successful call rates of two SNPs genotyping were both 100%.

RNA extraction, reverse transcription, and quantitative real-time polymerase chain reaction

White blood cells were separated from peripheral blood by gradient centrifugation and stored at −20°C. Peripheral leukocyte was reserved in RNA protective additive (Eaglink, EGEN2026, China) at −20°C. Total RNA was extracted using the Whole Blood RNA Extraction Kit (Yuan, Yu-BR02-1, China) and quantified using a NanoDrop 2000 spectrophotometer (Thermo Fisher Scientific, Waltham, MA). Isolated RNA was reversely transcribed into cDNA using the PrimeScript™ RT Reagent Kit (Takara, RR047A, Japan). *THBS1* gene mRNA expression of peripheral leukocyte was measured using SYBR Green quantitative real-time polymerase chain reaction (RT-qPCR), and the housekeeping gene Glyceraldehyde-3-Phosphate Dehydrogenase (*GAPDH*) was tested as an endogenous control. The qPCR reaction system included Platinum® SYBR® Green qPCR SuperMix-UDG (Invitrogen, 11733-046, USA), RNase free dH_2O, forward primer, reverse primer, and cDNA. Samples were incubated at 95°C for 5 min, followed by 40 cycles of 95°C for 10 s, 57°C for 20 s, and 72°C for 20 s on the QuantStudio™ 7 Flex Real-Time PCR System platform (Applied Biosystems, 4485700, CA). All samples were analyzed in three parallels, and cycle threshold values were recorded. The $2^{-\Delta\Delta CT}$ method was used to calculate relative expression levels of *THBS1* normalized by *GAPDH*. *THBS1* mRNA's forward primer sequence (5′–3′) was AGACTCCGCATCGCAAAGG, and the reverse primer sequence (5′–3′) was TCACCACGTTGTTGTCAAGGG. *GAPDH* mRNA's forward primer sequence (5′–3′) was GGAGCGAGATCCCTCCAAAAT, and the reverse primer sequence (5′–3′) was GGCTGTTGTCATACTTCTCATGG.

Statistical analysis

We used EpiData 3.1 software (The EpiData Association, Odense, Denmark) for duplicate entry and consistency check of the collected data. Continuous variables were presented as median [inter-quartile range (IQR)] for non-parametric data. Categorical variables were presented as frequencies and percentages. For group-wise comparisons, the Kruskal–Wallis test or Mann–Whitney test was used for continuous variables with abnormal distribution. The chi-square test (χ^2) was used to compare the differences in categorical variables between case and control groups. The Fisher's exact test was used to estimate whether the genotype frequencies in controls and IS group met the Hardy–Weinberg equilibrium (HWE) law. Binary logistic regression was applied to calculate the odds ratios (*ORs*) and corresponding 95% confidence intervals (*CIs*) for the association of *THBS1* variants and IS with adjustment for covariates (age, gender, smoking, drinking, hypertension, diabetes, and dyslipidemia). We used Cox proportional hazard regression to estimate the association with hazard ratios (*HRs*) and 95% *CIs* as well as after adjustment for covariates in the cohort study. Kruskal-Wallis H test was conducted to test the trend in mRNA levels among different groups of SNP genotypes. We used Spearman's rank correlation to evaluate the correlations between *THBS1* mRNA expression and NIHSS scores and MRS Scores after discharge in IS cases. We also used restricted cubic splines (RCS) with four knots at the 20th, 40th, 60th, and 80th centiles to flexibly model the

1 https://manticore.niehs.nih.gov/snpinfo/snpfunc.html

association of *THBS1* mRNA expression with the risk of long-term deaths in IS patients.

Haplotype association analyses as outlined by Schaid et al. (2002) were performed to test the associations of statistically inferred Haplotype with IS weighted with their estimated probability. All data analyses were carried out using SAS software 9.4 (SAS Inc., Cary, N.C., USA) and R 4.1.1 version.[2] A two−tailed *P*-value < 0.05 was considered statistically significant.

Results

Demographic and clinical characteristics of the study population

Table 1 shows the detailed demographic and clinical characteristics of 4,584 IS cases and 4,663 matched controls in the genetic case-control study. The median age of IS group (66 years) was comparable with that of the control group (66 years, $P = 0.355$). IS group had higher proportions of male (59.4%) and smokers (22.1%) while a lower proportion of drinkers (13.4%) than control group (41.6, 20.1, and 19.6%; $P < 0.05$). There were significant differences in SBP, DBP, GLU, TC, HDL-C, and LDL-C levels ($P < 0.001$) between the IS cases and controls. IS group had higher prevalence of hypertension (84.0%), diabetes (27.4%), and dyslipidemia (41.3%) than controls (50.1, 14.2 and 38.0%; $P \leq 0.001$).

In the case-control study for transcriptome level analysis, IS group presented higher level of SBP but lower levels of GLU, TC, and HDL-C than control group (**Table 1**). Age and gender were both matched for case and control. IS group had lower proportions of smokers (15.3%) and drinkers (9.9%) than control group (26.1% and 29.9%; $P \leq 0.001$). IS group had higher prevalence of hypertension (86.6%) while a lower prevalence of dyslipidemia (23.2%) than control group (72.9 and 51.6%; $P < 0.001$). **Table 1** also listed the characteristics of participants in the cohort study for the risk of IS incidence. The clinical characteristic of the follow-up study for the long-term death after IS were presented in **Supplementary Table 2**.

Association analyses of the thrombospondin-1 variants with IS in the case-control study

As shown in **Table 2**, the genotype and allele distributions of SNP rs2236741 followed *HWE* both in the control and IS groups (both *P*-values > 0.05). Even though we have double-checked the genotyping results and controlled the quality by comparing the genotype frequencies of cases and controls of each plate, the allele frequencies of rs3743125 did not accord with the *HWE* in controls ($P = 0.024$) but accord with *HWE* in IS cases ($P = 0.098$).

No significant association of the two tagSNPs at *THBS1* with IS was observed in the case-control study (**Supplementary Table 3**). The adjusted *ORs* (95%*CIs*) for the addictive model of rs2236741 and rs3743125 were 0.955 (0.872–1.047) and 0.955 (0.890–1.025) after adjustment for covariates. No significant association was observed for the dominant and recessive models of the two SNPs with IS (**Table 2**). Further stratification analyses by age, gender, smoking, drinking, hypertension, diabetes, and dyslipidemia did not reveal any significant association (**Supplementary Tables 4**, **5**). There was no significant association between *THBS1* variants and TOAST subtypes of IS in the case-control study (**Supplementary Table 6**).

Haplotype analyses of rs2236741–rs3743125

Compared with C-G haplotype of rs2236741 and rs3743125, the haplotype C-A, T-G, and T-A were identified to have no significant association with IS (**Supplementary Table 7**), even after adjustment for covariates [Adjusted *ORs* (95%*CIs*): 0.974 (0.894–1.062), 1.103 (0.829–1.469), and 0.933 (0.845–1.030), respectively] (**Table 3**). In addition, the haplotypes C-A, T-G, and T-A were not associated with LAA and SVO (**Supplementary Table 8**).

Association analyses for the incidence risk of ischemic stroke in the cohort study

After an average of 10.15-year follow-up for 4098 subjects free of stroke at baseline, 319 incident IS cases (10.30%) were observed and the incidence density was 63.08 (per 10^4 person-year). The variants of rs2236741 and rs3743125 were not associated with the incident risk of IS (**Supplementary Table 9**), even after adjustment for covariates [Adjusted *HRs* (95%*CIs*) for the addictive model: 1.025 (0.821–1.281) and 0.984 (0.829–1.168)] (**Table 4**).

Association analyses of thrombospondin-1 variants and the risk of long-term death after ischemic stroke

The variants of rs2236741 and rs3743125 were not associated with the long-term death after IS (**Supplementary Table 10**). Adjusted *HRs* (95%*CIs*) of the addictive model of rs2236741 and rs3743125 for all-cause death, stroke death, IS death, and HS death were 1.014 (0.848–1.212), 1.052 (0.820–1.349), 0.990 (0.723–1.356), 0.948 (0.553–1.626), and adjusted

2 http://cran.r-project.org/

TABLE 2 Association analyses of *THBS1* variants and the risk of ischemic stroke in the case-control study.

SNP	Group	WT/HT/MT	*OR* (95% *CI*)[a]			Allele			*P* for *HWE*
			Additive model	Dominant model	Recessive model	Major/Minor	*OR* (95% *CI*)	*P*[b]	
rs2236741	Control	3445/1116/102	0.955 (0.872–1.047)	0.973 (0.877–1.078)	0.753 (0.548–1.035)	0.858/0.142	1.001 (0.921–1.087)	0.991	0.301
(C>T)	IS	3384/1107/93	*P* = 0.331	*P* = 0.599	*P* = 0.080	0.859/0.141			0.824
rs3743125	Control	2185/2062/416	0.955 (0.890–1.025)	0.940 (0.858–1.029)	0.955 (0.815–1.120)	0.690/0.310	0.984 (0.925–1.048)	0.619	0.024
(G>A)	IS	2178/1998/408	*P* = 0.199	*P* = 0.181	*P* = 0.574	0.693/0.307			0.098

WT, wild type; HT, heterozygote type; MT, mutant type; HWE, Hardy-Weinberg; IS, ischemic stroke. [a]Adjusted for age, gender, smoking, drinking, hypertension, diabetes, and dyslipidemia. [b]*P*-value of χ^2-test for comparison of allele frequencies between the case and control groups.

TABLE 3 Haplotype frequencies of rs2236741–rs3743125 and association analyses with ischemic stroke.

Haplotype[a]	All (*n* = 9247)	IS (*n* = 4584)	Control (*n* = 4663)	*OR* (95% *CI*)[c]	*P*[c]
C-G[b]	0.678	0.678	0.677	Reference	–
C-A	0.181	0.181	0.182	0.974 (0.894–1.062)	0.668
T-G	0.014	0.015	0.013	1.103 (0.829–1.469)	0.462
T-A	0.127	0.126	0.128	0.933 (0.845–1.030)	0.199

[a]Loci are arranged in the order rs2236741–rs3743125. [b]C-G was chosen to be the reference. [c]Adjusted for age, gender, smoking, drinking, hypertension, diabetes, and dyslipidemia.

TABLE 4 Association analyses of *THBS1* variants with the incidence risk of ischemic stroke in the cohort study.

SNP	Genotype	Incident cases	Person-years	Incidence density (/10^4 person-years)	*HR* (95% *CI*)[a]		
					Additive model	Dominant model	Recessive model
rs2236741	CC	235	37497.42	62.67	1.025 (0.821–1.281)	1.041 (0.811–1.337)	0.915 (0.407–2.056)
	CT	78	11947.78	65.28	*P* = 0.827	*P* = 0.752	*P* = 0.829
	TT	6	1127.20	53.23			
rs3743125	GG	155	23845.56	65.00	0.984 (0.829–1.168)	0.944 (0.758–1.177)	1.097 (0.757–1.589)
	GA	133	21951.53	60.59	*P* = 0.856	*P* = 0.608	*P* = 0.626
	AA	31	4775.31	64.92			

[a]Adjusted for age, gender, smoking, drinking, hypertension, diabetes, and dyslipidemia.

*HR*s (95%*CI*s) of the addictive model of rs3743125 for all-cause death, stroke death, IS death, and HS death were 1.125 (0.982–1.289), 0.985 (0.809–1.199), 1.030 (0.810–1.310), 0.887 (0.583–1.351), respectively. The dominant and recessive models of the two SNPs had no association with the long-term death either (Table 5).

Comparisons of thrombospondin-1 mRNA expression between ischemic stroke cases and controls

The mRNA expression level of *THBS1* in IS cases was approximately equal to that in controls (1.01 vs. 0.99, *P* = 0.833). Further subgroup analyses by age, gender, smoking, drinking, hypertension, diabetes, and dyslipidemia did not observed significant differences in *THBS1* mRNA expression was detected between IS cases and controls (Supplementary Table 11). Additionally, no significant difference in *THBS1* mRNA expression was detected between the three TOAST subgroup of IS and control group (Figure 1). As shown in Figure 2, the *THBS1* mRNA expression levels significantly differed across rs3743125 GG, GA, and AA carriers in the control group (*P* = 0.016), but not in IS group (*P* = 0.454).

Association analyses of the thrombospondin-1 mRNA expression with the prognosis of ischemic stroke cases

RCS regression analyses did not identify significant linear or non-linear correlation between *THBS1* mRNA expression and the risk of all-cause death, stroke death, and IS death in IS patients (Figure 3). The adjusted *HR*s (95%*CI*s) for all-cause death, stroke death, and IS death were 0.962 (0.842–1.099), 0.986 (0.908–1.071), 0.975 (0.821–1.158), respectively (Supplementary Table 12). Furthermore, *THBS1*

TABLE 5 Association analyses of *THBS1* variants with the risk of long-term death after stroke*.

Outcome	SNP	Genotype	Events	Person-years	Density (/10^4 person-years)	*HR* (95% *CI*)[a]		
						Additive model	Dominant model	Recessive model
All cause death	rs2236741	CC	364	13654.01	266.59	1.014 (0.848–1.212)	0.995 (0.811–1.220)	1.201 (0.691–2.086)
		CT	111	4445.22	249.71	*P* = 0.883	*P* = 0.958	*P* = 0.516
		TT	13	415.70	312.73			
	rs3743125	GG	225	8885.69	253.22	1.125 (0.982–1.289)	1.125 (0.941–1.346)	1.262 (0.943–1.688)
		GA	212	7982.88	265.57	*P* = 0.091	*P* = 0.196	*P* = 0.117
		AA	51	1646.36	309.78			
Stroke death	rs2236741	CC	182	13654.01	133.29	1.052 (0.820–1.349)	1.011 (0.758–1.346)	1.500 (0.740–3.039)
		CT	55	4445.22	123.73	*P* = 0.690	*P* = 0.943	*P* = 0.260
		TT	8	415.70	192.45			
	rs3743125	GG	120	8885.69	135.05	0.985 (0.809–1.199)	0.993 (0.772–1.277)	0.946 (0.598–1.496)
		GA	105	7982.88	131.53	*P* = 0.883	*P* = 0.955	*P* = 0.813
		AA	20	1646.36	121.48			
Ischemic stroke death	rs2236741	CC	122	13654.01	89.35	0.990 (0.723–1.356)	0.940 (0.655–1.349)	1.429 (0.585–3.487)
		CT	34	4445.22	76.49	*P* = 0.952	*P* = 0.738	*P* = 0.433
		TT	5	415.70	120.28			
	rs3743125	GG	77	8885.69	86.66	1.030 (0.810–1.310)	1.047 (0.767–1.429)	1.012 (0.584–1.753)
		GA	70	7982.88	87.69	*P* = 0.808	*P* = 0.773	*P* = 0.967
		AA	14	1646.36	85.04			
Hemorrhagic stroke death	rs2236741	CC	43	13654.01	31.49	0.948 (0.553–1.626)	0.867 (0.466–1.614)	1.630 (0.396–6.708)
		CT	11	4445.22	24.75	*P* = 0.847	*P* = 0.654	*P* = 0.498
		TT	2	415.70	48.11			
	rs3743125	GG	29	8885.69	32.64	0.887 (0.583–1.351)	0.874 (0.517–1.480)	0.820 (0.296–2.272)
		GA	23	7982.88	28.81	*P* = 0.577	*P* = 0.617	*P* = 0.703
		AA	4	1646.36	24.30			

*Ischemic stroke cases aged between 35 and 80 years were selected. [a]Adjusted for age, gender, smoking, drinking, hypertension, diabetes, and dyslipidemia.

mRNA expression has no significant relevance to NIHSS scores of discharges ($\rho = -0.042$, $P = 0.462$), 1 month after discharge ($\rho = 0.064$, $P = 0.445$), 3 months after discharge ($\rho = 0.044$, $P = 0.601$), and 6 months after discharge ($\rho = 0.065$, $P = 0.441$) in IS cases (Figure 4). Similarly, there is no correlation between *THBS1* mRNA expression and mRS scores of discharges ($\rho = -0.010$, $P = 0.864$), 1 month after discharge ($\rho = 0.030$, $P = 0.716$), 3 months after discharge ($\rho = 0.043$, $P = 0.608$), and 6 months after discharge ($\rho = 0.066$, $P = 0.434$) in IS cases (Figure 5).

Discussion

In this research, we investigated the association of variations and mRNA expression of *THBS1* with the risk of IS and long-term death after stroke. Our results demonstrated that there was no significant association between tagSNPs of *THBS1* and IS as following aspects. In the case control study, genotype and haplotype analyses identified no significant association with IS and TOAST subtypes of IS. Furthermore, cohort studies did not indicate significant associations between *THBS1* variants and the risk of IS incidence or long-term death after stroke. Previous study showed that the coding polymorphism rs2292305 which is closely linked with rs3743125 we selected ($r^2 = 0.932$) was identified no significant with cerebral infarction in a Chinese population (Liu et al., 2004). This result was consistent with our results. In addition, the *THBS1* mRNA expression in IS cases was approximately equal to that in controls not only in the total population but also in different subgroups. *THBS1* mRNA expression had no significant association with the prognosis of IS, including NIHSS scores, mRS scores, and long-term deaths after discharge. Thus, there is no significant association of *THBS1* variants and leukocyte mRNA expression with the risk of IS and long-term death after stroke.

Ischemic stroke is one of the most vital causes of neurological morbidity and mortality in the world (Virani et al., 2021). Numerous studies confirmed that the inflammatory reaction that occurs in the cerebral tissue takes part in acute pathologies of ischemic stroke. The

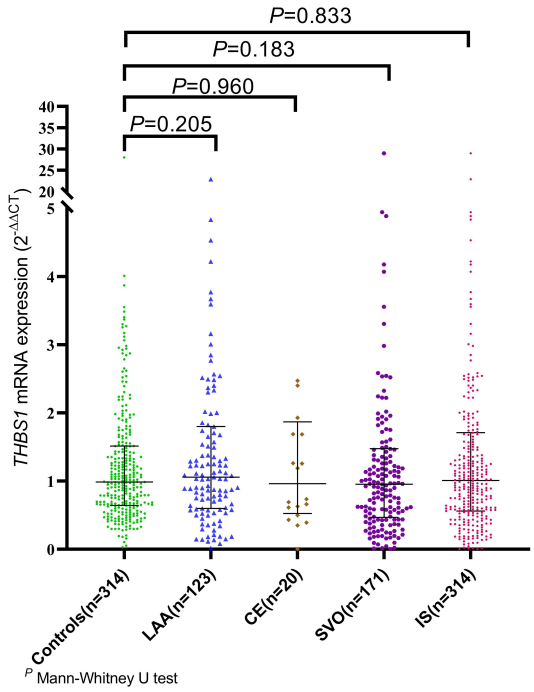

FIGURE 1
The mRNA expression of *THBS1* common variants in IS cases with different TOAST types and controls. The mRNA expression level of *THBS1* in IS cases was approximately equal to that in controls (1.01 vs. 0.99, $P = 0.833$). Additionally, no significant difference in the *THBS1* mRNA expression was detected between the three TOAST subgroups of IS cases and control group [LAA vs. controls: (1.09 vs. 0.99, $P = 0.205$), CE vs. controls: (0.96 vs. 0.99, $P = 0.960$), SVO vs. controls: (0.96 vs. 0.99, $P = 0.183$)].

function damage to the brain following ischemic stroke results in necrosis and apoptosis; all of these could trigger the inflammatory reaction controlled by the release of ROS, chemokines, and cytokines (Brea et al., 2009). The thrombospondin (THBS) family of secreted matricellular glycoproteins consisting of five members (THBS1-5) are stress and injury mediators of cellular attachment dynamics and extracellular matrix protein production (Schips et al., 2019). Della-Morte et al. (2012) observed that variation in the von Willebrand factor (*VWF*), *THBS1*, and *SERPINE1* genes may involve in the pathogenesis of atherosclerotic plaque and that suggested *THBS1* had the ability to interact with *VWF*, to be an candidate gene for arterial thrombosis (Bonnefoy et al., 2006). Nonetheless, no strong evidence supported the role of *THBS1* in the occurrence of arterial thrombosis (van Schie et al., 2011), and the correlation between peripheral THBS1 levels and long-term outcome of IS (Gao et al., 2015; Al Qawasmeh et al., 2020) merely displayed a concomitant effect rather than sequential relationship of causality. Therefore, the causal relationship between *THBS1* and IS was still lack of sufficient evidence.

Isenberg and Roberts (2020) concluded that the *THBS1* mutation alone may not be sufficient to cause pulmonary artery hypertension (PAH), and *THBS1* was proposed to be a modifier gene for familial PAH. The frequency of common *THBS1* polymorphisms did not differ between PAH and control cohorts (Isenberg and Roberts, 2020). *THBS1* induced lethal cardiac atrophy and played a vital role in intermittent hypoxia-induced fibroblast activation and cardiac fibrosis when overexpressed (Bao et al., 2020; Vanhoutte et al., 2021). Furthermore, hsa-miR-4443 protected atrial fibrillation (AF) by targeting *THBS1* (Xiao et al., 2021), as a biomarker in the development of AF and AF-related complications (Liu et al., 2021). Cardioembolic stroke caused by the embolus forming in the heart and occluding cerebral arteries is rising largely (Maida et al., 2020). AF is one of the risk factors for cardioembolic stroke. A previous study verified that subjects affected by AF have a risk of cerebral ischemia 3–5 times

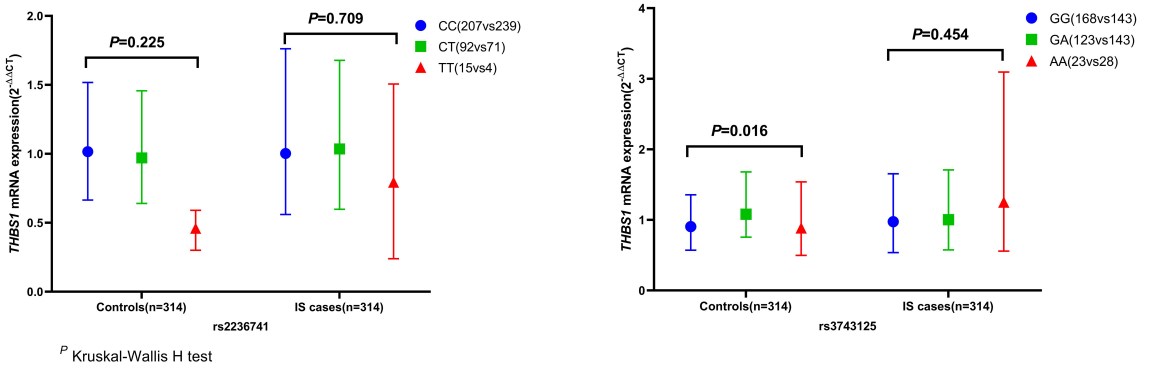

FIGURE 2
THBS1 gene mRNA expression ($2^{-\Delta\Delta CT}$) among different genotypes of rs2236741 and rs3743125. The *THBS1* mRNA expression levels significantly differed across rs3743125 GG, GA, and AA carriers in the control group (0.91 vs. 1.08 vs. 0.89, $P = 0.016$) but were not significantly different in IS group (0.97 vs. 1.00 vs. 1.25, $P = 0.454$). Besides, there were no significant differences across rs2236741 CC, CT, and TT carriers in the control group (1.02 vs. 0.97 vs. 0.54, $P = 0.225$) or in the IS cases (1.00 vs. 1.04 vs. 0.79, $P = 0.709$).

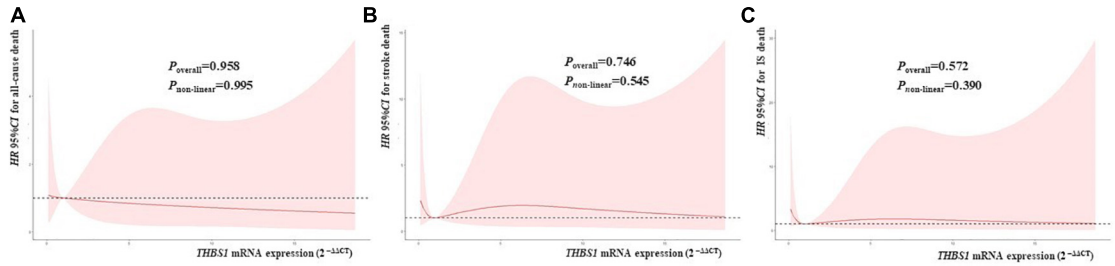

FIGURE 3
THBS1 mRNA expression with the *HRs* with 95%CIs for long-term deaths of IS patients. The *HRs* with 95%CIs for all-cause death, stroke death, and IS death had no correlation to *THBS1* mRNA expression in IS patients. (all *P*-values > 0.05).

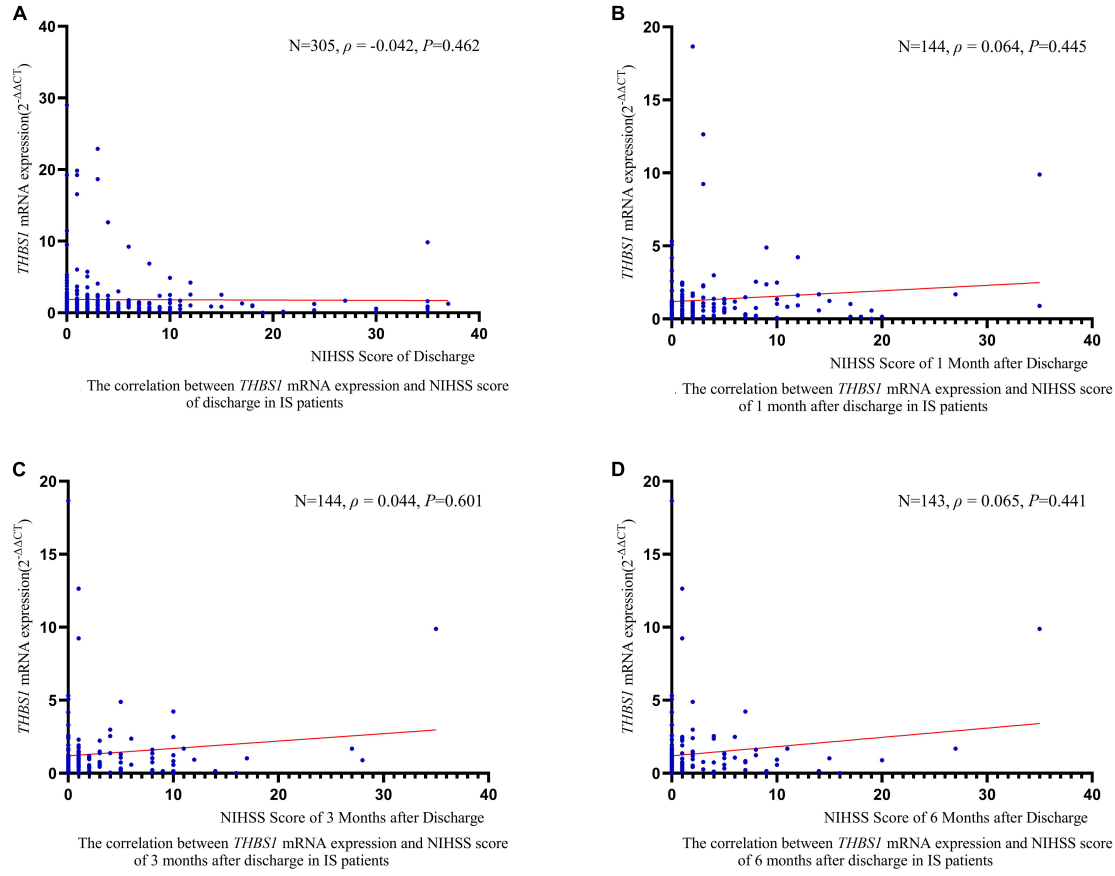

FIGURE 4
The correlation between *THBS1* mRNA expression and NIHSS scores of different periods after discharge in IS patients. *THBS1* mRNA expression has no significant relevance to NIHSS scores of different periods after discharge in IS patients (all *P*-values > 0.05).

higher than the average (Wolf et al., 1991). Consequently, *THBS1* may have relation to cardioembolic stroke. However, our research did not observe a positive association between *THBS1* and IS not only in the IS case-control study but also in the cohort studies. The reason may be that cardioembolic stroke accounts for only 5.4% of all IS cases in our study.

Although previous study indicated that *THBS1* may related to cardioembolic stroke, there was no significant difference of *THBS1* mRNA expression between CE cases and controls in this study. Consequently, these findings did not support the etiological role of *THBS1* in IS. However, Li et al. found several key genomic expressions (CCL20, *THBS1*, EREG, and IL6 etc.) were dramatically down-regulated in 5 and 24 h after

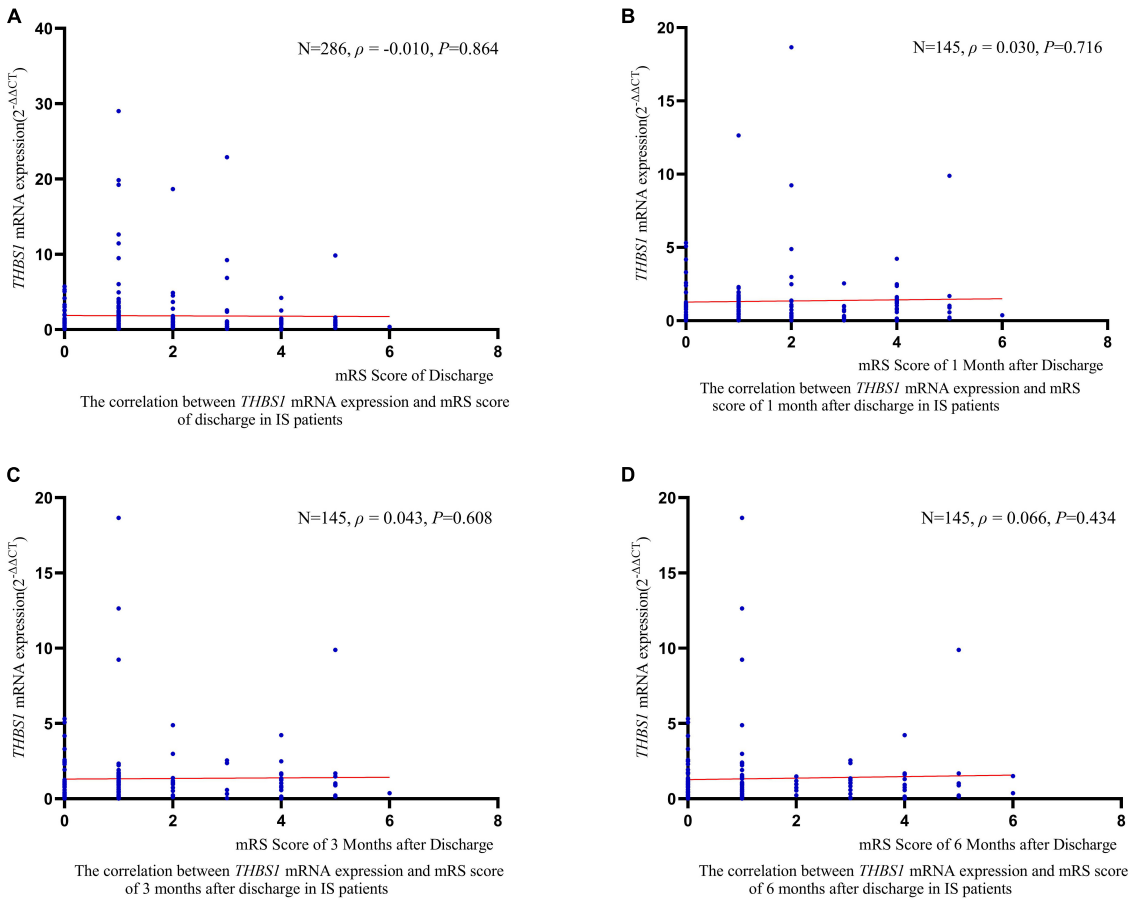

FIGURE 5
The correlation between *THBS1* mRNA expression and mRS scores of different periods after discharge in IS patients. *THBS1* mRNA expression has no significant relevance to mRS scores of different periods after discharge in IS patients (all *P*-values > 0.05).

ischemic stroke compared to controls (Li et al., 2017). On the contrary, expression of *THBS1* was noted in the ischemic brain with different temporal expression profiles from different cellular origins after focal cerebral ischemia/reperfusion (Lin et al., 2003). Besides, an animal study suggested that *THBS1* may increase the recruitment of monocytes into the clot and promote the transformation of monocytes into macrophages (Zhou et al., 2010). In advance, it has been reported that *THBS1* could block vascular endothelial growth factor (VEGF)-induced angiogenesis (Iruela-Arispe et al., 1999), so the change of *THBS1* expression in ischemic brains may confer a negative-feedback mechanism in angiogenesis (Kyriakides et al., 1998). In this study, THBS1 mRNA expression levels significantly differed across rs3743125 GG, GA, and AA carriers in the control group but not in IS group. The results may imply the latent biological function of rs3743125 on regulating mRNA expression in the population free of stroke while the effect disappears at IS occurrence. Since no significant association of THBS1 genetic variations and mRNA level was observed with IS or long-term death after IS, the value of this difference is limited to verify the pathogenesis of IS.

Though our current data did not suggest any significant association between the *THBS1* variants or mRNA expression and IS, this research with no doubt has notable strengths. First of all, our study differs from previous *THBS1* relevant studies that focused on the relationship between *THBS1* protein levels in plasma and IS (Gao et al., 2015; Moin et al., 2021). This study is unique since we integrated analyses of the genomic level and the transcriptomic level of *THBS1*. Moreover, we explored the association of *THBS1* candidate SNPs with not only the future new-onset IS but also the long-term outcomes of IS by combining the case-control study and the cohort study. In addition, the large sample size and the experiments with high-quality control ensured the accuracy and reliability of our results. However, some limitations are also worth mentioning. First, we did not detect serum THBS1 protein. Second, we selected candidate SNPs at the *THBS1* gene with the criterion of MAF $\geq$ 0.05, so could have missed the rare variants

with MAF < 0.05 that may have substantial biological effects on the IS occurrence and long-term death after IS.

In conclusion, although these findings need to be validated, our results indicated that there was no significant association between *THBS1* polymorphisms and the risk of IS incidence or long-term death of IS, and no significant difference in *THBS1* mRNA expression observed between IS patients and controls. Our findings, though negative, might as well contribute to verifying that the *THBS1*variants and expression do not affect the susceptibility to IS, and may provide useful evidence and guidance regarding the correlation between THBS1 and IS.

Data availability statement

The data analyzed in this study is subject to the following licenses/restrictions: "The datasets presented in this article are not available due to participants' confidentiality." Requests to access these datasets should be directed to corresponding author.

Ethics statement

Informed consent was obtained from each participant and this study was approved by the Research Ethics Committee of Nanjing Medical University (#2018571). The patients/participants provided their written informed consent to participate in this study.

Author contributions

CS designed the study, edited, and proofed the manuscript. CC performed the experiment work, analyzed the data, and wrote the manuscript. XC edited and proofed the manuscript. SY, LW, YJ, LL, and YW collected the data. QL, ZR, JL, and YY collected the samples. XG, FL, and JM performed the experiment work. All authors agreed to be accountable for the content of the work.

Funding

This work was supported by the National Natural Science Foundation of China (Grant Nos. 81872686 and 82173611) and the Priority Academic Program for the Development of Jiangsu Higher Education Institutions (Public Health and Preventive Medicine).

Acknowledgments

We would like to thank Hankun Xie for helping to edit the English language.

Conflict of interest

The authors declare that the research was conducted in the absence of any commercial or financial relationships that could be construed as a potential conflict of interest.

Publisher's note

All claims expressed in this article are solely those of the authors and do not necessarily represent those of their affiliated organizations, or those of the publisher, the editors and the reviewers. Any product that may be evaluated in this article, or claim that may be made by its manufacturer, is not guaranteed or endorsed by the publisher.

Supplementary material

The Supplementary Material for this article can be found online at: https://www.frontiersin.org/articles/10.3389/fnagi.2022.1006473/full#supplementary-material

References

Aburima, A., Berger, M., Spurgeon, B. E. J., Webb, B. A., Wraith, K. S., Febbraio, M., et al. (2021). Thrombospondin-1 promotes hemostasis through modulation of cAMP signaling in blood platelets. *Blood* 137, 678–689. doi: 10.1182/blood.2020005382

Al Qawasmeh, M., Alhusban, A., and Alfwaress, F. (2020). An evaluation of the ability of thrombospondin-1 to predict stroke outcomes and mortality after ischemic stroke. *Int. J. Neurosci.* 1–4. [Epub ahead of print]. doi: 10.1080/00207454.2020.1825417

August, P., and Suthanthiran, M. (2006). Transforming growth factor beta signaling, vascular remodeling, and hypertension. *N. Engl. J. Med.* 354, 2721–2723. doi: 10.1056/NEJMcibr062143

Baenziger, N. L., Brodie, G. N., and Majerus, P. W. (1972). Isolation and properties of a thrombin-sensitive protein of human platelets. *J. Biol. Chem.* 247, 2723–2731.

Bao, Q., Zhang, B., Suo, Y., Liu, C., Yang, Q., Zhang, K., et al. (2020). Intermittent hypoxia mediated by TSP1 dependent on STAT3 induces cardiac

fibroblast activation and cardiac fibrosis. *Elife* 9:e49923. doi: 10.7554/eLife.49923

Bevan, S., Traylor, M., Adib-Samii, P., Malik, R., Paul, N. L., Jackson, C., et al. (2012). Genetic heritability of ischemic stroke and the contribution of previously reported candidate gene and genomewide associations. *Stroke* 43, 3161–3167. doi: 10.1161/strokeaha.112.665760

Bonnefoy, A., Daenens, K., Feys, H. B., De Vos, R., Vandervoort, P., Vermylen, J., et al. (2006). Thrombospondin-1 controls vascular platelet recruitment and thrombus adherence in mice by protecting (sub)endothelial VWF from cleavage by ADAMTS13. *Blood* 107, 955–964. doi: 10.1182/blood-2004-12-4856

Brea, D., Sobrino, T., Ramos-Cabrer, P., and Castillo, J. J. C. D. (2009). Inflammatory and neuroimmunomodulatory changes in acute cerebral ischemia. *Cerebrovasc. Dis.* 27, 48–64. doi: 10.1159/000200441

Campbell, B. C. V., De Silva, D. A., Macleod, M. R., Coutts, S. B., Schwamm, L. H., Davis, S. M., et al. (2019). Ischaemic stroke. *Nat. Rev. Dis. Primers* 5:70. doi: 10.1038/s41572-019-0118-8

Contreras-Ruiz, L., Ryan, D. S., Sia, R. K., Bower, K. S., Dartt, D. A., and Masli, S. (2014). Polymorphism in THBS1 gene is associated with post-refractive surgery chronic ocular surface inflammation. *Ophthalmology* 121, 1389–1397. doi: 10.1016/j.ophtha.2014.01.033

Della-Morte, D., Beecham, A., Dong, C., Wang, L., McClendon, M. S., Gardener, H., et al. (2012). Association between variations in coagulation system genes and carotid plaque. *J. Neurol. Sci.* 323, 93–98. doi: 10.1016/j.jns.2012.08.020

Dong, J., Yang, S., Zhuang, Q., Sun, J., Wei, P., Zhao, X., et al. (2021). The Associations of Lipid Profiles With Cardiovascular Diseases and Death in a 10-Year Prospective Cohort Study. *Front. Cardiovasc. Med.* 8:745539. doi: 10.3389/fcvm.2021.745539

Feigin, V. L., Nguyen, G., Cercy, K., Johnson, C. O., Alam, T., Parmar, P. G., et al. (2018). Global, Regional, and Country-Specific Lifetime Risks of Stroke, 1990 and 2016. *N. Engl. J. Med.* 379, 2429–2437. doi: 10.1056/NEJMoa1804492

Gao, J. B., Tang, W. D., Wang, H. X., and Xu, Y. (2015). Predictive value of thrombospondin-1 for outcomes in patients with acute ischemic stroke. *Clin. Chim. Acta* 450, 176–180. doi: 10.1016/j.cca.2015.08.014

Hong, B. B., Chen, S. Q., Qi, Y. L., Zhu, J. W., and Lin, J. Y. (2015). Association of THBS1 rs1478605 T>C in 5′-untranslated regions with the development and progression of gastric cancer. *Biomed. Rep.* 3, 207–214. doi: 10.3892/br.2015.414

Iruela-Arispe, M. L., Lombardo, M., Krutzsch, H. C., Lawler, J., and Roberts, D. D. (1999). Inhibition of angiogenesis by thrombospondin-1 is mediated by 2 independent regions within the type 1 repeats. *Circulation* 100, 1423–1431. doi: 10.1161/01.cir.100.13.1423

Isenberg, J. S., and Roberts, D. D. (2020). THBS1 (thrombospondin-1). *Atlas Genet. Cytogenet. Oncol. Haematol.* 24, 291–299. doi: 10.4267/2042/70774

Isenberg, J. S., Romeo, M. J., Yu, C., Yu, C. K., Nghiem, K., Monsale, J., et al. (2008). Thrombospondin-1 stimulates platelet aggregation by blocking the antithrombotic activity of nitric oxide/cGMP signaling. *Blood* 111, 613–623. doi: 10.1182/blood-2007-06-098392

Jacob, S. A., Novelli, E. M., Isenberg, J. S., Garrett, M. E., Chu, Y., Soldano, K., et al. (2017). Thrombospondin-1 gene polymorphism is associated with estimated pulmonary artery pressure in patients with sickle cell anemia. *Am. J. Hematol.* 92, E31–E34. doi: 10.1002/ajh.24635

Jaffe, E. A., Ruggiero, J. T., and Falcone, D. J. (1985). Monocytes and macrophages synthesize and secrete thrombospondin. *Blood* 65, 79–84.

Kyriakides, T. R., Zhu, Y. H., Smith, L. T., Bain, S. D., Yang, Z., Lin, M. T., et al. (1998). Mice that lack thrombospondin 2 display connective tIS casesue abnormalities that are associated with disordered collagen fibrillogenesis, an increased vascular density, and a bleeding diathesis. *J. Cell. Biol.* 140, 419–430. doi: 10.1083/jcb.140.2.419

Li, W. X., Qi, F., Liu, J. Q., Li, G. H., Dai, S. X., Zhang, T., et al. (2017). Different impairment of immune and inflammation functions in short and long-term after ischemic stroke. *Am. J. Transl. Res.* 9, 736–745.

Lin, T. N., Kim, G. M., Chen, J. J., Cheung, W. M., He, Y. Y., and Hsu, C. Y. (2003). Differential regulation of thrombospondin-1 and thrombospondin-2 after focal cerebral ischemia/reperfusion. *Stroke* 34, 177–186. doi: 10.1161/01.str.0000047100.84604.ba

Liu, H., Yang, J., Zhang, J., Zheng, T., and Zhai, Y. (2021). THBS1: a potential biomarker for atrial fibrillation. *Int. J. Cardiol.* 345:129. doi: 10.1016/j.ijcard.2021.10.152

Liu, X. N., Song, L., Wang, D. W., Liao, Y. H., Ma, A. Q., Zhu, Z. M., et al. (2004). [Correlation of thrombospondin-1 G1678A polymorphism to stroke: a study in Chinese population]. *Zhonghua Yi Xue Za Zhi* 84, 1959–1962.

Maida, C. D., Norrito, R. L., Daidone, M., Tuttolomondo, A., and Pinto, A. (2020). Neuroinflammatory Mechanisms in Ischemic Stroke: Focus on Cardioembolic Stroke, Background, and Therapeutic Approaches. *Int. J. Mol. Sci.* 21:6454. doi: 10.3390/ijms21186454

Matsuo, Y., Tanaka, M., Yamakage, H., Sasaki, Y., Muranaka, K., Hata, H., et al. (2015). Thrombospondin 1 as a novel biological marker of obesity and metabolic syndrome. *Metabolism* 64, 1490–1499. doi: 10.1016/j.metabol.2015.07.016

Moin, A. S. M., Nandakumar, M., Al-Qaissi, A., Sathyapalan, T., Atkin, S. L., and Butler, A. E. (2021). Potential Biomarkers to Predict Acute Ischemic Stroke in Type 2 Diabetes. *Front. Mol. Biosci.* 8:744459. doi: 10.3389/fmolb.2021.744459

Navarro-Sobrino, M., Rosell, A., Hernández-Guillamon, M., Penalba, A., Boada, C., Domingues-Montanari, S., et al. (2011). A large screening of angiogenesis biomarkers and their association with neurological outcome after ischemic stroke. *Atherosclerosis* 216, 205–211. doi: 10.1016/j.atherosclerosis.2011.01.030

O'Donnell, M. J., Xavier, D., Liu, L., Zhang, H., Chin, S. L., Rao-Melacini, P., et al. (2010). Risk factors for ischaemic and intracerebral haemorrhagic stroke in 22 countries (the INTERSTROKE study): a case-control study. *Lancet* 376, 112–123. doi: 10.1016/s0140-6736(10)60834-3

Schaid, D. J., Rowland, C. M., Tines, D. E., Jacobson, R. M., and Poland, G. A. (2002). Score tests for association between traits and haplotypes when linkage phase is ambiguous. *Am. J. Hum. Genet.* 70, 425–434. doi: 10.1086/338688

Schips, T. G., Vanhoutte, D., Vo, A., Correll, R. N., Brody, M. J., Khalil, H., et al. (2019). Thrombospondin-3 augments injury-induced cardiomyopathy by intracellular integrin inhibition and sarcolemmal instability. *Nat. Commun.* 10:76. doi: 10.1038/s41467-018-08026-8

Sweetwyne, M. T., and Murphy-Ullrich, J. E. (2012). Thrombospondin1 in tissue repair and fibrosis: TGF-β-dependent and independent mechanisms. *Matrix Biol.* 31, 178–186. doi: 10.1016/j.matbio.2012.01.006

van Schie, M. C., van Loon, J. E., de Maat, M. P., and Leebeek, F. W. (2011). Genetic determinants of von Willebrand factor levels and activity in relation to the risk of cardiovascular disease: a review. *J. Thromb. Haemost.* 9, 899–908. doi: 10.1111/j.1538-7836.2011.04243.x

Vanhoutte, D., Schips, T. G., Vo, A., Grimes, K. M., Baldwin, T. A., Brody, M. J., et al. (2021). Thbs1 induces lethal cardiac atrophy through PERK-ATF4 regulated autophagy. *Nat. Commun.* 12:3928. doi: 10.1038/s41467-021-24215-4

Varma, V., Yao-Borengasser, A., Bodles, A. M., Rasouli, N., Phanavanh, B., Nolen, G. T., et al. (2008). Thrombospondin-1 is an adipokine associated with obesity, adipose inflammation, and insulin resistance. *Diabetes* 57, 432–439. doi: 10.2337/db07-0840

Virani, S. S., Alonso, A., Aparicio, H. J., Benjamin, E. J., Bittencourt, M. S., Callaway, C. W., et al. (2021). Heart Disease and Stroke Statistics-2021 Update: A Report From the American Heart Association. *Circulation* 143, e254–e743. doi: 10.1161/cir.0000000000000950

Wolf, P. A., Abbott, R. D., and Kannel, W. B. (1991). Atrial fibrillation as an independent risk factor for stroke: the Framingham Study. *Stroke* 22, 983–988. doi: 10.1161/01.str.22.8.983

Xiao, J., Zhang, Y., Tang, Y., Dai, H., OuYang, Y., Li, C., et al. (2021). hsa-miR-4443 inhibits myocardial fibroblast proliferation by targeting THBS1 to regulate TGF-β1/α-SMA/collagen signaling in atrial fibrillation. *Braz. J. Med. Biol. Res.* 54:e10692. doi: 10.1590/1414-431x202010692

Zhou, H. J., Zhang, H. N., Tang, T., Zhong, J. H., Qi, Y., Luo, J. K., et al. (2010). Alteration of thrombospondin-1 and −2 in rat brains following experimental intracerebral hemorrhage. Laboratory investigation. *J. Neurosurg.* 113, 820–825. doi: 10.3171/2010.1.Jns09637

frontiers | Frontiers in Aging Neuroscience

TYPE Original Research
PUBLISHED 14 October 2022
DOI 10.3389/fnagi.2022.1013295

OPEN ACCESS

EDITED BY
John Wesson Ashford,
United States Department of Veterans Affairs, United States

REVIEWED BY
Eva Bagyinszky,
Gachon University, South Korea
Elena Milanesi,
Victor Babes National Institute of Pathology (INCDVB), Romania
Shigeki Kawabata,
Sompo Care Inc., Japan
Marc Tambini,
Rutgers University, Newark, United States

*CORRESPONDENCE
Bin Jiao
4011070@csu.edu.cn
Lu Shen
shenlu@csu.edu.cn

SPECIALTY SECTION
This article was submitted to Alzheimer's Disease and Related Dementias, a section of the journal Frontiers in Aging Neuroscience

RECEIVED 06 August 2022
ACCEPTED 12 September 2022
PUBLISHED 14 October 2022

CITATION
Liu Y, Xiao X, Liu H, Liao X, Zhou Y, Weng L, Zhou L, Liu X, Bi X-y, Xu T, Zhu Y, Yang Q, Zhang S, Hao X, Zhang W, Wang J, Jiao B and Shen L (2022) Clinical characteristics and genotype-phenotype correlation analysis of familial Alzheimer's disease patients with pathogenic/likely pathogenic amyloid protein precursor mutations.
Front. Aging Neurosci. 14:1013295.
doi: 10.3389/fnagi.2022.1013295

Clinical characteristics and genotype-phenotype correlation analysis of familial Alzheimer's disease patients with pathogenic/likely pathogenic amyloid protein precursor mutations

Yingzi Liu[1], Xuewen Xiao[1], Hui Liu[1], Xinxin Liao[2,3,4,5,6], Yafang Zhou[2,3,4,5,6], Ling Weng[1,2,4,5,6], Lu Zhou[1], Xixi Liu[1], Xiang-yun Bi[1], Tianyan Xu[1], Yuan Zhu[1], Qijie Yang[1], Sizhe Zhang[1], Xiaoli Hao[1], Weiwei Zhang[2,4,5,6,7], Junling Wang[1,2,4,5,6], Bin Jiao[1,2,4,5,6]* and Lu Shen[1,2,4,5,6,8]*

[1]Department of Neurology, Xiangya Hospital, Central South University, Changsha, China, [2]National Clinical Research Center for Geriatric Disorders, Central South University, Changsha, China, [3]Department of Geriatrics, Xiangya Hospital, Central South University, Changsha, China, [4]Engineering Research Center of Hunan Province in Cognitive Impairment Disorders, Central South University, Changsha, China, [5]Hunan International Scientific and Technological Cooperation Base of Neurodegenerative and Neurogenetic Diseases, Changsha, China, [6]Key Laboratory of Hunan Province in Neurodegenerative Disorders, Central South University, Changsha, China, [7]Department of Radiology, Xiangya Hospital, Central South University, Changsha, China, [8]Key Laboratory of Organ Injury, Aging and Regenerative Medicine of Hunan Province, Changsha, China

Alzheimer's disease (AD) is a progressive neurodegenerative disease associated with aging, environmental, and genetic factors. Amyloid protein precursor (*APP*) is a known pathogenic gene for familial Alzheimer's disease (FAD), and now more than 70 *APP* mutations have been reported, but the genotype-phenotype correlation remains unclear. In this study, we collected clinical data from patients carrying APP mutations defined as pathogenic/likely pathogenic according to the American college of medical genetics and genomics (ACMG) guidelines. Then, we reanalyzed the clinical characteristics and identified genotype-phenotype correlations in APP mutations. Our results indicated that the clinical phenotypes of *APP* mutations are generally consistent with typical AD despite the fact that they show more non-demented symptoms and neurological symptoms. We also performed genotype-phenotype analysis according to the difference in APP processing

caused by the mutations, and we found that there were indeed differences in onset age, behavioral and psychological disorders of dementia (BPSD) and myoclonus.

KEYWORDS

Alzheimer's disease, APP mutations, clinical characteristics, genotype-phenotypic, non-dementia symptoms, neurological symptoms

Introduction

Alzheimer's disease (AD) is a progressive neurodegenerative disease characterized by progressive memory loss and cognitive decline (Sperling et al., 2011). According to the World Alzheimer Report 2018, 50 million people were living with dementia worldwide in 2018 (Alzheimer's Disease International Consortium, 2018), and the number will more than triple to 152 million by 2050. The typical pathological feature of AD is extracellular deposits of amyloid-β (Aβ) plaques and intracellular neurofibrillary tangles (Braak and Braak, 1996). Although the pathological changes of AD are relatively clear, the exact pathogenesis of this disease is still uncertain (Scheltens et al., 2016). AD is widely believed to be associated with aging, environmental and genetic factors (Farrer et al., 1997; Flicker, 2010; Barnes and Yaffe, 2011).

Alzheimer's disease can be divided into familial Alzheimer's disease (FAD) and sporadic Alzheimer's disease (SAD), depending on whether there is a positive family history. Mutations in the amyloid protein precursor (*APP*), presenilin-1 (*PSEN1*), and presenilin-2 (*PSEN2*) genes can cause FAD. These three causative genes explained 5–10% of FAD (Loy et al., 2014; Cacace et al., 2016), and over 200 mutations in these genes have been described so far (Alzforum mutation database).[1]

Amyloid protein precursor mutations are the second most common pathogenic gene for AD, with an estimated mutation frequency of 1% (Cacace et al., 2016; Hinz and Geschwind, 2017). *APP* gene is positioned on chromosome 21q21.2–21q21.3 and has several different isoforms, of which the three most common isoforms are the 695 amino acid form, the 751, and the 770 amino acid forms (Bayer et al., 1999). APP695 is mainly produced by neurons, while APP751 and APP770 are primarily expressed on peripheral cells and platelets (Hardy, 1997; Guerreiro et al., 2012). All three isoforms consist of a single membrane-spanning domain, a large extracellular glycosylated *N*-terminus, and a shorter cytoplasmic *C*-terminus (Muresan and Ladescu Muresan, 2015) and can generate Aβ after sequential sequencing cleavages by β-secretase and γ-secretase (Nunan and Small, 2000). More than 70 *APP* mutations have been reported possibly associated with FAD since the first mutation V717I was discovered (Goate et al., 1991), and most of the mutations were found to increase the production of Aβ or alter the ratio of $A\beta_{42}/A\beta_{40}$ (Citron et al., 1992; De Jonghe et al., 2001; Kirkitadze et al., 2001; Nilsberth et al., 2001). Despite one research summarizing the *APP* missense mutations and their impacts on APP Processing (Theuns et al., 2006), the research on the genotype-phenotype of *APP* mutation is limited (Lindquist et al., 2009; Ryan et al., 2016; Jiang et al., 2019). Only a part of *APP* mutations targeted at specific populations was described, and there was no systematic summary of all *APP* mutations. However, to study the pathogenesis of AD better, it is imperative to fully understand its clinical characteristics and the correlations between genotype and phenotype.

In a previous study, we had systematically re-evaluated *APP*, *PSEN1*, and *PSEN2* mutations according to the American college of medical genetics and genomics and the association for molecular pathology (ACMG-AMP) guidelines (Xiao et al., 2021). In this study, we collected detailed clinical data from FAD with *APP* mutations that were re-evaluated as pathogenic/likely pathogenic based on previous research. Then we reanalyzed the clinical characteristics and identified the genotype-phenotype correlations in AD caused by pathogenic/likely pathogenic *APP* mutations.

Materials and methods

Data sources and selection

We conducted a literature search using databases from the Alzforum mutation database (see text footnote 1) and PubMed with the keywords "APP" and "Alzheimer's disease." All the articles we included in this research described either clinical characteristics and/or neuropathological features. Almost all cases in these articles were diagnosed with AD according to the National Institute of Neurological and Communicative Disorders and Stroke-Alzheimer's Disease and Related Disorders Association (NINCDS-ADRDA) (McKhann et al., 1984) criteria or the National Institute on Aging-Alzheimer's Association (NIA-AA) (McKhann et al., 2011). *APP* mutations defined as variant of uncertain clinical significance

1 https://www.alzforum.org/mutations

(VUS) and benign/likely benign were excluded. Asymptomatic individuals and mild cognitive impairment (MCI) were also ruled out from the study.

Data extraction

The information collected directly from relevant manuscripts was related to the demographic data (origin, gender), age at onset (AAO), onset symptom, clinical feature, disease duration (calculated only for deceased patients), *APOE* allele, neuroimaging, electroencephalography (EEG), cerebrospinal fluid (CSF) biomarkers and the neuropathology for individually affected patients. Data were also extracted when the exact AAO and disease duration were unavailable in the article and the mean AAO, range, and number of patients.

Statistical analysis

The statistical analyses have been performed using the ANOVA test for continuous variables, chi-square for categorical variables, and correlation analysis for clinical phenotypes. All data were tested for normality and homogeneity of variance using the Shapiro-Wilk and Levene variance equality tests. All data were analyzed with IBM SPSS Statistics (version 23.0) and visualized using Prism 8 (GraphPad). Tests were considered statistically significant for $P < 0.05$.

Results

The overall clinical characteristics of pathogenic/likely pathogenic amyloid protein precursor mutations

A total of 31 *APP* mutations were re-evaluated as pathogenic/likely pathogenic based on the previous study, among which 28 mutations related to AD were included in this study, including 26 missense mutations, one double codon mutation, and only one mutation had a single base deletion. All the mutations were located in exon 16 (n = 7) and exon 17 (n = 21), near the splice site of α secretase, β secretase, and γ secretase. Several other mutations were near α, β, or γ secretase cleavage sites such as V669L or in the other region of *APP* than exon 16–17, but their pathogenic nature was questioned according to ACMG-AMP guidelines. Overall, 63 pedigrees exhibiting *APP* mutations were reported in this research, accounting for 180 affected subjects. **Figure 1** shows the locations of *APP* gene mutations, the number of families and individuals affected by the mutations. The most frequently reported mutations were KM670/671NL (n = 43, near β cleavage site) and V717I (n = 69, near γ_{42} cleavage site).

The clinical characteristics of *APP* gene mutations are summarized in **Supplementary Table 1**. The overall mean AAO in *APP* mutations was 50.7 years, ranging from 31 to 65 years. Gender information was available in 130 patients, including 55 male patients and 75 female patients (the ratio was 1:1.36). 74 cases reported the onset symptoms, and 170 described the clinical manifestations. Most cases had typical characteristics of memory loss (90.59%, 154/170), some patients also had non-amnestic clinical features including disorientation (39.41%, 67/170), visuospatial disorder (12.94%, 22/170) language impairment (27.65%, 47/170), apraxia/agnosia (49.41%, 84/170), dyscalculia (8.24%, 14/170), behavioral and psychological disorders of dementia (BPSD) (53.53%, 91/170). Some patients with *APP* mutations (e.g., A673V, A692G, and E693del) described neurological symptoms such as extrapyramidal symptoms (EPS), myoclonus, seizures, spastic paraplegia, and ataxia. And for those individuals who reported *APOE* allele, 70.49% (43/61) were *APOE* ε4 negative, 21.31% (13/61) had one *APOE* ε4, and 8.20% (5/61) had two copies of *APOE* ε 4.

The age at onset and disease duration

Age at onset data were available in 123 subjects, in which only 9 (7.32%) patients had AAO <40 years old, and 12 (9.76%) had AAO >60 years old. The AAO of most patients was between 40 and 60 years old. Considering the different mutations, the lowest mean AAO was observed among the A673V and I716F mutations (36.0 and 38.0 years, respectively), while the highest was in the I716M mutation (64 years). We also noted that the AAO in some mutations (e.g., K687N and A692G) were roughly the same, while some mutations (e.g., D678N) showed wide variation. Age at onset could be significantly different among the affected individuals, even within the same family. In our research, the *APOE* allele did not affect the overall mean AAO of *APP* mutations, whereas, in the V717I mutation, carriers of the ε4 allele had an earlier AAO (p = 0.005).

The course of AD with *APP* mutations was slow. The mean duration of the disease ranged from 3 to 18 years, with an average of 8.7 years. A faster disease duration with a mean duration of 4 years was observed in the T714I carriers, while the patients with the V717I and V715M mutation experienced a more extended period of the disease (mean duration of 9.9 and 10.0 years, respectively). Similar to the AAO, the course of AD was found to vary widely in the same mutations, even within the same pedigrees.

The first symptoms and clinical presentation

Most of the patients reported amnesia as the first symptom (82.43%, 61/74), which was throughout almost all subjects

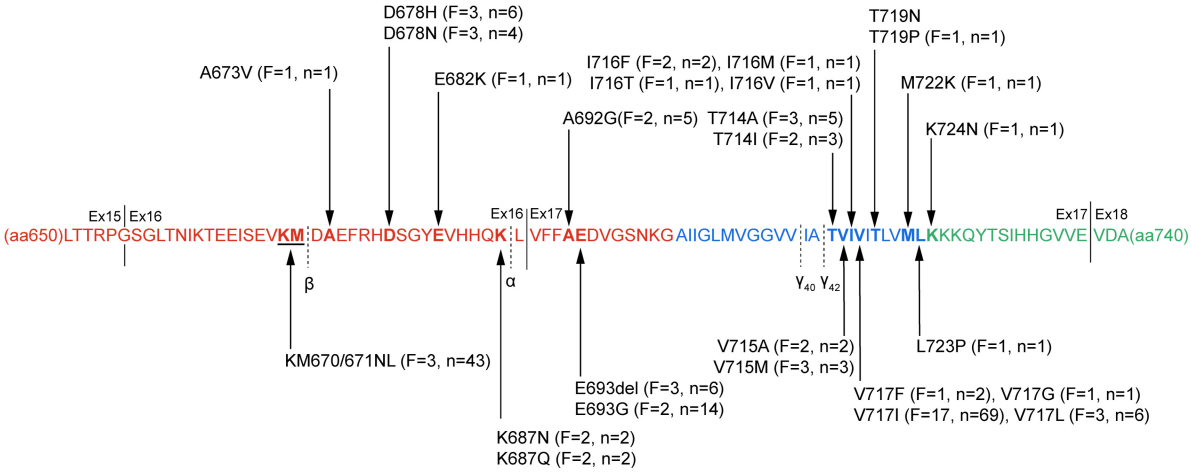

FIGURE 1
The pathogenic/likely pathogenic mutations in amyloid protein precursor (APP) protein. APP protein sequence from amino acid residue 650–740 is presented. The sequence in red depicts the extracellular domain, the transmembrane domain blue, and the intracellular domain green. Black arrow markers indicate pathogenic/likely pathogenic mutation sites, and the specific information on the mutation is described. The numbers of families and individuals affected are also shown in the figure. The cleavage sites of α-, β-, and γ secretases are marked with black dotted lines, and solid lines separate the different exons. *F*, the number of families affected in the mutations; *n*, the number of affected individuals; Ex, exon.

and gradually aggravated. Disorientation, BPSD, or functional executive function impairment could be the initial symptoms in some individuals, accounting for 12.16% (9/74) in total. Besides, some patients (5.41%, 4/74) could also exhibit headache, vertigo, and other non-dementia symptoms as the first clinical manifestation. In comparison, no cases reported language impairment and dyscalculia at the onset.

With the progression of dementia, BPSD became the second most common clinical feature after amnesia. BPSD were classified into three subsyndromes, including psychotic syndrome (hallucinations and/or delusions), affective syndrome (agitation and/or depression and/or anxiety and/or irritability), and behavior syndrome (euphoria and/or apathy and/or disinhibition and/or aberrant motor behavior) (Garre-Olmo et al., 2010). Among the above three subsyndromes, the affective syndrome has the highest frequency (75.0%, 63/84) in carriers who reported BPSD, with depression and anxiety being the most common. Hallucinations and delusions of psychiatric symptoms were also frequent in *APP* mutations; **Supplementary Table 1**). Apraxia/agnosia was also a frequent clinical manifestation in AD, occurring in nearly half of the cases. Over 25% of subjects had disorientation and language impairment, while dyscalculia was rarely reported in dementia cases. We also found that individuals in the same pedigrees tended to be impaired in similar cognitive domains.

Neurological symptoms were concentrated in some of these *APP* mutations, with more than half of the cases clustered in the V717I mutation. In contrast, the A673V and D678N mutations only showed neurological symptoms in one and two patients, respectively. EPS was the most common atypical neurological feature in pathogenic/likely pathogenic *APP* mutations. Patients reported with EPS have at least one clinical manifestation of bradykinesia, rigidity, dystonia, stooped posture, and shuffling gait. Some patients also had other neurological symptoms besides EPS, such as myoclonus, seizures, spastic paraplegia, and ataxia. Pathological reflexes and frontal release signs were shown in *APP* mutations as well. Myoclonus, seizures, spastic paraplegia, and ataxia occur similarly in our research. However, myoclonus and seizures appeared in almost all mutations that reported neurological symptoms, whereas spastic paraplegia was only present in A673V, E693del, T714A, and V717I, ataxia only in E693del, I716F, and V717I. In addition to typical clinical features and neurological symptoms, a tiny percentage of individuals had headaches, vertigo, sleep disturbance, and other non-dementia symptoms (**Supplementary Table 1**).

The diagnostic findings

The neuroimaging, CSF, EEG, and neuropathology results were collected in **Table 1**. Most cases undergoing CT/MRI examination showed diffuse cerebral atrophy or a local involvement of parietal and temporal lobes or hippocampal region, accompanying with or without white matter lesion and other signs. All patients who received positron emission tomography (PET) and/or single-photon emission computed tomography (SPECT) were confirmed to have the following pattern, a temporal and parietal hypoperfusion/hypometabolism at first, then a progressive involvement in the frontal and occipital regions, even the

TABLE 1 Neuroimaging, electroencephalography, cerebrospinal fluid (CSF) analysis, and neuropathology findings in pathogenic/likely pathogenic amyloid protein precursor (*APP*) mutations.

Exon	Mutation	CT/MRI	PET/SPECT	EEG	CSF	Neuropathology	References
16	KM670/671NL	–	–	–	–	*n* = 3 AP, NFTs	Mullan et al., 1992; Bogdanovic et al., 2002
	A673V	*n* = 1 diffuse atrophy white mater lesion	–	*n* = 1 diffuse slow waves	*n* = 1 $A\beta_{42}\downarrow$	–	Di Fede et al., 2009
	D678H	*n* = 3 diffuse atrophy *n* = 2 diffuse atrophy white mater lesion *n* = 1 diffuse atrophy amyloid angiopathy	*n* = 5 ^{18}F-AV-45 PET F-T-P-Pre C-O hypometabolism *n* = 1 SPECT P-T hypoperfusion	*n* = 1 diffuse slow waves	–	–	Chen et al., 2012; Huang et al., 2019
	D678N	*n* = 3 diffuse atrophy *n* = 1 P-T atrophy	*n* = 1 SPECT P-T hypoperfusion	–	*n* = 1 $A\beta_{42}\downarrow$, T-Tau↑, P-Tau↑	–	Wakutani et al., 2004; Han et al., 2020; Mao et al., 2021
	E682K	*n* = 1 hippocampal atrophy	*n* = 1 ^{11}C-PIB hypometabolism	–	*n* = 1 $A\beta_{42}\downarrow$, T-Tau↑, P-Tau↑	-	Zhou et al., 2011
	K687N	*n* = 1 diffuse atrophy *n* = 1 diffuse atrophy white mater lesion	–	–	*n* = 1 $A\beta_{42}\downarrow$, T-Tau↑, P-Tau↑	–	Kaden et al., 2012; Xu et al., 2018
	K687Q	*n* = 1 diffuse atrophy	–	–	–	–	Jiang et al., 2019
17	A692G	*n* = 1 local cerebral hemorrhage *n* = 1 diffuse atrophy white mater lesion	–	*n* = 1 Alpha rhythm, disturbance of frontal activity	–	*n* = 3 AP, NFTs	Cras et al., 1998; Brooks et al., 2004
	E693del	*n* = 4 diffuse atrophy	*n* = 1 ^{18}F-FDG hypometabolism *n* = 2 ^{11}C-PIB normal *n* = 1 ^{11}C-PIB T-P-O slight hypometabolism *n* = 1 ^{11}C-PIB F-T-P slight hypometabolism	–	*n* = 2 $A\beta_{42}\downarrow$, T-Tau↑, P-Tau↑ *n* = 1 T-Tau -, P-Tau -	–	Tomiyama et al., 2008; Shimada et al., 2011, 2020; Kutoku et al., 2015
	E693G	*n* = 3 diffuse atrophy *n* = 4 white mater lesion	*n* = 1 SPECT normal *n* = 4 SPECT P hypoperfusion *n* = 1 SPECT P-T hypoperfusion	–	–	*n* = 4 AP, NFTs	Basun et al., 2008; Kalimo et al., 2013
	T714A	*n* = 2 diffuse atrophy *n* = 1 white mater lesion	*n* = 1 ^{18}F-FDG hypometabolism SPECT P-T hypoperfusion	–	*n* = 1 $A\beta_{42}\downarrow$, T-Tau↑, P-Tau↑	–	Pasalar et al., 2002; Zekanowski et al., 2003; Lindquist et al., 2008, 2009
	T714I	*n* = 2 diffuse atrophy	–	–	*n* = 1 $A\beta_{42}\downarrow$, T-Tau↑	*n* = 1 AP, NFTs	Kumar-Singh et al., 2000; Edwards-Lee et al., 2005
	V715A	–	*n* = 1 SPECT P-O hypoperfusion	–	–	–	Cruts et al., 2003; Zekanowski et al., 2003
	V715M	*n* = 1 diffuse atrophy *n* = 1 temporal atrophy	–	*n* = 1 diffuse slow waves	–	*n* = 1 AP, NFTs	Ancolio et al., 1999; Park et al., 2008; Nan et al., 2014
	I716F	*n* = 1 temporal atrophy *n* = 1 P-F atrophy	*n* = 1 SPECT P hypoperfusion	*n* = 1 diffuse slow waves	*n* = 1 $A\beta_{42}\downarrow$	*n* = 2 AP, NFTs, α-Synuclein	Guardia-Laguarta et al., 2010; Pera et al., 2013; Sieczkowski et al., 2015
	I716M	*n* = 1 hippocampal atrophy	–	–	*n* = 1 $A\beta_{42}\downarrow$, T-Tau↑, P-Tau↑	–	Blauwendraat et al., 2016
	I716V	*n* = 1 diffuse atrophy	–	–	–	–	Eckman et al., 1997
	V717F	*n* = 1 diffuse atrophy	–	*n* = 1 T-P-O triphasic, delta waves and sharp waves	*n* = 1 $A\beta_{42}\downarrow$, T-Tau -, P-Tau -	–	Zádori et al., 2017

(Continued)

TABLE 1 (Continued)

Exon	Mutation	CT/MRI	PET/SPECT	EEG	CSF	Neuropathology	References
	V717G	*n* = 1 diffuse atrophy	–	–	–	–	Knight et al., 2009
	V717I	*n* = 3 temporal atrophy *n* = 2 hippocampal atrophy *n* = 9 diffuse atrophy *n* = 4 white mater lesion *n* = 1 cerebral infarction	*n* = 1 SPECT F-P-O hypoperfusion *n* = 2 SPECT diffuse hypoperfusion	*n* = 2 diffuse slow waves *n* = 1 diffuse slow waves and occasional theta wave *n* = 1 normal *n* = 1non-specifically abnormal	–	*n* = 2 AP, NFTs *n* = 2 AP, NFTs, LBs	Mullan et al., 1993b; Brooks et al., 1995; Matsumura et al., 1996; Halliday et al., 1997; Ishimaru et al., 2013; Jiao et al., 2014; Zhang et al., 2017; Lloyd et al., 2020; Zhou et al., 2020
	V717L	*n* = 1 P-T atrophy *n* = 3 diffuse atrophy	*n* = 1 SPECT diffuse hypoperfusion	*n* = 1 normal			Murrell et al., 2000; Godbolt et al., 2006; Abe et al., 2012
	T719P	*n* = 1 temporal atrophy					Ghidoni et al., 2009
	M722K	*n* = 1 diffuse atrophy					Wang et al., 2015
	L723P	*n* = 1 diffuse atrophy					Kwok et al., 2000

CT, computed tomography; MRI, magnetic resonance imaging; PET, positron emission tomography; SPECT, single-photon emission computed tomography; EEG, electroencephalography; CSF, cerebrospinal fluid; ^{18}F-AV-45, ^{18}F-Florbetapir (AV-45/Amyvid); ^{18}F-FDG, ^{18}F-fluorodeoxyglucose; ^{11}C-PIB, ^{11}C-labeled Pittsburgh Compound B; AP amyloid plaques; NTFs, neurofibrillary tangles; LBs, Lewy bodies; T-Tau, total-Tau; P-Tau, phospho-Tau; F, frontal; P, parietal; T, temporal; pre C, precuneus; O, occipital.

precuneus, and finally the entire cerebral. However, two patients with E693del showed no difference in ^{11}C-labeled Pittsburgh compound B (^{11}C-PIB) imaging compared with non-demented people, and one harboring E693G mutation had no abnormal results in SPECT.

Cerebrospinal fluid analysis was available in only 12 patients. Almost all cases matched the typical features of AD, the reduced $A\beta_{42}$ levels and the increased levels of total-Tau (T-Tau) and phospho-Tau (P-Tau). However, one with E693G mutation and one with V717F mutation had normal levels of T-Tau and p-Tau. EEG was presented in 12 cases as well. And the results were as follows: 7 showed diffuse slow waves, two were normal, one was a non-specific abnormality, one had an alpha rhythm with disturbance of frontal activity, and one indicated T-P-O triphasic, delta waves, and sharp waves.

A total of 18 brain autopsies were performed in all studies. All the neuropathological findings fulfilled the Consortium to Establish a Registry for Alzheimer's disease (CERAD) (Mirra et al., 1991) criteria, characterized by amyloid plaques and neurofibrillary tangles. In addition to amyloid plaques and neurofibrillary tangles, patients with I716F mutation have α-Synuclein in their brains, and Lewy bodies (LBs) were also present in patients with V717I mutation.

The genotype-phenotype correlations

Amyloid protein precursor mutations may alter APP processing, which may in turn diversify phenotypes. We collected the effects on APP processing in pathogenic/likely pathogenic *APP* mutations in **Supplementary Table 2**. The results showed that the mutation site adjacent to α/β secretase mainly increased the amount of total Aβ, while mutations near γ secretase alter the ratio of $A\beta_{42}/A\beta_{40}$. Based on the difference in biochemical results, we divided the pathogenic/likely pathogenic *APP* mutations into two groups: mutations close to α/β secretase and mutations near γ secretase, and compared their clinical features. Atypical mutations such as E693del were ruled out. A total of 130 cases (Complete data not available for all cases) were included in the study of genotype-phenotype correlation analyses, of which 38 were close to α/β secretase, and 92 belonged to the group near γ secretase. The clinical manifestations of the two groups were recorded in **Table 2**. The phenotype was mostly consistent (**Figure 2**). However, the AAO in the mutations near the α/β secretase site group was 52.2, a little later than 50.3 in group γ secretase (P = 0.049). The frequency of clinical BPSD was also less than that in group γ secretase (P = 0.008), and the incidence of myoclonus in the α/β secretase group was higher (P = 0.037).

V717I mutation is the most frequently reported and clinically detailed *APP* mutation, and we also compared V717I mutation to all pathogenic/likely pathogenic *APP* mutations. A total of 147 patients were included in genotype-phenotype correlation analyses, with 60 carrying V717I mutation. There was little difference between the two groups except that the visuospatial impairment on V717I was very low, only 3.2% (**Supplementary Figure 1**). However, when comparing V717I alone with other *APP* mutations (**Supplementary Tables 3**, **4**), we found that patients with the V717I mutation had a later onset and tended to have dyscalculia but had less damage in linguistic and visuospatial regions. V717I mutation carriers also had a

higher prevalence of ataxia and spastic paraplegia regarding neurological symptoms (**Supplementary Figure 2**).

We also performed correlation analysis for clinical phenotypes. Apraxia/agnosia showed a weak positive correlation with language impairment (r = 0.308, p = 0.001), and BPS was negatively correlated with the visuospatial disorder (r = −0.301, p = 0.001). And the individuals with ataxia were more likely to have spastic paraplegia (r = 0.468, $p = 1.711 \times 10^{-7}$).

Discussion

This is the first study to collect clinical data on *APP* mutations defined as pathogenic/likely pathogenic according to ACMG and describe genotype-phenotype correlations of FAD cases with *APP* mutations. Although *APP* mutations are the second most common pathogenic gene for AD, the information on clinical manifestations of *APP* mutations was relatively limited. In general, *APP* mutations are consistent with the typical AD phenotype, even if there are some specific and heterogeneous features. And there are also some differences in clinical manifestations between *APP* mutations and *PSEN1/PSEN2*.

Previous studies verified that the pedigrees with *APP* mutations have an earlier mean AAO than those with *PSEN2* mutations but later than families with *PSEN1* mutations (Mullan et al., 1993a; Jayadev et al., 2010). A study of clinical phenotypic and genetic association analysis of autosomal dominant FAD in the UK demonstrated that the mean AAO of *PSEN1* and *APP* mutations was 43.6 and 50.4, respectively (Ryan et al., 2016). The AAO of our study was 50.7, the same as the AAO of *APP* mutations in their research and later than that of *PSEN1* mutations. *APOE* ε4 is a well-established risk factor for LOAD. *APOE* ε4 carriers had a significantly earlier AAO of AD than ε4 non-carriers. A study showed a decrease in 3.02 years in AAO for each unit increase in the number of ε4 alleles (Sorbi et al., 1995; Thambisetty et al., 2013). However, the *APOE* allele only affected the AAO of V717I mutation in our research. The limited data and confounding factors interfered with our ability to analyze the correlations between AAO and *APOE* alleles in other pathogenic/likely pathogenic *APP* mutations other than V717I. Moreover, since AAO measurement is usually retrospective and prone to recall bias, the accuracy of AAO itself remains to be determined.

TABLE 2 The demographics and the frequencies of clinical features in mutations near α/β secretase and mutations near γ secretase.

	α /β secretase	γ secretase	*P*-value
AAO (years), mean ± SD	52.2 ± 5.2	50.5 ± 7.1	0.049*
Gender (M/F)	10/11	39/53	0.663
Amnesia (*n*, %)	21, 100%	79,85.9%	0.058
Non-amnestic clinical phenotype (*n*, %)			
Disorientation	10, 47.6%	46, 50.0%	0.879
Visuospatial disorder	6, 28.6%	14, 15.2%	0.141
Language impairment	9, 42.9%	33, 35.7%	0.527
Apraxia/agnosia	13, 61.9%	65, 70.7%	0.455
Dyscalculia	3, 14.3%	11, 12.0%	0.575
BDSP	8, 38.1%	64, 69.6%	0.008*
Neurological symptoms (*n*, %)			
EPS	4, 19.0%	26, 28.3%	0.520
Myoclonus	11, 28.2%	12, 13.0%	0.037*
Seizures	12 30.8%	16, 17.4%	0.088
Ataxia	0, 0.0%	14, 15.2%	0.069
Spastic paraplegia	0, 0.0%	14, 15.2%	0.069
Pathologic reflex	0, 0.0%	7, 8.2%	0.214
Frontal release signs	0, 0.0%	4, 4.3%	0.355

SD, standard deviation; BPSD, behavioral and psychological disorders of dementia; EPS, extrapyramidal symptoms. Clinical features are all shown as numbers and proportions (%). *Statistically significant for $P < 0.05$.

Our results indicated that *APP* pathogenic/likely pathogenic mutations all have the following clinical characteristics. First, most cases start with amnesia. Second, the disease progresses relatively slowly. Third, patients rarely exhibit pure progressive amnesia and usually present with impairment in multiple cognitive domains. Fourth, BPSD frequently occurs in the progression of dementia and manifests in various forms, among which affective symptoms represented by depression and anxiety are the most common. Fifth, the neuroimaging, CSF biochemical, and neuropathological findings are typical in most cases. The clinical phenotype of *APP* mutations is similar to the SAD (Swearer et al., 1992), but some specificity and heterogeneity remain. For instance, patients with *APP* mutations are more likely to have apraxia/agnosia and perform worse than LOAD (Koedam et al., 2010; Smits et al., 2012).

Regarding BPSD, anxiety and depression are the most common in *APP* mutations, while depression and irritability are more frequent in LOAD (Gumus et al., 2021). The higher incidence of anxiety and depression with less irritability is also well represented in *PSEN*1 and *PSEN2* (Kaiser et al., 2014; Panegyres and Chen, 2014), but they tend to have more hallucinations and delusions compared with *APP* mutations (Larner and Doran, 2006; Canevelli et al., 2014). The consistency and heterogeneity of the three pathogenic genes in BPSD may be related to both AAO and genes. In order to clarify whether there is a connection, it is necessary to pay more attention to the relationship between each subtype of BPSD in patients with dementia and AAO and genetics in future research. In addition, the disease progression of early-onset FAD is faster than that of late-onset SAD, with more extensive cognitive impairment and higher mortality (Jacobs et al., 1994), and this was broadly to our study. While in our study, the disease duration was not as short as previously reported, the average time from onset to death is only 6.6 years (Vermunt et al., 2019; Brück et al., 2021).

10.3389/fnagi.2022.1013295

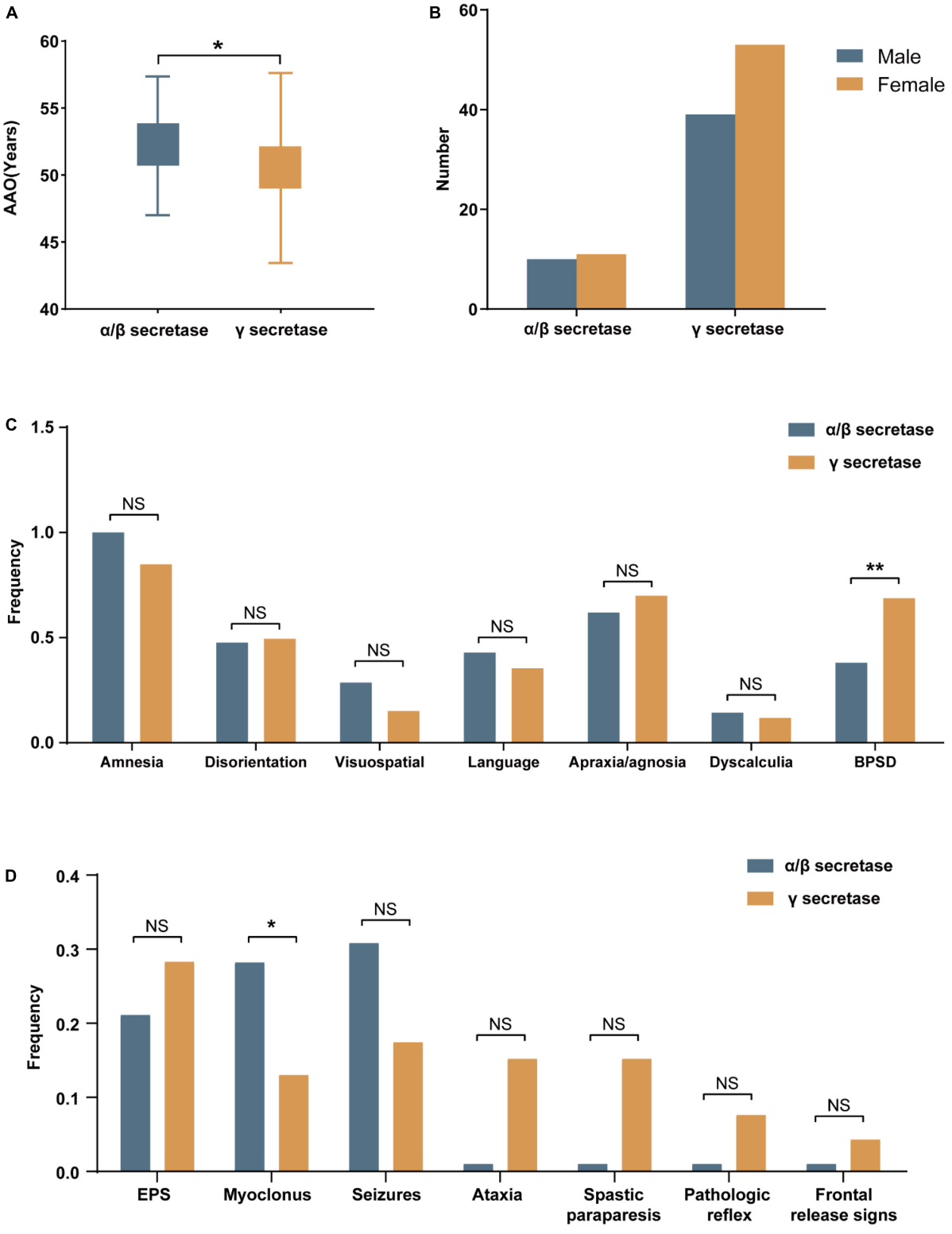

FIGURE 2
The demographics and the frequencies of clinical features in mutations near α/β secretase and near γ secretase. **(A)** The age at onset (AAO) and **(B)** The gender of mutations near α/β secretase and near γ secretase. **(C)** The frequencies of amnesia and non-amnestic clinical phenotype. **(D)** The frequencies of neurological symptoms (NS, no significance, *$p < 0.05$, **$p < 0.01$).

Similar to the non-amnestic phenotypes, neurological symptoms have higher morbidity in early-onset FAD than in late-onset SAD (Bateman et al., 2011), especially in pedigrees with AAO <40 years (Ryan and Rossor, 2010). Cases with *APP*, *PSEN1*, or *PSEN2* mutations in FAD also differ in neurological symptoms. A study in autosomal dominant familial AD reported that apart from seizures and myoclonus, patients with *PSEN1* mutations can present with other neurological symptoms while patients with *APP* mutations do not (Ryan et al., 2016). Differently, patients with *APP* mutation in this study also presented with EPS, spastic paraparesis, pathologic reflex, and ataxia. EPS is even more frequently in *APP* than in *PSEN1,* and the proportions of patients with myoclonus or seizures are the same. In the same study, Ryan et al. (2016) also pointed out that individuals with myoclonus tended to develop more seizures than those without myoclonus, yet this was not confirmed in our research. Instead, we found that patients with EPS or ataxia were more likely to have spastic paraplegia. Moreover, we also found that the severity of neurological symptoms would gradually increase as dementia progresses (Vöglein et al., 2019). Similarly, patients with neurological symptoms such as EPS experience a faster cognitive decline (Chui et al., 1994).

We conducted genotype-phenotype correlation analysis of *APP* mutations and found that biochemical differences due to mutations can lead to differences in clinical manifestations, which can occur in AAO, non-demented symptoms, and neurological symptoms. However, the clinical data of the patients we obtained were somewhat limited, which may have affected our interpretation of the results. Future studies need to focus more on the heterogeneity of clinical manifestations caused by differences in APP processing, Aβ amount, and the ratio of $A\beta_{42}/A\beta_{40}$, which may offer a better understanding of amyloid pathways in AD. Furthermore, the differences between V717I and all pathogenic/likely pathogenic *APP* mutations suggest that each *APP* mutation may have the diverse characteristic. For example, V715M and V717L have an earlier AAO than V717I. Some *APP* mutations had visuospatial and language impairments in addition to amnesia, while others had minor damage in these cognitive areas but showed more dyscalculia (e.g., V717I). And mutations in exon 16 are rare to show neurological symptoms compared to mutations in exon 17. Therefore, attention to the clinical manifestations of each mutation is highly warranted.

For the most reported V717I mutation, there was consistency in the pattern of symptoms between cases. There is a cognitive decline initially, with visuospatial impairment, disorientation, and language impairment. Dyscalculia, agnosia/apraxia and neurological symptoms occur as the disease progresses. However, there are differences in clinical manifestations among pedigrees (Mullan et al., 1993b). For instance, the APPV717I mutation in the Chinese population mainly manifests as affective symptoms, executive dysfunction and disorientation in the early stage, and spastic paraparesis and ataxia in the late stage are more common (Zhang et al., 2017). In addition, we also found differences in AAO and clinical manifestations within the same family. This may be due to variability in the expression of these mutations or related to other genetic or epigenetic factors (Román et al., 2019).

Although most pathogenic/likely pathogenic *APP* mutations are complete penetrance, some have been demonstrated to behave as incomplete dominant. A Caucasian woman with the homozygous mutation D678N had memory difficulties early in her third decade and developed full-blown clinical symptoms 10 years later. Her heterozygous affected siblings were generally diagnosed with dementia in their 60 s (Mastromoro et al., 2019). We also found asymptomatic carriers reported in some other pathogenic/likely pathogenic *APP* mutations, which may be due to incomplete dominant mutations or maybe just because of the individual differences as well as environmental factors that lead to a later onset in those carriers, and the researchers did not follow them up. And unlike other *APP* mutations (Zhou et al., 2011; Huang et al., 2019), A673V is a particular mutation caused by recessive homozygous mutation. It has a high amyloidosis effect in the homozygous state and an anti-amyloidosis effect in the heterozygous state (Di Fede et al., 2009). In addition, different mutations in the same site of *APP* can lead to different diseases. For example, E693K (Bugiani et al., 2010), E693Q (Wattendorff et al., 1982; Luyendijk and Bots, 1986) can lead to Cerebral Amyloid Angiopathy (CAA), E693G, and E693del lead to AD, D694N (Grabowski et al., 2001) mutation near 693 can lead to vascular dementia (VD). All of these suggest that there may be some discrepancy in the structure and toxicity of the mutant product Aβ, or other mechanisms related to other APP cleavage products besides Aβ such as APP intracellular domain (AICD). It is essential to use these atypical mutations as tools to study the pathogenesis of AD.

The limited clinical evidence makes it difficult to conduct further genotype-phenotype association analyses, especially to evaluate the clinical manifestations of different mutations at the same locus. And the reliability of the clinical data we collected remains to be determined. We are not able to be sure whether the specific manifestations unreported were because they were really absent or emerged after the study, or were just not mentioned in the articles. Besides, we only analyzed *APP* mutations and did not compare them with the other two pathogenic genes.

In conclusion, we collected the clinical data from patients with pathogenic/likely pathogenic *APP* mutations and performed an analysis of genotype-phenotypic association, which may help better understand the relationship between genotype and phenotype and may be beneficial for clinical practice prediction, diagnosis, and genetic counseling.

Data availability statement

Publicly available datasets were analyzed in this study. This data can be found here: https://www.alzforum.org/mutations.

Author contributions

YL and XX contributed to the conception and design of the study. YL collected the data, performed the statistical analysis, and wrote the first draft of the manuscript. All authors contributed to manuscript revision, read, and approved the submitted version.

Funding

We are grateful to all subjects for participation in our study. This study was supported by the National Natural Science Foundation of China (Nos. 81671075 to LS, 81971029 to LS, 81701134 to BJ, 81901171 to XLu), the National Key R&D Program of China (Nos. 2017YFC0840100 and 2017YFC0840104 to LS, 2018YFC1312003 to JW), the Provincial Key Plan for Research and Development of Hunan (No. 2017SK2031 to LS), the Provincial Technology Innovation Guidance Plan Project of Hunan (No. 2018SK52601 to BJ).

Conflict of interest

The authors declare that the research was conducted in the absence of any commercial or financial relationships that could be construed as a potential conflict of interest.

Publisher's note

All claims expressed in this article are solely those of the authors and do not necessarily represent those of their affiliated organizations, or those of the publisher, the editors and the reviewers. Any product that may be evaluated in this article, or claim that may be made by its manufacturer, is not guaranteed or endorsed by the publisher.

Supplementary material

The Supplementary Material for this article can be found online at: https://www.frontiersin.org/articles/10.3389/fnagi.2022.1013295/full#supplementary-material

References

Abe, M., Sonobe, N., Fukuhara, R., Mori, Y., Ochi, S., Matsumoto, T., et al. (2012). Phenotypical difference of amyloid precursor protein (APP) V717L mutation in Japanese family. *BMC Neurol.* 12:38. doi: 10.1186/1471-2377-12-38

Alzheimer's Disease International Consortium (2018). *World Alzheimer report 2018*. London: Alzheimer's Disease International.

Ancolio, K., Dumanchin, C., Barelli, H., Warter, J. M., Brice, A., Campion, D., et al. (1999). Unusual phenotypic alteration of beta amyloid precursor protein (betaAPP) maturation by a new Val-715 –> Met betaAPP-770 mutation responsible for probable early-onset Alzheimer's disease. *Proc. Natl. Acad. Sci. U.S.A.* 96, 4119–4124. doi: 10.1073/pnas.96.7.4119

Barnes, D. E., and Yaffe, K. (2011). The projected effect of risk factor reduction on Alzheimer's disease prevalence. *Lancet Neurol.* 10, 819–828. doi: 10.1016/S1474-4422(11)70072-2

Basun, H., Bogdanovic, N., Ingelsson, M., Almkvist, O., Näslund, J., Axelman, K., et al. (2008). Clinical and neuropathological features of the arctic APP gene mutation causing early-onset Alzheimer disease. *Arch. Neurol.* 65, 499–505. doi: 10.1001/archneur.65.4.499

Bateman, R. J., Aisen, P. S., De Strooper, B., Fox, N. C., Lemere, C. A., Ringman, J. M., et al. (2011). Autosomal-dominant Alzheimer's disease: a review and proposal for the prevention of Alzheimer's disease. *Alzheimers Res. Ther.* 3:1. doi: 10.1186/alzrt59

Bayer, T. A., Cappai, R., Masters, C. L., Beyreuther, K., and Multhaup, G. (1999). It all sticks together–the APP-related family of proteins and Alzheimer's disease. *Mol. Psychiatry* 4, 524–528. doi: 10.1038/sj.mp.4000552

Blauwendraat, C., Wilke, C., Jansen, I. E., Schulte, C., Simón-Sánchez, J., Metzger, F. G., et al. (2016). Pilot whole-exome sequencing of a German early-onset Alzheimer's disease cohort reveals a substantial frequency of PSEN2 variants. *Neurobiol. Aging* 37, 208.e11–208.e17. doi: 10.1016/j.neurobiolaging.2015.09.016

Bogdanovic, N., Corder, E., Lannfelt, L., and Winblad, B. (2002). APOE polymorphism and clinical duration determine regional neuropathology in Swedish APP(670, 671) mutation carriers: implications for late-onset Alzheimer's disease. *J. Cell. Mol. Med.* 6, 199–214. doi: 10.1111/j.1582-4934.2002.tb00187.x

Braak, H., and Braak, E. (1996). Evolution of the neuropathology of Alzheimer's disease. *Acta Neurol. Scand. Suppl.* 165, 3–12. doi: 10.1111/j.1600-0404.1996.tb05866.x

Brooks, W. S., Kwok, J. B., Halliday, G. M., Godbolt, A. K., Rossor, M. N., Creasey, H., et al. (2004). Hemorrhage is uncommon in new Alzheimer family with Flemish amyloid precursor protein mutation. *Neurology* 63, 1613–1617. doi: 10.1212/01.WNL.0000142965.10778.C7

Brooks, W. S., Martins, R. N., De Voecht, J., Nicholson, G. A., Schofield, P. R., Kwok, J. B., et al. (1995). A mutation in codon 717 of the amyloid precursor protein gene in an Australian family with Alzheimer's disease. *Neurosci. Lett.* 199, 183–186. doi: 10.1016/0304-3940(95)12046-7

Brück, C. C., Wolters, F. J., Ikram, M. A., and de Kok, I. (2021). Heterogeneity in reports of dementia disease duration and severity: A review of the literature. *J. Alzheimers Dis.* 84, 1515–1522. doi: 10.3233/JAD-210544

Bugiani, O., Giaccone, G., Rossi, G., Mangieri, M., Capobianco, R., Morbin, M., et al. (2010). Hereditary cerebral hemorrhage with amyloidosis associated with the E693K mutation of APP. *Arch. Neurol.* 67, 987–995. doi: 10.1001/archneurol.2010.178

Cacace, R., Sleegers, K., and Van Broeckhoven, C. (2016). Molecular genetics of early-onset Alzheimer's disease revisited. *Alzheimers Dement.* 12, 733–748. doi: 10.1016/j.jalz.2016.01.012

Canevelli, M., Piscopo, P., Talarico, G., Vanacore, N., Blasimme, A., Crestini, A., et al. (2014). Familial Alzheimer's disease sustained by presenilin 2 mutations: systematic review of literature and genotype-phenotype correlation. *Neurosci. Biobehav. Rev.* 42, 170–179. doi: 10.1016/j.neubiorev.2014.02.010

Chen, W. T., Hong, C. J., Lin, Y. T., Chang, W. H., Huang, H. T., Liao, J. Y., et al. (2012). Amyloid-beta (Aβ) D7H mutation increases oligomeric Aβ42 and alters properties of Aβ-zinc/copper assemblies. *PLoS One* 7:e35807. doi: 10.1371/journal.pone.0035807

Chui, H. C., Lyness, S. A., Sobel, E., and Schneider, L. S. (1994). Extrapyramidal signs and psychiatric symptoms predict faster cognitive decline in Alzheimer's disease. *Arch. Neurol.* 51, 676–681. doi: 10.1001/archneur.1994.00540190056015

Citron, M., Oltersdorf, T., Haass, C., McConlogue, L., Hung, A. Y., Seubert, P., et al. (1992). Mutation of the beta-amyloid precursor protein in familial Alzheimer's disease increases beta-protein production. *Nature* 360, 672–674. doi: 10.1038/360672a0

Cras, P., van Harskamp, F., Hendriks, L., Ceuterick, C., van Duijn, C. M., Stefanko, S. Z., et al. (1998). Presenile Alzheimer dementia characterized by amyloid angiopathy and large amyloid core type senile plaques in the APP 692Ala–>Gly mutation. *Acta Neuropathol.* 96, 253–260. doi: 10.1007/s004010050892

Cruts, M., Dermaut, B., Rademakers, R., Van den Broeck, M., Stögbauer, F., and Van Broeckhoven, C. (2003). Novel APP mutation V715A associated with presenile Alzheimer's disease in a German family. *J. Neurol.* 250, 1374–1375. doi: 10.1007/s00415-003-0182-5

De Jonghe, C., Esselens, C., Kumar-Singh, S., Craessaerts, K., Serneels, S., Checler, F., et al. (2001). Pathogenic APP mutations near the gamma-secretase cleavage site differentially affect Abeta secretion and APP C-terminal fragment stability. *Hum. Mol. Genet.* 10, 1665–1671. doi: 10.1093/hmg/10.16.1665

Di Fede, G., Catania, M., Morbin, M., Rossi, G., Suardi, S., Mazzoleni, G., et al. (2009). A recessive mutation in the APP gene with dominant-negative effect on amyloidogenesis. *Science* 323, 1473–1477. doi: 10.1126/science.1168979

Eckman, C. B., Mehta, N. D., Crook, R., Perez-tur, J., Prihar, G., Pfeiffer, E., et al. (1997). A new pathogenic mutation in the APP gene (I716V) increases the relative proportion of A beta 42(43). *Hum. Mol. Genet.* 6, 2087–2089. doi: 10.1093/hmg/6.12.2087

Edwards-Lee, T., Ringman, J. M., Chung, J., Werner, J., Morgan, A., St George Hyslop, P., et al. (2005). An African American family with early-onset Alzheimer disease and an APP (T714I) mutation. *Neurology* 64, 377–379. doi: 10.1212/01.WNL.0000149761.70566.3E

Farrer, L. A., Cupples, L. A., Haines, J. L., Hyman, B., Kukull, W. A., Mayeux, R., et al. (1997). Effects of age, sex, and ethnicity on the association between apolipoprotein E genotype and Alzheimer disease. A meta-analysis. APOE and Alzheimer Disease Meta Analysis Consortium. *JAMA* 278, 1349–1356. doi: 10.1001/jama.1997.03550160069041

Flicker, L. (2010). Modifiable lifestyle risk factors for Alzheimer's disease. *J. Alzheimers Dis.* 20, 803–811. doi: 10.3233/JAD-2010-091624

Garre-Olmo, J., López-Pousa, S., Vilalta-Franch, J., de Gracia Blanco, M., and Vilarrasa, A. B. (2010). Grouping and trajectories of the neuropsychiatric symptoms in patients with Alzheimer's disease, part I: symptom clusters. *J. Alzheimers Dis.* 22, 1157–1167. doi: 10.3233/JAD-2010-101212

Ghidoni, R., Albertini, V., Squitti, R., Paterlini, A., Bruno, A., Bernardini, S., et al. (2009). Novel T719P AbetaPP mutation unbalances the relative proportion of amyloid-beta peptides. *J. Alzheimers Dis.* 18, 295–303. doi: 10.3233/JAD-2009-1142

Goate, A., Chartier-Harlin, M. C., Mullan, M., Brown, J., Crawford, F., Fidani, L., et al. (1991). Segregation of a missense mutation in the amyloid precursor protein gene with familial Alzheimer's disease. *Nature* 349, 704–706. doi: 10.1038/349704a0

Godbolt, A. K., Beck, J. A., Collinge, J. C., Cipolotti, L., Fox, N. C., and Rossor, M. N. (2006). A second family with familial AD and the V717L APP mutation has a later age at onset. *Neurology* 66, 611–612. doi: 10.1212/01.WNL.0000197791.53828.2C

Grabowski, T. J., Cho, H. S., Vonsattel, J. P., Rebeck, G. W., and Greenberg, S. M. (2001). Novel amyloid precursor protein mutation in an Iowa family with dementia and severe cerebral amyloid angiopathy. *Ann. Neurol.* 49, 697–705. doi: 10.1002/ana.1009

Guardia-Laguarta, C., Pera, M., Clarimón, J., Molinuevo, J. L., Sánchez-Valle, R., Lladó, A., et al. (2010). Clinical, neuropathologic, and biochemical profile of the amyloid precursor protein I716F mutation. *J. Neuropathol. Exp. Neurol.* 69, 53–59. doi: 10.1097/NEN.0b013e3181c6b84d

Guerreiro, R. J., Gustafson, D. R., and Hardy, J. (2012). The genetic architecture of Alzheimer's disease: beyond APP, PSENs and APOE. *Neurobiol. Aging* 33, 437–456. doi: 10.1016/j.neurobiolaging.2010.03.025

Gumus, M., Multani, N., Mack, M. L., and Tartaglia, M. C. (2021). Progression of neuropsychiatric symptoms in young-onset versus late-onset Alzheimer's disease. *Geroscience* 43, 213–223. doi: 10.1007/s11357-020-00304-y

Halliday, G., Brooks, W., Arthur, H., Creasey, H., and Broe, G. A. (1997). Further evidence for an association between a mutation in the APP gene and Lewy body formation. *Neurosci. Lett.* 227, 49–52. doi: 10.1016/S0304-3940(97)00294-2

Han, L. H., Xue, Y. Y., Zheng, Y. C., Li, X. Y., Lin, R. R., Wu, Z. Y., et al. (2020). Genetic analysis of Chinese patients with early-onset dementia using next-generation sequencing. *Clin. Interv. Aging* 15, 1831–1839. doi: 10.2147/CIA.S271222

Hardy, J. (1997). Amyloid, the presenilins and Alzheimer's disease. *Trends Neurosci.* 20, 154–159. doi: 10.1016/S0166-2236(96)01030-2

Hinz, F. I., and Geschwind, D. H. (2017). Molecular genetics of neurodegenerative dementias. *Cold Spring Harb. Perspect. Biol.* 9:a023705. doi: 10.1101/cshperspect.a023705

Huang, C. Y., Hsiao, I. T., Lin, K. J., Huang, K. L., Fung, H. C., Liu, C. H., et al. (2019). Amyloid PET pattern with dementia and amyloid angiopathy in Taiwan familial AD with D678H APP mutation. *J. Neurol. Sci.* 398, 107–116. doi: 10.1016/j.jns.2018.12.039

Ishimaru, T., Ochi, S., Matsumoto, T., Yoshida, T., Abe, M., Toyota, Y., et al. (2013). [A case report of early-onset Alzheimer's disease with multiple psychotic symptoms, finally diagnosed as APPV717I mutation by genetic testing]. *Seishin Shinkeigaku Zasshi* 115, 1042–1050.

Jacobs, D., Sano, M., Marder, K., Bell, K., Bylsma, F., Lafleche, G., et al. (1994). Age at onset of Alzheimer's disease: relation to pattern of cognitive dysfunction and rate of decline. *Neurology* 44, 1215–1220. doi: 10.1212/WNL.44.7.1215

Jayadev, S., Leverenz, J. B., Steinbart, E., Stahl, J., Klunk, W., Yu, C. E., et al. (2010). Alzheimer's disease phenotypes and genotypes associated with mutations in presenilin 2. *Brain* 133(Pt 4), 1143–1154. doi: 10.1093/brain/awq033

Jiang, B., Zhou, J., Li, H. L., Chen, Y. G., Cheng, H. R., Ye, L. Q., et al. (2019). Mutation screening in Chinese patients with familial Alzheimer's disease by whole-exome sequencing. *Neurobiol. Aging* 76, 215.e15–215.e21. doi: 10.1016/j.neurobiolaging.2018.11.024

Jiao, B., Tang, B., Liu, X., Xu, J., Wang, Y., Zhou, L., et al. (2014). Mutational analysis in early-onset familial Alzheimer's disease in Mainland China. *Neurobiol. Aging* 35, 1957.e1–1957.e6. doi: 10.1016/j.neurobiolaging.2014.02.014

Kaden, D., Harmeier, A., Weise, C., Munter, L. M., Althoff, V., Rost, B. R., et al. (2012). Novel APP/Aβ mutation K16N produces highly toxic heteromeric Aβ oligomers. *EMBO Mol. Med.* 4, 647–659. doi: 10.1002/emmm.201200239

Kaiser, N. C., Liang, L. J., Melrose, R. J., Wilkins, S. S., Sultzer, D. L., and Mendez, M. F. (2014). Differences in anxiety among patients with early- versus late-onset Alzheimer's disease. *J. Neuropsychiatry Clin. Neurosci.* 26, 73–80. doi: 10.1176/appi.neuropsych.12100240

Kalimo, H., Lalowski, M., Bogdanovic, N., Philipson, O., Bird, T. D., Nochlin, D., et al. (2013). The Arctic AβPP mutation leads to Alzheimer's disease pathology with highly variable topographic deposition of differentially truncated Aβ. *Acta Neuropathol. Commun.* 1:60. doi: 10.1186/2051-5960-1-60

Kirkitadze, M. D., Condron, M. M., and Teplow, D. B. (2001). Identification and characterization of key kinetic intermediates in amyloid beta-protein fibrillogenesis. *J. Mol. Biol.* 312, 1103–1119. doi: 10.1006/jmbi.2001.4970

Knight, W. D., Ahsan, R. L., Jackson, J., Cipolotti, L., Warrington, E. K., Fox, N. C., et al. (2009). Pure progressive amnesia and the APPV717G mutation. *Alzheimer Dis. Assoc. Disord.* 23, 410–414. doi: 10.1097/WAD.0b013e31819cb7f3

Koedam, E. L., Lauffer, V., van der Vlies, A. E., van der Flier, W. M., Scheltens, P., and Pijnenburg, Y. A. (2010). Early-versus late-onset Alzheimer's disease: more than age alone. *J. Alzheimers Dis.* 19, 1401–1408. doi: 10.3233/JAD-2010-1337

Kumar-Singh, S., De Jonghe, C., Cruts, M., Kleinert, R., Wang, R., Mercken, M., et al. (2000). Nonfibrillar diffuse amyloid deposition due to a gamma(42)-secretase site mutation points to an essential role for N-truncated A beta(42) in Alzheimer's disease. *Hum. Mol. Genet.* 9, 2589–2598. doi: 10.1093/hmg/9.18.2589

Kutoku, Y., Ohsawa, Y., Kuwano, R., Ikeuchi, T., Inoue, H., Ataka, S., et al. (2015). A second pedigree with amyloid-less familial Alzheimer's disease harboring an identical mutation in the amyloid precursor protein gene (E693delta). *Intern. Med.* 54, 205–208. doi: 10.2169/internalmedicine.54.3021

Kwok, J. B., Li, Q. X., Hallupp, M., Whyte, S., Ames, D., Beyreuther, K., et al. (2000). Novel Leu723Pro amyloid precursor protein mutation increases amyloid beta42(43) peptide levels and induces apoptosis. *Ann. Neurol.* 47, 249–253. doi: 10.1002/1531-8249(200002)47:2<249::AID-ANA18>3.0.CO;2-8

Larner, A. J., and Doran, M. (2006). Clinical phenotypic heterogeneity of Alzheimer's disease associated with mutations of the presenilin-1 gene. *J. Neurol.* 253, 139–158. doi: 10.1007/s00415-005-0019-5

Lindquist, S. G., Nielsen, J. E., Stokholm, J., Schwartz, M., Batbayli, M., Ballegaard, M., et al. (2008). Atypical early-onset Alzheimer's disease caused by the Iranian APP mutation. *J. Neurol. Sci.* 268, 124–130. doi: 10.1016/j.jns.2007.11.021

Lindquist, S. G., Schwartz, M., Batbayli, M., Waldemar, G., and Nielsen, J. E. (2009). Genetic testing in familial AD and FTD: mutation and phenotype spectrum in a Danish cohort. *Clin. Genet.* 76, 205–209. doi: 10.1111/j.1399-0004.2009.01191.x

Lloyd, G. M., Trejo-Lopez, J. A., Xia, Y., McFarland, K. N., Lincoln, S. J., Ertekin-Taner, N., et al. (2020). Prominent amyloid plaque pathology and cerebral amyloid angiopathy in APP V717I (London) carrier – phenotypic variability in autosomal dominant Alzheimer's disease. *Acta Neuropathol. Commun.* 8:31. doi: 10.1186/s40478-020-0891-3

Loy, C. T., Schofield, P. R., Turner, A. M., and Kwok, J. B. (2014). Genetics of dementia. *Lancet* 383, 828–840. doi: 10.1016/S0140-6736(13)60630-3

Luyendijk, W., and Bots, G. T. (1986). Hereditary cerebral hemorrhage. *Scand. J. Clin. Lab. Invest.* 46:391. doi: 10.3109/00365518609083687

Mao, C., Li, J., Dong, L., Huang, X., Lei, D., Wang, J., et al. (2021). Clinical phenotype and mutation spectrum of Alzheimer's disease with causative genetic mutation in a Chinese cohort. *Curr. Alzheimer Res.* 18, 265–272. doi: 10.2174/1567205018666210608120339

Mastromoro, G., Gambardella, S., Marchionni, E., Campopiano, R., Traversa, A., Di Bonaventura, C., et al. (2019). Unusual segregation of APP mutations in monogenic Alzheimer disease. *Neuro Degener. Dis.* 19, 96–100. doi: 10.1159/000502906

Matsumura, Y., Kitamura, E., Miyoshi, K., Yamamoto, Y., Furuyama, J., and Sugihara, T. (1996). Japanese siblings with missense mutation (717Val –> Ile) in amyloid precursor protein of early-onset Alzheimer's disease. *Neurology* 46, 1721–1723. doi: 10.1212/WNL.46.6.1721

McKhann, G. M., Knopman, D. S., Chertkow, H., Hyman, B. T., Jack, C. R. Jr., Kawas, C. H., et al. (2011). The diagnosis of dementia due to Alzheimer's disease: recommendations from the National Institute on Aging-Alzheimer's Association workgroups on diagnostic guidelines for Alzheimer's disease. *Alzheimers Dement.* 7, 263–269. doi: 10.1016/j.jalz.2011.03.005

McKhann, G., Drachman, D., Folstein, M., Katzman, R., Price, D., and Stadlan, E. M. (1984). Clinical diagnosis of Alzheimer's disease: report of the NINCDS-ADRDA Work Group under the auspices of department of health and human services task force on Alzheimer's Disease. *Neurology* 34, 939–944. doi: 10.1212/WNL.34.7.939

Mirra, S. S., Heyman, A., McKeel, D., Sumi, S. M., Crain, B. J., Brownlee, L. M., et al. (1991). The consortium to establish a registry for Alzheimer's Disease (CERAD). Part II. Standardization of the neuropathologic assessment of Alzheimer's disease. *Neurology* 41, 479–486. doi: 10.1212/WNL.41.4.479

Mullan, M., Crawford, F., Axelman, K., Houlden, H., Lilius, L., Winblad, B., et al. (1992). A pathogenic mutation for probable Alzheimer's disease in the APP gene at the N-terminus of beta-amyloid. *Nat. Genet.* 1, 345–347. doi: 10.1038/ng0892-345

Mullan, M., Houlden, H., Crawford, F., Kennedy, A., Rogues, P., and Rossor, M. (1993a). Age of onset in familial early onset Alzheimer's disease correlates with genetic aetiology. *Am. J. Med. Genet.* 48, 129–130. doi: 10.1002/ajmg.1320480303

Mullan, M., Tsuji, S., Miki, T., Katsuya, T., Naruse, S., Kaneko, K., et al. (1993b). Clinical comparison of Alzheimer's disease in pedigrees with the codon 717 Val–>Ile mutation in the amyloid precursor protein gene. *Neurobiol. Aging* 14, 407–419. doi: 10.1016/0197-4580(93)90099-W

Muresan, V., and Ladescu Muresan, Z. (2015). Amyloid-β precursor protein: Multiple fragments, numerous transport routes and mechanisms. *Exp. Cell Res.* 334, 45–53. doi: 10.1016/j.yexcr.2014.12.014

Murrell, J. R., Hake, A. M., Quaid, K. A., Farlow, M. R., and Ghetti, B. (2000). Early-onset Alzheimer disease caused by a new mutation (V717L) in the amyloid precursor protein gene. *Arch. Neurol.* 57, 885–887. doi: 10.1001/archneur.57.6.885

Nan, S. J., Han, Y. Q., Fan, J., and Chen, Q. H. (2014). Blepharospasm in familial AD secondary to an APP mutation (V715M). *Acta Neurol. Belg.* 114, 333–334. doi: 10.1007/s13760-014-0291-1

Nilsberth, C., Westlind-Danielsson, A., Eckman, C. B., Condron, M. M., Axelman, K., Forsell, C., et al. (2001). The 'Arctic' APP mutation (E693G) causes Alzheimer's disease by enhanced Abeta protofibril formation. *Nat. Neurosci.* 4, 887–893. doi: 10.1038/nn0901-887

Nunan, J., and Small, D. H. (2000). Regulation of APP cleavage by alpha-, beta- and gamma-secretases. *FEBS Lett.* 483, 6–10. doi: 10.1016/S0014-5793(00)02076-7

Panegyres, P. K., and Chen, H. Y. (2014). Early-onset Alzheimer's disease: a global cross-sectional analysis. *Eur. J. Neurol.* 21, 1149–54, e64–e65. doi: 10.1111/ene.12453

Park, H. K., Na, D. L., Lee, J. H., Kim, J. W., and Ki, C. S. (2008). Identification of PSEN1 and APP gene mutations in Korean patients with early-onset Alzheimer's disease. *J. Korean Med. Sci.* 23, 213–217. doi: 10.3346/jkms.2008.23.2.213

Pasalar, P., Najmabadi, H., Noorian, A. R., Moghimi, B., Jannati, A., Soltanzadeh, A., et al. (2002). An Iranian family with Alzheimer's disease caused by a novel APP mutation (Thr714Ala). *Neurology* 58, 1574–1575. doi: 10.1212/WNL.58.10.1574

Pera, M., Alcolea, D., Sánchez-Valle, R., Guardia-Laguarta, C., Colom-Cadena, M., Badiola, N., et al. (2013). Distinct patterns of APP processing in the CNS in autosomal-dominant and sporadic Alzheimer disease. *Acta Neuropathol.* 125, 201–213. doi: 10.1007/s00401-012-1062-9

Román, G. C., Mancera-Páez, O., and Bernal, C. (2019). Epigenetic factors in late-onset Alzheimer's disease: MTHFR and CTH gene polymorphisms, metabolic transsulfuration and methylation pathways, and B vitamins. *Int. J. Mol. Sci.* 20:319. doi: 10.3390/ijms20020319

Ryan, N. S., and Rossor, M. N. (2010). Correlating familial Alzheimer's disease gene mutations with clinical phenotype. *Biomark. Med.* 4, 99–112. doi: 10.2217/bmm.09.92

Ryan, N. S., Nicholas, J. M., Weston, P. S. J., Liang, Y., Lashley, T., Guerreiro, R., et al. (2016). Clinical phenotype and genetic associations in autosomal dominant familial Alzheimer's disease: a case series. *Lancet Neurol.* 15, 1326–1335. doi: 10.1016/S1474-4422(16)30193-4

Scheltens, P., Blennow, K., Breteler, M. M., de Strooper, B., Frisoni, G. B., Salloway, S., et al. (2016). Alzheimer's disease. *Lancet* 388, 505–517. doi: 10.1016/S0140-6736(15)01124-1

Shimada, H., Ataka, S., Tomiyama, T., Takechi, H., Mori, H., and Miki, T. (2011). Clinical course of patients with familial early-onset Alzheimer's disease potentially lacking senile plaques bearing the E693Δ mutation in amyloid precursor protein. *Dement. Geriatr. Cogn. Disord.* 32, 45–54. doi: 10.1159/000330017

Shimada, H., Minatani, S., Takeuchi, J., Takeda, A., Kawabe, J., Wada, Y., et al. (2020). Heavy tau burden with subtle amyloid β accumulation in the cerebral cortex and cerebellum in a case of familial Alzheimer's disease with APP Osaka mutation. *Int. J. Mol. Sci.* 21:4443. doi: 10.3390/ijms21124443

Sieczkowski, E., Milenkovic, I., Venkataramani, V., Giera, R., Ströbel, T., Höftberger, R., et al. (2015). I716F AβPP mutation associates with the deposition of oligomeric pyroglutamate amyloid-β and α-synucleinopathy with Lewy bodies. *J. Alzheimers Dis.* 44, 103–114. doi: 10.3233/JAD-141524

Smits, L. L., Pijnenburg, Y. A., Koedam, E. L., van der Vlies, A. E., Reuling, I. E., Koene, T., et al. (2012). Early onset Alzheimer's disease is associated with a distinct neuropsychological profile. *J. Alzheimers Dis.* 30, 101–108. doi: 10.3233/JAD-2012-111934

Sorbi, S., Nacmias, B., Forleo, P., Piacentini, S., Latorraca, S., and Amaducci, L. (1995). Epistatic effect of APP717 mutation and apolipoprotein E genotype in familial Alzheimer's disease. *Ann. Neurol.* 38, 124–127. doi: 10.1002/ana.410380120

Sperling, R. A., Aisen, P. S., Beckett, L. A., Bennett, D. A., Craft, S., Fagan, A. M., et al. (2011). Toward defining the preclinical stages of Alzheimer's disease: recommendations from the National Institute on Aging-Alzheimer's Association workgroups on diagnostic guidelines for Alzheimer's disease. *Alzheimers Dement.* 7, 280–292. doi: 10.1016/j.jalz.2011.03.003

Swearer, J. M., O'Donnell, B. F., Drachman, D. A., and Woodward, B. M. (1992). Neuropsychological features of familial Alzheimer's disease. *Ann. Neurol.* 32, 687–694. doi: 10.1002/ana.410320513

Thambisetty, M., An, Y., and Tanaka, T. (2013). Alzheimer's disease risk genes and the age-at-onset phenotype. *Neurobiol. Aging* 34, 2696.e1–2696.e5. doi: 10.1016/j.neurobiolaging.2013.05.028

Theuns, J., Marjaux, E., Vandenbulcke, M., Van Laere, K., Kumar-Singh, S., Bormans, G., et al. (2006). Alzheimer dementia caused by a novel mutation located in the APP C-terminal intracytosolic fragment. *Hum. Mutat.* 27, 888–896. doi: 10.1002/humu.20402

Tomiyama, T., Nagata, T., Shimada, H., Teraoka, R., Fukushima, A., Kanemitsu, H., et al. (2008). A new amyloid beta variant favoring oligomerization in Alzheimer's-type dementia. *Ann. Neurol.* 63, 377–387. doi: 10.1002/ana.21321

Vermunt, L., Sikkes, S. A. M., van den Hout, A., Handels, R., Bos, I., van der Flier, W. M., et al. (2019). Duration of preclinical, prodromal, and dementia stages of Alzheimer's disease in relation to age, sex, and APOE genotype. *Alzheimers Dement.* 15, 888–898. doi: 10.1016/j.jalz.2019.04.001

Vöglein, J., Paumier, K., Jucker, M., Preische, O., McDade, E., Hassenstab, J., et al. (2019). Clinical, pathophysiological and genetic features of motor symptoms in autosomal dominant Alzheimer's disease. *Brain* 142, 1429–1440. doi: 10.1093/brain/awz050

Wakutani, Y., Watanabe, K., Adachi, Y., Wada-Isoe, K., Urakami, K., Ninomiya, H., et al. (2004). Novel amyloid precursor protein gene missense mutation (D678N) in probable familial Alzheimer's disease. *J. Neurol. Neurosurg. Psychiatry* 75, 1039–1042. doi: 10.1136/jnnp.2003.010611

Wang, Q., Jia, J., Qin, W., Wu, L., Li, D., Wang, Q., et al. (2015). A novel AβPP M722K mutation affects amyloid-β secretion and tau phosphorylation and may cause early-onset familial Alzheimer's disease in Chinese individuals. *J. Alzheimers Dis.* 47, 157–165. doi: 10.3233/JAD-143231

Wattendorff, A. R., Bots, G. T., Went, L. N., and Endtz, L. J. (1982). Familial cerebral amyloid angiopathy presenting as recurrent cerebral haemorrhage. *J. Neurol. Sci.* 55, 121–135. doi: 10.1016/0022-510X(82)90094-6

Xiao, X., Liu, H., Liu, X., Zhang, W., Zhang, S., and Jiao, B. (2021). *APP*, *PSEN1*, and *PSEN2* variants in Alzheimer's disease: systematic re-evaluation according to ACMG guidelines. *Front. Aging Neurosci.* 13:695808. doi: 10.3389/fnagi.2021.695808

Xu, Y., Liu, X., Shen, J., Tian, W., Fang, R., Li, B., et al. (2018). The whole exome sequencing clarifies the genotype- phenotype correlations in patients with early-onset dementia. *Aging Dis.* 9:696–705. doi: 10.14336/AD.2018.0208

Zádori, D., Füvesi, J., Timár, E., Horváth, E., Bencsik, R., Szépfalusi, N., et al. (2017). The report of p.Val717Phe mutation in the APP gene in a Hungarian family with Alzheimer disease: a phenomenological study. *Alzheimer Dis. Assoc. Disord.* 31, 343–345. doi: 10.1097/WAD.0000000000000206

Zekanowski, C., Styczyńska, M., Pepłońska, B., Gabryelewicz, T., Religa, D., Ilkowski, J., et al. (2003). Mutations in presenilin 1, presenilin 2 and amyloid precursor protein genes in patients with early-onset Alzheimer's disease in Poland. *Exp. Neurol.* 184, 991–996. doi: 10.1016/S0014-4886(03)00384-4

Zhang, G., Xie, Y., Wang, W., Feng, X., and Jia, J. (2017). Clinical characterization of an APP mutation (V717I) in five Han Chinese families with early-onset Alzheimer's disease. *J. Neurol. Sci.* 372, 379–386. doi: 10.1016/j.jns.2016.10.039

Zhou, J., Chen, Y., Meng, F., Zhang, K., Liu, X., and Peng, G. (2020). Presenilin 1 and APP gene mutations in early-onset AD families from a Southeast region of China. *Curr. Alzheimer Res.* 17, 540–546. doi: 10.2174/1567205017666200624195809

Zhou, L., Brouwers, N., Benilova, I., Vandersteen, A., Mercken, M., Van Laere, K., et al. (2011). Amyloid precursor protein mutation E682K at the alternative β-secretase cleavage β′-site increases Aβ generation. *EMBO Mol. Med.* 3, 291–302. doi: 10.1002/emmm.201100138

frontiers | Frontiers in Aging Neuroscience

TYPE Brief Research Report
PUBLISHED 08 December 2022
DOI 10.3389/fnagi.2022.1085406

OPEN ACCESS

EDITED BY
Prabhjyot Saini,
Emory University,
United States

REVIEWED BY
Emanuele Buratti,
International Centre for Genetic Engineering and Biotechnology, Italy
Chiara Fenoglio,
University of Milan,
Italy

*CORRESPONDENCE
Giacomina Rossi
giacomina.rossi@istituto-besta.it

SPECIALTY SECTION
This article was submitted to Neurocognitive Aging and Behavior, a section of the journal Frontiers in Aging Neuroscience

RECEIVED 31 October 2022
ACCEPTED 21 November 2022
PUBLISHED 08 December 2022

CITATION
Rossi G, Salvi E, Mehmeti E, Ricci M, Villa C, Prioni S, Moda F, Di Fede G, Tiraboschi P, Redaelli V, Coppola C, Koch G, Canu E, Filippi M, Agosta F, Giaccone G and Caroppo P (2022) Semantic and right temporal variant of FTD: Next generation sequencing genetic analysis on a single-center cohort.
Front. Aging Neurosci. 14:1085406.
doi: 10.3389/fnagi.2022.1085406

Semantic and right temporal variant of FTD: Next generation sequencing genetic analysis on a single-center cohort

Giacomina Rossi[1]*, Erika Salvi[2], Elkadia Mehmeti[2], Martina Ricci[1], Cristina Villa[1], Sara Prioni[3], Fabio Moda[1], Giuseppe Di Fede[1], Pietro Tiraboschi[1], Veronica Redaelli[1], Cinzia Coppola[4], Giacomo Koch[5], Elisa Canu[6], Massimo Filippi[6,7,8,9,10], Federica Agosta[6,7,8], Giorgio Giaccone[1] and Paola Caroppo[1]

[1]Neurology V and Neuropathology Unit, Fondazione IRCCS Istituto Neurologico Carlo Besta, Milan, Italy, [2]Neuroalgology Unit, Fondazione IRCCS Istituto Neurologico Carlo Besta, Milan, Italy, [3]Clinical Neuropsychology Unit, Fondazione IRCCS Istituto Neurologico Carlo Besta, Milan, Italy, [4]Department of Advanced Medical and Surgical Sciences, University of Campania "L. Vanvitelli", Naples, Italy, [5]Non Invasive Brain Stimulation Unit/Department of Behavioral and Clinical Neurology, Santa Lucia Foundation IRCCS, Rome, Italy, [6]Neuroimaging Research Unit, Division of Neuroscience, IRCCS San Raffaele Scientific Institute, Milan, Italy, [7]Neurology Unit, IRCCS San Raffaele Scientific Institute, Milan, Italy, [8]Vita-Salute San Raffaele University, Milan, Italy, [9]Unit of Neurorehabilitation, IRCCS San Raffaele Scientific Institute, Milan, Italy, [10]Neurophysiology Service, IRCCS San Raffaele Scientific Institute, Milan, Italy

Semantic and right temporal variant of frontotemporal dementia (svFTD and rtvFTD) are rare clinical phenotypes in which, in most cases, the underlying pathology is TDP-43 proteinopathy. They are usually sporadic disorders, but recent evidences suggest a higher frequency of genetic mutations for the right temporal versus the semantic variant. However, the genetic basis of these forms is not clear. In this study we performed a genetic screening of a single-center cohort of svFTD and rtvFTD patients, aiming at identifying the associated genetic variants. A panel of 73 dementia candidate genes has been analyzed by NGS target sequencing including both causal and risk/modifier genes in 23 patients (15 svFTD and 8 rtvFTD) and 73 healthy age-matched controls. We first performed a single variant analysis considering rare variants and then a gene-based aggregation analysis to evaluate the cumulative effects of multiple rare variants in a single gene. We found 12 variants in nearly 40% of patients (9/23), described as pathogenic or classified as VUS/likely pathogenic. The overall rate was higher in svFTD than in rtvFTD. Three mutations were located in *MAPT* gene and single mutations in the following genes: *SQSTM1, VCP, PSEN1, TBK1, OPTN, CHCHD10, PRKN, DCTN1*. Our study revealed the presence of variants in genes involved in pathways relevant for the pathology, especially autophagy and inflammation. We suggest that molecular analysis should be performed in all svFTD and rtvFTD patients, to better understand the genotype–phenotype correlation and the pathogenetic mechanisms that could drive the clinical phenotypes in FTD.

KEYWORDS

frontotemporal dementia, semantic variant, right temporal variant, next generation sequencing, genetic variant, pathogenic, mutation

Introduction

The term semantic variant of frontotemporal dementia (svFTD) usually refers to the form of FTD characterized by an early impairment of verbal semantic knowledge, that manifests as anomia and impaired single word comprehension, linked to the predominant atrophy of the left anterior temporal lobe and the diagnosis is based on current clinical criteria (Gorno-tempini et al., 2011). The right temporal variant of FTD (rtvFTD), a rarer clinical phenotype, originally considered a right variant of svFTD, has distinct clinical features and predominantly right hemisphere involvement. Patients with rtvFTD exhibit early behavioral symptoms, particularly empathy deficits and psychiatric disorders (Ulugut Erkoyun et al., 2020), but the diagnosis is challenging, and patients are often misdiagnosed as behavioral variant of FTD (bvFTD; Younes et al., 2022). A motor neuron involvement is rare in svFTD, but it has been found in up to 28% of rtvFTD cases in a recent neuropathological cohort (Ulugut et al., 2021).

While pathology can be highly heterogeneous in bvFTD, most of patients affected by svFTD and rtvFTD has TDP-43 neuronal accumulation, particularly the Type C pathology (Rohrer et al., 2010). In a minority of patients with rtvFTD a recent study reported also tauopathy as pathological substrate of the disease (Ulugut et al., 2021).

FTD has a prominent genetic basis, with up to 40% of cases presenting a family history (Mann and Snowden, 2017). To date three major genes have been described as linked to FTD: microtubule-associated protein tau (*MAPT*), progranulin (*GRN*) and Chromosome 9 open reading frame 72 (*C9ORF72*; Mann and Snowden, 2017). Furthermore, other causative genes have been disclosed, underlining rarer familial cases: Sequestosome 1 (*SQSTM1*), Valosin-Containing Protein (*VCP*), Charged Multivesicular Body Protein 2B (*CHMP2B*), TAR DNA Binding Protein, 43-KD (*TARDBP*), Fused in Sarcoma (*FUS*), Triggering Receptor Expressed on Myeloid cells 2 (*TREM2*), Tank-Binding Kinase 1 (*TBK1*) (see Fenoglio et al., 2018 for review). Left and right variants of FTD are usually sporadic, but recent evidence suggests a higher frequency of genetic mutations for the right versus the left variant (Ulugut Erkoyun et al., 2021). However, the genetic basis of these forms is not clear and genotype–phenotype correlations need to be elucidated, to allow accurate genetic counseling.

In this study, we used a next generation sequencing (NGS) approach to perform a genetic screening of a single-center cohort of patients with svFTD and rtvFTD, aiming at evaluating the genetic contribution in those disorders, by confirming candidate or discovering new genetic variants that could be associated with these clinical phenotypes.

Materials and methods

Cohort description

Twenty-three patients with clinical diagnosis of svFTD and rtvFTD (15 and 8 respectively) were retrospectively selected from FTD patients followed-up at Fondazione IRCCS Istituto Neurologico Carlo Besta from 2015 to 2020. One of them, carrying a *MAPT* mutation has been recently published (Villa et al., 2022). Clinical diagnosis of svFTD was made on the basis of current criteria (Gorno-Tempini et al., 2011). For the diagnosis of rtvFTD we followed the clinical and neuroimaging proposed framework (Ulugut Erkoyun et al., 2020). All patients underwent a complete clinical, neuropsychological and neuroimaging assessment. Analysis of markers of neurodegeneration (amyloid-β 1–42 – Aβ42, total tau and T181-phosphorylated-tau) was performed on cerebrospinal fluid (CSF) of 16 patients using LUMIPULSE G (Fujirebio, Malvern, PA, United States). Seventy-three age-matched healthy subjects from an in-house cohort were used as control group (healthy controls, HC). Written informed consent was obtained from all patient and healthy subjects.

Next generation sequencing

DNA of patients was obtained, after informed consent, from peripheral blood lymphocytes. We designed a targeted enrichment panel to capture the coding and 25 bp flanking intron sequences of 73 dementia genes, including both causal genes and risk/modifier factors (Supplementary material S1). Nextera Flex for Enrichment system (Illumina, San Diego, CA, United States) coupled with gene-specific probes (Integrated DNA Technologies, Coralville, IA, United States) and the MiSeq instrument (Illumina, San Diego, CA, United States) were used for sequencing. A first quality control step was performed with FastQC software to identify base quality drops across cycles and adapter contamination, and to evaluate overall data quality. We performed both adapter trimming and quality trimming using Trimmomatic (version 0.36; Bolger et al., 2014). High-quality reads were mapped to the hg19 reference genome using bwa v. 0.7.17-r1188 (mem algorithm; Li and Durbin, 2010). Hence, we performed duplicated read marking, local realignment, and base quality score recalibration as suggested by GATK best practices (DePristo et al., 2011). We performed single-nucleotide variant (SNV) and insertion/deletion (INDEL) calling using the GATK module Haplotype Caller (version 4.1.9) over the target region. For the variant annotation we used the SnpEff software (Cingolani et al., 2012) that annotates and predicts the effects of genetic variants on

TABLE 1 Clinical and demographic features of study groups.

	Total	svFTD	rtvFTD	HC
N (M/F)	23 (13/10)	15(7/8)	8 (6/2)	73 (56/17)
Age at onset (mean±SD)	60.09 (±8.03)	60.27 (±8.69)	59.75 (±7.17)	–
Predominant symptom at onset		Loss of semantic knowledge	Memory impairment and behavioral alterations	–
MND	1/23	1/15	0	–
Family history of dementia	9/23	8/15	1/8	–
CSF (N)	16	11	5	
CSF Tau (pg/ml)	339.25 (±170.37)	351.36 (±193.27)	312.6 (±119.06)	
CSF p-tau (pg/ml)	38.32 (±19.85)	38.56 (±22.61)	37.65 (±11.61)	
CSF Abeta42 (pg/ml)	737.375 (±193.05)	783.45 (±177.46)	636 (±205.77)	

FTD = Frontotemporal dementia; sv = semantic variant; rtv = right temporal variant; HC = healthy controls; SD = standard deviation; N = number; M = male; F = female; MND = Motor neuron disease; CSF = cerebrospinal fluid. Patients and HC did not show significant difference in term of sex ($p = 0.11$) and age ($p = 0.18$).

genes and proteins. Variants that did not pass the variant filtering (total reads count≤20, alternative allele depth ≤ 10 and allele balance of 25%) were removed. Visual inspection of bam files was performed using IGV software (Thorvaldsdóttir et al., 2013).

Single variant and gene-based aggregation analysis

In our cohort of 23 patients and 73 HC we first performed a single-variant analysis considering non-synonymous (missense, splicing, frameshift, STOP gain/loss) rare variants, that is variants with minor allele frequency (MAF) <0.01 in Genome Aggregation Database – Exomes – Non Finnish Europeans (GNOMEX_NFE). Franklin by Genoox[1] and/or Varsome[2] were used to report the classification according the criteria of the American College of Medical Genetics (ACMG).

Furthermore, we performed a gene-based aggregation analysis to evaluate the cumulative effects of multiple rare and low frequency (MAF <0.05) variants in a gene. All non-synonymous variants with MAF <0.05 in the studied cohort and reaching at least 80% of call rate were collapsed into single genes. Genes mapped by only one variant were not considered. To test whether there is an excess of variants in patients in comparison with HC, we applied both the combined burden and variance-component SKAT-O (Lee et al., 2012) and the simple burden method as implemented in EPACTS software (Efficient and Parallelizable Association Container Toolbox).[3] Rho statistic indicates the direction of the effects, with rho = 1 referring to high percentage of causality in the same direction and rho = 0 to the simultaneous presence of causal and non-causal variants with opposing directions.

All the analyses were corrected for sex and age as covariates.

Genotyping of *C9ORF72* exanucleotide repeat

The GGGGCC hexanucleotide repeat in the *C9ORF72* gene (DeJesus-Hernandez et al., 2011) was assessed by a repeat-primed PCR reaction using the AmplideX® PCR/CE C9orf72 Kit (Asuragen, Austin, TX, United States), according to the manufacturer's instructions. PCR products were analyzed on an ABI3130xl Genetic Analyzer.

Results

Demographic and clinical data of overall cohort are reported in Table 1. Patients and HC did not show significant difference in term of sex ($p = 0.11$) and age ($p = 0.18$). 39% (9/23) of patients had a family history of dementia (53% of svFTD).

Semantic impairment with naming deficits was the first symptom of svFTD patients, while rtvFTD patients showed early changes in their personality and behaviour (among them, eating behavior changes, loss of empathy, compulsive behaviors), memory loss, prosopagnosia and topographical disorientation. According with clinical diagnosis, brain magnetic resonance imaging and fluorodeoxyglucose-positron emission tomography showed predominant atrophy and hypometabolism in left anterior temporal lobe in svFTD and a predominant right temporal involvement in all rtvFTD. CSF biomarkers were in the normal range in 13/16 patients, 3 patients had isolated reduction of Abeta42. Total tau was elevated in 2 patients and one of them had also elevated p-tau, but normal Abeta42.

Single variant analysis

By single variant analysis, we found 12 variants described as pathogenic in the scientific literature (reported in Human Gene Mutation Database, HGMD) or classified as variant of unknown significance (VUS)/likely pathogenic in 9 patients (39% of patients) and none in control subjects (Table 2).

1 https://franklin.genoox.com/clinical-db/home

2 https://varsome.com

3 http://genome.sph.umich.edu/wiki/EPACTS

TABLE 2 Variants present in patients.

Patient	FTD (rtv/sv)	Gene	Codon	Reference	Associated disease (HGMD)	ACMG	Notes on pathogenicity	AF_ GNOMEX_ NFE
P01	rtv	*MAPT*	N621N (N286N)*	NM_001123066.3:c.1863C>T	nr	Likely benign	Splicing enhancer alteration	2.38E-05
		PSEN1	M93V	NM_000021.3:c.277A>G	nr	Likely pathogenic	Within a mutational hot spot	8.95E-06
P05	sv	*MAPT*	P636L (P301L)*	NM_001123066.3:c.1907C>T	FTD	Pathogenic	Several reports on genetics, function, neuropathology, animal models	1.32E-05
P06	sv	*OPTN*	Q314L	NM_021980.4:c.941A>T	ALS	VUS-LP	15 pathogenicity scores[$]	2.78E-04
		DCTN1	R795H	NM_004082.4:c.2384G>A	CMT	VUS-LP	18 pathogenicity scores[$]	4.48E-05
P10	rtv	*CHCHD10*	P80L	NM_213720.1:c.239C>T	ALS	VUS	9 pathogenicity scores[$]	2.31E-04
P11	sv	*PRKN*	T240M	NM_004562.2:c.719C>T	PD	Pathogenic	Functional studies	2.51E-04
P12	sv	*MAPT*	Q671H (Q336H)*	NM_001123066.3:c.2013G>T	FTD	VUS-LP	Reports on genetics, function, neuropathology	0
P20	sv	*SQSTM1*	E280/del	NM_003900.4:c.838_840delGAG	FTD	VUS-LP	Susceptibility factor	1.79E-05
P21	sv	*VCP*	G376E	NM_007126.3:c.1127G>A	nr	VUS-LP	New, absent in population databases, 19 pathogenicity scores[$]	0
		TBK1	I207T	NM_013254.3:c.620T>C	ALS	VUS	10 pathogenicity scores[$]	1.08E-04
P23	sv	*SQSTM1*	P387L	NM_003900.4:c.1160C>T	FTD, ALS, PBD	VUS-LP	Reports on genetics	5.97E-04

FTD = Frontotemporal dementia; rtv = right temporal variant; sv = semantic variant; *NM_005910; HGMD = Human Gene Mutation Database; nr = not reported; ALS = Amyotrophic lateral sclerosis; CMT = - Charcot–Marie-Tooth; PD = Parkinson's disease; PDB =. Paget disease of bone; ACMG = American College of Medical Genetics; VUS = variant of unknown significance; VUS-LP = VUS near likely pathogenic.
[$]https://varsome.com; AF_GNOMEX_NFE = Allele frequency from Genome Aggregation Database - Exome - Non Finnish Europeans.

We found three mutations in the microtubule-associated protein tau (*MAPT*) gene, which was the first causative gene to be linked to FTD: P301L, Q336H (Villa et al., 2022) and N286N. In addition, we discovered single mutations in the following genes: *SQSTM1*, *VCP*, presenilin 1 (*PSEN1*), *TBK1*, optineurin (OPTN), coiled-coil-helix-coiled-coil-helix domain containing protein 10 (*CHCHD10*), parkin (*PRKN*) and dynactin 1 (*DCTN1*). Three patients carried two mutations each: P01, N286N *MAPT* and M93V *PSEN1*; P06, Q314L *OPTN* and R795H *DCTN1*; P21, G376E *VCP* and I207T *TBK1*. All the variants are singletons (present only in 1 patient) and not present in control subjects. Clinical characteristics of the 9 patients carrying the variants are reported in Table 3.

Gene-based aggregation analysis

None of the genes reached the Bonferroni corrected threshold (for the total number of genes considered, $p = 0.001$). However, the SKAT-O test highlighted 4 genes with suggestive value of $p < 0.05$, enriched for rare variants: *CD33*, *PSEN1*, *OPTN* and *ABCA1* (Table 4).

OPTN with a rho value equal to 1 showed a unidirectional risk association, reflected by the fact that the two rare variants are exclusively present or more frequent in cases than in HC: M98K was present in 6.5% of patients and 2.1% of HC, whereas Q314L was carried by one patient (Table 5). The simple burden test showed *OPTN* as conferring a risk 7.89-fold higher in patients compared to HC ($p = 0.0395$, OR = 7.89).

A rho value equal to 0.1, for *CD33* and *PSEN1*, indicated a simultaneous presence of causal and non-causal variants with opposing directions. *CD33* is enriched of 4 rare/low frequency variants in 7 patients and 5 HC: the frameshift G156fs was shared by patients and HC with a similar frequency, S305P was present in 4 of 23 patients (8.7%) and one HC (0.7%), F243L and V267I were exclusively carried by one patient (Table 5). In *PSEN1*, E318G was found in 4.3% of patients and 0.7% of controls, the M93V was exclusively

carried by one patient whereas D333V was present in one control.

As for *ABCA1* (Table 5), a rho value of 0 indicates the simultaneous presence of causal and non-causal variants with opposing directions. In fact, out of 9 variants, 4 were present in patients and 5 in a high number of HC, showing opposite directions in terms of risk association.

Genotyping of *C9ORF72* exanucleotide repeat

None of the patients carried an expanded allele (>30 repeats).

Discussion

In this study we found several pathogenic or VUS/likely pathogenic variants, in nearly 40% of patients.

P301L, carried by P05, is one of the most known and studied *MAPT* mutations, whose pathogenicity has been demonstrated in several genetic, functional and neuropathological studies, as well as in animal models (Hutton et al., 1998; Barghorn et al., 2000; Lewis et al., 2000; Rossi et al., 2008). Different FTD clinical phenotypes have been associated with the mutation, including svFTD (Ishizuka et al., 2011). Q336H *MAPT* mutation, carried by patient P12, was recently published as associated with svFTD (Villa et al., 2022). This mutation had been previously functionally and neuropathologically characterized as pathogenic (Tacik et al., 2015). Patient P01 carried the N286N *MAPT* and M93V *PSEN1* variants. As for the N286N *MAPT* variant, only once cited without additional details (Rohrer et al., 2009), the classification as likely benign does not take into account the pathogenetic mechanism typical of some silent *MAPT* mutations localized in exon 10, that is the alteration of an exon 10 splicing enhancer or silencer (D'Souza and Schellenberg, 2002; Qian and Liu, 2014). In fact, an *in silico* functional analysis demonstrated the effect on exon 10 splicing of this variant (Tubeuf et al., 2020). The M93V variant in *PSEN1*, so far never described, is very interesting as localized in a mutational hot spot in a critical region for the protein function, the transmembrane domain 1: in fact, the adjacent mutations C92S (Zhang et al., 2000; Tedde et al., 2003) and V94M (Arango et al., 2001; Somavarapu and Kepp, 2016) are associated with Alzheimer's disease (AD). In addition, several other pathogenic AD mutations have been described in the same protein region. It is well known that *PSEN1* mutations give rise to Alzheimer's disease by affecting the beta amyloid levels; however, a few mutations have been reported as associated with a FTD phenotype, even pathologically confirmed as a tauopathy (Dermaut et al., 2004), although how loss of functional presenilin 1 could predispose to tauopathy has not been clarified. Our patient had a clinical phenotype of rtvFTD with early memory deficits and behavioural disturbances including lack of empathy, hyperphagia and loss of inhibition, the clinical phenotype suggesting the prevalence of FTD neurodegeneration pathway, while the AD pathway may cooperate in the pathology. Moreover, amyloid-PET was negative in our patient, making AD diagnosis unlikely.

MAPT mutations have been previously identified in 4 rtvFTD cases (Ulugut Erkoyun et al., 2021). However, in our cohort, both svFTD (P05 and P12) and rtvFTD (P01) patients carried *MAPT* mutations, not confirming a prevalent association of *MAPT* mutations with rtvFTD.

Patient P06 had Q314L *OPTN* and R795H *DCTN1* variants. *OPTN*, earlier reported as causative of primary open-angle glaucoma, was afterwards linked to ALS (Maruyama et al., 2010), or to FTD (Dominguez et al., 2021), with dominant or recessive transmission. Heterozygous Q314L in *OPTN* was described in some sporadic ALS cases (Del Bo et al., 2011; Pensato et al., 2020). *DCTN1*, firstly linked to ALS and Perry syndrome, was then associated with progressive supranuclear palsy and FTD phenotypes (Caroppo et al., 2014). R795H variant was only described in a case of Charcot–Marie-Tooth. These variants are classified as VUS-near likely pathogenic and may contribute to the FTD pathology in our patient, although with very different mechanisms, as *OPTN* is involved in autophagy whereas *DCTN1*, binding to microtubules and to dynein, has a role in retrograde axonal transport (LaMonte et al., 2002). Patient P21 carried the G376E *VCP* and I207T *TBK1* variants. Mutations in *VCP* were identified as the cause of inclusion body myopathy with Paget disease of bone and frontotemporal dementia (IBMPF); (Watts et al., 2004). Afterwards, *VCP* mutations were also found in cases of pure FTD (Saracino et al., 2018). The G376E variant has never been described and is not present in population databases, constituting a possible new mutation. In fact, it is adjacent to the ATPase domain 1, where other mutations have been described (Mol et al., 2021), and it is classified as VUS-near likely pathogenic, having at least 19 pathogenicity scores. I207T in *TBK1* was described in a patient affected by sporadic ALS (Tohnai et al., 2018). The mutation is within the serine/threonine kinase domain and has 10 pathogenicity scores. *TBK1* is now recognized also as a FTD gene (van Mossevelde et al., 2018). Since *VCP* has several functions, including the maintenance of lysosomal homeostasis (Arhzaouy et al., 2019), it may cooperate with *TBK1*, whose principal role is in the autophagy. The coexistence of variants in genes involved in the same pathway reinforces their pathogenic role and may explain the pathology. Both P06 and P21 patients were svFTD, without any sign of ALS.

Patients P20 and P23, both svFTD, carried a *SQSTM1* mutation. *SQSTM1* mutations were firstly identified as causative of Paget Disease of Bone (PDB; Laurin et al., 2002), and afterwards this gene was disclosed to be also causative of ALS (Fecto et al., 2011) and FTD (Le Ber et al., 2013). The P387L mutation, carried by patient P23, was previously described in patients affected by PDB (Johnson-Pais et al., 2003), and also in familiar cases of FTD, where a segregation with the disease was demonstrated (Le Ber et al., 2013). The amino acid deletion E280, carried by patient P20,

TABLE 3 Clinical and demographic characteristics of the 9 patients carrying the variants.

	P01	*P05*	*P06*	*P10*	*P11*	*P12*	*P20*	*P21*	*P23*
Clinical variant	rtv	sv	sv	rtv	sv	sv	sv	sv	sv
Gender	M	M	F	M	M	F	F	M	F
Family history	pos	pos	neg	neg	pos	pos	neg	pos	pos
Age at onset	50	47	59	67	65	37	63	61	58
Disease duration	5	12	na	5	8	7	6	6	2
Gene variant	*MAPT* N286N *PSEN1* M93V	*MAPT* P301L	*OPTN* Q314L *DCTN1* R795H	*CHCHD10* P80L	*PRKN* T240M	*MAPT* Q336H	*SQSTM1* E280/del	*VCP* G376E *TBK1* I207T	*SQSTM1 P387L*
CSF analysis/ amyloid-PET	PET-amyloid neg	Normal CSF	Normal CSF	Normal CSF	Normal CSF	Reduced Aβ42, normal tau and p-tau	na	Normal Aβ42, elevated tau and p-tau	na
MMSE (/30)	18*	4*	25	27*	na	9*	26	12*	na
MoCA (/30)	na	na	na	na	na	na	na	na	22*
FAB (/18)	13*	na	na	12*	na	9*	15	4*	16
FBI (/72)	33	na	na	14	na	21	12	8	na

rtv = right temporal variant; sv = semantic variant; na = not available; CSF = cerebrospinal fluid; PET = positron emission tomography; MMSE = Mini-Mental State Examination; MoCA = Montreal Cognitive Assessment; FAB = Frontal Assessment Battery; FBI = Frontal Behavioral Inventory.*under cut-off; pos = positive; neg = negative. For *MAPT*, reference NM_005910 is used.

TABLE 4 Genes enriched by rare/low frequency variants after gene-based analysis with a SKAT-O *p* value <0.05.

			SKAT-O		BURDEN	
GENE	**N tested variants**	**N Singleton variants**	**Rho**	**Value of *p***	**Value of *p***	**OR**
CD33	4	2	0.1	3.28E-03	2.71E-02	4.57
PSEN1	3	2	0.1	2.99–02	3.60E-02	5.91
OPTN	2	1	1	4.46E-02	3.95E-02	7.89
ABCA1	9	6	0	4.83E-02	2.61E-01	0.56

SKAT-O, Optimized sequence kernel association test; OR, Odds Ratio. The results are ordered by SKAT-O p-value. Rho statistic indicates the direction of the effects, with rho = 1 referring to high percentage of causality in the same direction and rho = 0 to the simultaneous presence of causal and non-causal variants with opposing directions.

was described as a susceptibility factor for FTD (Van Der Zee et al., 2014).

Patient P10, rtvFTD, had the P80L *CHCHD10* mutation, previously reported in patients affected by familial or sporadic ALS (Ronchi et al., 2015; Zhang et al., 2015). *CHCHD10* codes for a mitochondrial protein associated not only with ALS but also with FTD (Chaussenot et al., 2014).

While homozygous or heterozygous compound mutations in *PRKN* lead to early-onset Parkinson's disease (PD; Lücking et al., 2000), the role of heterozygous mutations is still controversial, ranging from benign condition to susceptibility factor (Marder et al., 2010; Moura et al., 2013). *PRKN* T240M mutation, carried by the svFTD patient P11, is predicted to eliminate a phosphorylation site for casein kinase II and occurs in the same codon as other mutations (T240R and T240K), indicating that this is an important functional residue. Furthermore, functional studies in neuronal cell cultures demonstrated that this mutation impairs glutamatergic signaling (Zhu et al., 2018). Biallelic mutations in *PKRN* can lead to FTD (Zimmermann et al., 2018), whereas we suppose that heterozygous mutations may only constitute a susceptibility factor.

In summary, as for single variant findings, we found 12 mutations in 9 patients out of 23, evidencing a strong genetic component in FTD phenotypes usually regarded as sporadic. We also showed that the mutations appeared to be more associated with svFTD (7/15, 47%) than with rtvFTD (2/8, 25%) at variance with what suggested by others (Ulugut Erkoyun et al., 2021). Our data show that a gene strongly involved in our cohort of patients is *MAPT*, one of the three major genes causative of the FTD spectrum. Along with *DCTN1*, the involvement of this gene clearly demonstrates the relevance of the correct microtubule dynamics and transport in the nervous system. The mutations found in our patients outline cell pathways whose alterations are common to different neurodegenerative diseases such as FTD, ALS and Parkinson's disease (PD). Lysosomal and autophagic functions are sustained by *VCP*, which plays a role in lysosome homeostasis, and by *SQSTM1*, *TBK1* and *OPTN*, which interact in the autophagy (Abramzon et al., 2020; Fleming et al., 2022), all mutated in ALS and FTD. In addition, mitophagy, a specialized form of autophagy concerning mitocondria, is

TABLE 5 Variants present in the enriched genes (gene-based aggregation analysis).

Gene	codon	Reference	Associated disease (HGMD)	ACMG	AF_ GNOMEX_ NFE	Cohort MAF	% pts	% HC	N pts ($n = 22$)	N HC ($n = 73$)
CD33	S305P	NM_001772.3:c.913 T > C	nr	benign	2.15E-02	2.60%	8.70%	0.70%	4	1
CD33	G156fs	NM_001772.3:c.466_469delGGCC	AD risk	benign	2.43E-02	2.60%	2.20%	2.70%	1	4
CD33	F243L	NM_001772.3:c.727 T > C	nr	benign	3.58E-04	0.50%	2.20%	0.00%	1	0
CD33	V267I	NM_001772.3: c.799G > A	nr	benign	4.39E-04	0.50%	2.20%	0.00%	1	0
PSEN1	E318G	NM_000021.3:c.953A > G	AD risk	benign	1.86E-02	1.60%	4.30%	0.70%	2	1
PSEN1	M93V	NM_000021.3:c.277A > G	nr	Likely pathogenic	8.95E-06	0.50%	2.20%	0.00%	1	0
PSEN1	D333V	NM_000021.3:c.998A > T	nr	Likely pathogenic*	0	0.50%	0.00%	0.70%	0	1
OPTN	M98K	NM_001008211.1:c.293 T > A	glaucoma risk	Likely benign	2.80E-02	3.10%	6.50%	2.10%	3	3
OPTN	Q314L	NM_001008211.1:c.941A > T	ALS	VUS-LP	2.78E-04	0.50%	2.20%	0.00%	1	0
ABCA1	Q2196H	NM_005502.3:c.6588G > C	HDL deficiency	VUS-LP	2.25E-04	0.50%	2.20%	0.00%	1	0
ABCA1	R909Q	NM_005502.3:c.2726G > A	nr	VUS	2.69E-05	0.50%	0.00%	0.70%	0	1
ABCA1	T774P	NM_005502.3:c.2320A > C	Increased cholesterol	Likely benign	3.15E-03	0.50%	0.00%	0.70%	0	1
ABCA1	M674L	NM_005502.3:c.2020A > C	nr	VUS	0	0.50%	2.20%	0.00%	1	0
ABCA1	V285M	NM_005502.3:c.853G > A	nr	VUS	1.79E-05	0.50%	2.20%	0.00%	1	0
ABCA1	.	NM_005502.3:c.814-7A > G	nr	VUS	.	0.50%	2.20%	0.00%	1	0
ABCA1	K776N	NM_005502.3:c.2328G > C	Risk ischemic heart disease	Benign	3.38E-03	1.00%	0.00%	1.40%	0	2
ABCA1	E1172D	NM_005502.3:c.3516G > C	Coronary heart disease	Benign	2.90E-02	4.20%	0.00%	5.50%	0	7
ABCA1	V771M	NM_005502.3:c.2311G > A	Altered cholesterol levels	Benign	3.32E-02	4.70%	0.00%	6.20%	0	8

HGMD = Human Gene Mutation Database; nr = not reported; ALS = Amyotrophic lateral sclerosis; AD = Alzheimer's disease; HDL = high-density lipoprotein; ACMG = American College of Medical Genetics; VUS = variant of unknown significance; VUS-LP = VUS near likely pathogenic; AF_GNOMEX_NFE = Allele frequency from Genome Aggregation Database - Exome - Non Finnish Europeans. MAF = Minor allele frequency; *for cardiovascular disease; N = number; pts = patients; HC = Healthy controls.

carried out by the interaction of *TBK1*, *PRKN* and *OPTN* (Harding et al., 2021). Mitochondrial homeostasis is the function of *CHCHD10*, linked to FTD, ALS and PD (Jiang et al., 2022).

We also performed a gene-level association analysis (burden analysis) in order to disclose genes which may contain a significantly higher number of variants in patients than in controls, suggesting the gene to be relevant to the pathology. We are aware of the small size of our cohorts, partly justified by the rarity of the disease, and in fact we did not achieved the Bonferroni significant threshold, but only suggestive *p* values highlighting 4 genes: *CD33, PSEN1* and *ABCA1*, showing a simultaneous presence of causal and non-causal variants with opposing directions, and *OPTN,* showing unidirectional risk association with rare variants exclusively present or more frequent in patients than in HC.

CD33 is a transmembrane protein and a sialic acid-binding immunoglobulin-like lectin that regulates innate immunity. In the CNS, it is expressed by the microglia. CD33 has an immunoreceptor tyrosine-based inhibitory motif (ITIM) and one ITIM-like domain that facilitates an inhibitory signal. When CD33 is activated by sialic-acid-containing glycoproteins and glycolipids, it results in inhibition of microglia phagocytosis. Genome-wide association studies (GWAS) identified several genetic loci associated with increased susceptibility to late onset Alzheimer's disease, including CD33 (Naj et al., 2011). Some polymorphisms increase CD33 expression, giving rise to reduced microglial phagocytosis and amyloid clearance. Although most polymorphisms were related to AD dementia, others were described as associated with a FTD phenotype (Rendina et al., 2020). In our cohorts we found 4 CD33 rare or low frequency variants. In particular, S305P was found in 9.1% of patients and 0.7% of control subjects, while F243L and V267I were only found in one patient each and no controls. G156fs was found approximately with the same frequency in patients and controls. All these variants are classified as benign. Besides the involvement in amyloid clearance, a pathological feature of AD, CD33 may be regarded as a gene more generally involved in immune and

inflammatory pathways, which are also altered in FTD (Ferrari et al., 2014, 2015).

We have already discussed the contribution of a *PSEN1* likely pathogenic variant, M93V, to FTD phenotype (see above); in addition, the gene-based analysis revealed the presence of the E318G variant, previously described as a risk factor for AD but afterwards producing conflicting results (Dermaut et al., 1999). The D333V variant, present in a control subject, was never reported before and it is classified as likely pathogenic for cardiovascular disease (Li et al., 2006). As for *OPTN*, we have already described the Q341L variant (see above), while the M98K is reported in databases as likely benign.

ABCA1 is an ATP-binding cassette transporter that controls whole brain cholesterol homeostasis. Polymorphisms in *ABCA1* have been demonstrated to influence susceptibility to dementia, in particular to AD (Lupton et al., 2014; Chen et al., 2016). In our cohorts we found 9 *ABCA1* rare or low frequency variants. Four of them were found in patients and the others in controls, showing opposite directions in terms of risk association, that is not giving a true causal significance to this gene as regards to FTD phenotypes. Literature data about *ABCA1* concern primarily cardiovascular disease and variants classified as benign due to their relatively high frequency in the population are often associated with a certain level of risk for these diseases. As for dementias, in experimental models, *ABCA1* activities appear to influence neuroinflammation and neurodegeneration (Karasinska et al., 2013), thus possibly affecting different forms of dementia, including FTD.

In conclusion, our study revealed the presence of variants in genes involved in pathways relevant for the pathology, especially autophagy and inflammation, common to different neurodegenerative diseases such as FTD, ALS, AD and PD. The findings support the role of these pathways in semantic phenotypes of FTD, as recently suggested (Pascual et al., 2021). Molecular analysis of dementia-related genes should be performed in all patients with svFTD and rtvFTD, to better understand the genotype–phenotype correlations and to study the pathogenetic mechanisms that could drive the clinical phenotypes in FTD.

Data availability statement

The original contributions presented in the study are included in the article/Supplementary material, further inquiries can be directed to the corresponding author.

Ethics statement

The studies involving human subjects were reviewed and approved by Ethics Committee of Fondazione IRCCS Istituto Neurologico Carlo Besta (Prot. n.39–05/04/2017). All the subjects provided their written informed consent to participate in this study.

Author contributions

GR and PC: conceptualization. ES, EM, and MR: formal analysis. CV, SP, FM, GF, PT, VR, CC, GK, EC, MF, and FA: investigation. FA and GG: funding acquisition. GR, ES, and EM: methodology. GR, PC, and ES: writing – original draft. GR, PC, and FA: writing – review and editing. All authors contributed to the article and approved the submitted version.

Funding

This research was funded by the European Research Council (StG-2016_714388_NeuroTRACK) and the Italian Ministry of Health, Ricerca Corrente RRC.

Conflict of interest

EC has received research supports from the Italian Ministry of Health. MF is Editor-in-Chief of the *Journal of Neurology*; received compensation for consulting services and/or speaking activities from Bayer, Biogen Idec, Merck-Serono, Novartis, Roche, Sanofi Genzyme, Takeda, and Teva Pharmaceutical Industries; and receives research support from Biogen Idec, Merck-Serono, Novartis, Roche, Teva Pharmaceutical Industries, Italian Ministry of Health, Fondazione Italiana Sclerosi Multipla, and ARiSLA (Fondazione Italiana di Ricerca per la SLA). FA is Section Editor of *NeuroImage: Clinical*; has received speaker honoraria from Biogen Idec, Roche and Zambon; and receives or has received research supports from the Italian Ministry of Health, AriSLA (Fondazione Italiana di Ricerca per la SLA), the European Research Council and the Foundation Research on Alzheimer Disease.

The remaining authors declare that the research was conducted in the absence of any commercial or financial relationships that could be construed as a potential conflict of interest.

Publisher's note

Supplementary material

The Supplementary material for this article can be found online at: https://www.frontiersin.org/articles/10.3389/fnagi.2022.1085406/full#supplementary-material

References

Abramzon, Y. A., Fratta, P., Traynor, B. J., and Chia, R. (2020). The overlapping genetics of amyotrophic lateral sclerosis and frontotemporal dementia. *Front. Neurosci.* 14:42. doi: 10.3389/fnins.2020.00042

Arango, D., Cruts, M., Torres, O., Backhovens, H., Serrano, M. L., Villareal, E., et al. (2001). Systematic genetic study of Alzheimer disease in Latin America: mutation frequencies of the amyloid beta precursor protein and presenilin genes in Colombia. *Am. J. Med. Genet.* 103, 138–143. doi: 10.1002/1096-8628(20011001)103:2<138::aid-ajmg1529>3.0.co;2-8

Arhzaouy, K., Papadopoulos, C., Schulze, N., Pittman, S. K., Meyer, H., and Weihl, C. C. (2019). VCP maintains lysosomal homeostasis and TFEB activity in differentiated skeletal muscle. *Autophagy* 15, 1082–1099. doi: 10.1080/15548627.2019.1569933

Barghorn, S., Zheng-Fischhöfer, Q., Ackmann, M., Biernat, J., von Bergen, M., Mandelkow, E. M., et al. (2000). Structure, microtubule interactions, and paired helical filament aggregation by tau mutants of frontotemporal dementias. *Biochemistry* 39, 11714–11721. doi: 10.1021/bi000850r

Bolger, A. M., Lohse, M., and Usadel, B. (2014). Trimmomatic: a flexible trimmer for Illumina sequence data. *Bioinformatics* 30, 2114–2120. doi: 10.1093/bioinformatics/btu170

Caroppo, P., Le Ber, I., Clot, F., Rivaud-Péchoux, S., Camuzat, A., De Septenville, A., et al. (2014). Dctn1 mutation analysis in families with progressive supranuclear palsy–like phenotypes. *JAMA Neurol.* 71, 208–215. doi: 10.1001/jamaneurol.2013.5100

Chaussenot, A., Le Ber, I., Ait-El-Mkadem, S., Camuzat, A., de Septenville, A., and Bannwarth, S. (2014). Screening of CHCHD10 in a French cohort confirms the involvement of this gene in frontotemporal dementia with amyotrophic lateral sclerosis patients. *Neurobiol. Aging* 35, 2884.e1–2884.e4. doi: 10.1016/j.neurobiolaging.2014.07.022

Chen, Q., Liang, B., Wang, Z., Cheng, X., Huang, Y., Liu, Y., et al. (2016). Influence of four polymorphisms in ABCA1 and PTGS2 genes on risk of Alzheimer's disease: a meta-analysis. *Neurol. Sci.* 37, 1209–1220. doi: 10.1007/s10072-016-2579-9

Cingolani, P., Platts, A., Wang, L., Coon, M., Nguyen, T., Wang, L., et al. (2012). A program for annotating and predicting the effects of single nucleotide polymorphisms, SnpEff: SNPs in the genome of Drosophila melanogaster strain w1118; iso-2; iso-3. *Fly* 6, 80–92. doi: 10.4161/fly.19695

D'Souza, I., and Schellenberg, G. D. (2002). Tau exon 10 expression involves a bipartite intron 10 regulatory sequence and weak 5′ and 3′ splice sites. *J. Biol. Chem.* 277, 26587–26599. doi: 10.1074/jbc.M203794200

DeJesus-Hernandez, M., Mackenzie, I. R., Boeve, B. F., Boxer, A. L., Baker, M., Rutherford, N. J., et al. (2011). Expanded GGGGCC hexanucleotide repeat in noncoding region of C9ORF72 causes chromosome 9p-linked FTD and ALS. *Neuron* 72, 245–256. doi: 10.1016/j.neuron.2011.09.011

Del Bo, R., Tiloca, C., Pensato, V., Corrado, L., Ratti, A., Ticozzi, N., et al. (2011). Novel optineurin mutations in patients with familial and sporadic amyotrophic lateral sclerosis. *J. Neurol. Neurosurg. Psychiatry* 82, 1239–1243. doi: 10.1136/jnnp.2011.242313

DePristo, M. A., Banks, E., Poplin, R., Garimella, K. V., Maguire, J. R., Hartl, C., et al. (2011). A framework for variation discovery and genotyping using next-generation DNA sequencing data. *Nat. Genet.* 43, 491–498. doi: 10.1038/ng.806

Dermaut, B., Cruts, M., Slooter, A. J., Van Gestel, S., De Jonghe, C., Vanderstichele, H., et al. (1999). The Glu318Gly substitution in presenilin 1 is not causally related to Alzheimer disease. *Am. J. Hum. Genet.* 64, 290–292. doi: 10.1086/302200

Dermaut, B., Kumar-Singh, S., Engelborghs, S., Theuns, J., Rademakers, R., Saerens, J., et al. (2004). A novel presenilin 1 mutation associated with Pick's disease but not beta-amyloid plaques. *Ann. Neurol.* 55, 617–626. doi: 10.1002/ana.20083

Dominguez, J., Yu, J. T., Tan, Y. J., Ng, A., De Guzman, M. F., Natividad, B., et al. (2021). Novel optineurin frameshift insertion in a family with frontotemporal dementia and parkinsonism without amyotrophic lateral sclerosis. *Front. Neurol.* 12:645913. doi: 10.3389/fneur.2021.645913

Fecto, F., Yan, J., Vemula, S. P., Liu, E., Yang, Y., Chen, W., et al. (2011). SQSTM1 mutations in familial and sporadic amyotrophic lateral sclerosis. *Arch. Neurol.* 68, 1440–1446. doi: 10.1001/archneurol.2011.250

Fenoglio, C., Scarpini, E., Serpente, M., and Galimberti, D. (2018). Role of genetics and epigenetics in the pathogenesis of alzheimer's disease and frontotemporal dementia1. *J. Alzheimers Dis.* 62, 913–932. doi: 10.3233/JAD-170702

Ferrari, R., Grassi, M., Salvi, E., Borroni, B., Palluzzi, F., Pepe, D., et al. (2015). A genome-wide screening and SNPs-to-genes approach to identify novel genetic risk factors associated with frontotemporal dementia. *Neurobiol. Aging* 36, 2904.e13–2904.e26. doi: 10.1016/j.neurobiolaging.2015.06.005

Ferrari, R., Hernandez, D. G., Nalls, M. A., Rohrer, J. D., Ramasamy, A., Kwok, J. B. J., et al. (2014). Frontotemporal dementia and its subtypes: a genome-wide association study. *Lancet Neurol.* 13, 686–699. doi: 10.1016/S1474-4422(14)70065-1

Fleming, A., Bourdenx, M., Fujimaki, M., Karabiyik, C., Krause, G. J., Lopez, A., et al. (2022). The different autophagy degradation pathways and neurodegeneration. *Neuron* 110, 935–966. doi: 10.1016/j.neuron.2022.01.017

Gorno-Tempini, M. L., Hillis, A. E., Weintraub, S., Kertesz, A., Mendez, M., Cappa, S. F., et al. (2011). Classification of primary progressive aphasia and its variants. *Neurology* 76, 1006–1014. doi: 10.1212/WNL.0b013e31821103e6

Harding, O., Evans, C. S., Ye, J., Cheung, J., Maniatis, T., and Holzbaur, E. L. F. (2021). ALS- and FTD-associated missense mutations in TBK1 differentially disrupt mitophagy. *Proc. Natl. Acad. Sci. U.S.A* 118:e2025053118. doi: 10.1073/pnas.2025053118

Hutton, M., Lendon, C. L., Rizzu, P., Baker, M., Froelich, S., Houlden, H., et al. (1998). Association of missense and 5′-splice-site mutations in tau with the inherited dementia FTDP-17. *Nature* 393, 702–705. doi: 10.1038/31508

Ishizuka, T., Nakamura, M., Ichiba, M., and Sano, A. (2011). Familial semantic dementia with P301L mutation in the tau gene. *Dement. Geriatr. Cogn. Disord.* 31, 334–340. doi: 10.1159/000328412

Jiang, T., Wang, Y., Wang, X., and Xu, J. (2022). CHCHD2 and CHCHD10: future therapeutic targets in cognitive disorder and motor neuron disorder. *Front. Neurosci.* 16:988265. doi: 10.3389/fnins.2022.988265

Johnson-Pais, T. L., Wisdom, J. H., Weldon, K. S., Cody, J. D., Hansen, M. F., Singer, F. R., et al. (2003). Three novel mutations in SQSTM1 identified in familial Paget's disease of bone. *J. Bone Miner. Res.* 18, 1748–1753. doi: 10.1359/jbmr.2003.18.10.1748

Karasinska, J. M., de Haan, W., Franciosi, S., Ruddle, P., Fan, J., Kruit, , et al. (2013). ABCA1 influences neuroinflammation and neuronal death. *Neurobiol. Dis.* 54, 445–455. doi: 10.1016/j.nbd.2013.01.018

LaMonte, B. H., Wallace, K. E., Holloway, B. A., Shelly, S. S., Ascaño, J., Tokito, M., et al. (2002). Disruption of dynein/dynactin inhibits axonal transport in motor neurons causing late-onset progressive degeneration. *Neuron* 34, 715–727. doi: 10.1016/s0896-6273(02)00696-7

Laurin, N., Brown, J. P., Morissette, J., and Raymond, V. (2002). Recurrent mutation of the gene encoding sequestosome 1 (SQSTM1/p62) in Paget disease of bone. *Am. J. Hum. Genet.* 70, 1582–1588. doi: 10.1086/340731

Le Ber, I., Camuzat, A., Guerreiro, R., Bouya-Ahmed, K., Bras, J., Nicolas, G., et al. (2013). SQSTM1 mutations in French patients with frontotemporal dementia or frontotemporal dementia with amyotrophic lateral sclerosis. *JAMA Neurol.* 70, 1403–1410. doi: 10.1001/jamaneurol.2013.3849

Lee, S., Emond, M. J., Bamshad, M. J., Barnes, K. C., Rieder, M. J., Nickerson, D. A., et al. (2012). Optimal unified approach for rare-variant association testing with application to small-sample case-control whole-exome sequencing studies. *Am. J. Hum. Genet.* 91, 224–237. doi: 10.1016/j.ajhg.2012.06.007

Lewis, J., McGowan, E., Rockwood, J., Melrose, H., Nacharaju, P., Van Slegtenhorst, M., et al. (2000). Neurofibrillary tangles, amyotrophy and progressive motor disturbance in mice expressing mutant (P301l) tau protein. *Nat. Genet.* 25, 402–405. doi: 10.1038/78078

Li, H., and Durbin, R. (2010). Fast and accurate long-read alignment with burrows-wheeler transform. *Bioinformatics* 26, 589–595. doi: 10.1093/bioinformatics/btp698

Li, D., Parks, S. B., Kushner, J. D., Nauman, D., Burgess, D., Ludwigsen, S., et al. (2006). Mutations of presenilin genes in dilated cardiomyopathy and heart failure. *Am. J. Hum. Genet.* 79, 1030–1039. doi: 10.1086/509900

Lücking, C. B., Dürr, A., Bonifati, V., Vaughan, J., De Michele, G., Gasser, T., et al. (2000). Association between early-onset Parkinson's disease and mutations in the parkin gene. *N. Engl. J. Med.* 342, 1560–1567. doi: 10.1056/NEJM200005253422103

Lupton, M. K., Proitsi, P., Lin, K., Hamilton, G., Daniilidou, M., Tsolaki, M., et al. (2014). The role of ABCA1 gene sequence variants on risk of Alzheimer's disease. *J. Alzheimers Dis.* 38, 897–906. doi: 10.3233/JAD-131121

Mann, D. M. A., and Snowden, J. S. (2017). Frontotemporal lobar degeneration: pathogenesis, pathology and pathways to phenotype: frontotemporal lobar degeneration. *Brain Pathol.* 27, 723–736. doi: 10.1111/bpa.12486

Marder, K. S., Tang, M. X., Mejia-Santana, H., Rosado, L., Louis, E. D., Comella, C. L., et al. (2010). Predictors of parkin mutations in early-onset parkinson disease: the consortium on risk for early-onset parkinson disease study. *Arch. Neurol.* 67, 731–738. doi: 10.1001/archneurol.2010.95

Maruyama, H., Morino, H., Ito, H., Izumi, Y., Kato, H., and Watanabe, Y. (2010). Mutations of optineurin in amyotrophic lateral sclerosis. *Nature* 465, 223–226. doi: 10.1038/nature08971

Mol, M. O., van Rooij, J. G. J., Wong, T. H., Melhem, S., Verkerk, A. J. M. H., Kievit, A. J. A., et al. (2021). Underlying genetic variation in familial frontotemporal dementia: sequencing of 198 patients. *Neurobiol. Aging* 97, 148.e9–148.e16. doi: 10.1016/j.neurobiolaging.2020.07.014

Moura, K. C. V., Campos Junior, M., de Rosso, A. L. Z., Nicaretta, D. H., Pereira, J. S., Silva, D. J., et al. (2013). Genetic analysis of park2 and pink1 genes in brazilian patients with early-onset parkinson's disease. *Dis. Markers* 35, 181–185. doi: 10.1155/2013/597158

Naj, A. C., Jun, G., Beecham, G. W., Wang, L.-S., Vardarajan, B. N., Buros, J., et al. (2011). Common variants at MS4A4/MS4A6E, CD2AP, CD33 and EPHA1 are associated with late-onset Alzheimer's disease. *Nat. Genet.* 43, 436–441. doi: 10.1038/ng.801

Pascual, B., Funk, Q., Zanotti-Fregonara, P., Cykowski, M. D., Veronese, M., Rockers, E., et al. (2021). Neuroinflammation is highest in areas of disease progression in semantic dementia. *Brain* 144, 1565–1575. doi: 10.1093/brain/awab057

Pensato, V., Magri, S., Bella, E. D., Tannorella, P., Bersano, E., Sorarù, G., et al. (2020). Sorting rare als genetic variants by targeted re-sequencing panel in italian patients: Optn, vcp, and sqstm1 variants account for 3% of rare genetic forms. *J. Clin. Med.* 9:E412. doi: 10.3390/jcm9020412

Qian, W., and Liu, F. (2014). Regulation of alternative splicing of tau exon 10. *Neurosci. Bull.* 30, 367–377. doi: 10.1007/s12264-013-1411-2

Rendina, A., Drongitis, D., Donizetti, A., Fucci, L., Milan, G., Tripodi, F., et al. (2020). Cd33 and siglecl1 immunoglobulin superfamily involved in dementia. *J. Neuropathol. Exp. Neurol.* 79, 891–901. doi: 10.1093/jnen/nlaa055

Rohrer, J. D., Geser, F., Zhou, J., Gennatas, E. D., Sidhu, M., Trojanowski, J. Q., et al. (2010). TDP-43 subtypes are associated with distinct atrophy patterns in frontotemporal dementia. *Neurology* 75, 2204–2211. doi: 10.1212/WNL.0b013e318202038c

Rohrer, J. D., Guerreiro, R., Vandrovcova, J., Uphill, J., Reiman, D., Beck, J., et al. (2009). The heritability and genetics of frontotemporal lobar degeneration. *Neurology* 73, 1451–1456. doi: 10.1212/WNL.0b013e3181bf997a

Ronchi, D., Riboldi, G., Del Bo, R., Ticozzi, N., Scarlato, M., Galimberti, D., et al. (2015). CHCHD10 mutations in Italian patients with sporadic amyotrophic lateral sclerosis. *Brain* 138:e372. doi: 10.1093/brain/awu384

Rossi, G., Dalprà, L., Crosti, F., Lissoni, S., Sciacca, F. L., Catania, M., et al. (2008). A new function of microtubule-associated protein tau: involvement in chromosome stability. *Cell Cycle* 7, 1788–1794. doi: 10.4161/cc.7.12.6012

Saracino, D., Clot, F., Camuzat, A., Anquetil, V., Hannequin, D., Guyant-Maréchal, L., et al. (2018). Novel VCP mutations expand the mutational spectrum of frontotemporal dementia. *Neurobiol. Aging* 72, 187.e11–187.e14. doi: 10.1016/j.neurobiolaging.2018.06.037

Somavarapu, A. K., and Kepp, K. P. (2016). Loss of stability and hydrophobicity of presenilin 1 mutations causing Alzheimer's disease. *J. Neurochem.* 137, 101–111. doi: 10.1111/jnc.13535

Tacik, P., DeTure, M., Hinkle, K. M., Lin, W. L., Sanchez-Contreras, M., Carlomagno, Y., et al. (2015). A novel tau mutation in exon 12, p.Q336H, causes hereditary pick disease. *J. Neuropathol. Exp. Neurol.* 74, 1042–1052. doi: 10.1097/NEN.0000000000000248

Tedde, A., Nacmias, B., Ciantelli, M., Forleo, P., Cellini, E., Bagnoli, S., et al. (2003). Identification of new presenilin gene mutations in early-onset familial Alzheimer disease. *Arch. Neurol.* 60, 1541–1544. doi: 10.1001/archneur.60.11.1541

Thorvaldsdóttir, H., Robinson, J. T., and Mesirov, J. P. (2013). Integrative genomics viewer (IGV): high-performance genomics data visualization and exploration. *Brief. Bioinform.* 14, 178–192. doi: 10.1093/bib/bbs017

Tohnai, G., Nakamura, R., Sone, J., Nakatochi, M., Yokoi, D., and Katsuno, M. (2018). Frequency and characteristics of the TBK1 gene variants in Japanese patients with sporadic amyotrophic lateral sclerosis. *Neurobiol. Aging* 64, 158.e15–158.e19. doi: 10.1016/j.neurobiolaging.2017.12.005

Tubeuf, H., Charbonnier, C., Soukarieh, O., Blavier, A., Lefebvre, A., Dauchel, H., et al. (2020). Large-scale comparative evaluation of user-friendly tools for predicting variant-induced alterations of splicing regulatory elements. *Hum. Mut.* 41, 1811–1829. doi: 10.1002/humu.24091

Ulugut, H., Dijkstra, A. A., Scarioni, M., Netherlands Brain BankBarkhof, F., Scheltens, P., et al. (2021). Right temporal variant frontotemporal dementia is pathologically heterogeneous: a case-series and a systematic review. *Acta Neuropathol. Commun.* 9:131. doi: 10.1186/s40478-021-01229-z

Ulugut Erkoyun, H., Groot, C., Heilbron, R., Nelissen, A., van Rossum, J., Jutten, R., et al. (2020). A clinical-radiological framework of the right temporal variant of frontotemporal dementia. *Brain* 143, 2831–2843. doi: 10.1093/brain/awaa225

Ulugut Erkoyun, H., van der Lee, S. J., Nijmeijer, B., van Spaendonk, R., Nelissen, A., Scarioni, , et al. (2021). The right temporal variant of frontotemporal dementia is not genetically sporadic: a case series. *J. Alzheimers Dis.* 79, 1195–1201. doi: 10.3233/JAD-201191

van der Zee, J., Van Langenhove, T., Kovacs, G. G., Dillen, L., Deschamps, W., Engelborghs, , et al. (2014). Rare mutations in SQSTM1 modify susceptibility to frontotemporal lobar degeneration. *Acta Neuropathol.* 128, 397–410. doi: 10.1007/s00401-014-1298-7

Van Mossevelde, S., Engelborghs, S., van der Zee, J., and Van Broeckhoven, C. (2018). Genotype–phenotype links in frontotemporal lobar degeneration. *Nat. Rev. Neurol.* 14, 363–378. doi: 10.1038/s41582-018-0009-8

Villa, C., Rossi, G., Bizzozero, I., Prioni, S., Boiocchi, C., Agosta, F., et al. (2022). MAPT Q336H mutation: Intrafamilial phenotypic heterogeneity in a new Italian family. *Eur. J. Neurol.* 29, 1529–1533. doi: 10.1111/ene.15250

Watts, G. D. J., Wymer, J., Kovach, M. J., Mehta, S. G., Mumm, S., Darvish, D., et al. (2004). Inclusion body myopathy associated with Paget disease of bone and frontotemporal dementia is caused by mutant valosin-containing protein. *Nat. Genet.* 36, 377–381. doi: 10.1038/ng1332

Younes, K., Borghesani, V., Montembeault, M., Spina, S., Mandelli, M. L., Welch, A. E., et al. (2022). Right temporal lobe and socioemotional semantics: semantic behavioural variant frontotemporal dementia. *Brain* 145, 4080–4096. doi: 10.1093/brain/awac217

Zhang, D. M., Levitan, D., Yu, G., Nishimura, M., Chen, F., Tandon, A., et al. (2000). Mutation of the conserved N-terminal cysteine (Cys92) of human presenilin 1 causes increased a beta42 secretion in mammalian cells but impaired notch/lin-12 signalling in C. elegans. *Neuroreport* 11, 3227–3230. doi: 10.1097/00001756-200009280-00035

Zhang, M., Xi, Z., Zinman, L., Bruni, A. C., Maletta, R. G., Curcio, S. A., et al. (2015). Mutation analysis of CHCHD10 in different neurodegenerative diseases. *Brain* 138:e380. doi: 10.1093/brain/awv082

Zhu, M., Cortese, G. P., and Waites, C. L. (2018). Parkinson's disease-linked Parkin mutations impair glutamatergic signaling in hippocampal neurons. *BMC Biol.* 16:100. doi: 10.1186/s12915-018-0567-7

Zimmermann, M., Wilke, C., Schulte, C., Hoffmann, J., Klopfer, J., Reimold, M., et al. (2018). Biallelic Parkin (Park2) mutations can cause a bvFTD phenotype without clinically relevant parkinsonism. *Parkinsonism Relat. Disord.* 55, 145–147. doi: 10.1016/j.parkreldis.2018.06.006

frontiers | Frontiers in Aging Neuroscience

TYPE Brief Research Report
PUBLISHED 25 January 2023
DOI 10.3389/fnagi.2023.1087823

OPEN ACCESS

EDITED BY
Shunsuke Koga,
Mayo Clinic Florida,
United States

REVIEWED BY
Che Norma Mat Taib,
Universiti Putra Malaysia,
Malaysia
David J. Koss,
Newcastle University,
United Kingdom
Jifeng Guo,
Central South University,
China

*CORRESPONDENCE
Xian Zhang
✉ xianzhang@xmu.edu.cn

†These authors have contributed equally to this work and share first authorship

SPECIALTY SECTION
This article was submitted to Parkinson's Disease and Aging-related Movement Disorders, a section of the journal Frontiers in Aging Neuroscience

RECEIVED 02 November 2022
ACCEPTED 05 January 2023
PUBLISHED 25 January 2023

CITATION
Wang Z, Yang D, Jiang Y, Wang Y, Niu M, Wang C, Luo H, Xu H, Li J, Zhang Y-w and Zhang X (2023) Loss of RAB39B does not alter MPTP-induced Parkinson's disease-like phenotypes in mice.
Front. Aging Neurosci. 15:1087823.
doi: 10.3389/fnagi.2023.1087823

Loss of RAB39B does not alter MPTP-induced Parkinson's disease-like phenotypes in mice

Zijie Wang[1,2†], Dingting Yang[1,2†], Yiru Jiang[1], Yong Wang[1], Mengxi Niu[1], Chong Wang[3], Hong Luo[1], Huaxi Xu[1], Jingwen Li[2], Yun-wu Zhang[1] and Xian Zhang[1*]

[1]Fujian Provincial Key Laboratory of Neurodegenerative Disease and Aging Research, School of Medicine, Center for Brain Sciences, The First Affiliated Hospital of Xiamen University, Institute of Neuroscience, Xiamen University, Xiamen, China, [2]Department of Neurosurgery, Xiang'an Hospital of Xiamen University, Xiamen, China, [3]Department of Basic Medical Sciences, School of Medicine, Xiamen University, Xiamen, China

Parkinson's disease (PD) is a common neurodegenerative movement disorder with undetermined etiology. A major pathological hallmark of PD is the progressive degeneration of dopaminergic neurons in the substantia nigra. Loss-of-function mutations in the *RAB39B* gene, which encodes a neuronal-specific small GTPase RAB39B, have been associated with X-linked intellectual disability and pathologically confirmed early-onset PD in multiple families. However, the role of RAB39B in PD pathogenesis remains elusive. In this study, we treated *Rab39b* knock-out (KO) mice with MPTP to explore whether RAB39B deficiency could alter MPTP-induced behavioral impairments and dopaminergic neuron degeneration. Surprisingly, we found that MPTP treatment impaired motor activity and led to loss of tyrosine hydroxylase-positive dopaminergic neurons and gliosis in both WT and *Rab39b* KO mice. However, RAB39B deficiency did not alter MPTP-induced impairments. These results suggest that RAB39B deficiency does not contribute to PD-like phenotypes through compromising dopaminergic neurons in mice; and its role in PD requires further scrutiny.

KEYWORDS

MPTP, RAB39B, Pakinson's disease, mouse behavior, dopaminergic neurons

1. Introduction

Parkinson's disease (PD) is the second most common central neurodegenerative disease after Alzheimer's disease (von Campenhausen et al., 2005; Tysnes and Storstein, 2017). PD affects about 1–2% of the population over the age of 60 and about 5% of the population over the age of 85 (Van Den Eeden et al., 2003; de Lau and Breteler, 2006; Masato et al., 2019). With an increase in population aging worldwide, PD has been causing serious social and economic burden. The clinical diagnosis of PD is based on the motor symptoms, including bradykinesia, muscular rigidity, rest tremor, and postural and gait impairment (Gibb and Lees, 1988; Gelb et al., 1999). The pathologic hallmarks of PD are progressive loss of dopaminergic neurons in the substantia nigra pars compacta (SNpc) and presence of intracellular inclusions of aggregated α-synuclein called Lewy bodies (LBs). In addition, neuroinflammation plays an important role in the progression of PD. Activated microglia and release of toxins may be involved in the process of neurodegeneration (Hirsch and Hunot, 2000). The environmental and genetic causes have long been considered important risk factors for PD, but the exact etiology of PD remains unknown.

The *RAB39B* gene consists of two exons spanning 3,764 bp of human genomic DNA on the X chromosome and encodes a neuronal-specific protein named RAB39B which is localized in the Golgi compartment (Stankovic et al., 1997; Cheng et al., 2002; Giannandrea et al., 2010). As a small GTPase, RAB39B primarily plays a role in intracellular vesicle trafficking (Chavrier et al., 1990; Cheng et al., 2002). Mutations in *RAB39B* gene are associated with a variety of neurological disorders including X-linked intellectual disability (XLID), autism, epilepsy, macrocephaly and early-onset Parkinson's disease (EOPD) (Giannandrea et al., 2010; Wilson et al., 2014; Mata et al., 2015; Shi et al., 2016; Woodbury-Smith et al., 2017; Gao et al., 2020).

A loss-of-function mutation in *RAB39B* was originally found in pathologically confirmed EOPD who have extensive dopaminergic neuron loss in substantia nigra and widespread Lewy body pathology (Wilson et al., 2014). Subsequently, additional *RAB39B* mutations associated with EOPD have been reported. Most of these mutations result in complete loss of RAB39B (Lesage et al., 2015; Güldner et al., 2016; Shi et al., 2016; Ciammola et al., 2017; Woodbury-Smith et al., 2017), and some of them lead to subcellular mislocalization of RAB39B (c.574G > A; p.G192R) (Mata et al., 2015) and dysregulated protein homeostasis (c.503C > A; p.T168K) (Wilson et al., 2014; Gao et al., 2020). However, *RAB39B* mutations were not detected in several large-scale cohort screenings of familial PD, indicating that *RAB39B* mutations might be rare in PD (Yuan et al., 2015; Hodges et al., 2016; Löchte et al., 2016; Lin et al., 2017). Some studies have demonstrated that RAB39B is involved in the regulating the homeostasis, oligomerization and aggregation of α-synuclein *in vitro* (Wilson et al., 2014; Gonçalves et al., 2016), but the underlying mechanism is largely unclear.

In our previous study, we found that *Rab39b* KO mice predominately exhibited impairments of learning and memory and synaptic plasticity, whereas their motor behavior impairment was not obvious (Niu et al., 2020). Since PD is considered to be the result of a complex interaction of multiple risk factors, including genetic factors, environmental factors, age, sex, and other factors (Kalia and Lang, 2015), it is possible that the effect of RAB39B deficiency on PD requires the involvement of other factors. In this study, we induced PD-like phenotypes including motor deficits and dopaminergic neuron degeneration in wild type and *Rab39b* KO mice by MPTP, and explored whether RAB39B deficiency could alter MPTP-induced impairments.

2. Methods

2.1. Animals

C57BL/6J *Rab39b* knock-out (KO) mice were generated and genotyped as previously described (Niu et al., 2020). C57BL/6J wild type (WT) mice were provided by Xiamen University Laboratory Animal Center. Mice were kept at 20–25°C with a 12 h light/dark cycle and with free access to food and water. Male *Rab39b* KO or wild-type (WT) littermates at 9–15 weeks of age were subjected to the experiments. All procedures and protocols involving animals were performed in accordance with the guidelines of the National Institutes of Health Guide for the Care and Use of Laboratory Animals, and were approved by the Animal Ethics Committee of Xiamen University (XMULAC20170207).

2.2. MPTP administration

Rab39b KO mice and their littermate wild-type (WT) control mice were acclimated for 7 days and were subjected to a rotarod training at 10 rpm for 10 min once a day for 5 days for optimum performance (Figure 1A). Mice were then randomly divided into WT control group (saline-WT), *Rab39b* KO control group (saline-KO), MPTP treated WT group (MPTP-WT) and MPTP treated *Rab39b* KO group (MPTP-KO). Mice in each group were intraperitoneally injected with saline once 1 day before the first injection of MPTP. MPTP-WT and MPTP-KO groups were intraperitoneally injected with MPTP (30 mg/kg in 150 μl saline, once a day; MedChemExpress) for 7 consecutive days. Saline-WT and saline-KO groups were given 150 μl saline instead (Figure 1A).

2.3. Motor behavioral tests

Mice were tested for motor behaviors after the last injection of MPTP (Figure 1A), and a 30-min adaptation to the experimental environment was provided every day before the test. The experimental environment was soundproof with suitable light intensity and temperature.

2.3.1. Pole test

Mice were placed head-down on top of a vertical wooden pole (55 cm in height and 1 cm in diameter) and the time required to reach the bottom of the pole was measured. The test was repeated three times for each mouse, and the average descending time was calculated for comparison. Two-way ANOVA followed by Tukey's *post hoc* test was used for the test.

2.3.2. Hanging wire test

A wire with a diameter of 1.5 mm was placed horizontally 40 cm above a thick layer of cotton bedding. Mice were suspended by placing their fore paws on the wire for 30 s and were graded according to the status of their hind paws grasping the wire: both hind paws grasping the wire was scored 3, only one hand paw grasping the wire was scored 2, non-hind paws grasping the wire was scored 1, and mouse falling off the wire was scored 0. Two-way ANOVA followed by Tukey's *post hoc* test was used for the test.

2.3.3. Rotarod test

The rotarod test was performed as described previously (Niu et al., 2020). Before MPTP injection, mice were trained on a rotating rod at a speed of 10 rpm for 10 min once a day for 5 consecutive days. After the last injection of MPTP, mice were tested on a rotating rod at a constant speed of 10 rpm. Tests were repeated three times at an interval of at least 30 min. The latency to fall off the rotating rod was recorded, and the average of the latencies were calculated and compared. Two-way ANOVA followed by Tukey's *post hoc* test was used for the test.

2.3.4. Gait analysis

Gait dynamics of mice were captured and analyzed using the DigiGait gait analysis system (Mouse Specifics), as previously described (Quarta et al., 2017; Liu et al., 2019; Wozniak et al., 2019). Mice were placed inside an acrylic compartment (5 cm (W) × 25 cm (L)) with a transparent treadmill belt at the bottom. Each mouse was tested individually on the treadmill; and each paw's movement was measured. Prior to video recording, mice were allowed to acclimatize for 5 min in

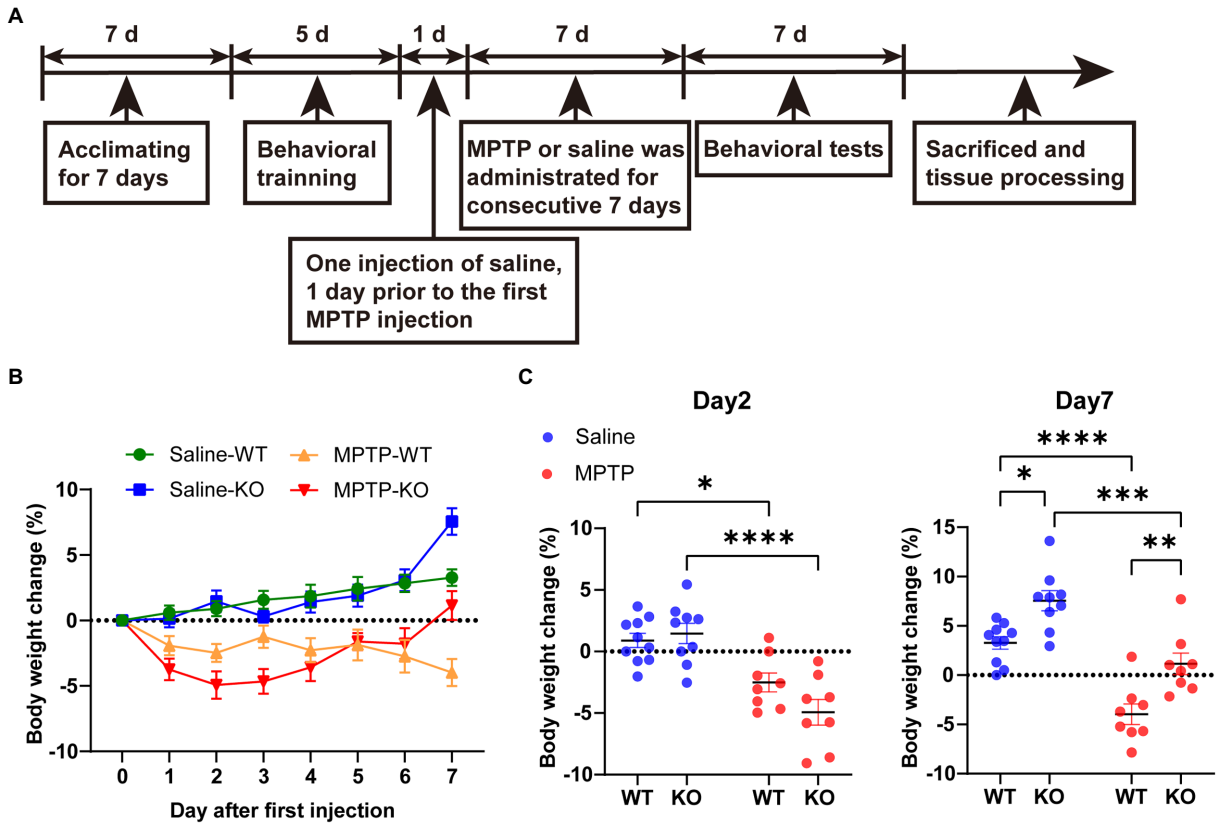

FIGURE 1
MPTP treatment. **(A)** A schematic diagram of MPTP treatment in *Rab39b* KO and WT mice. **(B)** Percentage of body weight change in MPTP-treated *Rab39b* KO and WT mice or respective saline-treated control mice at different time points after first MPTP injection. **(C)** Percentage of body weight change in MPTP-treated *Rab39b* KO and WT mice or respective saline-treated control mice on days 2 and 7 after first MPTP injection, respectively. Data represent mean±SEM, n=10 for Saline-WT, n=9 for Saline-KO, and n=8 for both MPTP-WT and MPTP-KO. *p<0.05, **p<0.01, ***p<0.001, ****p<0.0001, two-way ANOVA followed by Tukey's *post hoc* test.

the compartment and then run at 10 cm/s for another 5 min to adapt. When mice were stably walking, the belt speed was adjusted and maintained at 25 cm/s. Videos of at least 5 s of uninterrupted mouse running were recorded to provide an adequate number of sequential strides. Once the 5 s videos were obtained, 2.5 s of video length was post-processed and analyzed by the software provided with the DigiGait system. Each video was individually adjusted with a binary threshold adjustment tool to remove any noise and to establish well defined paw areas. Data were manually adjusted to remove any artifacts in the paw area-plots the system. The various measurements were defined or calculated as described below: (1) Stride duration = the stance duration when the paw of a limb was in contact with the treadmill belt; (2) Stride length = speed/stride frequency; and (3) Stride frequency = the number of gait signals over time. Two-way ANOVA followed by Tukey's *post hoc* test was used for the test.

2.4. Immunofluorescence staining

Mice were anesthetized with 1% sodium pentobarbital in saline and perfused with 0.01 M PBS. Whole brain was fixed in 4% paraformaldehyde at 4°C for 24 h, and then dehydrated in 30% sucrose. Tissues were embedded in OCT and 35 μm brain sections were collected by a cryostat microtome (Leica). Mouse brain sections were permeabilized and blocked in buffer composed of 0.2% Triton X-100 and 5% goat serum in PBS for 1 h at room temperature, and then incubated with anti-tyrosine hydroxylase primary antibody (Millipore, ab152, 1: 800), anti-α-synuclein primary antibody (ABclonal, A7215, 1:100), anti-GFAP primary antibody (Proteintech, 16,825-1-AP, 1:200) and anti-IBA1 primary antibody (Wako, 019–19,741, 1:200) overnight at 4°C. After incubating with appropriate fluorescence-conjugated secondary antibodies (Thermo Fisher Scientific, A11008, 1:400) for 1 h at room temperature, z-stack images were obtained using an A1R (Nikon) confocal microscope or an FV1000MPE-B confocal laser scanning biological microscope (OLYMPUS). The number of TH-positive cells in the fluorescence image was counted by particles analysis using Image J. The numbers of α-synuclein-positive cells were counted manually. The mean positive cell number of multiple brain slice images from each mouse was quantified and used for comparison.

2.5. Immunoblot analysis

Mouse brains were sliced in pre-cooled brain molds (RWD) and then the substantia nigra was isolated on ice under an optical microscope. Substantia nigra tissues were homogenized and lysed in RIPA lysis buffer (150 mM NaCl, 25 mM Tris–HCl, pH 7.5, 0.1% sodium dodecyl sulfate, and 1% Nonidet P-40) supplemented with the Complete Protease and Phosphatase Inhibitor Cocktail (MedChemExpress). Protein concentration was determined using the Pierce BCA Protein

Assay (Thermo Fisher Scientific). Equal amounts of protein lysates were separated by SDS-polyacrylamide gel electrophoresis and transferred to polyvinylidene fluoride membrane. Membrane was blocked with 5% skim milk at room temperature for 1 h, and incubated first with appropriate primary antibody diluent and then with horseradish peroxidase (HRP)-conjugated secondary antibodies. The membranes were incubated with an appropriate amount of ECL (Bio-Rad) solution, which was added dropwise and then imaged with a chemiluminescence imaging system (Azure 300). Protein band intensity was quantified using ImageJ.

2.6. Statistical analysis

Statistical analysis was performed using the Prism 8 software (GraphPad). Data represent mean ± standard error of means (SEM). $p < 0.05$ was considered statistically significant.

3. Results

3.1. MPTP treatment and mouse body weight analysis

Our previous study found that 2-month-old *Rab39b* KO mice showed impaired motor skill learning and decreased midbrain dopamine levels (Niu et al., 2020). To further determine the role of *Rab39b* deficiency in the pathophysiology of PD, we treated *Rab39b* KO and WT control mice with MPTP for 7 consecutive days (Figure 1A). The body weights of mice were recorded right before each injection (Figure 1B). The body weight change in saline-treated WT mice gradually increased during the 7 days. The trend of the body weight change in saline-treated *Rab39b* KO mice was similar to that of saline-treated WT mice (Figure 1B). But on day 7, the body weight gain was much more in saline-treated *Rab39b* KO mice than in saline-treated WT mice (Figure 1C). On the other hand, the body weight change in WT and *Rab39b* KO mice treated with MPTP decreased significantly after the first injection, when compared to respective saline-treated control group. The body weight loss in WT mice kept increasing throughout the MPTP treatment. However, after the first three injections of MPTP, *Rab39b* KO mice loss more weight than WT mice with no significant difference, then the weight of *Rab39b* KO mice began to recover, and after the last injection the weight of *Rab39b* KO mice even exceeded that before treatment. In addition, the weight gain in *Rab39b* KO mice was also higher than that of WT group after the seventh injection of saline (Figures 1B,C).

3.2. Loss of *Rab39b* does not alter MPTP-induced motor behavior impairment

After the induction of MPTP, the mice were tested for motor behaviors. In the pole test, the latency to descend from the top to the bottom in MPTP-treated WT and *Rab39b* KO mice was significantly longer than that in respective saline-treated control group. However, there was no significant difference between *Rab39b* KO and WT mice in either MPTP or saline treatment group (Figure 2A). Similarly, in the hanging wire test, the scores in MPTP-treated WT and *Rab39b* KO mice were significantly lower than those in corresponding saline-treated mice, but there was no significant difference between *Rab39b* KO and WT mice in either MPTP or saline treatment group (Figure 2B). In the rotarod test, although MPTP induction did not significantly change the motor ability of *Rab39b* KO mice, the average latency to fall in *Rab39b* KO mice was significantly reduced when compared to corresponding WT mice in both MPTP and saline treatment groups (Figure 2C). In addition, mice were subjected to gait analysis tests (Figure 2D). Consistently, MPTP-treated WT and *Rab39b* KO mice walked with significantly shorter stride time and stride length, as well as higher stride frequency, compared to the respective saline-treated control group. Furthermore, compared to the corresponding WT mice in MPTP and saline treatment groups, both *Rab39b* KO mice showed longer stride time and stride length, as well as lower stride frequency (Figures 2E–G). These results suggest that MPTP treatment causes motor activity impairment in mice, but loss of *Rab39b* does not alter MPTP-induced motor behavior impairment.

3.3. *Rab39b* deficiency does not alter MPTP-induced pathology of PD in SNpc

Dopaminergic neurons in SNpc are subjected to progressive loss in PD. Therefore, we performed immunofluorescence staining to quantitatively analyze the number of tyrosine hydroxylase (TH)-positive dopaminergic neurons in SNpc of mice. The number of TH-positive cells in SNpc of MPTP-treated WT and *Rab39b* KO mice was significantly lower than that of respective saline-treated mice, the number of TH-positive cells in SNpc was not significantly changed between WT and *Rab39b* KO mice in either MPTP or saline treatment group (Figures 3A,B). Meanwhile, western blotting of the substantia nigra showed significant decrease of TH protein levels in MPTP-treated WT and *Rab39b* KO mice compared to respective saline-treated mice, and the TH protein level was not significantly changed between WT and *Rab39b* KO mice in either MPTP or saline treatment group (Figures 3C,D). In addition, we quantified α-synuclein-positive neurons in the substantia nigra region by immunofluorescence. In the saline control group, most of the neuronal bodies lacked detectable α-synuclein staining, whereas fluorescence was mainly manifested in the neuronal fibers. Compared to the respective saline control group, the number of α-synuclein-positive cells in substantia nigra of MPTP-treated WT and *Rab39b* KO mice was significantly elevated (Figures 3E,F). However, *Rab39b* KO mice showed no change compared to WT levels under the MPTP-induced pathological context. These results suggest that MPTP induction decreases the number of dopaminergic neurons and increases α-synuclein reactivity of neurons in substantia nigra of mice, but deletion of RAB39B does not further affect these pathologies of PD induced by MPTP.

3.4. Loss of *Rab39b* does not alter MPTP-induced gliosis

We then studied the role of *Rab39b* deficiency in MPTP-induced gliosis in mice. Immunofluorescence staining and quantitative analysis demonstrated that the number of GFAP-positive astrocytes and IBA1-positive microglia was significantly increased in SNpc of MPTP-treated WT and *Rab39b* KO mice when compared to respective saline-treated mice, but there was no significant difference between WT and *Rab39b* KO mice in either MPTP or saline treatment group (Figures 4A–C). These results suggest that MPTP toxicity causes gliosis of astrocytes and

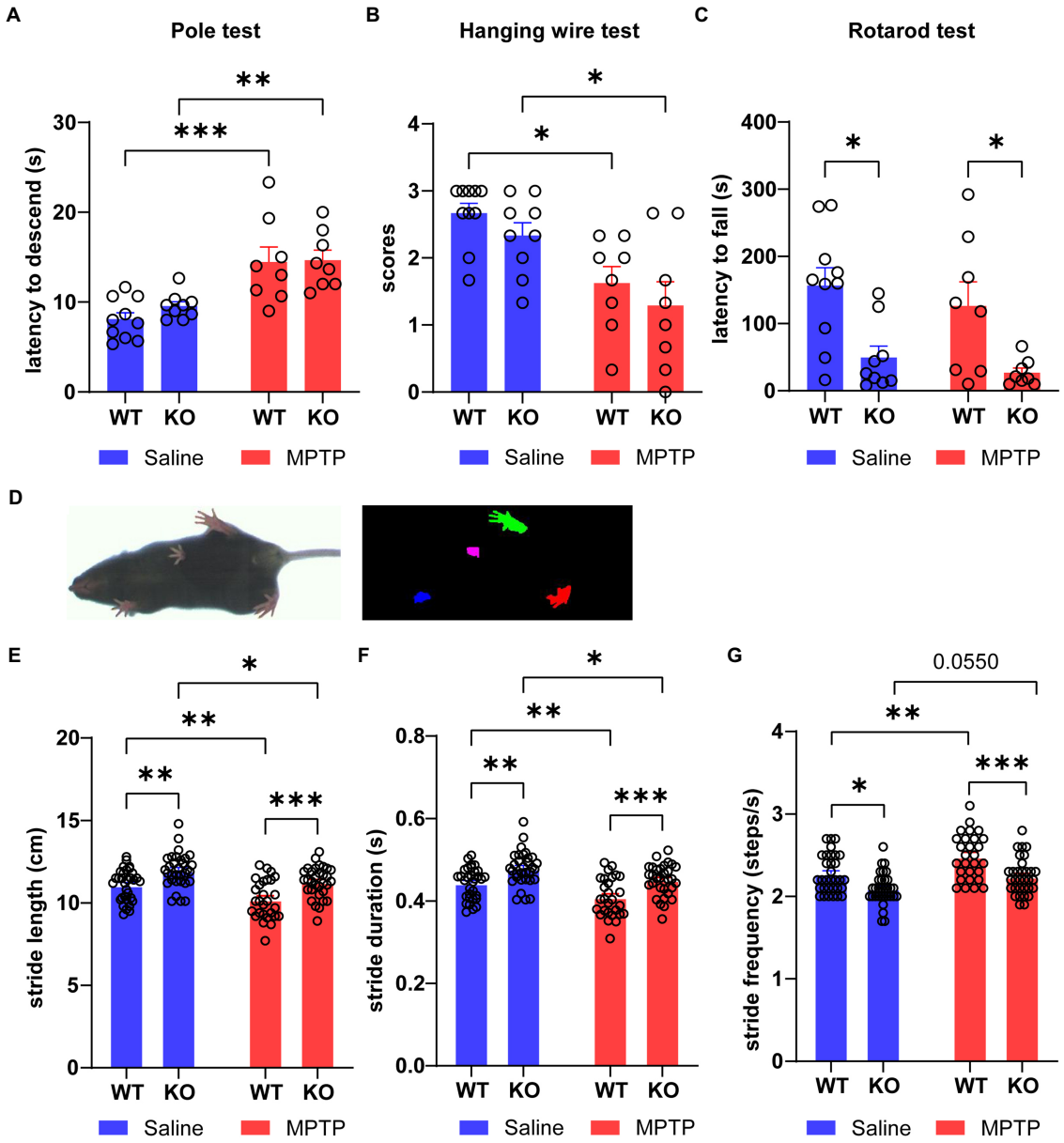

FIGURE 2
Loss of *Rab39b* does not alter motor behavior impairment in MPTP-induced mice. **(A)** Latency of descending from the top to the bottom in MPTP-treated *Rab39b* KO and WT mice or respective saline-treated control mice was recorded in pole test for comparison. n=10 for Saline-WT, n=9 for Saline-KO, and n=8 for both MPTP-WT and MPTP-KO. **(B)** Hanging wire test was performed in MPTP-treated *Rab39b* KO and WT mice or respective saline-treated control mice and the scores were calculated for comparison. n=10 for Saline-WT, n=9 for Saline-KO, and n=8 for both MPTP-WT and MPTP-KO. **(C)** MPTP-treated *Rab39b* KO and WT mice or respective saline-treated control mice were subjected to the rotarod test and the average latency to fall was calculated for comparison. n=10 for Saline-WT, n=9 for Saline-KO, and n=8 for both MPTP-WT and MPTP-KO. **(D)** Representative image of a mouse subjected to video recording of gait analysis (left) and digital image of the ventral surface of the gait footprints during the analysis (right). **(E-G)** The stride length, stride duration, and stride frequency in MPTP-treated *Rab39b* KO and WT mice or respective saline-treated control mice. n=32 paws from 8 mice for Saline-WT, Saline-KO and MPTP-KO, and n=28 paws from 7 mice for MPTP-WT. Data represent mean±SEM, *p<0.05, **p<0.01, ***p<0.001, two-way ANOVA followed by Tukey's *post hoc* test.

microglia, but loss of *Rab39b* does not affect gliosis, nor does it alter glial activation in response to MPTP toxicity.

4. Discussion

Recent studies have reported an increasing number of *RAB39B* mutations associated with early-onset PD as well as Lewy body diseases (LBDs) (Wilson et al., 2014; Lesage et al., 2015; Mata et al., 2015; Güldner et al., 2016; Shi et al., 2016; Ciammola et al., 2017). Most of these mutations cause the loss of RAB39B protein function. But the molecular mechanism underlying PD pathogenesis caused by *RAB39B* mutations remains to be clarified. Previous studies have shown that loss of RAB39B compromises motor learning but does not affect mobility in 2-month-old mice (Niu et al., 2020; Zhang et al., 2020). Herein, we constructed a PD model induced by intraperitoneal injection of

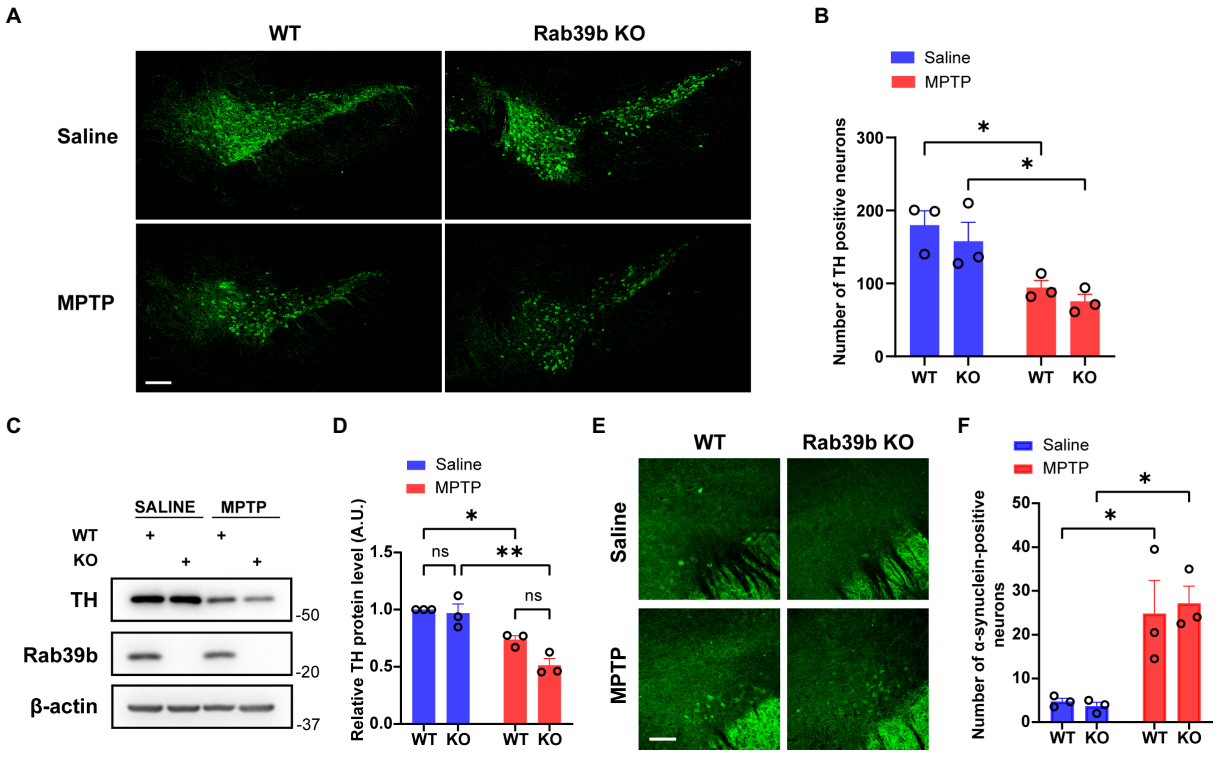

FIGURE 3
Loss of *Rab39b* does not alter MPTP-induced pathology of PD in SNpc. **(A)** Representative images of TH immunostaining of SNpc in MPTP-treated *Rab39b* KO and WT mice or respective saline-treated control mice. Scale bar, 200μm. **(B)** Quantitative analysis of TH positive cell numbers in **(A)**. *n*=3 mice per group, average of 2–4 brain slices from each mouse. **(C)** Western blotting of proteins in substantia nigra tissue lysates of mice. **(D)** Protein levels were quantified and normalized to those of β-actin for comparison. *n*=3 mice per group. **(E)** Representative images of α-synuclein immunostaining of substantia nigra in MPTP-treated *Rab39b* KO and WT mice or respective saline-treated control mice. Scale bar, 80μm. **(F)** Quantitative analysis of α-synuclein positive cell numbers in **(E)**. *n*=3 mice per group, average of 2–4 brain slices from each mouse. Data represent mean±SEM, ns: not significant, **p*<0.05, ***p*<0.01, two-way ANOVA followed by Tukey's *post hoc* test.

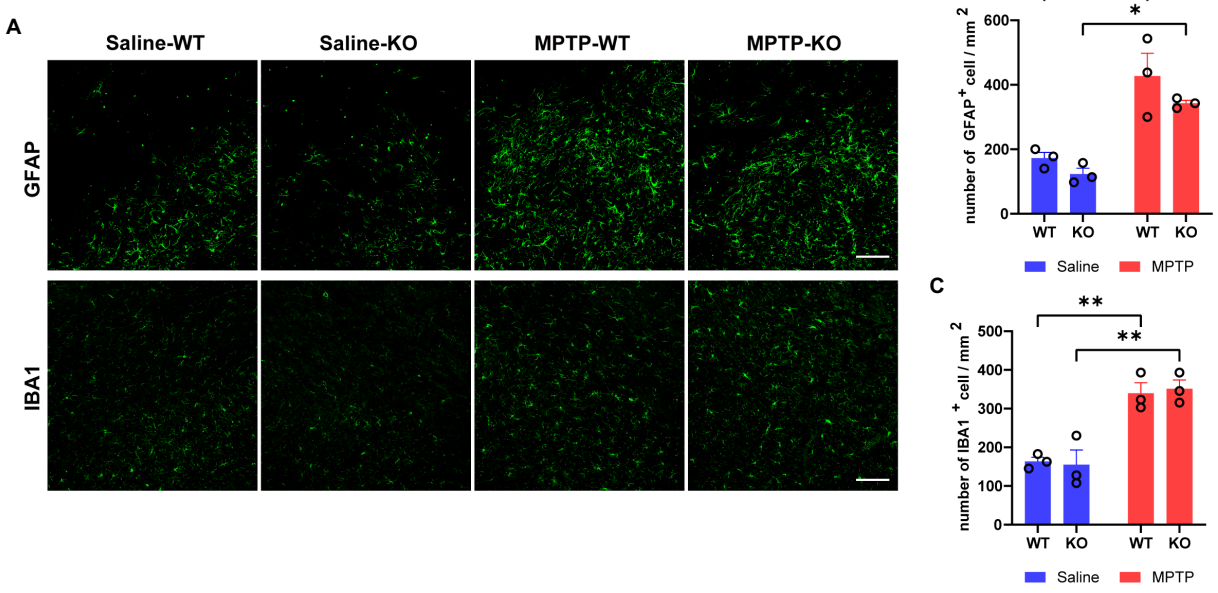

FIGURE 4
Loss of *Rab39b* does not alter reactive gliosis in SNpc of MPTP-induced mice. **(A)** Representative images of GFAP and IBA1 immunostaining of SNpc in MPTP-treated *Rab39b* KO and WT mice or respective saline-treated control mice. Scale bars, 100μm. **(B)** Quantitative analysis of GFAP-positive cells in **(A)**. **(C)** Quantitative analysis of IBA1-positive cells in **(A)**. *n*=3 mice per group, average of 2–3 brain slices from each mouse. Data represent mean±SEM, **p*<0.05, ***p*<0.01, two-way ANOVA followed by Tukey's *post hoc* test.

MPTP in *Rab39b* KO mice to explore the possible consequences of RAB39B deficiency in PD pathology. *RAB39B* is an X-linked gene and EOPD associated with RAB39B mutations are more common in men than women, so we focused on male mice in this study.

MPTP treatment is a classic and widely used method to generate animal model of PD (Jackson-Lewis and Przedborski, 2007). MPTP can pass through the blood–brain barrier (BBB) and is metabolized by astrocytic monoamine oxidase-B (MAO-B) to form the active toxicant 1-methyl-4-phenylpyridinium (MPP^+), which accumulates in the mitochondrial matrix and inhibits complex I of the respiratory chain, resulting in degeneration and death of nigra-striatal dopaminergic neurons (Heikkila et al., 1984; Di Monte et al., 1991, 1992). During the MPTP treatment, we found a significant and persistent decrease in the body weight in MPTP-treated mice compared to respective control mice after the first injection. Interestingly, although the weight loss of *Rab39b* KO mice was more significant than that of WT mice after the first three injections of MPTP, the weight of *Rab39b* KO mice began to recover and returned to the level before MPTP treatment after the last injection. In previous studies, *Rab39b* KO mice showed some weight loss compared to littermate control WT at 2 months of age or throughout the early stage of growth (P7-P90), regardless of the mouse strains (Niu et al., 2020; Mignogna et al., 2021). The loss of body weight in *Rab39b* KO mice could be attributed to a significant reduction in the volume of abdominal adipose tissue, whereas there were no significant differences in the weight of organs, food and water intake, body temperature, and glucose consumption in each brain region between genotypes (Mignogna et al., 2021). Lack of activity caused by MPTP treatment translate into reduced food and water intake and a possible slight weight loss (Jackson-Lewis and Przedborski, 2007). At the beginning of intraperitoneal injection of MPTP (the first three injections), *Rab39b* KO mice with less abdominal adipose tissue may be more sensitive to drug reactivity. Given that saline-injected *Rab39b* KO mice on the seventh day also gained more weight than saline-injected WT mice, this abnormal weight gain may be due to that *Rab39b* KO mice are still in a growth and development stage with unknown reason. Future investigation on the water and food intake and metabolic indexes of mice during injection period may help solve this puzzle.

The results of pole test and hanging wire test showed that MPTP-treated mice had deficits in motor abilities, but loss of RAB39B did not exacerbate these impairments. In the rotarod test, the latency to fall from the rotating rod in *Rab39b* KO mice was significantly lower than that in corresponding WT mice in both MPTP and saline treatment groups, but there was no difference between MPTP-and saline-treated *Rab39b* KO mice. These results are consistent with previous studies suggesting that loss of RAB39B impairs motor ability learning (Niu et al., 2020; Zhang et al., 2020), and further indicate that loss of RAB39B does not alter motor deficits upon MPTP toxicity. In gait analysis test, we found that both saline-and MPTP-treated Rab39B KO mice exhibited increased stride length and duration and decreased stride frequency when compared to respective WT controls. While upon MPTP treatment, both WT and *Rab39b* KO mice had decreased stride length and duration and increased stride frequency; and this is consistent with the phenotype of MPTP-induced mice reported by Liu et al. (2019). These findings further support that RAB39B deficiency does not affect MPTP-induced motor deficits in mice. Moreover, our results revealed that RAB39B deficiency had no effect on dopaminergic neuronal loss and neuroinflammatory response in SNpc of MPTP-induced mice. Together, in the current study, we demonstrate that RAB39B deficiency does not contribute to PD through compromising dopaminergic neurons in MPTP-induced PD mouse model.

The α-synuclein protein is highly expressed in brain and is a primary component of Lewy bodies in PD (Goedert et al., 2017; Khan and Khan, 2022). Missense mutations, as well as multiplications of the gene encoding α-synuclein (*SNCA*) are directly related to familial PD (Menšíková et al., 2022). RAB39B was found to be involved in the regulation of α-synuclein homeostasis in some previous studies (Wilson et al., 2014; Gonçalves et al., 2016). Wilson et al. reported that the loss of RAB39B in primary hippocampal neurons and P19 neuroblastoma reduced steady-state levels of α-synuclein (Wilson et al., 2014). Subsequently, Gonçalves et al. found that the RAB39B silencing promoted the oligomerization and aggregation of α-synuclein independent of the levels of α-synuclein in human H4 neuroglial cells (Gonçalves et al., 2016). Herein, we found that MPTP treatment significantly increased the number of α-synuclein-positive cells in substantia nigra of both WT and *Rab39b* KO mice; and these results are consistent with previous studies showing an up-regulation of α-synuclein in dopaminergic neurons in substantia nigra after injection of MPTP in both mice and non-human primates (Vila et al., 2000; Purisai et al., 2005). However, loss of RAB39B did not further affect the number of a-synuclein-positive cells exposed to MPTP toxicity. Future studies to explore whether RAB39B deficiency contributes to α-synuclein pathology *in vivo*, using Lewy body pathological models such as the A53T transgenic mice (Koprich et al., 2017) may help determine the mechanism underlying the pathogenesis of PD caused by *RAB39B* mutations.

Data availability statement

The original contributions presented in the study are included in the article/supplementary material, further inquiries can be directed to the corresponding author.

Ethics statement

The animal study was reviewed and approved by Animal Ethics Committee of Xiamen University.

Author contributions

ZW, Y-wZ, and XZ designed the research and wrote the manuscript. ZW and DY performed most molecular and animal experiments. YJ, YW, and MN helped with animal experiments. CW, HL, HX, and JL made intellectual contributions. All authors reviewed the manuscript.

Funding

This work was supported by grants from National Natural Science Foundation of China (81771377, U21A20361 and 82130039 to Y-wZ).

Conflict of interest

The authors declare that the research was conducted in the absence of any commercial or financial relationships that could be construed as a potential conflict of interest.

Publisher's note

References

Chavrier, P., Parton, R. G., Hauri, H. P., Simons, K., and Zerial, M. (1990). Localization of low molecular weight GTP binding proteins to exocytic and endocytic compartments. *Cells* 62, 317–329. doi: 10.1016/0092-8674(90)90369-P

Cheng, H., Ma, Y., Ni, X., Jiang, M., Guo, L., Ying, K., et al. (2002). Isolation and characterization of a human novel RAB (RAB39B) gene. *Cytogenet. Genome Res.* 97, 72–75. doi: 10.1159/000064047

Ciammola, A., Carrera, P., Di Fonzo, A., Sassone, J., Villa, R., Poletti, B., et al. (2017). X-linked parkinsonism with intellectual disability caused by novel mutations and somatic mosaicism in RAB39B gene. *Parkinsonism Relat. Disord.* 44, 142–146. doi: 10.1016/j.parkreldis.2017.08.021

De Lau, L. M., and Breteler, M. M. (2006). Epidemiology of Parkinson's disease. *Lancet Neurol.* 5, 525–535. doi: 10.1016/S1474-4422(06)70471-9

Di Monte, D. A., Wu, E. Y., Irwin, I., Delanney, L. E., and Langston, J. W. (1991). Biotransformation of 1-methyl-4-phenyl-1,2,3,6-tetrahydropyridine in primary cultures of mouse astrocytes. *J. Pharmacol. Exp. Ther.* 258, 594–600. PMID: 1907660

Di Monte, D. A., Wu, E. Y., Irwin, I., Delanney, L. E., and Langston, J. W. (1992). Production and disposition of 1-methyl-4-phenylpyridinium in primary cultures of mouse astrocytes. *Glia* 5, 48–55. doi: 10.1002/glia.440050108

Gao, Y., Martínez-Cerdeño, V., Hogan, K. J., Mclean, C. A., and Lockhart, P. J. (2020). Clinical and neuropathological features associated with loss of RAB39B. *Mov. Disord.* 35, 687–693. doi: 10.1002/mds.27951

Gelb, D. J., Oliver, E., and Gilman, S. (1999). Diagnostic criteria for Parkinson disease. *Arch. Neurol.* 56, 33–39. doi: 10.1001/archneur.56.1.33

Giannandrea, M., Bianchi, V., Mignogna, M. L., Sirri, A., Carrabino, S., D'elia, E., et al. (2010). Mutations in the small GTPase gene RAB39B are responsible for X-linked mental retardation associated with autism, epilepsy, and macrocephaly. *Am. J. Hum. Genet.* 86, 185–195. doi: 10.1016/j.ajhg.2010.01.011

Gibb, W. R., and Lees, A. J. (1988). The relevance of the Lewy body to the pathogenesis of idiopathic Parkinson's disease. *J. Neurol. Neurosurg. Psychiatry* 51, 745–752. doi: 10.1136/jnnp.51.6.745

Goedert, M., Jakes, R., and Spillantini, M. G. (2017). The Synucleinopathies: twenty years on. *J. Parkinsons Dis.* 7, S51–S69. doi: 10.3233/JPD-179005

Gonçalves, S. A., Macedo, D., Raquel, H., Simões, P. D., Giorgini, F., Ramalho, J. S., et al. (2016). shRNA-based screen identifies endocytic recycling pathway components that act as genetic modifiers of alpha-Synuclein aggregation secretion and toxicity. *PLoS Genet* 12:e1005995. doi: 10.1371/journal.pgen.1005995

Güldner, M., Schulte, C., Hauser, A. K., Gasser, T., and Brockmann, K. (2016). Broad clinical phenotype in parkinsonism associated with a base pair deletion in RAB39B and additional POLG variant. *Parkinsonism Relat. Disord.* 31, 148–150. doi: 10.1016/j.parkreldis.2016.07.005

Heikkila, R. E., Manzino, L., Cabbat, F. S., and Duvoisin, R. C. (1984). Protection against the dopaminergic neurotoxicity of 1-methyl-4-phenyl-1,2,5,6-tetrahydropyridine by monoamine oxidase inhibitors. *Nature* 311, 467–469. doi: 10.1038/311467a0

Hirsch, E. C., and Hunot, S. (2000). Nitric oxide, glial cells and neuronal degeneration in Parkinsonism. *Trends Pharmacol. Sci.* 21, 163–165. doi: 10.1016/S0165-6147(00)01471-1

Hodges, K., Brewer, S. S., Labbé, C., Soto-Ortolaza, A. I., Walton, R. L., Strongosky, A. J., et al. (2016). RAB39B gene mutations are not a common cause of Parkinson's disease or dementia with Lewy bodies. *Neurobiol. Aging* 45, 107–108. doi: 10.1016/j.neurobiolaging.2016.03.021

Jackson-Lewis, V., and Przedborski, S. (2007). Protocol for the MPTP mouse model of Parkinson's disease. *Nat. Protoc.* 2, 141–151. doi: 10.1038/nprot.2006.342

Kalia, L. V., and Lang, A. E. (2015). Parkinson's disease. *Lancet* 386, 896–912. doi: 10.1016/S0140-6736(14)61393-3

Khan, A. N., and Khan, R. H. (2022). Protein misfolding and related human diseases: a comprehensive review of toxicity, proteins involved, and current therapeutic strategies. *Int. J. Biol. Macromol.* 223, 143–160. doi: 10.1016/j.ijbiomac.2022.11.031

Koprich, J. B., Kalia, L. V., and Brotchie, J. M. (2017). Animal models of α-synucleinopathy for Parkinson disease drug development. *Nat. Rev. Neurosci.* 18, 515–529. doi: 10.1038/nrn.2017.75

Lesage, S., Bras, J., Cormier-Dequaire, F., Condroyer, C., Nicolas, A., Darwent, L., et al. (2015). Loss-of-function mutations in RAB39B are associated with typical early-onset Parkinson disease. *Neurol Genet* 1:e9. doi: 10.1212/NXG.0000000000000009

Lin, H. H., Wu, R. M., Lin, H. I., Chen, M. L., Tai, C. H., and Lin, C. H. (2017). Lack of RAB39B mutations in early-onset and familial Parkinson's disease in a Taiwanese cohort. *Neurobiol. Aging* 50, 169.e3–169.e4. doi: 10.1016/j.neurobiolaging.2016.10.021

Liu, Y., Zong, X., Huang, J., Guan, Y., Li, Y., Du, T., et al. (2019). Ginsenoside Rb1 regulates prefrontal cortical GABAergic transmission in MPTP-treated mice. *Aging (Albany NY)* 11, 5008–5034. doi: 10.18632/aging.102095

Löchte, T., Brüggemann, N., Vollstedt, E. J., Krause, P., Domingo, A., Rosales, R., et al. (2016). RAB39B mutations are a rare finding in Parkinson disease patients. *Parkinsonism Relat. Disord.* 23, 116–117. doi: 10.1016/j.parkreldis.2015.12.014

Masato, A., Plotegher, N., Boassa, D., and Bubacco, L. (2019). Impaired dopamine metabolism in Parkinson's disease pathogenesis. *Mol. Neurodegener.* 14:35. doi: 10.1186/s13024-019-0332-6

Mata, I. F., Jang, Y., Kim, C. H., Hanna, D. S., Dorschner, M. O., Samii, A., et al. (2015). The RAB39B p.G192R mutation causes X-linked dominant Parkinson's disease. *Mol. Neurodegener.* 10:50. doi: 10.1186/s13024-015-0045-4

Menšíková, K., Matěj, R., Colosimo, C., Rosales, R., Tučková, L., Ehrmann, J., et al. (2022). Lewy body disease or diseases with Lewy bodies? *NPJ Parkinsons Dis* 8:3. doi: 10.1038/s41531-021-00273-9

Mignogna, M. L., Musardo, S., Ranieri, G., Gelmini, S., Espinosa, P., Marra, P., et al. (2021). RAB39B-mediated trafficking of the GluA2-AMPAR subunit controls dendritic spine maturation and intellectual disability-related behaviour. *Mol. Psychiatry* 26, 6531–6549. doi: 10.1038/s41380-021-01155-5

Niu, M., Zheng, N., Wang, Z., Gao, Y., Luo, X., Chen, Z., et al. (2020). RAB39B deficiency impairs learning and memory partially through compromising autophagy. *Front. Cell Dev. Biol.* 8:598622. doi: 10.3389/fcell.2020.598622

Purisai, M. G., Mccormack, A. L., Langston, W. J., Johnston, L. C., and Di Monte, D. A. (2005). Alpha-synuclein expression in the substantia nigra of MPTP-lesioned non-human primates. *Neurobiol. Dis.* 20, 898–906. doi: 10.1016/j.nbd.2005.05.028

Quarta, M., Cromie, M., Chacon, R., Blonigan, J., Garcia, V., Akimenko, I., et al. (2017). Bioengineered constructs combined with exercise enhance stem cell-mediated treatment of volumetric muscle loss. *Nat. Commun.* 8:15613. doi: 10.1038/ncomms15613

Shi, C. H., Zhang, S. Y., Yang, Z. H., Yang, J., Shang, D. D., Mao, C. Y., et al. (2016). A novel RAB39B gene mutation in X-linked juvenile Parkinsonism with basal ganglia calcification. *Mov. Disord.* 31, 1905–1909. doi: 10.1002/mds.26828

Stankovic, T., Byrd, P. J., Cooper, P. R., Mcconville, C. M., Munroe, D. J., Riley, J. H., et al. (1997). Construction of a transcription map around the gene for ataxia telangiectasia: identification of at least four novel genes. *Genomics* 40, 267–276. doi: 10.1006/geno.1996.4595

Tysnes, O.-B., and Storstein, A. (2017). Epidemiology of Parkinson's disease. *J. Neural Transm.* 124, 901–905. doi: 10.1007/s00702-017-1686-y

Van Den Eeden, S. K., Tanner, C. M., Bernstein, A. L., Fross, R. D., Leimpeter, A., Bloch, D. A., et al. (2003). Incidence of Parkinson's disease: variation by age, gender, and race/ethnicity. *Am. J. Epidemiol.* 157, 1015–1022. doi: 10.1093/aje/kwg068

Vila, M., Vukosavic, S., Jackson-Lewis, V., Neystat, M., Jakowec, M., and Przedborski, S. (2000). Alpha-synuclein up-regulation in substantia nigra dopaminergic neurons following administration of the parkinsonian toxin MPTP. *J. Neurochem.* 74, 721–729. PMID: 10646524

Von Campenhausen, S., Bornschein, B., Wick, R., Bötzel, K., Sampaio, C., Poewe, W., et al. (2005). Prevalence and incidence of Parkinson's disease in Europe. *Eur. Neuropsychopharmacol.* 15, 473–490. doi: 10.1016/j.euroneuro.2005.04.007

Wilson, G. R., Sim, J. C., Mclean, C., Giannandrea, M., Galea, C. A., Riseley, J. R., et al. (2014). Mutations in RAB39B cause X-linked intellectual disability and early-onset Parkinson disease with α-synuclein pathology. *Am. J. Hum. Genet.* 95, 729–735. doi: 10.1016/j.ajhg.2014.10.015

Woodbury-Smith, M., Deneault, E., Yuen, R. K. C., Walker, S., Zarrei, M., Pellecchia, G., et al. (2017). Mutations in RAB39B in individuals with intellectual disability, autism spectrum disorder, and macrocephaly. *Mol. Autism.* 8:59. doi: 10.1186/s13229-017-0175-3

Wozniak, D. F., Valnegri, P., Dearborn, J. T., Fowler, S. C., and Bonni, A. (2019). Conditional knockout of UBC13 produces disturbances in gait and spontaneous locomotion and exploration in mice. *Sci. Rep.* 9:4379. doi: 10.1038/s41598-019-40714-3

Yuan, L., Deng, X., Song, Z., Yang, Z., Ni, B., Chen, Y., et al. (2015). Genetic analysis of the RAB39B gene in Chinese Han patients with Parkinson's disease. *Neurobiol. Aging* 36, 2907.e11–2907.e12. doi: 10.1016/j.neurobiolaging.2015.06.019

Zhang, W., Ma, L., Yang, M., Shao, Q., Xu, J., Lu, Z., et al. (2020). Cerebral organoid and mouse models reveal a RAB39b-PI3K-mTOR pathway-dependent dysregulation of cortical development leading to macrocephaly/autism phenotypes. *Genes Dev.* 34, 580–597. doi: 10.1101/gad.332494.119

frontiers | Frontiers in Aging Neuroscience

TYPE Original Research
PUBLISHED 17 February 2023
DOI 10.3389/fnagi.2023.1098034

OPEN ACCESS

EDITED BY
Emilia Vitale,
Institute of Biochemistry and Cell Biology,
Department of Biomedical Sciences,
National Research Council (CNR), Italy

REVIEWED BY
Nobuyuki Kimura,
Okayama University of Science, Japan
Kundlik Gadhave,
Johns Hopkins University,
United States

*CORRESPONDENCE
Kun Zou
✉ kunzou@med.nagoya-cu.ac.jp
Makoto Michikawa
✉ michi@med.nagoya-cu.ac.jp

SPECIALTY SECTION
This article was submitted to Alzheimer's Disease and Related Dementias, a section of the journal Frontiers in Aging Neuroscience

RECEIVED 14 November 2022
ACCEPTED 20 January 2023
PUBLISHED 17 February 2023

CITATION
Gao Y, Sun Y, Islam S, Nakamura T, Tomita T, Zou K and Michikawa M (2023) Presenilin 1 deficiency impairs Aβ42-to-Aβ40- and angiotensin-converting activities of ACE. *Front. Aging Neurosci.* 15:1098034. doi: 10.3389/fnagi.2023.1098034

Presenilin 1 deficiency impairs Aβ42-to-Aβ40- and angiotensin-converting activities of ACE

Yuan Gao[1], Yang Sun[1], Sadequl Islam[1], Tomohisa Nakamura[1], Taisuke Tomita[2], Kun Zou[1]* and Makoto Michikawa[1]*

[1]Department of Biochemistry, Graduate School of Medical Sciences, Nagoya City University, Nagoya, Japan, [2]Laboratory of Neuropathology and Neuroscience, Faculty of Pharmaceutical Sciences, University of Tokyo, Bunkyo, Japan

Introduction: Alzheimer's disease (AD) is associated with amyloid β-protein 1-42 (Aβ42) accumulation in the brain. Aβ42 and Aβ40 are the major two species generated from amyloid precursor protein. We found that angiotensin-converting enzyme (ACE) converts neurotoxic Aβ42 to neuroprotective Aβ40 in an ACE domain– and glycosylation-dependent manner. Presenilin 1 (PS1) mutations account for most of cases of familial AD and lead to an increased Aβ42/40 ratio. However, the mechanism by which *PSEN1* mutations induce a higher Aβ42/40 ratio is unclear.

Methods: We over expressed human ACE in mouse wild-type and PS1-deficient fibroblasts. The purified ACE protein was used to analysis the Aβ42-to-Aβ40- and angiotensin-converting activities. The distribution of ACE was determined by Immunofluorescence staining.

Result: We found that ACE purified from PS1-deficient fibroblasts exhibited altered glycosylation and significantly reduced Aβ42-to-Aβ40- and angiotensin-converting activities compared with ACE from wild-type fibroblasts. Overexpression of wild-type PS1 in PS1-deficient fibroblasts restored the Aβ42-to-Aβ40- and angiotensin-converting activities of ACE. Interestingly, PS1 mutants completely restored the angiotensin-converting activity in PS1-deficient fibroblasts, but some PS1 mutants did not restore the Aβ42-to-Aβ40-converting activity. We also found that the glycosylation of ACE in adult mouse brain differed from that of embryonic brain and that the Aβ42-to-Aβ40-converting activity in adult mouse brain was lower than that in embryonic brain.

Conclusion: PS1 deficiency altered ACE glycosylation and impaired its Aβ42-to-Aβ40- and angiotensin-converting activities. Our findings suggest that PS1 deficiency and *PSEN1* mutations increase the Aβ42/40 ratio by reducing the Aβ42-to-Aβ40-converting activity of ACE.

KEYWORDS

Alzheimer's disease, angiotensin-converting enzyme, amyloid β-protein, presenilin 1, familial AD

Introduction

Alzheimer's disease (AD) is a degenerative disease of the central nervous system characterized by amyloid β-protein (Aβ) accumulation, intraneuronal neurofibrillary tangles, and neuronal loss (Goedert and Spillantini, 2006; Selkoe, 2011; Selkoe and Hardy, 2016). Aβ is produced by the hydrolysis of a type I transmembrane protein, amyloid precursor protein (APP), mediated by β-and γ-secretase (Haass et al., 1993; Kimberly and Wolfe, 2003). The most abundant form of Aβ is Aβ40 (containing 40 amino acids), which comprises 90% of all secreted Aβ (Selkoe and Hardy, 2016). Aβ40 exerts neuroprotective effects, functions as an antioxidant against metal-induced oxidative damage, and inhibits Aβ42 toxicity and Aβ42 accumulation in the brain (Zou et al., 2002, 2003; Kim

et al., 2007; Kuperstein et al., 2010). In contrast, Aβ42 is more prone to aggregate and exhibit toxicity than Aβ40, and it is essential for amyloid deposition in the brain (McGowan et al., 2005; Selkoe and Hardy, 2016). Abnormal accumulation of Aβ42 in the brain is considered the cause of neurodegeneration and cognitive decline in AD patients (Selkoe and Hardy, 2016).

γ-Secretase, an aspartyl intramembrane protease complex that catalyzes the proteolysis of type I membrane proteins (De Strooper et al., 2012), is composed of four subunits, presenilin 1 (*PSEN1*, PS1) or presenilin 2 (*PSEN2*, PS2), Pen-2, Aph-1, and nicastrin (NCT) (Kimberly et al., 2003; Bai et al., 2015). PS1 and PS2 constitute the catalytic subunit of γ-secretase. Most *PSEN* FAD mutations are situated within or flanking the conserved hydrophobic TMDs and are missense mutations resulting in single amino acid changes, such as PS1L166P and PS1G384A (Wanngren et al., 2014). In addition, an AD-associated mutation within the PS1 gene deletes exon 9 (PS1Δexon9) due to a splicing error and results in the accumulation of the uncleaved full-length protein (Steiner et al., 1999). Mutations in *PSEN1* and *PSEN2* account for most cases of early onset familial AD (FAD) and are thought to affect Aβ generation by changing the cleavage site of γ-secretase, thereby increasing the amount of Aβ42 relative to Aβ40, which in turn triggers FAD (Bentahir et al., 2006; Kuperstein et al., 2010). However, the mechanism underlying the increase in the Aβ42/40 ratio associated with *PSEN* mutations is unclear. In addition to serving as the catalytic subunit of the γ-secretase complex, PS also has other functions. Previous studies showed that PS, especially PS1, also plays roles in protein trafficking and the maturation and cellular localization of NCT, APP, TrkB, N-cadherin, neurotrophin receptor–like death domain protein, epidermal growth factor receptor and integrin β1 (Naruse et al., 1998; Leem et al., 2002; Herreman et al., 2003; Uemura et al., 2003; Gowrishankar et al., 2004; Zou et al., 2008). In the absence of PS1 and PS2, maturation and cell-surface delivery of NCT are completely inhibited, whereas the maturation and cell-surface delivery of integrin β1 are enhanced, suggesting that PS regulates protein maturation in a bidirectional manner (Zou et al., 2008).

We previously reported that angiotensin-converting enzyme (ACE) converts toxic Aβ42 to neuroprotective Aβ40 and reduces the Aβ42/40 ratio (Zou et al., 2007; Zou and Michikawa, 2008). Inhibition of ACE or heterozygous ACE deletion significantly enhances Aβ42 deposition and increases Aβ42/40 ratio in the brain of AD model mice. ACE inhibitors are widely used clinically for the treatment of hypertension, however, compared with non–ACE inhibitor antihypertensive medications, ACE inhibitors can reduce IQ in male hypertensive patients (Liu et al., 2019). ACE plays a central role in blood pressure regulation *via* the renin-angiotensin-aldosterone system (Turner and Hooper, 2002). Somatic ACE consists of two homologous catalytic domains, the C-domain and the N-domain (Hooper and Turner, 2003). Although these domains are highly homologous, they have distinct physiological functions (Fuchs et al., 2008; Zou et al., 2009). Interestingly, only the N-domain of ACE exhibits Aβ42-to-Aβ40-converting activity, whereas the C-domain primarily exhibits angiotensin-converting activity. Notably, both of these activities are impaired after de-glycosylation of the *N*-glycan (Zou et al., 2007, 2009). The earliest-deposited Aβ species, Aβ43, can be converted to Aβ41, and this activity requires both active domains of ACE. Inhibition of ACE *via* treatment with the ACE inhibitor captopril leads to a significant increase in Aβ43 deposition in mouse brain (Zou et al., 2013). In addition, successive catalysis by ACE and ACE2 convert Aβ43 to Aβ40 (Liu et al., 2014).

Most *PSEN1* mutations found in FAD induce an increase in the Aβ42/40 ratio, but the underlying mechanism is unclear (Selkoe and Hardy, 2016). Thus, we hypothesized that the increase in the Aβ42/40 ratio associated with *PSEN1* mutations results from impairment of the Aβ42-to-Aβ40-converting activity of ACE. Here, we examined the effects of PS1 deficiency and *PSEN1* mutations on the maturation and glycosylation of ACE protein and its Aβ42-to-Aβ40-converting and angiotensin-converting activities. We found that ACE protein purified from PS1-knockout (PS1-KO) fibroblasts shows altered glycosylation and markedly impaired Aβ42-to-Aβ40-and angiotensin-converting activities. Transfection of wild-type (WT) PS1 restored these activities in PS1-KO cells; however, some PS mutants could not restore the Aβ42-to-Aβ40-converting activity of ACE in PS1-KO cells. These findings provide a novel mechanism underlying *PSEN1* mutations regulate Aβ42/40 ratio through ACE.

Results

PS1 deficiency altered ACE glycosylation and impaired its Aβ42-to-Aβ40-converting activity

To determine whether PS1 regulates ACE maturation and its Aβ42-to-Aβ40-converting activity, we purified three different recombinant ACE proteins from WT and PS1-KO fibroblasts. Full-domain ACE (F-ACE) includes both the N-terminal and C-terminal domain active sites. N-ACE includes only the N-terminal active site, whereas C-ACE includes only the C-terminal active site (Figure 1A; Zou et al., 2009). A 6-histidine tag was used to the C-terminus of all ACE mutants to facilitate purification. WT and PS1-KO fibroblasts transiently overexpressed F-ACE, N-ACE, and C-ACE. No endogenous ACE was detected in the lysate of fibroblasts transfected with empty vectors (mock) using anti-ACE and anti–6 × His-tag antibodies. The F-ACE, N-ACE, and C-ACE proteins were purified after overexpression in fibroblasts and then examined by Western blotting. The molecular weight of F-ACE and N-ACE from PS1-KO fibroblasts was slightly lower than that of the proteins from WT fibroblasts (Figure 1B), suggesting that PS1 deficiency affects the maturation or glycosylation of F-ACE and N-ACE. However, there was no difference in the molecular weight of C-ACE purified from WT and PS1-KO fibroblasts (Figure 1B).

As indicated above, ACE has two active domains, with the Aβ42-to-Aβ40-converting activity localized in the N-terminal domain and the angiotensin-converting activity localized in the C-terminal domain (Zou et al., 2009). Synthetic Aβ40 and Aβ42 were used to examine the specificity of the anti-Aβ40 and anti-Aβ42 antibodies, and no cross-reaction was observed (Figure 1C). To identify whether the generation of Aβ40 is dependent on Aβ42-to-Aβ40-converting activity of ACE, we incubated an ACE inhibitor captopril with the mixture of F-ACE and synthetic Aβ42. Aβ40 generation was completely inhibited by captopril (Figure 1D). To determine whether PS1 deficiency affects the Aβ42-to-Aβ40-converting activity of ACE, we incubated purified ACE proteins from WT or PS1-KO fibroblasts with Aβ42 and examined the generation of Aβ40 using anti-Aβ40 and

Abbreviations: AD, Alzheimer's disease; Aβ, amyloid β-protein; Aβ42, amyloid β-protein1-42; ACE, angiotensin-converting enzyme; PS, presenilin; PS1-CTF, C-terminal fragment of presenilin 1; NCT, nicastrin; APP, amyloid precursor protein; APH-1, anterior pharynx-defective-1; PEN-2, presenilin enhancer-2; FAD, Transmembrane domains.

10.3389/fnagi.2023.1098034

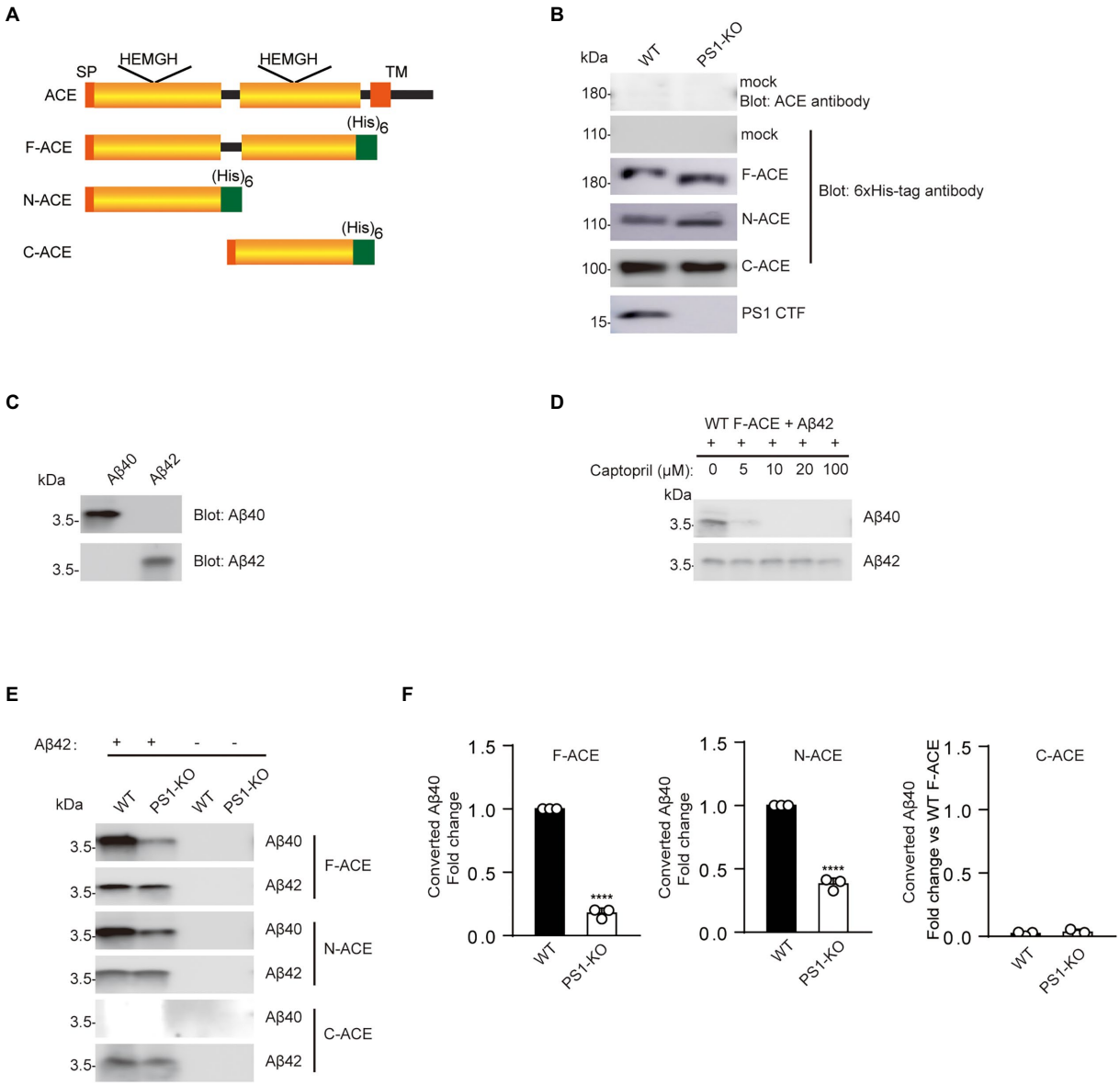

FIGURE 1
Recombinant F-ACE and N-ACE from PS1-KO fibroblasts exhibit decreased Aβ42-to-Aβ40-converting activity. **(A)** Schematic representation of human ACE and recombinant ACE proteins. The wild-type (WT) ACE protein consists of a signal peptide (SP), a single transmembrane domain (TM), and two homologous catalytic domains (yellow boxes). Recombinant ACE proteins (F-ACE, N-ACE and C-ACE) contain 6 histidine residues (green box) at the C-terminus and a SP at the N-terminus. **(B)** Western blots of 20μg protein from the lysate of WT and PS1-KO fibroblasts transfected with empty vectors (mock) were probed with anti-ACE and anti−6×His-tag antibodies (Upper two panels). Western blots of 20μg of purified F-, N-, and C-ACE proteins from WT or PS1-KO fibroblasts were probed with anti−6×His-tag or PS1-CTF antibodies (Lower four panels). **(C)** The specificity of the anti-Aβ40 and anti-Aβ42 antibodies was confirmed by Western blotting of 0.1μg of synthetic Aβ40 and Aβ42. **(D)** Captopril 0, 5, 10, 20, 100μM was incubated with purified F-ACE protein and synthetic Aβ42 for 2h. **(E)** Purified F-, N-, and C-ACE proteins were mixed with synthetic Aβ42 and incubated at 37°C for 2h. Western blots of the mixture were probed with anti-Aβ40 and anti-Aβ42 antibodies. The symbols (+) and (–) indicate with and without synthetic Aβ42. **(F)** Quantification of Aβ40 converted from Aβ42. F-and N-ACE purified from PS1-KO cells showed lower Aβ-converting activity (Aβ42-to-Aβ40−converting activity) compared with proteins from WT fibroblasts. C-ACE did not show any Aβ-converting activity. Values represent the mean±SEM; $n=3$; ****, $p<0.0001$, by unpaired two-tailed Student's *t* test. F-ACE, full-domain ACE; N-ACE, N-terminal domain ACE; C-ACE, C-terminal domain ACE.

anti-Aβ42 antibodies. As reported in our previous study, only the F-ACE and N-ACE domains exhibited Aβ42-to-Aβ40-converting activity (Figures 1E,F). Interestingly, F-ACE and N-ACE purified from PS1-KO cells showed significantly lower Aβ42-to-Aβ40-converting activity compared to the domains purified from WT cells (Figures 1E,F). These results suggest that PS1 deficiency affects the maturation/glycosylation of ACE and reduces the Aβ42-to-Aβ40-converting activity of F-ACE and N-ACE.

PS1 deficiency completely abolished the angiotensin-converting activity of ACE

We also examined the angiotensin-converting activity of F-ACE, N-ACE, and C-ACE purified from WT and PS1-KO fibroblasts. The angiotensin-converting activity of these proteins was analyzed by monitoring the cleavage of a synthetic *o*-aminobenzoyl peptide substrate to release a fluorophore. As previously reported, F-ACE and

10.3389/fnagi.2023.1098034

C-ACE purified from WT fibroblasts exhibited angiotensin-converting activity, whereas N-ACE did not (Figures 2A–C). Surprisingly, the angiotensin-converting activity of F-ACE and C-ACE purified from PS1-KO cells was completely abolished (Figures 2A,C). These results suggest that PS1 is essential for the angiotensin-converting activity ACE.

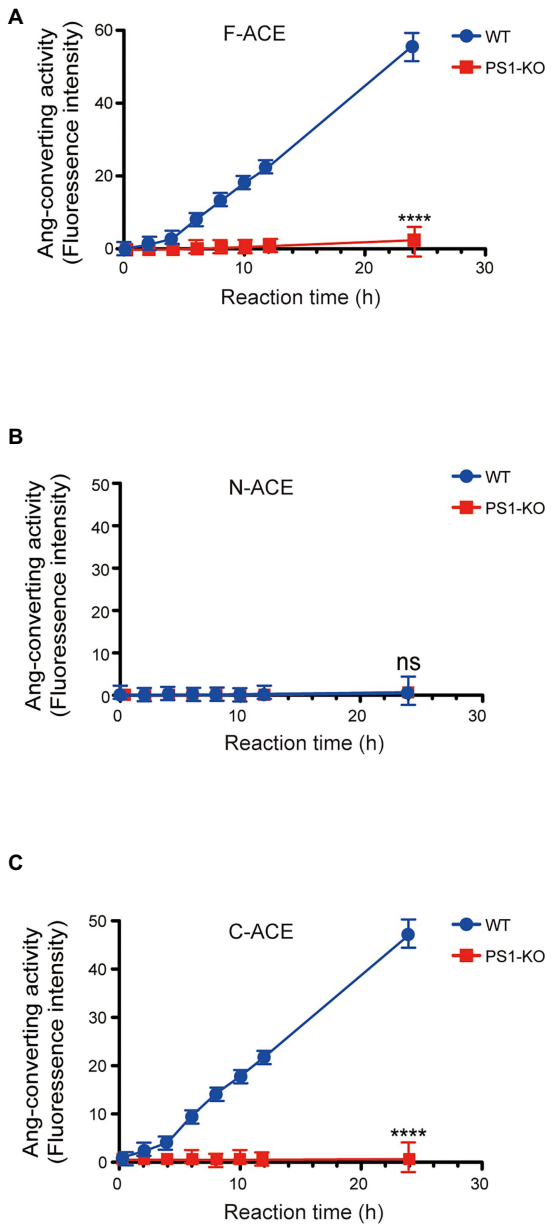

FIGURE 2
Loss of angiotensin-converting activity in recombinant F-and C-ACE from PS1-KO fibroblasts. Ang-converting (angiotensin-converting) activity was measured by incubating 2μg of ACE protein with the synthetic o-aminobenzoyl peptide substrate for 24h at 37°C. **(A)** F-ACE purified from WT fibroblasts showed Ang-converting activity, whereas PS1-KO fibroblasts did not show any Ang-converting activity. **(B)** N-ACE purified from WT and PS1-KO fibroblasts did not show any Ang-converting activity. **(C)** C-ACE purified from WT fibroblasts showed Ang-converting activity, whereas PS1-KO fibroblasts did not show any Ang-converting activity. Values represent the means ± SD; n=3; ****p<0.0001. NS, not significant, by unpaired two-tailed Student's t test.

PSEN1 mutations reduce the Aβ42-to-Aβ40-converting activity of ACE

To determine whether *PSEN1* mutations affect the Aβ42-to-Aβ40-converting activity of ACE, we transfected PS1WT, PS1L166P, PS1ΔE9, or PS1G384A into PS1-KO fibroblasts. We then transfected F-ACE, N-ACE, or C-ACE into these fibroblasts and purified the ACE proteins from the respective transfectants. Western blots of the purified ACE proteins are shown in Figure 3A. The PS1WT and PS1 mutants partially restored the maturation of the F-ACE and N-ACE proteins (Figure 3A). The level of mature NCT was significantly reduced in PS1-KO fibroblasts; however, NCT maturation was completed restored by transfection of the PS1WT and PS1 mutants (Figure 3A).

We then examined the Aβ42-to-Aβ40-converting activity of the ACE proteins by incubating them in the presence of Aβ42. Interestingly, PS1WT and PS1ΔE9 restored the Aβ42-to-Aβ40-converting activity of both F-ACE and N-ACE to levels similar to those of F-ACE and N-ACE from WT fibroblasts. However, PS1L166P and PS1G384A did not restore the Aβ42-to-Aβ40-converting activity of F-ACE and N-ACE compared with PS1WT (Figures 3B,C). As previously reported, none of the C-ACE proteins exhibited Aβ42-to-Aβ40-converting activity (Figures 3B,C). These results suggest that some *PSEN1* mutations increase the Aβ42/40 ratio by reducing the Aβ42-to-Aβ40-converting activity of ACE.

PS1WT and PS1 mutants restored the angiotensin-converting activity of ACE in PS1-KO fibroblasts

We also examined the angiotensin-converting activity of F-ACE, N-ACE, and C-ACE proteins purified from PS1-KO fibroblasts transfected with PS1WT, PS1L166P, PS1ΔE9, or PS1G384A. In contrast to the Aβ42-to-Aβ40-converting activity, all of the PS1WT and PS1 mutants of F-ACE and C-ACE proteins exhibited angiotensin-converting activity (Figures 4A,C). Because angiotensin-converting activity is not localized in the N-terminal domain of ACE, this activity was not detected after transfection of PS WT and PS1 mutants (Figure 4B). These results suggest that PS1 is essential for the angiotensin-converting activity of ACE and that FAD-linked PS1 mutants do not affect the angiotensin-converting activity.

PS1 deficiency and PS1 mutant reduced the Golgi apparatus distribution of ACE.

To gain mechanistic insights into the decreased Aβ42-to-Aβ40-and angiotensin-converting activities of ACE protein in PS1-KO fibroblasts, we investigated whether the Golgi apparatus distribution of ACE changed in the cells. We found that the localization of F-ACE protein in Golgi apparatus decreased in PS1-KO fibroblasts. Transfection of PS1WT, PSΔE9 and PS1G384A into PS1-KO fibroblasts restored the distribution of F-ACE in Golgi apparatus, however, PS1L166P did not restored the Golgi apparatus distribution of F-ACE (Figures 5A,B). These results suggest that reduced distribution of ACE in Golgi apparatus can decrease ACE maturation and impair its activities.

De-glycosylation of ACE abolished its Aβ42-to-Aβ40-and angiotensin-converting activities.

To examine which glycosylation is necessary for Aβ42-to-Aβ40-and angiotensin-converting activities, F-ACE, N-ACE, and C-ACE were incubated with *N*-glycanase, *O*-glycanase, or sialidase A. After

10.3389/fnagi.2023.1098034

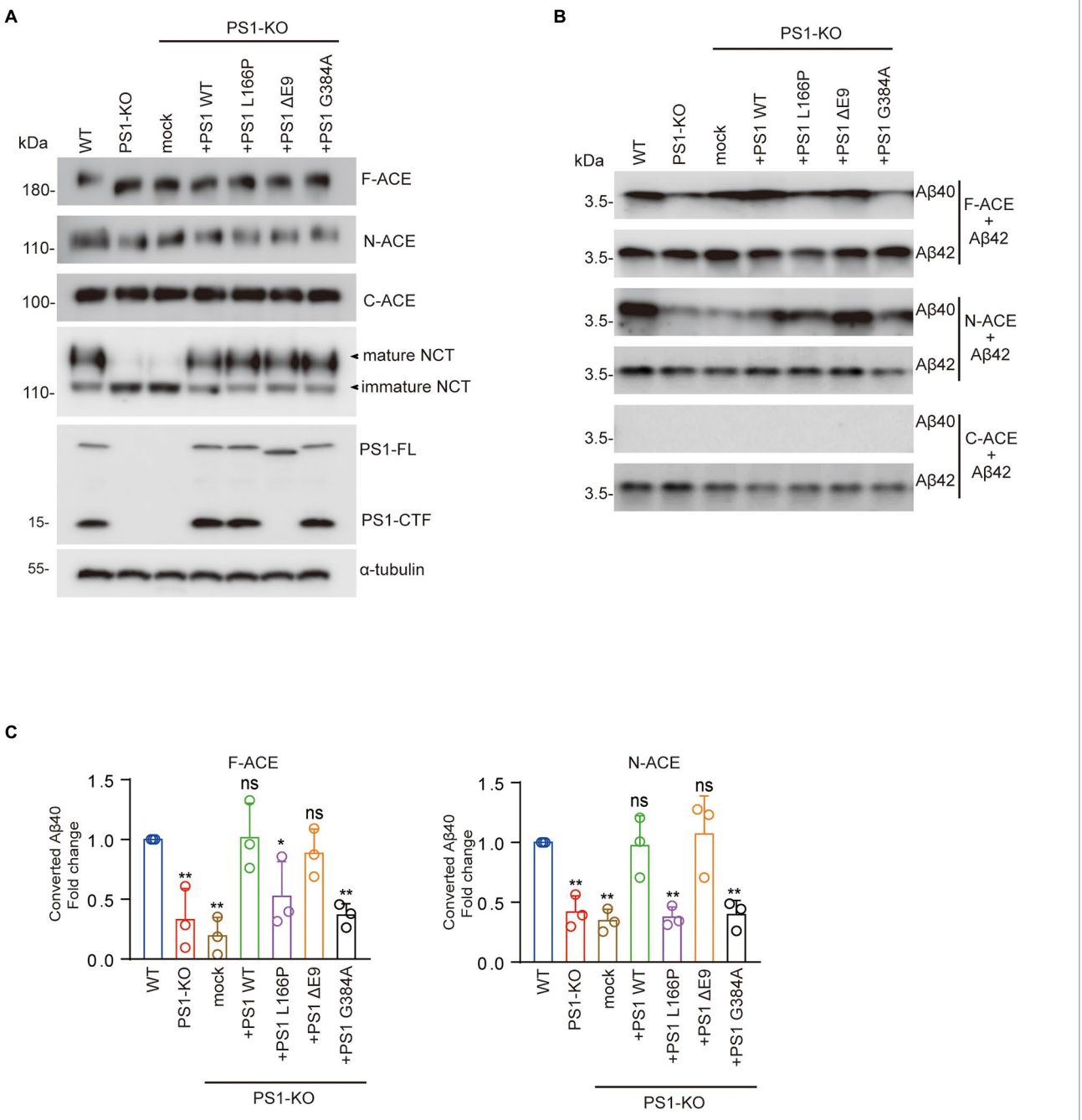

FIGURE 3
FAD-linked PS1L166P and PS1G384A mutations did not restore Aβ42-to-Aβ40–converting activity of ACE. **(A)** Fibroblasts were transfected with empty vector or PS1WT or PS1 mutant plasmids. Recombinant ACE proteins, NCT, PS1, and α-tubulin were detected by Western blotting. **(B)** F-, N-, and C-ACE purified from WT and PS1-KO fibroblasts or PS1-KO fibroblasts transfected with PS1WT or PS1 mutant were mixed with synthetic Aβ42 and incubated at 37°C for 2h. Western blots of the mixtures were probed with anti-Aβ40 and anti-Aβ42 antibodies. **(C)** Quantification of Aβ40 converted from Aβ42. PS1L166P and PS1G384A did not restore the Aβ42-to-Aβ40–converting activity of F-ACE and N-ACE proteins, whereas PS WT and PS1ΔE9 restored this activity. Values represent the mean±SD; n=3; *, p<0.05, **, p<0.01. NS, not significant, Holm-Sidak's multiple comparisons test.

treatment with *N*-glycanase, the molecular weight of F-ACE, N-ACE, and C-ACE was significantly reduced, indicating that most glycosylation of ACE is *N*-glycan. *O*-Glycanase and sialidase A treatment did not significantly reduce the molecular weight of the ACE proteins compared with *N*-glycanase (Figure 6A). We then incubated Aβ42 with the de-glycosylated F-ACE and N-ACE proteins. After de-glycosylation by *N*-glycanase, *O*-glycanase, or sialidase A, neither F-ACE nor N-ACE exhibited Aβ42-to-Aβ40-converting activity (Figure 6B). Similarly, the angiotensin-converting activity of F-ACE and C-ACE was also abolished by treatment with *N*-glycanase, *O*-glycanase, or sialidase A (Figure 6C).

Aβ42-to-Aβ40-converting activity was lower in adult mouse brain cortex than embryonic brain cortex.

To determine whether changes in brain Aβ42-to-Aβ40-converting activity are development dependent, we incubated cortex lysate from 17-day-old embryos or 3-month-old mice with synthetic Aβ42. The level

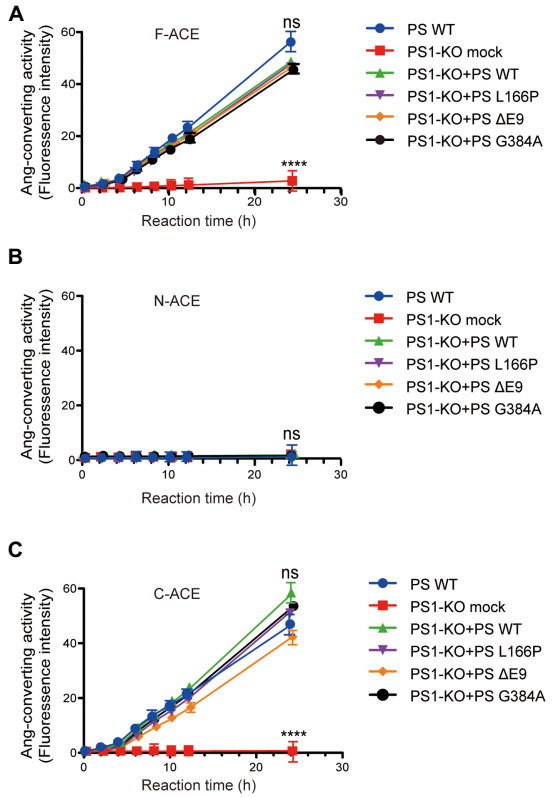

FIGURE 4
Transfection of PS1WT and PS1 mutants restored angiotensin-converting activity of F-ACE and C-ACE in PS1-KO fibroblasts. Ang-converting activity was measured by incubating 2μg of ACE protein with the synthetic o-aminobenzoyl peptide substrate for 24h at 37°C. **(A)** Transfection of PS1WT and PS1 mutants fully restored Ang-converting activity of F-ACE in PS1-KO fibroblasts. **(B)** N-ACE purified from WT, PS1-KO, and PS1-KO fibroblasts transfected with PS1WT and PS1 mutants did not show any ang-converting activity. **(C)** Transfection of PS1WT and PS1 mutants fully restored the Ang-converting activity of C-ACE in PS1-KO fibroblasts. PS1WT and PS1 mutants did not exert different effects on angiotensin-converting activity. Values represent the mean±SD; $n=3$; NS, not significant, ****$p<0.0001$, Holm-Sidak's multiple comparisons test.

of Aβ40 converted from Aβ42 in adult cortex was lower than that in embryonic cortex, indicating that embryonic cortex has higher Aβ42-to-Aβ40-converting activity than adult cortex (Figures 7A,B). However, there was no difference in angiotensin-converting activity between the cortex lysates from 17-day-old embryos and 3-month-old mice (Figure 7C). Interestingly, ACE protein in adult cortex showed two bands on Western blotting, whereas a single band corresponding to the upper band of ACE in adult brain was observed in the embryonic cortex (Figure 7D). After de-glycosylation with *N*-glycanase, the molecular weight of both adult and embryonic brain ACE decreased to a single band of approximately 150 kDa, whereas *O*-glycanase did not significantly change the molecular weight of ACE. Notably, sialidase A slightly reduced the molecular weight of the upper band of ACE from adult brain and ACE from embryonic brain (Figure 7D). Then we also examined the Aβ42-to-Aβ40-converting activity in the brain lysate after de-glycosylation. Aβ40 generation was not detected after de-glycosylation with *N*-glycanase, *O*-glycanase, or sialidase A (Figure 7E). These results suggest that the Aβ42-to-Aβ40-converting activity of ACE decreases with development in adult brain compared with embryonic brain and that glycosylation modulates the Aβ42-to-Aβ40-converting activity of ACE.

Materials and methods

Cell culture and transfection

WT and PS1-KO mouse embryonic fibroblasts (MEFs) were maintained in Dulbecco's modified Eagle's medium (Wako, Osaka, Japan) containing 10% fetal bovine serum (Corning, Woodland, CA) at 37°C in a 5% CO_2 atmosphere. To overexpress human ACE (F-ACE, N-ACE, and C-ACE with 6×His-tag) and the PS1WT and PS mutants (PS1L166P, PS1ΔE9, and PS1G384A), plasmids encoding the target cDNAs were transfected into platinum-E cells using FuGENE (Promega, Madison, WI, United States) for packaging. Conditioned medium was collected after 48 h and added to MEFs. In order to increase the transfection efficiency, polybrene was added at the same time to a final concentration of 5 μg/ml.

ACE protein purification

Cells transfected with F-ACE, N-ACE, and C-ACE were harvested in lysis buffer [50 mM Tris–HCl (pH 7.5) containing 0.5% NP40] and centrifuged at 15,000 *g* for 30 min. Next, 1 ml of TALON® metal affinity resin (Takara, Shiga, Japan) was used to purify ACE protein from 8 ml of MEF lysate. All of the abovementioned operations were carried out at 4°C. The concentration of purified ACE protein was determined using a Pierce™ BCA protein assay kit (Thermo Scientific, Rockford, IL, United States).

Mouse cortex sample

WT C57BL/6 J female mice at gestation day 17 were perfused with PBS (137 mM NaCl, 2.7 mM KCl, 10 mM Na_2HPO_4, 1.8 mM KH_2PO_4, 1 mM $CaCl_2$, and 0.5 mM $MgCl_2$). The cortex from 3-month-old mice and embryos was homogenized with lysis buffer [50 mM Tris–HCl (pH 7.5) containing 0.5% NP40] and centrifuged at 15000 *g* and 4°C for 30 min. The protein concentration of the brain lysate was determined using a Pierce™ BCA Protein assay kit (Thermo Scientific). The experiments in this study were performed in strict accordance with the recommendations of the Fundamental Guidelines for Proper Conduct of Animal Experiments and Related Activities in Academic Research Institutions, under the jurisdiction of the Ministry of Education, Culture, Sports, Science and Technology, Japan.

Western blot

A total of 5 μg of cell lysate protein or ACE and 20 μg of protein from adult and embryonic mouse cortex were separated by SDS-PAGE and transferred onto PVDF membranes (Sigma-Aldrich, St. Louis, MO, United States). The membranes were incubated overnight at 4°C with the proper primary antibodies. After incubating with appropriate peroxidase-conjugated secondary antibodies, the membranes were

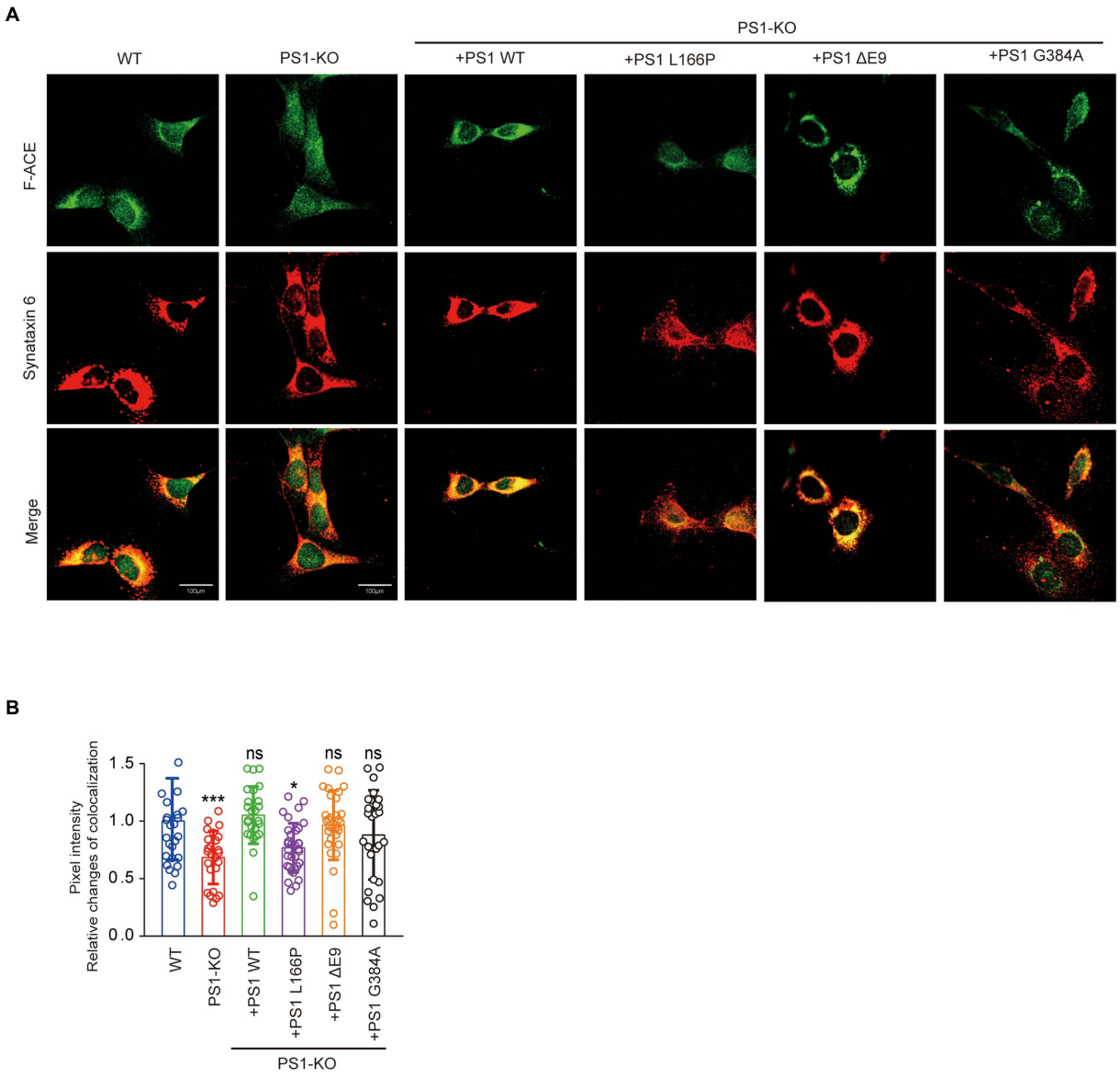

FIGURE 5
PS1 deficiency and PS1 mutant affected the localization of ACE. **(A)** Immunostaining for Golgi apparatus (red) and F-ACE (green) in WT, PS1-KO, and PS1-KO fibroblasts transfected with PS1WT and PS1 mutants. Scale bars, 100μm. **(B)** Quantification of ACE intensity in Golgi apparatus of WT, PS1-KO, and PS1-KO fibroblasts transfected with PS1WT and PS1 mutants. $n \geq 25$ different stained cells/group. *$p<0.05$, ***$p<0.001$. NS, not significant, Holm-Sidak's multiple comparisons test.

visualized using Super Signal Chemiluminescence (Wako) and an Amersham Imager 680. Detailed information regarding antibodies is provided in Supplementary Table S1.

Aβ42-to-Aβ40-converting activity assay

Purified ACE protein (25 μg) was mixed with freshly dissolved synthetic Aβ42 (PEPTIDE, Osaka, Japan) at a final concentration of 40 μM (Zou et al., 2009). The mixture was incubated at 37°C for 4 h and then dissolved in 2× SDS sample buffer [0.125 M Tris–HCl (pH 6.8), 20% glycerol, 4% SDS, 10% 2-mercaptoethanol, 0.004% bromophenol blue]. The mixture was separated by SDS-PAGE in tricine buffer and blotted onto a PVDF membrane. Aβ40 and Aβ42 were detected using anti-Aβ40 and anti-Aβ42 antibodies.

Angiotensin-converting activity assay

ACE activity was analyzed using an ACE activity assay kit (abcam, Cambridge, United Kingdom) according to the manufacturer's instructions. A total of 2 μg of ACE protein was mixed with a synthetic o-aminobenzoyl peptide substrate and incubated at 37°C. ACE activity was measured every 2 h using a fluorescence microplate reader at Ex/Em wavelengths of 330/340 nm.

ACE de-glycosylation

An ACE de-glycosylation kit (abcam) was used to de-glycosylate purified ACE protein according to the manufacturer's instructions. A total of 30 μg of ACE protein was mixed with PNGase F, *O*-glycosidase,

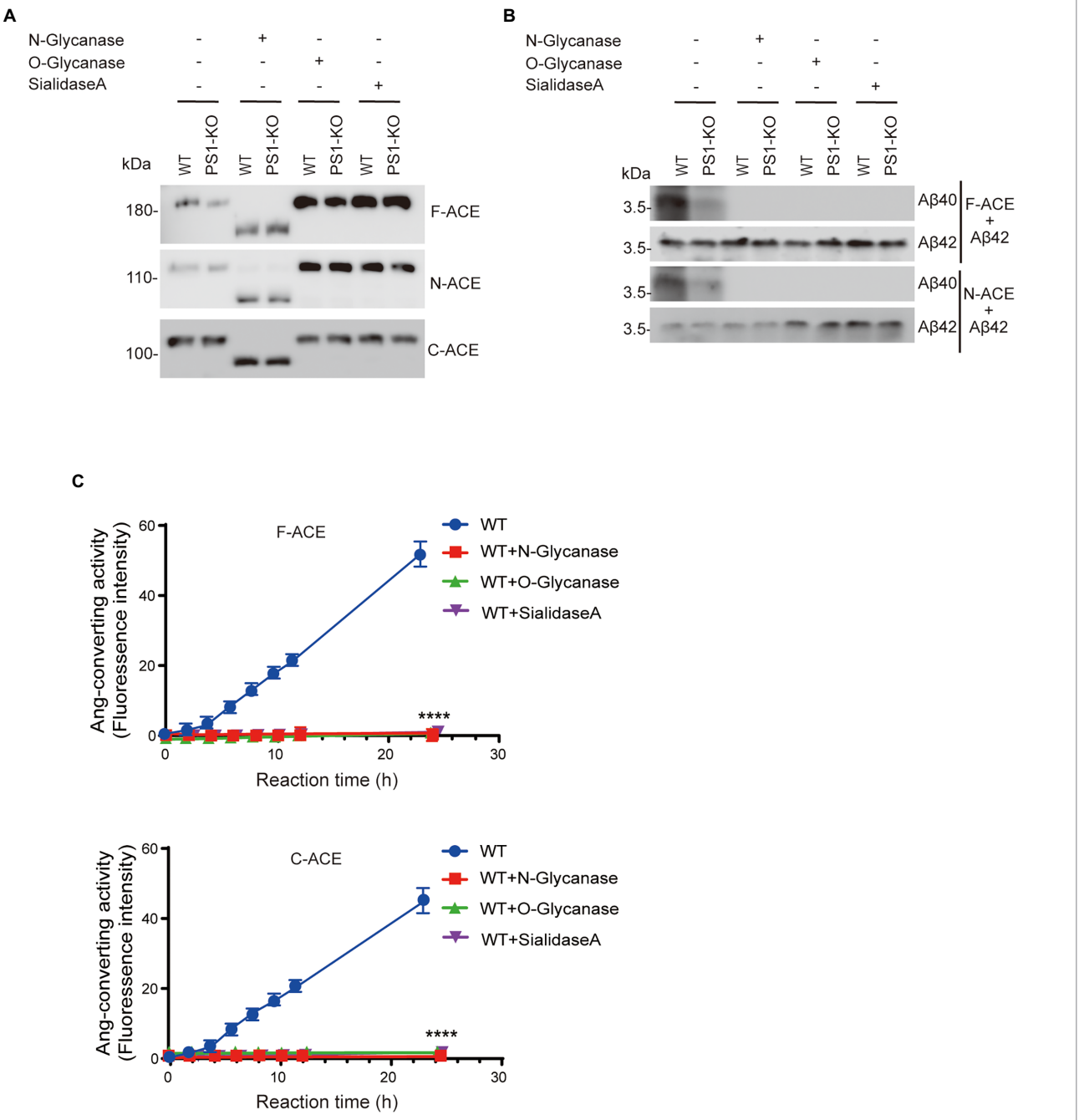

FIGURE 6
De-glycosylation abolished the Aβ42-to-Aβ40– and angiotensin-converting activity of ACE. **(A)** Purified F-ACE, N-ACE, and C-ACE (30μg each) from WT and PS1-KO fibroblasts was de-glycosylated using 1μl of *N*-glycanase, *O*-glycanase, or sialidase A for 2h at 37°C. Western blots of 20μg of de-glycosylated F-, N-, or C-ACE proteins from WT or PS1-KO fibroblasts were probed with an anti–6×His-tag antibody. **(B)** De-glycosylated F-ACE and N-ACE proteins were mixed with synthetic Aβ42 and incubated at 37°C for 2h. Western blots of the mixtures were probed with anti-Aβ40 and anti-Aβ42 antibodies. F-ACE and N-ACE did not exhibit Aβ-converting activity after de-glycosylation using *N*-glycanase, *O*-glycanase, or sialidase A. **(C)** F-ACE and C-ACE did not exhibit Ang-converting activity after de-glycosylation using *N*-glycanase, *O*-glycanase, or sialidase A. Values represent the mean±SD; *n*=3; ****, *p*<0.0001, Holm-Sidak's multiple comparisons test.

or α-2(3, 6, 8, 9)-neuraminidase to remove *N*-glycosylation, *O*-glycosylation, or sialic acid. De-glycosylated ACE was analyzed by Western botting, and its activity was examined.

Immunofluorescence staining

WT fibroblasts, PS1-KO fibroblasts transfected with F-ACE, and PS1-KO fibroblasts transfected with F-ACE and PS1 mutants were seeded using image culture dishes (Eppendorf) and incubated at 37°C for 24 h. We firstly fixed cells in 4% paraformaldehyde for 30 min at room temperature. The cells were then permeabilized with 0.1% Triton X-100 for 20 min and incubated in 10% donkey serum in Tris-buffered saline containing 0.05% Tween 20 for 1 h at room temperature. The cells were incubated overnight at 4°C with anti-syntaxin-6 and anti-ACE antibodies. Immunofluorescent labeling by staining with Alexa Fluor 488 or Alexa Fluor 568-conjugated secondary antibodies. Images were acquired with a confocal microscope (Olympus FV3000,

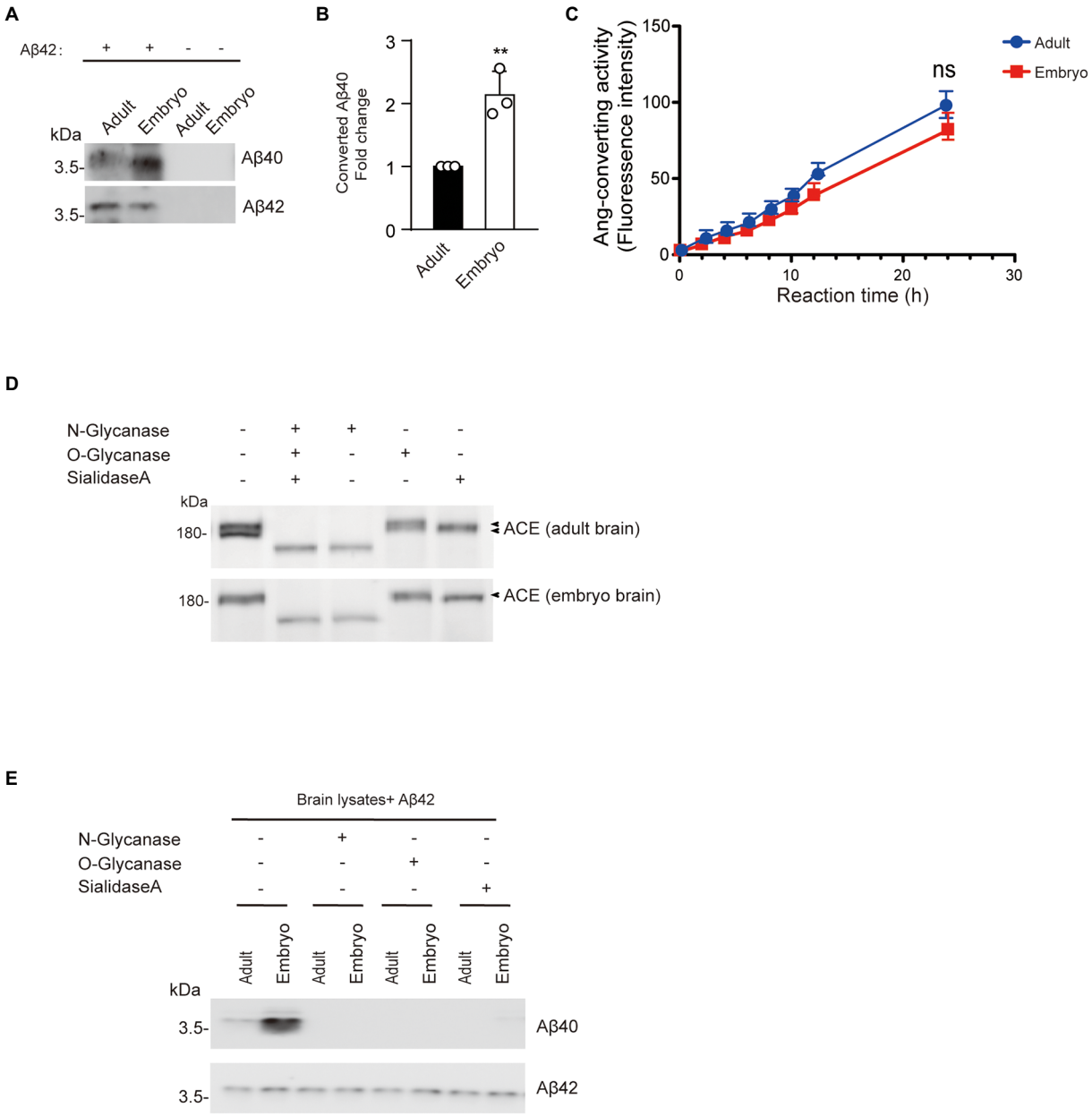

FIGURE 7
Aβ42-to-Aβ40-converting activity in adult mouse brain cortex is lower than that in embryonic brain cortex. **(A)** Synthetic Aβ42 protein (40μM) was incubated with 20μg of cortex lysate from 17-day-old embryos or 3-month-old mice. Aβ40 and Aβ42 were detected by Western blotting. **(B)** Quantification of Aβ40 converted from Aβ42. Embryo cortex exhibited higher Aβ42-to-Aβ40-converting activity than adult cortex. Values represent the mean±SEM; $n=3$; $^{**}p<0.001$, by unpaired two-tailed Student's t test. **(C)** Ang-converting activity was measured by incubating 2μg of total protein of cortex lysate from 17-day-old embryos or 3-month-old mice with the synthetic o-aminobenzoyl peptide substrate for 24h at 37°C. Values represent the mean±SD; $n=3$; NS, not significant, by unpaired two-tailed Student's t test. **(D)** Western blots of 20μg of total protein of cortex lysate from 17-day-old embryos or 3-month-old mice were probed with a polyclonal anti-ACE antibody. **(E)** 20μg protein of cortex lysate from 17-day-old embryos or 3-month-old mice were de-glycosylated and incubated with synthetic Aβ42. Aβ40 and Aβ42 were detected by Western blotting.

Tokyo, Japan). Details on the antibodies used are provided in Supplementary Table S1. ImageJ software was used to quantify the colocalization of ACE with the Golgi apparatus. The threshold intensity for both fluorescent signals is preset, which is determined using a colocalization threshold function. Colocalized pixels above a threshold intensity were automatically quantified and scored, and results were expressed as colocalized mean intensity positivity for both channels. Supplementary Table S1 provides details on antibodies and reagents.

Statistical analyzes

Prism 7.0 software (GraphPad Software, San Diego, CA) was used for statistical analyzes. All data are shown as the mean ± SEM or mean ± SD of at least three independent experiments, with $p<0.05$ considered statistically significant. Student's t tests were used to determine the significance of differences between two groups. Group differences were analyzed by one-way analysis of variance followed by ANOVA with Holm-Sidak's multiple comparisons tests for multiple

groups against the control group. All experiments produced similar results under the same or similar conditions, and normal distribution of the data was assumed.

Discussion

PS1-KO mice developed obvious developmental defects in the embryonic period and eventually died in the perinatal period (Donoviel et al., 1999). Presenilin gene mutations account for the majority of FAD cases. Most FAD-related mutations in PS1 are associated with increased Aβ42 levels or decreased Aβ40 levels, which results in an elevated Aβ42/40 ratio due to loss of PS1 function (Fernandez et al., 2014). These data also suggest that declines in neuroprotective Aβ40 levels may contribute to the pathogenesis of AD (Zou and Michikawa, 2008). However, how *PSEN1* mutations lead to an increase in the Aβ42/40 ratio is unclear. Here, we examined whether PS1 can regulate the activity of ACE, which converts neurotoxic Aβ42 to neuroprotective Aβ40. For the first time, we demonstrated that PS1 deficiency leads to significant lower Aβ42-to-Aβ40-converting activity of ACE (Figure 1). Strikingly, ACE purified from PS1-KO fibroblasts did not show any angiotensin-converting activity (Figure 2). These results suggest that PS plays a crucial role in ACE maturation and activity, and also in blood pressure regulation.

Overexpression of WT PS1 in PS1-KO fibroblasts restored the Aβ42-to-Aβ40-and angiotensin-converting activities of ACE. Interestingly, some PS1 mutants successfully restored the angiotensin-converting activity of ACE but not its Aβ42-to-Aβ40-converting activity, suggesting that *PSEN1* mutations increase the Aβ42/40 ratio by impairing the Aβ42-to-Aβ40-converting activity of ACE. A previous study found that Aβ40 levels are reduced to <5% of PS1WT levels in PS1/2-KO fibroblasts as a result of the FAD-linked *PSEN1* mutations L166P and G384A, whereas PS1ΔE9 fibroblasts exhibit higher Aβ40 levels than PS1L166P and PS1G384A fibroblasts (Heilig et al., 2013). Patients with PS1L166P, PS1G384A, and PS1ΔE9 exhibit mean AD onset at 24 years, 35 years, and 45.5 years, respectively (Julliams et al., 1999; Cacquevel et al., 2012). These results suggest that lower Aβ40 levels are associated with earlier FAD onset. NCT undergoes a typical ER-to-Golgi maturation pattern, with most mature species localized to the Golgi (Yang et al., 2002). Multiple studies have shown that complex glycosylation of NCT is dependent on PS1, with strong downregulation of mature NCT levels observed in cells lacking PS1 (Figure 3A; Edbauer et al., 2002; Herreman et al., 2003). In our study, PS1WT, PS1ΔE9, PS1L166P, and PS1G384A completely restored the maturation of NCT and angiotensin-converting activity (Figures 3A, 4). However, PS1L166P did not restore the localization of F-ACE protein localized in Golgi apparatus (Figures 5A,B). In addition, a study showed that overexpression of PS1 with a familial AD mutation (M146L) in the neuroblastoma cell line SH-SY5Y resulted in reduced sialylation of NCAM (Farquhar et al., 2003). Thus, PS1 mutants may also reduce sialylation of ACE in Golgi apparatus. The detail structure of ACE glycan in PS1 mutant cells need to be further analyzed. In contrast to PS1L166P and PS1G384A, only PS PS1ΔE9 restored the Aβ42-to-Aβ40-converting activity of ACE (Figure 3). Thus, our results suggest that the PS1L166P and PS1G384A mutations result in low Aβ42-to-Aβ40-converting activity, which leads to low Aβ40 levels and early onset of FAD.

Mammalian somatic ACEs contain two homology domains, an N-terminal domain (N-domain) and a C-terminal domain (C-domain), each with a zinc-dependent active site (Hooper and Turner, 2003). The presence of two active sites in ACE has inspired many attempts to determine whether the active sites differ functionally. ACE also hydrolyzes multiple polypeptide substrates, including substance P, luteinizing hormone–releasing hormone, acetyl-Ser-Asp-Lys-Pro (AcSDKP), and neurotensin (Turner and Hooper, 2002). AcSDKP, a peptide thought to inhibit myeloid maturation, is preferentially cleaved by the N-domain of ACE *in vitro* (Rousseau et al., 1995). In contrast, the ACE C-domain is the major site of angiotensin I cleavage *in vivo* (Fuchs et al., 2008).

Similar to our previous report, here, we also found that the angiotensin-converting activity of ACE is localized in the C-domain, whereas the Aβ42-to-Aβ40-converting activity is specifically localized in the N-domain (Figures 1E, 2B). We previously purified overexpressed F-ACE, N-ACE, and C-ACE proteins from cell culture medium (Zou et al., 2009). However, PS1-KO fibroblasts did not secrete any ACE protein after overexpression, possibly because PS1 deficiency impairs cellular secretion (Islam et al., 2022). Thus, we purified ACE protein from cell lysate, and this ACE protein exhibited activity similar to that of ACE purified from culture medium (Figures 1, 2).

Somatic ACE is highly glycosylated, and its glycan structure, as well as the location of the oligosaccharide chains, can vary with different protein sources (Kryukova et al., 2015). The sequence of human somatic ACE includes 17 potential *N*-glycosylation sites and 2 *O*-glycosylation sites (Anthony et al., 2010; Goth et al., 2015). We previously found that *N*-glycosylation is required for the Aβ42-to-Aβ40-and angiotensin-converting activities of ACE. Here, we found that removal of either *N*-glycosylation, *O*-glycosylation, or sialic acid abolished the Aβ42-to-Aβ40-and angiotensin-converting activities of ACE (Figures 4B,C). Our results suggest that the presence of *N*-glycosylation, *O*-glycosylation, or sialic acid plays an essential role in the Aβ42-to-Aβ40-and angiotensin-converting activities of ACE. NCT maturation has been reported to be reduced during rat brain development (Uchihara et al., 2006). We also found that glycosylation and Aβ42-to-Aβ40-converting activity of ACE decreases with development in adult brain compared with embryonic brain (Figures 7A,B).

Collectively, our data indicate that deletion of PS1 results in a significant decrease in both the Aβ42-to-Aβ40-converting activity and angiotensin-converting activity of ACE. Moreover, some FAD-linked *PSEN1* mutations were shown to impair the Aβ42-to-Aβ40-converting activity of ACE (Figure 8). Our results suggest that the increase in the Aβ42/40 ratio associated with FAD-linked *PSEN1* mutations results from not only altered γ-secretase cleavage but also the decrease in the Aβ42-to-Aβ40-converting activity of ACE. In addition, the presence of the *ACE I* allele with decreased serum and tissue ACE levels appears to be strongly associated with AD onset (Lehmann et al., 2005). Thus, approaches that maintain or enhance the Aβ42-to-Aβ40-converting activity of ACE will be useful for reducing the Aβ42/40 ratio and preventing the onset of AD. Taken together, our results suggest that enhancing PS-mediated trafficking and maturation of ACE may decrease Aβ42/40 ratio and can be used as a strategy for developing novel therapeutic regimens for AD patients.

Data availability statement

The original contributions presented in the study are included in the article/Supplementary material, further inquiries can be directed to the corresponding authors.

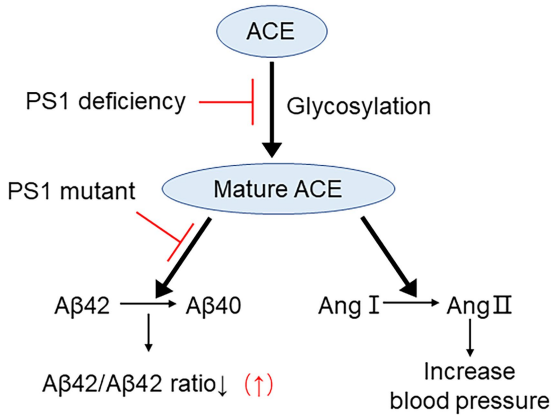

FIGURE 8
Proposed mechanism on PS1 mutant elevating Aβ42/40 ratio by impairing ACE maturation. ACE maturation/glycosylation is essential for its Aβ42-to-Aβ40-and angiotensin-converting activities and for reducing Aβ42/40 ratio. PS1 deficiency inhibits ACE maturation and both of these activities. PS1 mutant selectively inhibits Aβ42-to-Aβ40-converting activity of ACE and elevates Aβ42/40 ratio. However, PS1 mutants do not inhibit angiotensin converting activity of ACE.

Ethics statement

The animal study was reviewed and approved by The experiments in this study were performed in strict accordance with the recommendations of the Fundamental Guidelines for Proper Conduct of Animal Experiments and Related Activities in Academic Research Institutions, under the jurisdiction of the Ministry of Education, Culture, Sports, Science and Technology, Japan.

Author contributions

YG, YS, TN, TT, and KZ: data curation. YG, YS, SI, and KZ: formal analysis. YG, YS, and KZ: investigation. YG and KZ: writing—original draft. YG, KZ, and MM: writing—review and editing. KZ: conceptualization and supervision. KZ and MM: funding acquisition and project administration.

Funding

This work was supported by the Grant-in-Aid for Scientific Research C 19K07846 and 22K07352 (to KZ) from the Ministry of Education, Culture, Sports, Science, and Technology, Japan. This work was also supported by AMED under grant number JP20dk0207050h0001, JP20dk0207050h0002, JP20dk0207050h0003 and JP20de010702 (to MM), and by "the 24th General Assembly of the Japanese Association of Medical Sciences" (to KZ), the Daiko Foundation (to KZ), the Hirose International Scholarship Foundation (to KZ) and the Hori Sciences and Arts Foundation (to KZ).

Acknowledgments

We thank Bart De Strooper for providing Wild-type (WT) and PS1 knock-out (PS1-KO) mouse embryonic fibroblast (MEF) cells.

Conflict of interest

The authors declare that the research was conducted in the absence of any commercial or financial relationships that could be construed as a potential conflict of interest.

Publisher's note

All claims expressed in this article are solely those of the authors and do not necessarily represent those of their affiliated organizations, or those of the publisher, the editors and the reviewers. Any product that may be evaluated in this article, or claim that may be made by its manufacturer, is not guaranteed or endorsed by the publisher.

Supplementary material

The Supplementary material for this article can be found online at: https://www.frontiersin.org/articles/10.3389/fnagi.2023.1098034/full#supplementary-material

References

Anthony, C. S., Corradi, H. R., Schwager, S. L., Redelinghuys, P., Georgiadis, D., Dive, V., et al. (2010). The N domain of human angiotensin-I-converting enzyme: the role of N-glycosylation and the crystal structure in complex with an N domain-specific phosphinic inhibitor, RXP407. *J. Biol. Chem.* 285, 35685–35693. doi: 10.1074/jbc.M110.167866

Bai, X. C., Yan, C., Yang, G., Lu, P., Ma, D., Sun, L., et al. (2015). An atomic structure of human γ-secretase. *Nature* 525, 212–217. doi: 10.1038/nature14892

Bentahir, M., Nyabi, O., Verhamme, J., Tolia, A., Horré, K., Wiltfang, J., et al. (2006). Presenilin clinical mutations can affect gamma-secretase activity by different mechanisms. *J. Neurochem.* 96, 732–742. doi: 10.1111/j.1471-4159.2005.03578.x

Cacquevel, M., Aeschbach, L., Houacine, J., and Fraering, P. C. (2012). Alzheimer's disease-linked mutations in presenilin-1 result in a drastic loss of activity in purified γ-secretase complexes. *PLoS One* 7:e35133. doi: 10.1371/journal.pone.0035133

De Strooper, B., Iwatsubo, T., and Wolfe, M. S. (2012). Presenilins and γ-secretase: structure, function, and role in Alzheimer disease. *Cold Spring Harb. Perspect. Med.* 2, –a006304. doi: 10.1101/cshperspect.a006304

Donoviel, D. B., Hadjantonakis, A. K., Ikeda, M., Zheng, H., Hyslop, P. S., and Bernstein, A. (1999). Mice lacking both presenilin genes exhibit early embryonic patterning defects. *Genes Dev.* 13, 2801–2810. doi: 10.1101/gad.13.21.2801

Edbauer, D., Winkler, E., Haass, C., and Steiner, H. (2002). Presenilin and nicastrin regulate each other and determine amyloid beta-peptide production via complex formation. *Proc. Natl. Acad. Sci. U. S. A.* 99, 8666–8671. doi: 10.1073/pnas.132277899

Farquhar, M. J., Gray, C. W., and Breen, K. C. (2003). The over-expression of the wild type or mutant forms of the presenilin-1 protein alters glycoprotein processing in a human neuroblastoma cell line. *Neurosci. Lett.* 346, 53–56. doi: 10.1016/S0304-3940(03)00544-5

Fernandez, M. A., Klutkowski, J. A., Freret, T., and Wolfe, M. S. (2014). Alzheimer presenilin-1 mutations dramatically reduce trimming of long amyloid β-peptides (Aβ) by γ-secretase to increase 42-to-40-residue Aβ. *J. Biol. Chem.* 289, 31043–31052. doi: 10.1074/jbc.M114.581165

Fuchs, S., Xiao, H. D., Hubert, C., Michaud, A., Campbell, D. J., Adams, J. W., et al. (2008). Angiotensin-converting enzyme C-terminal catalytic domain is the main site of angiotensin I cleavage in vivo. *Hypertension* 51, 267–274.

Goedert, M., and Spillantini, M. G. (2006). A century of Alzheimer's disease. *Science* 314, 777–781. doi: 10.1126/science.1132814

Goth, C. K., Halim, A., Khetarpal, S. A., Rader, D. J., Clausen, H., and Schjoldager, K. T. (2015). A systematic study of modulation of ADAM-mediated ectodomain shedding by site-specific O-glycosylation. *Proc. Natl. Acad. Sci. U. S. A.* 112, 14623–14628. doi: 10.1073/pnas.1511175112

Gowrishankar, K., Zeidler, M. G., and Vincenz, C. (2004). Release of a membrane-bound death domain by gamma-secretase processing of the p75NTR homolog NRADD. *J. Cell Sci.* 117, 4099–4111. doi: 10.1242/jcs.01263

Haass, C., Hung, A. Y., Schlossmacher, M. G., Teplow, D. B., and Selkoe, D. J. (1993). Beta-amyloid peptide and a 3-kDa fragment are derived by distinct cellular mechanisms. *J. Biol. Chem.* 268, 3021–3024. doi: 10.1016/S0021-9258(18)53650-4

Heilig, E. A., Gutti, U., Tai, T., Shen, J., and Kelleher, R. J. 3rd. (2013). Trans-dominant negative effects of pathogenic PSEN1 mutations on γ-secretase activity and Aβ production. *J. Neurosci.* 33, 11606–11617. doi: 10.1523/JNEUROSCI.0954-13.2013

Herreman, A., Van Gassen, G., Bentahir, M., Nyabi, O., Craessaerts, K., Mueller, U., et al. (2003). Gamma-Secretase activity requires the presenilin-dependent trafficking of nicastrin through the Golgi apparatus but not its complex glycosylation. *J. Cell Sci.* 116, 1127–1136. doi: 10.1242/jcs.00292

Hooper, N. M., and Turner, A. J. (2003). An ACE structure. *Nat. Struct. Biol.* 10, 155–157. doi: 10.1038/nsb0303-155

Islam, S., Sun, Y., Gao, Y., Nakamura, T., Noorani, A. A., Li, T., et al. (2022). Presenilin is essential for ApoE secretion, a novel role of Presenilin involved in Alzheimer's disease pathogenesis. *J. Neurosci.* 42, 1574–1586. doi: 10.1523/JNEUROSCI.2039-21.2021

Julliams, A., Vanderhoeven, I., Kuhn, S., Van Broeckhoven, C., and De Jonghe, C. (1999). No influence of presenilin1 I143T and G384A mutations on endogenous tau phosphorylation in human and mouse neuroblastoma cells. *Neurosci. Lett.* 269, 83–86. doi: 10.1016/S0304-3940(99)00402-4

Kim, J., Onstead, L., Randle, S., Price, R., Smithson, L., Zwizinski, C., et al. (2007). Abeta 40 inhibits amyloid deposition in vivo. *J. Neurosci. Off. J. Soc. Neurosci.* 27, 627–633. doi: 10.1523/JNEUROSCI.4849-06.2007

Kimberly, W. T., LaVoie, M. J., Ostaszewski, B. L., Ye, W., Wolfe, M. S., and Selkoe, D. J. (2003). Gamma-secretase is a membrane protein complex comprised of presenilin, nicastrin, Aph-1, and pen-2. *Proc. Natl. Acad. Sci. U. S. A.* 100, 6382–6387. doi: 10.1073/pnas.1037392100

Kimberly, W. T., and Wolfe, M. S. (2003). Identity and function of gamma-secretase. *J. Neurosci. Res.* 74, 353–360. doi: 10.1002/jnr.10736

Kryukova, O. V., Tikhomirova, V. E., Golukhova, E. Z., Evdokimov, V. V., Kalantarov, G. F., Trakht, I. N., et al. (2015). Tissue specificity of human angiotensin I-converting enzyme. *PLoS One* 10:e0143455. doi: 10.1371/journal.pone.0143455

Kuperstein, I., Broersen, K., Benilova, I., Rozenski, J., Jonckheere, W., Debulpaep, M., et al. (2010). Neurotoxicity of Alzheimer's disease Aβ peptides is induced by small changes in the Aβ42 to Aβ40 ratio. *EMBO J.* 29, 3408–3420. doi: 10.1038/emboj.2010.211

Leem, J. Y., Saura, C. A., Pietrzik, C., Christianson, J., Wanamaker, C., King, L. T., et al. (2002). A role for presenilin 1 in regulating the delivery of amyloid precursor protein to the cell surface. *Neurobiol. Dis.* 11, 64–82. doi: 10.1006/nbdi.2002.0546

Lehmann, D. J., Cortina-Borja, M., Warden, D. R., Smith, A. D., Sleegers, K., Prince, J. A., et al. (2005). Large meta-analysis establishes the ACE insertion-deletion polymorphism as a marker of Alzheimer's disease. *Am. J. Epidemiol.* 162, 305–317. doi: 10.1093/aje/kwi202

Liu, S., Ando, F., Fujita, Y., Liu, J., Maeda, T., Shen, X., et al. (2019). A clinical dose of angiotensin-converting enzyme (ACE) inhibitor and heterozygous ACE deletion exacerbate Alzheimer's disease pathology in mice. *J. Biol. Chem.* 294, 9760–9770. doi: 10.1074/jbc.RA118.006420

Liu, S., Liu, J., Miura, Y., Tanabe, C., Maeda, T., Terayama, Y., et al. (2014). Conversion of Aβ43 to Aβ40 by the successive action of angiotensin-converting enzyme 2 and angiotensin-converting enzyme. *J. Neurosci. Res.* 92, 1178–1186. doi: 10.1002/jnr.23404

McGowan, E., Pickford, F., Kim, J., Onstead, L., Eriksen, J., Yu, C., et al. (2005). Abeta42 is essential for parenchymal and vascular amyloid deposition in mice. *Neuron* 47, 191–199. doi: 10.1016/j.neuron.2005.06.030

Naruse, S., Thinakaran, G., Luo, J. J., Kusiak, J. W., Tomita, T., Iwatsubo, T., et al. (1998). Effects of PS1 deficiency on membrane protein trafficking in neurons. *Neuron* 21, 1213–1221. doi: 10.1016/S0896-6273(00)80637-6

Rousseau, A., Michaud, A., Chauvet, M. T., Lenfant, M., and Corvol, P. (1995). The hemoregulatory peptide N-acetyl-Ser-asp-Lys-pro is a natural and specific substrate of the N-terminal active site of human angiotensin-converting enzyme. *J. Biol. Chem.* 270, 3656–3661. doi: 10.1074/jbc.270.8.3656

Selkoe, D. J. (2011). Alzheimer's disease. *Cold Spring Harb. Perspect. Biol.* 3:a004457. doi: 10.1101/cshperspect.a004457

Selkoe, D. J., and Hardy, J. (2016). The amyloid hypothesis of Alzheimer's disease at 25 years. *EMBO Mol. Med.* 8, 595–608. doi: 10.15252/emmm.201606210

Steiner, H., Romig, H., Grim, M. G., Philipp, U., Pesold, B., Citron, M., et al. (1999). The biological and pathological function of the presenilin-1 Deltaexon 9 mutation is independent of its defect to undergo proteolytic processing. *J. Biol. Chem.* 274, 7615–7618. doi: 10.1074/jbc.274.12.7615

Turner, A. J., and Hooper, N. M. (2002). The angiotensin-converting enzyme gene family: genomics and pharmacology. *Trends Pharmacol. Sci.* 23, 177–183. doi: 10.1016/S0165-6147(00)01994-5

Uchihara, T., Sanjo, N., Nakamura, A., Han, K., Song, S. Y., St George-Hyslop, P., et al. (2006). Transient abundance of presenilin 1 fragments/nicastrin complex associated with synaptogenesis during development in rat cerebellum. *Neurobiol. Aging* 27, 88–97. doi: 10.1016/j.neurobiolaging.2004.12.011

Uemura, K., Kitagawa, N., Kohno, R., Kuzuya, A., Kageyama, T., Chonabayashi, K., et al. (2003). Presenilin 1 is involved in maturation and trafficking of N-cadherin to the plasma membrane. *J. Neurosci. Res.* 74, 184–191. doi: 10.1002/jnr.10753

Wanngren, J., Lara, P., Ojemalm, K., Maioli, S., Moradi, N., Chen, L., et al. (2014). Changed membrane integration and catalytic site conformation are two mechanisms behind the increased Aβ42/Aβ40 ratio by presenilin 1 familial Alzheimer-linked mutations. *FEBS Open Bio* 4, 393–406. doi: 10.1016/j.fob.2014.04.006

Yang, D. S., Tandon, A., Chen, F., Yu, G., Yu, H., Arawaka, S., et al. (2002). Mature glycosylation and trafficking of nicastrin modulate its binding to presenilins. *J. Biol. Chem.* 277, 28135–28142. doi: 10.1074/jbc.M110871200

Zou, K., Gong, J. S., Yanagisawa, K., and Michikawa, M. (2002). A novel function of monomeric amyloid beta-protein serving as an antioxidant molecule against metal-induced oxidative damage. *J. Neurosci. Off. J. Soc. Neurosci.* 22, 4833–4841. doi: 10.1523/JNEUROSCI.22-12-04833.2002

Zou, K., Hosono, T., Nakamura, T., Shiraishi, H., Maeda, T., Komano, H., et al. (2008). Novel role of presenilins in maturation and transport of integrin beta 1. *Biochemistry* 47, 3370–3378. doi: 10.1021/bi7014508

Zou, K., Kim, D., Kakio, A., Byun, K., Gong, J. S., Kim, J., et al. (2003). Amyloid beta-protein (Abeta)1-40 protects neurons from damage induced by Abeta 1-42 in culture and in rat brain. *J. Neurochem.* 87, 609–619. doi: 10.1046/j.1471-4159.2003.02018.x

Zou, K., Liu, J., Watanabe, A., Hiraga, S., Liu, S., Tanabe, C., et al. (2013). Aβ43 is the earliest-depositing Aβ species in APP transgenic mouse brain and is converted to Aβ41 by two active domains of ACE. *Am. J. Pathol.* 182, 2322–2331. doi: 10.1016/j.ajpath.2013.01.053

Zou, K., Maeda, T., Watanabe, A., Liu, J., Liu, S., Oba, R., et al. (2009). Abeta42-to-Abeta40-and angiotensin-converting activities in different domains of angiotensin-converting enzyme. *J. Biol. Chem.* 284, 31914–31920. doi: 10.1074/jbc.M109.011437

Zou, K., and Michikawa, M. (2008). Angiotensin-converting enzyme as a potential target for treatment of Alzheimer's disease: inhibition or activation? *Rev. Neurosci.* 19, 203–212. PMID: 19145983

Zou, K., Yamaguchi, H., Akatsu, H., Sakamoto, T., Ko, M., Mizoguchi, K., et al. (2007). Angiotensin-converting enzyme converts amyloid beta-protein 1-42 (Abeta (1-42)) to Abeta (1-40), and its inhibition enhances brain Abeta deposition. *J. Neurosci.* 27, 8628–8635. doi: 10.1523/JNEUROSCI.1549-07.2007

Frontiers in
Aging Neuroscience

Explores the mechanisms of central nervous system aging and age-related neural disease

The third most-cited journal in the field of geriatrics and gerontology, with a focus on understanding the mechanistic processes associated with central nervous system aging.

Discover the latest Research Topics

See more →

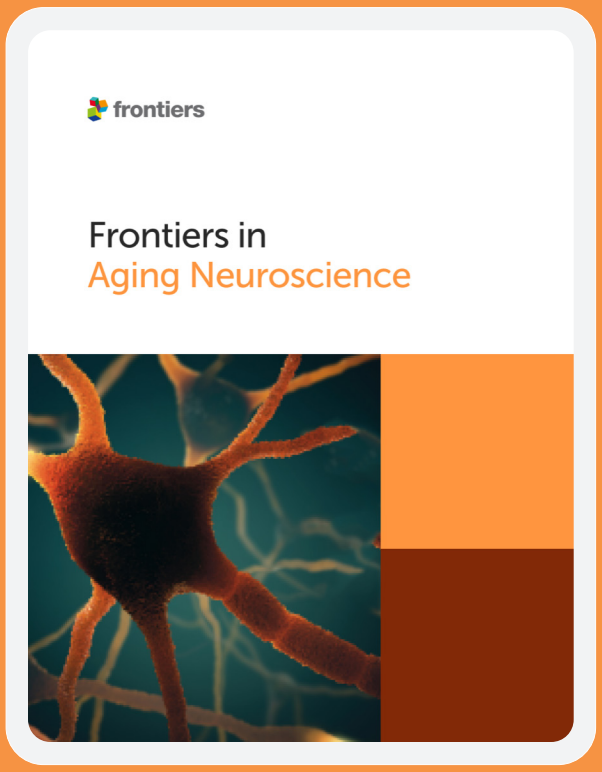

Frontiers

Avenue du Tribunal-Fédéral 34
1005 Lausanne, Switzerland
frontiersin.org

Contact us

+41 (0)21 510 17 00
frontiersin.org/about/contact